Geochimica et Cosmochimica Acta

JOURNAL OF THE GEOCHEMICAL SOCIETY

Executive Editors

C. W. CORRENS, *Göttingen.* E. INGERSON, *Austin, Texas.* L. R. WAGER, *Oxford.*

Editors

L. H. AHRENS, *Capetown.* S. R. NOCKOLDS, *Cambridge.* H. C. UREY, *La Jolla, Calif.*
JOHN VERHOOGEN, *Berkeley, Calif.* A. P. VINOGRADOV, *Moscow.*
W. A. WAHL, *Helsingfors.*

CONTENTS VOLUME 23, NOS. 1/2 APRIL 1961

TOM F. W. BARTH: Abundance of the elements, areal averages and geochemical cycles 1

M. H. CARR and K. K. TUREKIAN: The geochemistry of cobalt 9

W. J. KNAPP and H. FLOOD: Activities and structure of some borosilicate melts 61

J. F. EVERNDEN, G. H. CURTIS, J. OBRADOVICH and R. KISTLER: On the evaluation of glauconite and illite for dating sedimentary rocks by the potassium-argon method 78

R. R. BROOKS and L. H. AHRENS: Some observations on the distribution of thallium, cadmium and bismuth in silicate rocks and the significance of covalency on their degree of association with other elements 100

D. M. SHAW: Element distribution laws in geochemistry 116

H. W. FAIRBAIRN, P. M. HURLEY and W. H. PINSON: The relation of discordant Rb–Sr mineral and whole rock ages in an igneous rock to its time of crystallization and to the time of subsequent Sr^{87}/Sr^{86} metamorphism 135

Geochemical Notes:

R. R. BROOKS and L. H. AHRENS: The determination of indium and thallium in G–1, W–1 and other silicate rocks by a new technique 145

C. C. MCMULLEN, C. B. CRAGG and H. G. THODE: Absolute ratio of B^{11}/B^{10} in Searles Lake borax 147

Letter to the Editors:

E-AN ZEN: Partial molar volumes of some salts in aqueous solutions . . . 151

Academy of Sciences of the U.S.S.R.:

Abstracts from proceedings of the Institute for the geology of ore deposits, petrography, mineralogy and geochemistry 152

Errata: 154

PERGAMON PRESS OXFORD • LONDON • NEW YORK • PARIS

GEOCHIMICA ET COSMOCHIMICA ACTA

EXECUTIVE EDITORS

PROF. C. W. CORRENS (1959) *Sedimentpetrographisches Institut der Universität, Lotzestr.* 13, *Göttingen, Germany*
PROF. E. INGERSON (1959–1960) *Department of Geology, University of Texas, Austin* 12, *Texas, U.S.A.*
PROF. L. WAGER, F.R.S. (1959–1961) *Department of Geology and Mineralogy, The University Museum, Oxford, England*

EDITORS

PROF. L. H. AHRENS (1959–1960) *Department of Chemistry, University of Capetown, Rondebosch, Cape Province, South Africa*
Dr. S. R. NOCKOLDS *Department of Mineralogy and Petrology, The University, Cambridge, England*
PROF. H. C. UREY, For. Mem. R. S. (1959) *University of California, La Jolla, California, U.S.A.*
Dr. JOHN VERHOOGEN (1959–1961) *Department of Geology, University of California, Berkeley, California, U.S.A.*
PROF. A. P. VINOGRADOV (1959–1961) *Vernadsky Institute, Moscow, U.S.S.R.*
PROF. W. A. WAHL (1959–1961) *Observatoriegaten* 8, *Helsingfors, Finland*

EDITORIAL ADVISORY BOARD

EUROPE

T. F. W. BARTH, *Oslo*
L. CAPDECOMME, *Toulouse*
E. J. CONWAY, *Dublin*
P. ESKOLA, *Helsinki*
P. GALLITELLI, *Modena*
A. HADDING, *Lund*
O. HAHN, *Göttingen*
H. W. HARVEY, *Plymouth*
F. HEIDE, *Jena*
A. HOLMES, *Edinburgh*
W. Q. KENNEDY, *Leeds*
PH. H. KUENEN, *Gröningen*
S. LANDERGREN, *Stockholm*
F. MASHATSCHKI, *Vienna*
A. MUIR, *Harpenden*
J. ORCEL, *Paris*
E. RAGUIN, *Paris*
E. REINHARD, *Basle*
TH. G. SAHAMA, *Helsinki*
C. E. TILLEY, *Cambridge*
T. VOGT, *Trondheim*

AMERICAN CONTINENT

A. F. BUDDINGTON, *Princeton*
D. GUIMÃRAES, *Belo Horizonte*
G. E. HUTCHINSON, *New Haven*
B. H. MASON, *New York*
F. WHIPPLE, *Cambridge*
R. WILDT, *New Haven*
H. S. YODER, *Washington*

FAR EAST

T. WATANABE, *Tokyo*

AUSTRALIA

D. J. SWAINE, *Sydney*

Publishing Offices: Pergamon Press Ltd., Headington Hill Hall, Oxford

Four issues per volume, three volumes per year

Subscription *per annum* (including postage) (A) £21 (U.S.A. $60.00); (B) For individual subscribers who write directly to the publisher certifying that the Journal is for their private use, £7.7s. (U.S.A. $21.50). Members of the Geochemical Society, or non-members who occasionally publish papers in the Journal, £3. 11s. 6d. (U.S.A. $10.00) *per annum.*

Back numbers, £10 (U.S.A. $28.00) per volume

Single issues, £2. 10s. (U.S.A. $7.00) each

Copyright © 1961 Pergamon Press Ltd.

PERGAMON PRESS LTD.

HEADINGTON HILL HALL, OXFORD 122 EAST 55TH STREET, NEW YORK 22, N.Y.

PRINTED IN NORTHERN IRELAND AT THE UNIVERSITIES PRESS, BELFAST

PERGAMON PRESS

specialized journals for *specialized advertising!*

Advertise in GEOCHIMICA ET COSMOCHIMICA ACTA—

Space is available to all manufacturers of suitable products—the range which will appeal to readers of this journal is extensive and includes spectrometers, seismographs, seismic amplifiers and detectors, hydrometers, humidity instruments, monometers, galvanometers, radiation detectors and pyrometers, colorimeters, fluorometers, petrographic and other microscopes, flame photometers, surveying instruments, voltmeters, lenses and optical elements, mine ventilation instruments, X-ray microanalysers, pumps, pipe-lines, gas detection and measurement apparatus, microphotometers, X-ray films, plates and equipment, samplers of airborne dust and bacteria, telecommunications equipment, gyroscopic instruments, petroleum testing equipment, thermometers of all types, chemicals, oil boring equipment, electronic equipment . . . this list could easily be trebled!

We shall be happy to provide impartial advice as to the suitability of products not listed.

THIS IS ONE OF MORE THAN 60 INTERNATIONAL SCIENTIFIC JOURNALS. SPECIAL REDUCED "COMBINED RATES" ARE OFFERED TO MANUFACTURERS ADVERTISING IN MORE THAN ONE JOURNAL.

For details WRITE OR PHONE to

R. D. MILLER
Advertisement Manager

PERGAMON PRESS LIMITED
Pergamon House,
4 Fitzroy Square,
London W.1
Phone: EUSton 4455

PERGAMON PRESS INC.
122 East 55th Street,
New York 22, N.Y.,
U.S.A.
Phone: Plaza 3-9651

Appearing in 1961

International Series of Monographs on Pure and Applied Biology: Biochemistry Division

Physical Constants of Steroids

Edited by L. L. ENGEL

In this volume the diverse properties of steroid hormones and their metabolites which are useful in their isolation identification, and quantitative estimation are dealt with. Among the physical properties covered are fluorescence spectra, the chromogens formed upon treatment of steroids with sulphuric acid and correlation of the sulphuric acid chromogens with structure of the steroid. Laboratory workers in the field of steroid hormone metabolism and chemistry will find this an invaluable handbook.

Approx. £5 ($15.00)

Oxytocin

Proceedings of an International Symposium held in Montevideo

Edited by R. CALDEYRO-BARCIA and H. HELLER

This book represents the most comprehensive account of the physiology of oxytocin with special reference to its importance in human labour. The following recent advances and special aspects have been covered: extra-uterine effects of oxytocin; its actions as analysed by electrophysiological methods; its effect on the pregnant and parturient human uterus; the effects of synthetic analogues of oxytocin on uterine function; a comparison of oxytocin with other oxytocic drugs and the physiological (and possibly pathological) importance of oxytocinase, *i.e.* the oxytocin inactivating enzyme which appears in human blood during pregnancy.

Approx. 63s.

A Short Textbook of Colloid Chemistry

2nd Revised Edition

by B. JIRGENSONS and M. E. STRAUMANIS

This text is an introduction to colloids for those who are interested in the fundamentals of colloids and their applications in chemical industry, pharmacy, clinical medicine, biology and similar fields. All types of inorganic and organic colloids are treated, emphasising the effects of particle size and shape on the properties of the systems. The experimental procedures are described in detail, stressing the methods that are now used in industrial and clinical laboratories.

Approx. 63s. ($10.00)

International Series of Monographs on Pure and Applied Biology: Biochemistry Division

The Chromatography of Steroids

by I. E. BUSH

The available methods for the chromatography of steroids are reviewed in this book. Particular attention is given to the application of the theory of partition chromatography to the behaviour of steroids in chromatographic systems, and this is then used to give general indications of what types of chromatographic procedure are most suitable for particular problems in steroid biochemistry. Systematic application of the principles outlined in this book should lead to many more precise ways of identifying steroids by chromatographic means in the future.

Approx. 60s.

Absorption Spectra and Chemical Bonding in Complexes

by C. K. JORGENSEN

In this book the molecular orbital theory is shown to be the appropriate description of complexes, while the ligand field theory (in its electrostatic model) and the valency-bond model (especially Pauling's hybridisation hypothesis) are shown to be inadequate for the description of the energy levels and for the chemical bonding. Chapters on atomic spectroscopy and complex chemistry are included and a large number of references are given. This book will interest inorganic chemists and non-nuclear physicists at a fairly advanced level in addition to theorists of chemical physics.

Approx. 40s.

Descriptive leaflets will be sent on request

PERGAMON PRESS

OXFORD LONDON NEW YORK PARIS

Headington Hill Hall, Oxford 4 & 5 *Fitzroy Square, London W.*1

122 *East 55th Street, New York* 22, *N.Y.*

Geochimica et Cosmochimica Acta, 1961, Vol. 23, pp. 1 to 8. Pergamon Press Ltd. Printed in Northern Ireland

5856-29A

Abundance of the elements, areal averages and geochemical cycles*

Tom. F. W. Barth

We have no quantitative knowledge of the composition of the earth as a whole, or the composition of the individual parts. The concept of geochemical cycles explains some of the migration of the chemical species in the earth; but the quantitative relations of the cyclic processes are not known. Our ignorance is really shocking; the underlying data are inadequate and no final solution would seem possible today. So little is known that, in order to get a start, a series of hypotheses have to be introduced. Such hypotheses must be critically examined—this is the main object of the present paper. If the hypotheses can be shown to be plausible one may at least go ahead; if not, there is no use to proceed with subsequent calculations.

Our interpretation of the geochemical cycles is highly influenced by inherited notions, and our ideas of rock genesis have been through many and often sinuous changes during the 200 years growth of the earth sciences, from Werner's neptunism and Hutton's plutonism to present day. Whereas it is possible for us to see Werner and Hutton in a historical perspective, this is not yet possible in the case of the Rosenbusch system: In modern geochemistry the Rosenbusch ideas have prevailed; igneous rocks are regarded as primary, they come from the depths of the earth, from "die ewige Teufe", i.e., they are "juvenile", whereas sedimentary (and metamorphic) rocks are secondary and ultimately derived from igneous material.

Clarke and Washington adhered to this theory: The average composition of the crust is in effect that of igneous rocks; crustal abundances of the elements can be computed, therefore, by averaging the chemical analyses of the igneous rocks. The overall average of the 5159 analyses of igneous rocks compiled by Washington is still the accepted basis for nearly all geochemical calculations. V. M. Goldschmidt, a scientist of unusual capacity and founder of modern geochemistry was likewise deeply rooted in Rosenbusch's school; so was N. L. Bowen, an equally great man and the founder of modern petrology.

Thus the dead hand of the past is still directing our thinking: The average composition of the sedimentary rocks must correspond to that of the igneous rocks; for ultimately all sediments derive from igneous material. However, if this theory is applied to actual rocks, discrepancies are found, and sundry hypotheses have appeared to explain away the facts. A particularly disturbing difference is that of sodium: according to current calculations, the igneous rocks contain about three times as much sodium as do the sedimentary rocks.

In a paper of great consequence given before the German Mineralogische Gesellschaft in 1933 and repeated in his Hugo Müller lecture delivered before the

* Presidential Address presented before the Geochemical Society November 1, 1960, during its annual meeting in Denver, Colorado.

Chemical Society in London in 1937, and again repeated in his posthumous book of 1954, GOLDSCHMIDT maintained in principle*:

$$\text{Age of the Sea} = \frac{\text{Total amount of Na in the sea}}{\text{Na supplied per year}} \tag{1}$$

As a consequence of this GOLDSCHMIDT assumed:

$$\text{Total Weight of weathered rocks } W = \frac{\text{Total amount of Na in the sea}}{\text{Na\% of igneous rocks} - \text{Na\% of Sediments}} \tag{2}$$

His reasoning is well known: He thought that the sodium missing in the sediments is to be found in the sea.† The concentration of sodium in igneous rocks and in sediments are about 3 per cent and 1 per cent respectively. The total amount of sodium in the ocean corresponds to a mass of 3 kg per cm² of the earth's surface. From (2) we thus obtain, W total $= \frac{3}{3\% - 1\%} = 150$ kg per cm². By introducing the small corrections mentioned above GOLDSCHMIDT actually arrived at 160 kg per cm².

I have several objections to this kind of calculation, the most important are:

I. I do not believe that only igneous rocks or their derivatives make up the crust.

II. I do not believe that the weathered sodium stays in the ocean.

Ad. I

The source of the sediments is obviously the surface of the earth. In addition to older sediments which will be reworked, there are, at the surface, much more that 50 per cent of rocks of metamorphic origin (see Table 1). Metamorphites, in particular crystalline schists and gneisses, have been changed chemically by "juvenile" matter which derive from the same source as that of the igneous rocks. Consequently, there should *not* be a direct chemical correspondence between igneous and sedimentary rocks: all previous quantitative computations of crustal abundance are erroneous (see Table 2).

The composition of the surface of the earth at any one time, in particular that of the surface of the dry continents, is of the utmost importance. Not until such data are at hand, can we hope for a more quantitative knowledge of the geochemical migrations.

Unfortunately, we know very little about areal averages. This was again and most recently emphasized by FLEISCHER and CHAO before the International Geological Congress last summer (1960): "The need for better information was clearly stated by Daly in 1914, who pointed out that such data were required for many petrological problems. Essentially nothing has been attempted since. We can only repeat his hope that some international group should encourage the

* He made a modification by assuming that 33% of the sodium was locked up in evaporites and other sediments. It should also be added that he did not think that the present supply of Na (as observed in river water, etc.) should be used.

† He made a small correction in accordance with the fact that the total amount of sediments (shales) is slightly less than that of the igneous rocks (v.i.).

Table 1. Norway south of 65° N. 231500 km²

Relative Areas of Rock Species					
		I			
Caledonian Zone		144100 km²	62·3%		
1. T.hjemite-Opdalite	14·4%	2600 km²			
2. Gabbro-Amphibolite	16·0%	2900 km²			
3. Ultrabasics	3·9%	700 km²			
4. Thrust masses, acid	18·8%	3400 km²			
5. Thrust masses basic	47·0%	8500 km²			
Intrusives				18100 km²	12·5%
Devonian				2300 km²	1·6%
6. Valdres sparagmite		1100 km²			
7. Schists-Jotun-W. Coast		19500 km²			
8. Schists-T.hjem area		27000 km²			
9. Schists-Grong area		4300 km²			
Cambro-Silurian Supracrustals				51900 km²	36·0%
10. Sparagmite (arkoses)		18600 km²			
11. Meta-sparagmite in N.W.		1100 km²			
Eocambrian				19700 km²	13·7%
12. Fosen area		11000 km²			
13. Møre-Romsdal		40000 km²			
14. Haugesund		1100 km²			
Migmatite				52100 km²	36·2%
		II			
Oslo Graben		9900 km²	4·3%		
1. Subvolcanics	77·2%	6100 km²			
2. Basic lavas	3·8%	300 km²			
3. Romb Porphyries	17·7%	1400 km²			
4. Tuffs, etc.	1·3%	100 km²			
Igneous rocks				7900 km²	80·0%
Sedimentary rocks				2000 km²	20·0%
		III			
Precambrian		77500 km²	33·4%		
1. Mixed gneisses	48·0%	26000 km²			
2. Gneissic granites	33·2%	18000 km²			
3. Quartzites	12·0%	6500 km²			
4. Post-Granites	4·2%	2300 km²			
5. Anorthosite, etc.	2·2%	1200 km²			
6. Amphibolite	0·4%	200 km²			
W. of Oslo Graben				54200 km²	70·0%
Östfold-Trysil				19000 km²	24·5%
"Windows"				4300 km²	5·5%

Table 2. Chemical composition of the crust

Some Areal Averages
(cation per cent)

Averages for Norway

	Caledonian Zone	Precambrian	Oslo Igneous
Si	60·9	65·2	55·2
Ti	0·5	0·5	0·8
Al	17·1	15·5	18·3
Fe	1·6	1·0	2·1
Fe	2·8	2·0	1·6
Mn	0·1	—	0·1
Mg	4·0	2·3	1·7
Ca	3·7	2·8	3·1
Na	5·2	6·0	9·6
K	3·7	4·3	5·3
P	0·1	0·2	0·2
	100·0	100·0	100·0

Other Averages

	S. Norway Grand Total	Finland Sederholm 1925	Norw. Loams Goldschmidt 1933	Ign. Rocks Clark and Washington
Si	62·3	63·8	58·3	55·8
Ti	0·5	0·3	0·6	0·7
Al	16·6	16·8	18·4	17·0
Fe	1·5	0·9	2·5	2·2
Fe	2·6	2·3	3·0	3·0
Mn	0·1	0·1	0·1	0·1
Mg	3·4	2·4	4·9	4·9
Ca	3·4	3·5	3·2	5·2
Na	5·6	5·6	3·9	7·1
K	3·9	4·3	4·9	3·8
P	0·1	0·1	0·2	0·2
	100·0	100·0	100·0	100·0

compilation, country by country, of estimates of the relative areal extent of the various types of igneous rocks. Until this is done, estimates of abundance of elements must be of the nature of guesses".

Indeed, not only the igneous rocks, but also the areal extent of the various types of the sedimentary and metamorphic rocks must be estimated. I hope soon to finish the work of such a survey of Southern Norway.

Ad II

The accumulation of sodium in the ocean would mean a one way traffic in geochemistry, or, rather worse: The ocean becomes a kind of digestive organ of geochemistry: fed by rivers, wind and ice, it receives the weathered material, digesting certain elements for ever, whereas others are rejected and returned to the endless cycle of geochemistry.

This is not so! The ocean is just a channel through which the migrating elements are cycled. Some of the elements run fast through this channel, others are slow, and according to the speed the concentration will vary. There is no one-way traffic, but a dynamic equilibrium between supply and removal. Consequently it becomes in principle impossible to determine the age of the sea from its salt content, and all previous quantitative computations of the total mass of sediments are erroneous.

I prefer to look at the problem in a different way: If we assume perfect balance between input and output, it is possible to calculate how long each element remains in the sea before it is removed.* The period of passage, τ_i may be defined as the average time expressed in years necessary for an element i to pass through the sea in the geochemical cycle. From our assumptions we derive

$$\tau_i = \frac{\text{Total amount of an element in the sea}}{\text{Amount supplied per year}} \qquad \text{(I)}$$

Thus we find that a sodium ion spends an average of 208 million years in the sea but potassium only 10 million years (see data in Table 3). The attainment of such balances must have taken some time. So the query is: Is the span from the earliest to modern time long enough? Computations show that for all practical purposes equilibrium for an element will be attained after three times the period of passage. Thus for sodium within about 600 million years, for potassium within only 30 million years.

Equation I gives a totally different meaning to the Goldschmidt equation here quoted as (1). Obviously Goldschmidt's second equation will also be influenced. To simplify the following calculations I shall in the first approximation, limit myself to the typical geosynclinal sediments, shales and schists.

The problem may be formulated as follows:

Let W be the total weight of weathered rock in unit time (mainly derived from

* Many questions could be asked as to the justification of this assumption. But time does not permit to discuss it fully here. The main question is, perhaps, how sodium, which is conspicuously low in the sediments, can find its way from the sea and back into continental rocks. My answer to this is: By formation of evaporites, and by occlusion in the pore spaces of practically all sedimentary rocks (the efficiency of both processes will be proportional to the concentration in the sea). Part of the occluded sea water is leached out of the sediments and sodium carried in solution back to the sea, part of it manifests in sodium-bearing minerals of the metamorphosed sediments.

Table 3. Data for calculation of the amount of weathered rocks

	Ign. Rocks	Canada	Finland	Norway	Caledonian	Shale × 0·85
Mg	2·09	1·07	1·02	1·45	1·70	1·19
Ca	3·63	2·91	2·42	2·41	2·60	0·34
Na	2·84	2·70	2.27	2·28	2·15	0·85
K	2·59	2·55	2·95	2·72	2·60	2·16
			$c_i - 0{\cdot}85 \cdot s_i$			D_i
Mg	0·90	—	—	0·26	0·51	0·016
Ca	3·29	2·57	2·08	2·07	2·26	0·108
Na	1·99	1·85	1·42	1·43	1·30	0·014
K	0·43	0·39	0·79	0·56	0·44	0·011
			$D_i/c_i - 0{\cdot}85 \cdot s_i$			Average
Mg	1·8	neg.	neg.	6·2	3·1	—
Ca	3·3	4·2	5·2	5·2	4·8	*4·5*
Na	0·7	0·8	1·0	1·0	1·1	*0·9*
K	2·6	2·8	1·4	2·0	2·5	*2·3*
Average	2·1	—	—	3·6	2·9	2·7

The content of Mg, Ca, Na, and K expressed in weight per cent is given for Igneous rocks (CLARKE and WASHINGTON), Canadian Shield (GROUT, 1938), Findland (SEDERHOLM, 1925), Norway S of 65°N, and Caledonian rocks in Scandinavia S of 65°N. D_i is the amount delivered by rivers to the sea expressed as kg per cm² in a millon years, according to data by CONWAY (1942).

the continents). It will split into two parts: $W = \Sigma D_i + S$. ΣD_i is the sum of all dissolved ions that are carried into the sea, S is mainly the hydrolyzates that form the shales and schists. Let c_i and s_i be the average weight percentages of an element, i, in the continents and in the shales respectively. The following equation will be satisfied for each element.*

$$c_i W = D_i + s_i S$$

By making certain assumptions WICKMAN (1954) has found that $S = 0{\cdot}845\text{W}$, this factor does not affect the principles of the calculations, for convenience we shall use 0·85, and we obtain:

$$W = \frac{D_i}{c_i - 0{\cdot}85 s_i} \qquad \text{(II)}$$

If the total amount of an element in the sea is designated by M_i, and we use the other symbols as introduced above, we obtain in principle two sets of equations of similar form but of different meaning.

Goldschmidt: Age of the Sea $= \dfrac{M_{\text{Na}}}{D_{\text{Na}}}$ (1) $\qquad W_{\text{Total}} = \dfrac{M_{\text{Na}}}{c_{\text{Na}} - s_{\text{Na}}}$ (2)

Barth: Period of passage, $\tau_i = \dfrac{M_i}{D_i}$ (I) $\qquad W_{\text{Year}} = \dfrac{D_i}{c_i - s_i}$ (II)

* Provided there are no gains or losses in the geochemical cycle.

Combining (I) and (II) shows that $\tau_i W_{\text{Year}} = \frac{M_i}{c_i - s_i}$, or that GOLDSCHMIDT'S equation (2) does not give the total amount of weathered rock but, for each element, gives the amount that weathered during the "period of passage" of that particular element. Thus Goldschmidt's result, computed from the sodium balance, in the amount of 160 kg "total" weathered rock per cm^2 of the earth (and extensively quoted in the geochemical literature) actually applied to the amount of weathered rock during 208 million years (because $\tau_{Na} = 208$ million years is the period of passage of sodium through the sea).

My equations as distinct from those of Goldschmidt's apply in principle to all elements. But using shales (and schists) as the standard sediment they are, as previously explained, limited to the elements that go into ionic solutions virtually: magnesium, calcium, sodium, and potassium. Any of these elements used in equation II should give the same figure for W.

The amounts of these elements delivered by the rivers of the world into the sea were first estimated by Clarke. The latest and most accurate estimates are those of CONWAY (1943), they are used here. The composition of the average shale is taken from WICKMAN (1954). Based on these figures one may calculate from equation II the weight of weathered rocks per unit time, for example per a million years (see table 3). The figures refer to kg per cm^2 of the surface of the earth. The average comes out as 2·7 kg/cm^2 corresponding to an average erosion of 10 meters per million years. Putting the geological age of the earth at $3 \cdot 10^9$ years, the "total" erosion becomes 30 kilometers. This is a large figure, but it harmonizes quite well with other estimates of the total erosion based on geological evidence.

However, this figure is obviously inaccurate. It will have to be adjusted as more knowledge becomes available. But the principles involved in the present calculations come closer to the true conditions than did those of GOLDSCHMIDT. They expose to us a vista of the possibilities of some day arriving at an entirely new petrology.

If we assume that weathering and sedimentation have been restricted to the continents and their shelves, while the ocean troughs were passive, it means that a total erosion corresponding to a depth of more than 60 km must have taken place in the continents. If the order of magnitude of this figure is correct, we have to conclude that practically all continental matter has been reworked, i.e., there is no "juvenile" matter in the continents; all rocks have been sediments but modified and changed by metamorphism, metasomatism, and remelting under plutonic conditions, then again raised to the surface to become sediments. Said Hutton "In the economy of the world, I can find no traces of a beginning, no prospect of an end".

REFERENCES

CLARKE F. W. and WASHINGTON H. S. (1924) The composition of the Earth's crust. *U.S. Geol. Survey, Prof. Paper*, **127**.

CONWAY E. J. (1943) Mean geochemical data in relation to oceanic evolution. *Proc. Irish Royal Acad.* **48**, sect. B, No. 8.

FLEISCHER M. and CHAO E. C. T. (1960) Some problems in the estimation of the abundances of elements in the Earth's crust. XXI Int. Geol. Congress, Pt. 1, p. 141. (Copenhagen 1960).

Goldschmidt V. M. (1933) Grundlagen der quantitativen Geochemie. *Fortschr. der Mineral. Krist. und Petr.* **17**, p. 112.

Goldschmidt V. M. (1937) Principles of distribution of chemical elements in minerals and rocks. *Jour. Chem. Soc. London*, April, 1937, p. 655.

Goldschmidt V. M. (1954) *Geochemistry*. Clarendon Press, Oxford.

Grout F. F. (1938) Petrographic and Chemical data on the Canadian Shield. *J. Geol.* **46**, p. 486.

Sederholm J. J. (1925) The average composition of the Earth's crust in Finland. *Bull. comm. geol.* Finlande No. **70**.

Washington H. S. (1917) Chemical analyses of igneous rocks. *U.S. Geol. Survey, Prof. Paper* **99**.

Wickman F. E. (1954) The total amount of sediments and the composition of the average igneous rock. *Geochim. et Cosmochim. Acta* **5**, p. 97.

Geochimica et Cosmochimica Acta, 1961, Vol. 23, pp. 9 to 60. Pergamon Press Ltd. Printed in Northern Ireland

The geochemistry of cobalt

M. H. Carr* and K. K. Turekian
Department of Geology, Yale University, New Haven, Conn.

(*Received* 5 *October* 1960)

Abstract—Cobalt has been determined in a wide variety of geologically interesting materials using the combined techniques of emission spectrography and neutron activation analysis. Neutron activation was used to analyse standards for the emission spectrograph and materials low in cobalt. The following table is a summary of the results obtained with these methods.

	Co (p.p.m.)	Co/Fe ($\times 10^4$)	Co/Mg ($\times 10^4$)
Basaltic rocks	48	6·0	12
Granodiorites	7	2·5	7·0
Granites	1	0·6	6·4
Schists	40	5·3	9·3
Shales	19	4·9	14
"Pure" limestone	0·1	—	—
Quartzite	0·3	—	—

During differentiation of a basaltic magma (as in the case of the Stillwater complex) most of the cobalt enters the ferromagnesian minerals. The cobalt content of these minerals depends on the total number of Fe–Mg lattice sites and is independent of the Fe/Mg ratio. This relationship appears to hold for basaltic rocks in general. Cobalt is strongly coherent with magnesium in granitic rocks and behaves like magnesium in its partition relations between metamorphic minerals. The acceptance of both cobalt and magnesium is more selective at lower grades of metamorphism. These observed coherence relations require a re-evaluation of the geochemical laws governing the distribution of trace elements in the petrogenesis of igneous and metamorphic rocks and the partition of trace elements between co-existing minerals.

In sediments most of the cobalt is in the argillaceous fraction and seems to follow iron and magnanese. The cobalt economy in the deep sea is discussed and we conclude that with present knowledge, the cobalt accumulations in deep-sea sediments may be explained as the result of supply of detritally associated cobalt and dissolved cobalt from surface runoff rather than volcanic exhalations.

The crustal abundance of cobalt is calculated as 27 p.p.m. on the model of a crust of basalt and granodiorite in equal proportions.

Introduction

Before any accurate assessment of the processes causing dispersion and concentration of an element in the earth's crust can be made, accurate knowledge of the abundance of the element in various geologic materials is required. Adequate knowledge of the abundance of cobalt in many geologic materials has been previously lacking, particularly in the case of granites and non-pelitic sediments which normally have low cobalt concentrations and present analytical problems. By the use of the combined techniques of neutron activation and emission spectrography a large enough range of geologically interesting materials can be analysed to enable an evaluation of the behaviour of cobalt in the earth's crust to be made. Comparison of the behaviour of a trace element with that of some major elements, as well as consideration of absolute abundances may throw new light on laws governing the distribution of trace elements in geologic systems and such comparisons will be made for cobalt.

* Present address: Dept. of Geophysics, Univ. of Western Ontario, London, Ontario.

The type of broad study endeavoured here has assisted in the resolution of some petrogenetic and geochemical problems but naturally has uncovered a host of new ones which compel more extensive work for their elucidation.

Analytical Techniques

Previous work

The most commonly used analytical method for the determination of cobalt in geologically interesting materials has been d.c. arc emission spectroscopy. This technique is generally restricted to materials containing more than 5 p.p.m. cobalt if no procedure for concentrating the cobalt is used. Most basic and ultrabasic rocks and mafic minerals are high in cobalt hence this method is particularly useful for such materials (Faust *et al.*, 1956; Lundergardh, 1945, 1949, 1956, 1957; Nockolds and Allen, 1953, 1954, 1956; Nockolds and Mitchell, 1948; Wager and Mitchell, 1943, 1945, 1951, 1953). The cobalt content of common sulphides is also often high enough for spectrographic determination (Auger, 1941; Bjorlykke and Jarp, 1950; Fryklund and Harner, 1955; Hawley, 1952). Geologic materials containing less than 5 p.p.m. can be analysed spectrographically if the cobalt is concentrated before arcing. Scott and Mitchell (1943) at first used 8-hydroxyquinoline as an agent for extracting the cobalt, later modifying their procedure by using a mixture of 8-hydroxyquinoline, tannin and thionalide (Mitchell and Scott, 1947). Hirst and Nicholls (1958) used such a technique to determine cobalt in the acid-soluble fractions of limestone.

The chemical non-spectrographic techniques commonly involve the extraction of cobalt by an organic precipitant with subsequent determination gravimetrically colorimetrically, or polarographically. If the cobalt is present in small quantities, a carrier is commonly added to obtain a sufficiently bulky precipitate. Using dithizone as a precipitant, the cobalt contents of some granitic rocks have been determined colorimetrically by Sandell and Perlich (1939) and Sandell and Goldich (1943) and of some soils by Johnson and Graham (1952). Malyuga (1946) and Smythe and Gatehouse (1955) have determined cobalt in geologic materials using 1-nitroso-2-naphthol. Other workers, Clark (1958) and Warren and Delavault (1957) have preferred to use the more selective though less efficient isomer of this complex, 2-nitroso-1-naphthol. Stanton (1944) determined cobalt in a number of limestones using the nitroso-R-salt and the cobalt in spring waters has been determined using *o*-nitrosoresorcinol (Torii, 1955). Many of the above techniques have been outlined by Young (1948).

Smales *et al.* (1957) determined cobalt in a wide variety of materials by neutron activation.

Techniques Employed in Present Study

A. *Neutron activation*

The general principles of neutron activation analysis have been described by several authors (e.g. Meinke, 1955; Reed, 1959). The application of this technique to the determination of cobalt involves measuring the radioactivity of Co^{60} formed by an (n, γ) reaction with Co^{59}. The detailed procedure we have used is published elsewhere (Turekian and Carr, 1961).

Determinations down to 0·02 p.p.m. cobalt have been made using this technique and the precision at various concentrations is given in Table 1. To what degree inhomogeneities in the samples contribute to the loss of precision is not known, but it certainly may be an important factor, especially in coarse-grained rocks low in cobalt.

Table 1. Reproducibility of neutron activation analyses for cobalt

Material	No. of observations	p.p.m. Co	Coeff. var. (%)	Std. error (duplicate analyses) (%)
Diabase W–1	11	52	5·0	3·5
Granite G–1	12	2·4	10·4	7·4
Quartz	3	0·06	32	23

B. *Contamination during sample preparation*

Cobalt contamination may occur previous to analysis during the preparation of the sample powders by crushing and grinding. To estimate the extent of this contamination, two groups of three samples from the same piece of quartz were analysed for cobalt. The first group of samples was prepared by the routine method of crushing in a metal mortar and then grinding to a fine powder in an agate mortar. The second group was crushed and ground using only an agate mortar. The cobalt contents of these samples determined by neutron activation are given below:

	Agate mortar (p.p.m.)	Metal crusher (p.p.m.)
	0·088	0·08
	0·038	0·29
	0·066	0·17
Average	0·064	0·18

The difference between the mean cobalt contents of the two groups of samples is thought to represent the maximum contamination during sample preparation. A single piece of quartz was used for the experiment and this required more extensive crushing in the metal mortar than the less homogeneous rock samples. That this is the maximum extent of contamination is confirmed by duplicate analyses, in close agreement, on three granites which gave cobalt concentrations less than 0·12 p.p.m., the difference between the mean cobalt concentrations of the two groups of quartz samples above. Further, the cobalt contents of these granites fall on a Co–Mg curve for granites (Fig. 12), to be discussed later. The smallest concentration of cobalt measured in crystalline rocks was 0·06 p.p.m. for a graphic granite, and this latter figure may be a more real measure of the maximum contamination in sample preparation than the figure of 0·12 given above. Although the extent of contamination determined here is considerably less than that found by Myers and Barnett (1953), it is similar to that found by Sandell (1947).

C. *Spectrographic analysis*

Co, Fe and Mg have been determined spectrographically. Co is determined using Fe as a variable internal standard, hence determination of Fe was necessary for Co determination in those cases where Fe analyses were not available from other sources. Mg determinations were made for the purpose of geochemical arguments.

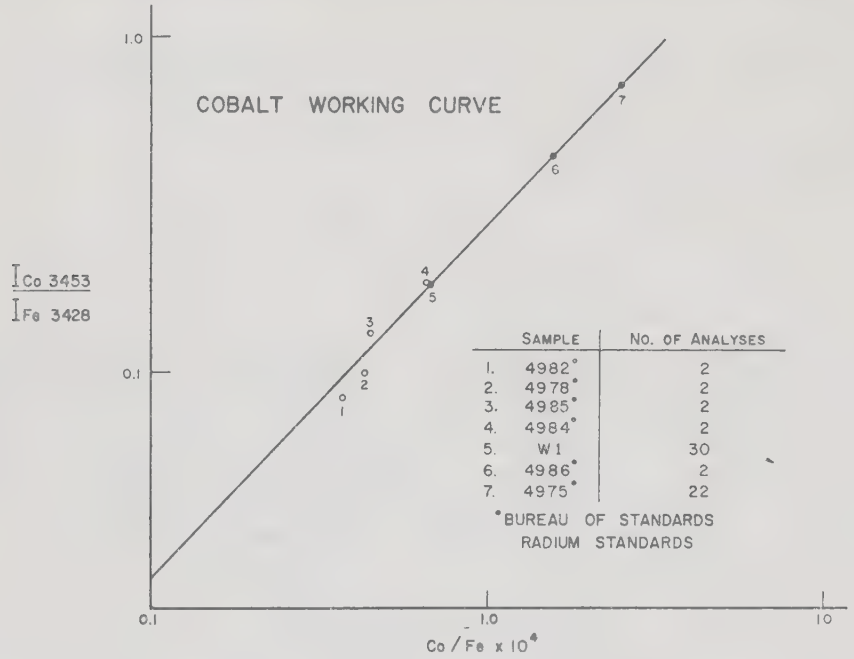

Fig. 1. Working curve for cobalt in silicates.

1. *Cobalt; Method of analysis*

(a) *Silicates.*

The technique used here is modified after Turekian (1957). Each powdered sample was mixed with analytical grade calcium carbonate in equal weight proportions. Five-milligram samples of this mixture were then weighed into $\frac{1}{8}$-in. deep, necked carbon electrodes, $\frac{1}{8}$-in. internal diameter, $\frac{3}{16}$-in. outside diameter (National Carbon Company L-4006). After preliminary burning for approximately 5 sec at 7·5 A (d.c. arc anode excitation) to prevent popping, the samples were arced to completion at 16·5 A with a 10μ slit and 100 per cent light transmission, using a Jarrel-Ash Ebert, 3·4 m, plane grating spectrograph. The spectra were recorded in the second order on Eastman Kodak Spectrum Analysis no. 2 plates which were processed in Kodak D-19 developer for 3 min at 20°C. The calcium carbonate provided a homogeneous base for a variety of rock types. A Jarrel–Ash console microphotometer was used for interpretation of the plates. The cobalt 3453 line was used as the analysis line and the Fe 3428 generally for the comparison line. The working curve shown in Fig. 1 was constructed using a series of rocks all

analysed for cobalt by neutron activation. Although use of internal standards alleviates the necessity of running standards on every plate, it has proven valuable to run two standards on each plate to detect any variation in procedure. These were the standard diabase W–1 and a dunite (Bureau of Standards, radium standard SS 4975).

(b) *Carbonates and deep sea sediments*

Carbonate sediments normally contain insufficient cobalt to be determined accurately spectrographically. However, deep-sea sediments were analysed by comparing intensities of the Co 3453 line for samples with those for standards which were prepared by mixing analytical grade calcium carbonate with pure cobaltic oxide. The samples were arced and the plates processed as for silicates. Kodak SA–1 high-contrast plates were used to obtain better results on the low cobalt values encountered. A typical working curve for these materials is given in Fig. 2.

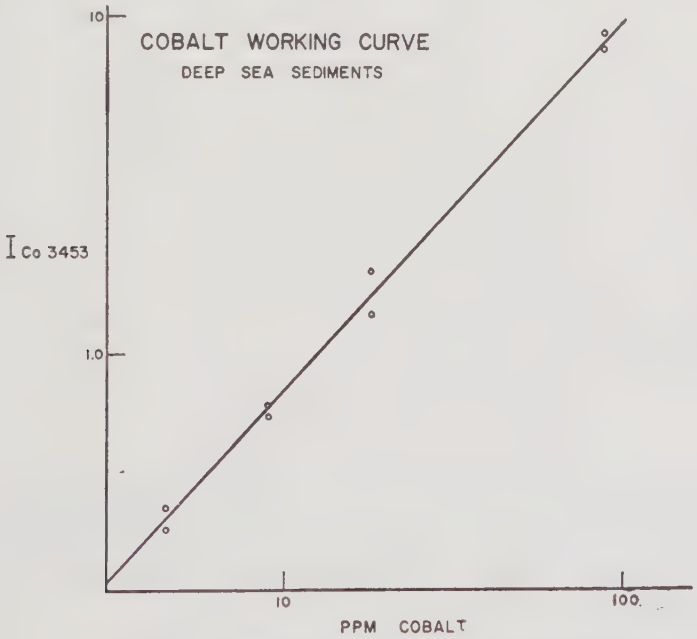

Fig. 2. Working curve for cobalt in deep-sea sediments.

(c) *Sulphides*

The sulphide samples were crushed and ground to a fine powder and mixed with graphite (National Carbon Co., SP–2 grade). Five-milligram samples of this mixture were arced to completion at 10 A.d.c. arc anode excitation in carbon electrodes (National Carbon Co. L-4006) with a 10μ slit and 100 per cent light transmission. The spectra were recorded, the plates processed and the line intensities measured as with the silicates.

Standards used to construct the working curve (Fig. 3) were prepared by mixing

pure Co_2O_3 in various proportions with a pyrite containing 9 p.p.m. cobalt (determined by neutron activation) and the cobalt in the samples determined using iron as an internal standard, the line Fe 3432 being most commonly used.

(d) *Iron and manganese ores*

The iron and manganese ores were mixed with graphite in proportions 1:2 by weight and arced under the same conditions as for sulphides. Also the plates were

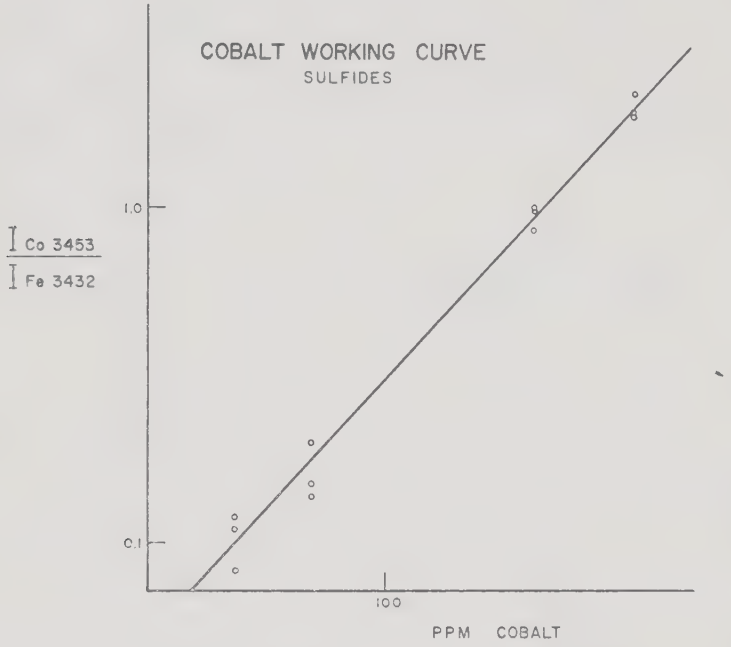

Fig. 3. Working curve for cobalt in sulphides.

processed and the lines interpreted using iron as an internal standard as for the sulphides. The working curve (Fig. 4) was constructed from standards prepared by mixing Co_2O_3 in various proportions with analytical grade Fe_2O_3 which was shown spectrographically to contain less than 4 p.p.m. cobalt.

Sources of error

Two possible sources of systematic error in the determination of the concentrations of an element using the emission spectrograph are lack of accurately known standards and matrix effects. The standards used for silicates were all analysed by neutron activation and the confidence limits for these standards are given in the section on neutron activation.

The accuracy of the sulphide standards was checked by comparing emission spectrographic and neutron activation values for cobalt on two pyrites. Assuming the neutron activation values to be the true values, the *t*-test can be applied to determine the significance of the differences between the cobalt determinations

using the two methods of analysis. Using the notation in Table 2, the t-statistic is calculated as

$$t = \frac{\bar{x} - \phi}{s/\sqrt{n}}$$

According to the usual statistical practice, the values for P in Table 2 indicate that the differences between the neutron activation and emission spectrographic results are not significant.

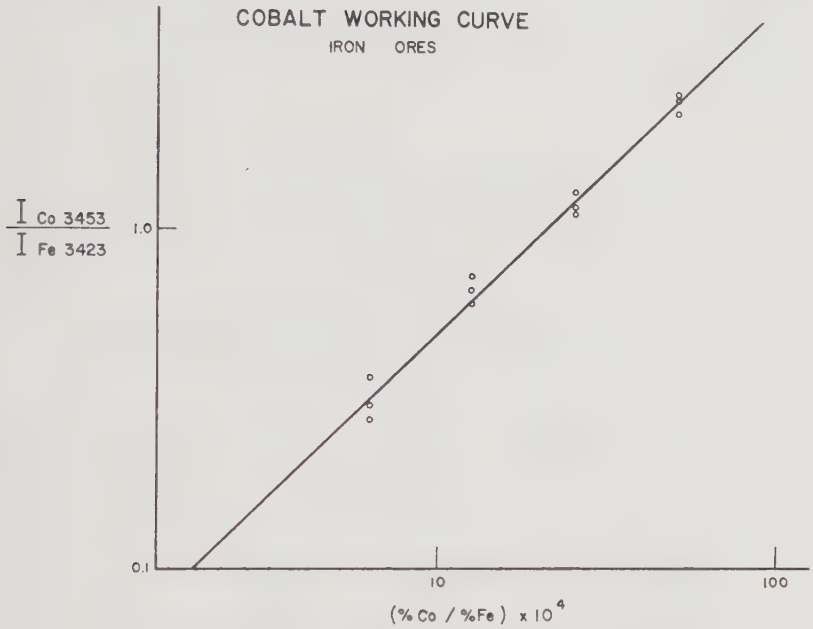

Fig. 4. Working curve for cobalt in iron ores.

The working curve for cobalt in silicates (Fig. 1) was constructed from rocks of different chemical composition and yet all of the deviations from the curve are within the experimental error. Thus the effect of mixing the samples with calcium carbonate is such as to render matrix effects negligible and to obviate the need to

Table 2. Comparison of determinations of cobalt in sulphides by emission spectrographic and neutron activation analyses

Sample	E.S. $\bar{x}_1$ (p.p.m.)	N	N.A. $\bar{x}_2$ (p.p.m.)	$\Delta\bar{x}$ $\bar{x}_1 - \bar{x}_2$	S	t	ϕ	P (%)
YCM-9	38	2	36	2	5·9	0·240	1	80–90
YCM-6	165	2	137	28	26·4	1·45	1	20–30

x_1 = mean of emission spectrographic observations, N = number of observations, x_2 = value by neutron activation analysis, S = standard deviation, calculated from data in Table 3, t = t-statistic, ϕ = degrees of freedom ($N - 1$), P = probability that difference is by chance (generally a 5 per cent probability or less is required to reject the null hypothesis).

make corrections for variable rock matrices. The sample carbonate and sulphide systems are much less subject to matrix effects than silicates.

Another possible source of error for those materials high in cobalt is self-absorption of the cobalt line. This is not likely for this line up to concentrations of at least 750 p.p.m.

Sensitivity and precision

Table 4 shows the reproducilibity of I_{Co}/I_{Fe} ratios on a single plate for silicates with various cobalt concentrations. Table 3 gives the same data for sulphides. Table 5 gives the statistics on silicate determinations from several plates.

Using the techniques described above cobalt can be determined satisfactorily down to about 4 p.p.m.

Table 3. Reproducibility of cobalt values for pyrites based on five runs for each sample

p.p.m. Co	Mean I_{Co}/I_{Fe}	Coeff. var. (%)	Std. error duplicate analyses (%)
27	0·117	14·7	10·6
55	0·210	19·6	13·8
273	1·13	10·0	7·1
546	2·16	16·0	11·3

Table 4. Reproducibility of cobalt analyses of silicates based on seven runs for each sample on a single plate

Sample	p.p.m. Co	I_{Co}/I_{Fe}	Coeff. var. (%)	Std. error duplicate analyses (%)
AS 55	7	0·099	28	20
B. of S. 98	16	0·283	20	14
AD 52	30	0·103	14	10
W–1	52	0·175	14	10
SS 4975	145	0·732	7	5

Table 5. Reproducibility of cobalt analyses on silicates from several plates

Sample	W–1	SS 4975
No. of runs	30	22
No. of plates	11	11
Mean I_{Co}/I_{Fe} ratio	0·174	0·743
Coeff. var. (%)	8·7	7·8

2. *Iron and magnesium; Method of analysis*

The powdered rock and mineral samples were mixed with two parts by weight of graphite (National Carbon Co., SP–2 grade). Exactly 5 mg of this mixture was arced to completion at 10 A d.c. arc anode excitation and the second-order spectrum was most commonly recorded on Kodak Spectrum Analysis no. 2 plates and processed as before. Standard granite G–1 and standard diabase W–1 were used as standards and the concentrations of iron and magnesium calculated by comparison of the absolute intensities of the iron and magnesium lines of the standards and samples. The Fe 3011 line was used for iron determination, and the Mg 2783 for magnesium determination below 3 per cent Mg and the Mg 3329 line used for determination of greater than 3 per cent Mg.

Sources of error, accuracy and precision

Because iron and magnesium concentrations are calculated from absolute intensities and not intensity ratios, the principal source of error is differential burning. This will be non-systematic and accounted for by the precision data listed in Table 6.

Table 6. Reproducibility of iron and magnesium analyses based on seven runs for each sample on the same plate

Line	Sample	% element	Intensity line	Coeff. var. (%)	Std. error duplicate analyses (%)
Fe 3011	G–1	1·41	0·41	10·3	7·3
	AS 20	3·20	0·97	10·0	7·1
	W–1	7·75	2·58	9·4	6·6
	AD 77	11·5	3·78	10·5	7·4
Mg 3329	G–1	0·32	0·15	28	20
	AS 20	0·80	0·34	25	18
	W–1	3·98	1·21	12	8·9
	AD 77	5·0	1·56	15	11
Mg 2783	G–1	0·23	2·04	22	16
	AS 20	0·80	12·6	7·0	5·0
	W–1	3·98	36	10	7·1

To test the accuracy of the method, a large number of wet-chemically analysed rocks (supplied by W. B. Hamilton, U. S. G. S., Denver) of a wide variety of types were analysed for iron and magnesium using the technique described above. Plots of log per cent Fe against log intensity of Fe 3100 and log per cent Mg against log intensity of Mg 3329 are given in Figs. 5 and 6, respectively. In the case of Fe, all points lie close to the 45° line, indicating that large systematic errors are not encountered with this analytical method. Two samples lie well off the 45° line on the magnesium plot. As the rest of the samples fall close to the 45° line, it is considered probable that deviation from the line for these two samples results from faulty

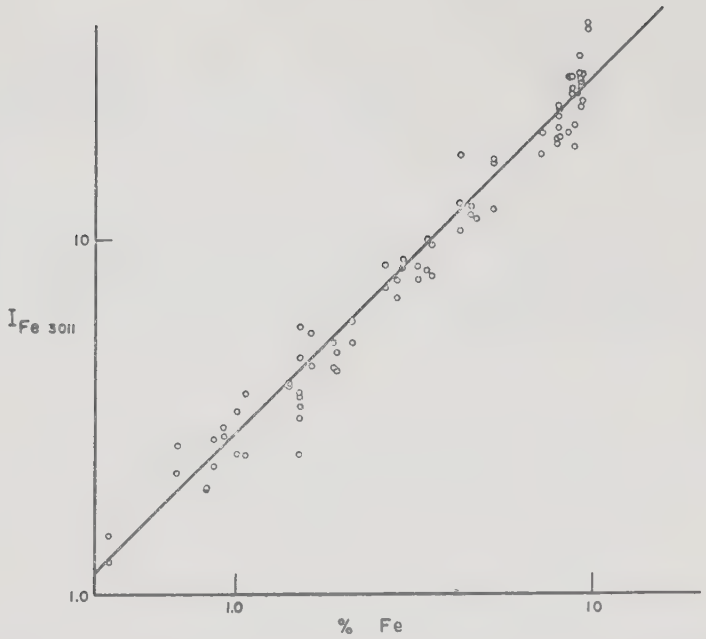

Fig. 5. Plot of $I_{Fe\ 3011}$ against percentage Fe for wet chemically analysed rocks.

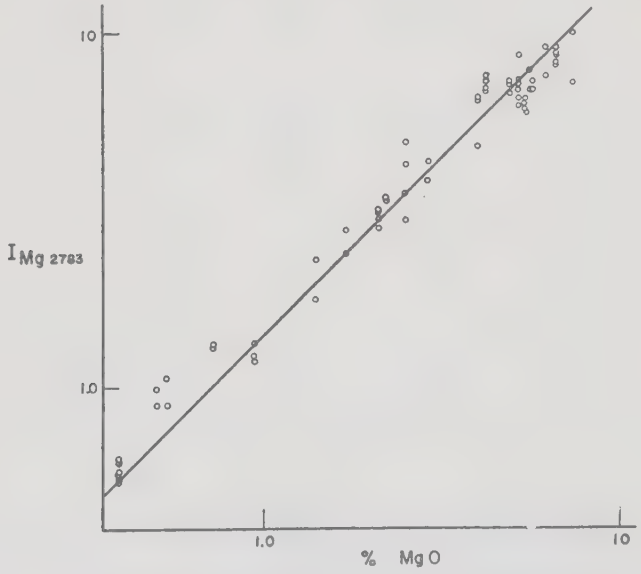

Fig. 6. Plot of $I_{Mg\ 2783}$ against percentage MgO for wet chemically analysed rocks.

wet-chemical determination of Mg, and large systematic errors are probably not involved in the emission spectrographic determinations.

Presentation of Results

Most of the analytical results are listed in Tables 7 to 16; however, several groups

Table 7. Neutron activation data on some standard rocks (from Turekian and Carr, 1961)

Number	Rock	Co (p.p.m.)	Avg. Co (p.p.m.)
G 1	granite	2·4, 2·6, 2·3, 1·9, 2·0, 2·8, 2·6, 2·5, 2·7, 2·5, 2·3, 2·0,	2·4
W 1	diabase	55, 56, 50, 55, 51, 54, 49, 52, 50, 49, 47.	52
Bureau of Standards: Radium Standards			
4975	dunite	154, 134	144
4976	limestone	0·61, 1·2	0·9
4977	sandstone	15*, 1·2	
4978	basalt	48	
4979	granite	0·85, 0·87, 0·93	0·88
4980	quartzite	0·22, 0·33, 0·25	0·27
4981	granite	0·32, 0·29	0·30
4982	gabbro–diorite	37, 40	38
4983	granite	0·44, 0·24	0·34
4984	diabase	47, 49	48
4985	basalt	49, 49	49
4986	kimberlite	64, 78	71
Bureau of Standards: Other Standards			
1a	argillaceous limestone	4·8, 4·5, 2·3	3·9
88	dolomite	0·37, 0·35, 0·14	0·29
97	flint clay	4·7, 4·1	4·4
98	plastic clay	17, 16	16·5
99	soda feldspar	0·69, 0·92, 0·73	0·78

* Possibly contaminated.

of analyses have been incorporated into the text where appropriate. Samples analysed by neutron activation have been listed separately from those analysed by emission spectrography. Otherwise, except for the readily available Bureau of Standards standard rocks, the samples are grouped according to the type of material analysed.

As iron was used as an internal standard in the spectrographic determination of cobalt, and as comparison of the distribution of iron and magnesium with that of cobalt has proven valuable in interpreting the data on silicates, iron and magnesium are given with all the silicate analyses. Also calcium contents are important in evaluating the data on granites and shales and the values listed here for these two rock types are taken from Turekian and Kulp (1956), who analysed for calcium and strontium most of the samples presented here.

Table 8. Neutron activation data on cobalt in granitic rocks

Number	Description	Ca (%)	Fe (%)	Mg (%)	Co (p.p.m.)	Avg. Co (p.p.m.)
AG 4	Granite, Loch Etive, Argyllshire, Scotland	1·8	2·2	1·2	6·7 6·6	6·6
AG 6	Shap granite, Westmorland, England	1·3	1·6	0·84	3·0 3·0	3·0
AG 11	Granodiorite, Slieve Garron, Newry, Northern Ireland	3·2	3·7	3·1	13·2 14·0	13·6
AG 13	Biotite-hornblende granite, Sherman granite, Laramie Range, Wy.	1·6	2·4	0·35	3·5 3·7	3·6
AG 17	Graphic granite, Whalen Canyon, Laramie Co., Wy.	0·22	0·04	0·01	0·047 0·083	0·055
AG 22	Granite, Mojave Mts., Colorado R., Ariz.	0·68	0·54	0·09	0·42 0·47	0·44
AG 27	Bushveld granite, S. Africa	0·41	1·0	0·02	0·11 0·09	0·10
AG 28	Vredeforte granite, S. Africa	1·11	0·68	0·17	1·00 0·97	0·98
AG 30	White granite, Little Cottonwood, Utah	0·72	1·5	0·22	1·86 1·87	1·86
AG 31	Granite, Independence Rock, Utah	1·1	2·3	0·52	1·31 1·38	1·34
AG 42	Granite, summit of Pikes Peak, Colorado	0·84	1·9	0·13	0·98 1·15	1·01
AG 48	Granite, Santa Fe, New Mexico	0·82	1·8	0·31	2·73 2·70	2·71
AG 59	Granite, Glamorgan batholith, Haliburton, Ont.	0·69	1·7	0·21	1·63 1·80	1·71
AG 69	Saganaga granite, N of Gunflint, Lake, Minn.	1·0	1·3	0·78	4·4 4·5	4·4
AG 85	Granite, Woodstock, Md.	1·1	1·5	0·43	3·6 3·6	3·6
AG 86	Granite, Mt. Airy, N.C.	1·4	0·78	0·18	1·5	1·5
AG 104	Braintree granite, Pine Hill, Quarry, Braintree, Mass.	0·11	2·8	0·078	0·14 0·19	0·16
AG 106	Granite, Weymouth, Mass.	0·67	1·5	0·098	1·7 1·3	1·5
AG 125	Biotite granite, Conway, New Hampshire	0·89	1·3	0·062	0·23 0·43	0·33
AG 127	Granitic gneiss "Bethlehem granodiorite", Bethlehem, N.H.	1·2	2·9	0·63	6·4 5·5	5·9
AG 129	Granite (peralkaline), Peabody Stock, Essex Co., Mass.	0·79	2·2	0·099	0·77 0·75	0·76
AG 132	Granite, Stony Creek, Conn.	0·96	2·6	0·50	3·0 3·3	3·1
AG 133	Killingworth granite, near Killingworth, Conn.	2·4	2·3	0·72	4·9 4·6	4·7
G 1*	Granite, Smith Granite Co., Westerly, R.I.	1·0	1·4	0·23	2·4	2·4
4979*	Granite, Chelmsford, Mass.	0·54	0·8	0·14	0·90	0·90

* Standard Rocks, see Table 10.

Table 8—(*contd.*)

Number	Description	Ca (%)	Fe (%)	Mg (%)	Co (p.p.m.)	Avg. Co (p.p.m.)
4981*	Granite, Sheanan Quarry, Graniteville, Mo.	0·46	1·2	0·048	0·30	0·30
4983*	Granite, Milford, N.H.	0·56	1·2	0·072	0·34	0·34
YCR 5	Composite of western North American granites	1·66	2·8	0·67	7·3 8·4	7·8
Rhyolites						
AG 44	Rhyolite, San Juan Mts., Ouray Co., Colorado	0·19	6·6	1·2	16·9 17·0	16·9
AG 64	S.E. Terrys Peak, Black Hills, S.D.	0·086	1·4	0·078	0·43 0·46	0·44
AG 67	Baraboo Range, Lower Narrows, Baraboo R., Wis.	0·045	2·1	0·073	0·60 0·95	0·77
AG 49	S side of Carson City, Nev.	0·58	0·53	0·13	0·53 0·50	0·51
AG 78	Little Belt Mts., Mont.	1·0	0·76	0·20	0·66 0·70	0·68

Table 9. Cobalt in recent shells by neutron activation

Sample	Description	Co (p.p.m.)	Avg. Co (p.p.m.)	$CaCo_3$* polymorph
YBF 1	Coral, *Oculina diffusa*, Bahamas	0·069 0·067	0·068	A
YBF 6	Coral, *Siderastrea radians* (Pallas), Bahamas	0·013	0·019	A
YAF 34	Pelecypod, *Macoma balthica*, L.I. Sound	0·17 0·32	0·24	A
YAF 62	Pelecypod, *Tellina modesta*, California	0·050 0·068	0·059	A
YAF 80	Pelecypod, *Pecten ventricosa*, Guaymas, Gulf of Calif.	0·073 0·055	0·064	C
YAF 85	Pelecypod, *Pecten pallium*,	0·11 0·12	0·11	C
YAF 95	Gastropod, *Conus papilionacens*, W. Africa	0·038	0·038	A
YAF 127	Gastropod, *Nerita fuviculatum*,	0·032 0·043	0·038	27% calcite

* A = 100% aragonite; C = mainly calcite.

Each neutron activation determination has been listed separately whereas the spectrographic data listed are means of two analyses. The analytical errors involved in the various determinations are discussed above.

Discussion of Results

The distribution of cobalt in various geologic systems may be discussed in two ways. First, its distribution in these systems may be evaluated without reference to specific major elements. Then, an attempt may be made to relate the distribution

Table 10. Miscellaneous neutron activation data

Sample	Description	Co (p.p.m.)	Avg. Co (p.p.m.)
YCR 3	Composite basalt	42 42	42
YCR 6	Mid-Atlantic Ridge basalt	48 50	49
YCR 7	Olivine basalt, Hawaii	53 50	52
YBS 2	Pierre shale, U.S.G.S. Lab, No. 259557	10·4	10·4
YAM 2	Gypsum, Eureka, Nevada	0·060 0·062	0·061
YAM 11	Anhydrite, Leopoldshall, Saxony	0·02 0·02	0·02
A 180–74*	Equatorial mid-Atlantic core, depth 16 cm	7·9	7·9
A 180–74*	As above, depth 106 cm	4·2 4·2	4·3
A 167–21	Deep sea carbonate ooze, 29°49′N, 76°35′W, depth 200 cm	2·4 2·4	2·4
A 167–29	Deep sea carbonate ooze, 28°26′N, 76°40′W, depth 400 cm	19 20	20
YBM 3*	Pyrite, French Creek, Pa.	8·9 9·0	9·0
YCM 6*	Pyrite, Carrol Mine, Central City District, Colo.	142 133	137
YCM 9*	Pyrite, as for YCM 6	35 37	36

* Used to monitor emission spectrographic results.

pattern of cobalt to that of some major elements. Since cobalt does not form any common silicate minerals, its distribution and concentration in the major rock units must be related to original concentrations in the source and the nature of the possible host lattices. Goldschmidt (1954) has suggested, on the basis of ionic radii, that the most likely sites in rock-forming minerals for the incorporation of cobalt are those occupied by iron and magnesium. The degree of coherence of cobalt with these two elements therefore receives special attention below.

Two works containing a compilation of some data on the geochemistry and biogeochemistry of cobalt are Benoit (1956) and Young (1957).

Previous Work

1. *Crystalline rocks*

The available analyses on crystalline rocks indicate that there is a relationship between cobalt concentration and dark mineral content, as would be expected from the above discussion. Ultrabasic rocks as a group have the highest concentrations of cobalt. Du Rietz (1955) and Lundegardh (1945) gave values of from 50 to 200 p.p.m. cobalt for some ultrabasic rocks of Sweden. Wager and Mitchell (1951) noted values of from 70 to 100 p.p.m. for picrites from Hawaii and Skaergaard, and similar values for picrites were given by Nockolds and Allen (1954, 1956) and

Table 11. Basaltic rocks analyzed spectrographically

Number	Description	Fe (%)	Mg (%)	Co (p.p.m.)
	I. *Oceanic Islands*			
	(A) Pacific			
	(i) Hawaii			
AD 22	Basalt, top of Mauna Loa	8·7	0·34	43
AD 23	Olivine basalt, Mauna Loa	9·4	2·9	64
AD 24	Basalt, falls near Hilo	8·2	4·0	53
AD 25	Olivine-rich basalt, crater of Kilauea	9·8	3·1	76
AD 26	Basalt, near Lahaina, Maui	11·8	2·4	69
AD 27	Basalt, summit of Mt. Haleakala, Maui	8·8	1·3	19
AD 28	Basalt, olivine free (Koolau series) Kaukonahua Gulch, Oahu	7·2	2·4	45
AD 29	Olivine basalt, Kaena Pt., Oahu	10·8	2·1	40
AD 30	Olivine basalt, Kolua, Kauaii	8·9	12·0	87
SD 4	Melilite basalt, with nepheline, Manuhonohono cave, Kauai	11·9	6·0	110
SD 5	Olivine basalt, prehistoric flow, from Mauna Loa	8·8	3·1	52
SD 6	Oligoclase andesite, Kohala Mt.	8·0	3·1	4
	(ii) Other intra-Pacific islands			
AD 31	Lava, Galapagos	9·2	3·1	57
AD 32	Scoria, Tahiti	8·2	6·2	49
AD 34	Ankaramite, Tahiti	8·2	7·4	61
AD 35	Basalt, NW side of Vita Levu, Fiji	7·4	2·5	46
RD 2	Basalt, labr. (β) Vanikoro	9·3	3·8	84
RD 3	Basalt, labr. (β), Ambryn eruption 1913	8·8	2·0	58
RD 4	Basalt, labr. (β), Mangareva	8·2	3·1	46
	(iii) Japan			
AD 1	Bronzite andesite, Noto Penin. Ishikawa	3·2	1·8	21
AD 2	Olivine basalt, Noto Penin. Ishikawa	7·3	3·8	34
AD 11	Non-porphyritic basalt, Shimotanna, Izu.	10·6	2·9	36
AD 12	Pigeonitic andesite, Hakone caldera, Shizuoka	9·6	3·9	38
KD 1	Olivine basalt, S of Saigo, Dogo, Oki Island	7·0	2·1	47
KD 3	Aphyric basalt, (Pliocene?), Okata Osima Island, Izu.	10·5	2·3	56
KD 4	Olivine trachybasalt (Pleistocene), Gembrudo, near Kyoto	6·8	2·6	35
KD 8	Olivine andesite (Miocene), N. of Kamitugu, Aita	6·5	1·9	27
KD 10	Dolerite (Miocene), near Semi, Yamagata	9·1	1·2	27
	(B) Atlantic and Indian Oceans			
AD 36	Olivine basalt, Jamestown, St. Helena	9·8	5·3	56
AD 37	Olivine basalt, Funchal, Madeira	9·7	9·4	72
AD 38	Olivine basalt, Ile de France, Mauritius	10·6	6·0	72
AD 39	Olivine basalt, Horta, Fayal, Azores	8·9	4·9	46
AD 40	Olivine basalt, San Cristobal, Santo Domingo, Haiti	6·2	3·8	33
	II. *Europe*			
AD 16	Dolerite (Tertiary), Muchraw, Linlithgow, Scotland	12·4	3·8	31
AD 17	Olivine basalt, Mauchline, Ayrshire, Scotland	10·2	3·6	36

Table 11—(*contd.*)

Number	Description	Fe (%)	Mg (%)	Co (p.p.m.)
AD 18	Gabbro, Carrock Fell, England	10·9	2·2	29
AD 19	Quartz dolerite, East Lothian, Scotland	9·6	2·9	37
AD 20	Olivine Basalt, Wannow, Bohemia	8·3	4·5	35
AD 43	Olivine dolerite, Scawt Hill, Antrim, Ireland	6·4	5·5	37
AD 44	Pyroxene rich dolerite, Scawt Hill, Antrim, Ireland	7·4	4·2	41
	III. *Africa*			
AD 14	Coarse-grained dolerite, Karroo	5·9	1·5	25
AD 15	Coarse-grained dolerite, Karroo	10·8	3·9	42
AD 45	Olivine basalt, Lake Kivu, Congo	8·1	2·6	44
AD 46	Olivine basalt, w. leucite, Lake Kivu	8·3	6·6	47
AD 47	Gabbro (norite), massif of Mt. Kakoulima, Guinea	5·4	8·4	65
FD 4	Basalt, Bulawayo dist., S. Rhodesia	9·9	2·0	37
FD 6	Basalt (lava no. 3), Wankie dist., S. Rhodesia	9·1	3·4	49
FD 7	Basalt (lava no. 5), Wankie dist.	9·7	1·8	53
FD 8	Basalt (lava no. 1), Wankie dist.	9·6	1·5	50
FD 9	Basalt (lava no. 2), Wankie dist.	9·3	2·0	53
FD 10	Basalt (lava no. 4), Wankie dist.	8·9	2·8	49
FD 21	Ol. basalt, borehole, S. Ndanga, S. Rhodesia	7·5	5·2	50
	IV. *S. America*			
AD 3	Diabase, Rio Caroni Heres, Bolivar Venezuela	9·0		53
AD 4	Gabbro, Guaharibos, Alto Orinoco, Terr. Amazonas, Venezuela	5·1	3·8	35
AD 5	Diabase, Uriman, Bolivar	9·6		57
AD 6	Diabase, Rio Tirika Heres, Bolivar	8·2		78
AD 7	Diabase, Quebrada, Virambaru Heres, Bolivar	6·7	4·9	34
AD 8	Basalt, Pico Maunoir, Alto Orinoco Terr. Amazonas, Venezuela	7·1	3·2	36
AD 9	Diabase, Uriman, Bolivar	8·0	2·9	49
AD 10	Diabase, Quebrada, Kuriaraparu, Bolivar, Venezuela	10·6	2·8	55
	V. *N. America*			
	(A) Eastern United States			
	(i) Triassic basaltic rocks			
AD 95	Diabase, Gulf Mills, Montgomery Co., Pa.	6·7	4·6	48
AD 97	Diabase, Radnor Twp., Pa.	9·7	4·1	84
AD 98	Diabase, Conshocken, Pa.	7·8	2·9	55
AD 99	Diabase, Frankford, Pa.	8·6	5·0	95
AD 100	Diabase, Big Hill, Cornwall, Pa.	7·6	2·9	53
AD 101	Granophyric diabase, Round Top, Gettysburg, Pa.	6·7	2·8	58
AD 102	Diabase, South Mtn., York Co., Pa.	8·0	2·6	58
AD 106	Diabase, Leesburg, Loudon Co., Va.	6·2	3·8	48
AD 107	Ol. Diabase, Charlotte, N. Carolina	8·2	7·7	74
AD 108	Diabase, First Watchung, Patterson, N.J.	6·9	4·1	47
AD 109	Basalt, Second Watchung, Haledon, N.J.	7·7	3·5	20
AD 119	Diabase, Hartford, Conn.	10·9	2·0	69

Table 11—(*contd.*)

Number	Description	Fe (%)	Mg (%)	Co (p.p.m.)
AD 110	Basalt, Snake Hill, N.J.	10·5	2·1	69
W 1	Diabase, near Centerville, Fairfax Co., Va.	7·7	4·0	52
	(ii) Pre-Triassic basaltic rocks			
AD 88	Gabbro (coronite), Peekshill, N.Y.	8·0	4·6	68
AD 90	Diabase, Trembleau Pt., Lake Champlain, N.Y.	10·8	6·3	67
AD 91	Diabase, Cascadeville, N.Y.	9·5	6·6	62
AD 93	Diabase, Thousand Islands, N.Y.	16·0	3·1	94
AD 94	Diorite, Harrison Diorite, Westchester Co., N.Y.	5·2	2·5	31
AD 96	Quartz diorite, Philadelphia, Pa.	7·9	4·6	37
AD 103	Dolerite, Iron Hill, S of Newark, Del.	2·9	4·6	31
AD 104	Gabbro diorite, Mt. Hope, Md.	6·9	2·8	41
AD 105	Gabbro, Ilchester, Md.	9·0	6·9	65
AD 121	Gabbro, Ascutney Notch, Vt.	6·1	0·97	18
	(iii) Adirondacks			
AD 86	Norite, Westport, N.Y.	7·2	0·98	30
AD 87	Anorthosite, Elizabethtown, N.Y.	0·32	0·26	4
AD 89	Anorthosite, Euba Mills, N.Y.	1·9	0·73	8
AD 92	Anorthosite, North Hudson, N.Y.	0·45	0·22	4
	(B) Midwestern and Canadian Pre-Cambrian			
	(i) Keweenawan rocks of Lake Superior Region			
AD 63	Ol. diabase, near S. Porcupine, Ontario, Canada	10·6	2·6	73
AD 64	Gabbro, Tatlock, Ontario	9·8	1·8	55
AD 65	Basalt, Isle Royal, Mich.	10·4	2·5	59
AD 66	Quartz diabase, Lighthouse Pt., Marquette, Mich.	12·6	2·5	73
AD 69	Gabbro, Beaver Bay, Minn.	9·8	1·7	55
AD 70	Ol. diabase, Beaver Bay, Minn.	6·5	2·2	51
AD 71	Ol. gabbro, Beaver Bay, Minn.	8·1	2·0	49
AD 72	Diabase, Beaver Bay, Minn.	10·1	1·8	48
AD 83	Anorthosite, Minn.	0·98	4·6	4
AD 84	Ol. diabase, Grand Portage, Minn.	15·4	2·9	55
	(ii) Duluth gabbro			
AD 74	Red rock, contaminated by early anorthosite	4·4	0·77	15
AD 75	Anorthosite, upper facies	4·3	0·94	16
AD 76	Aplitic red rock	7·7	1·1	21
AD 77	Main mass of banded gabbro	13·2	6·9	96
AD 78	Gabbro, above banded gabbro, below anorthosite	11·3	4·6	50
AD 79	Basal gabbro (?)	8·5	9·1	73
AD 80	Gabbro (at floor), contaminated by basalt hornfels	11·0	9·5	107
AD 81	Pegmatite mass at base of gabbro	12·4	14·0	92
AD 82	Average Ol. gabbro (near base)	7·0	5·5	58
	(C) Western United States			
	(i) Pacific Northwest: Columbia R. tholeiitic basalts (Miocene)			
QD 1	Waterville, Wash.	7·7	1·9	32
QD 2	Dike, Grande Ronde R., S. of Anatone, Wash.	9·9	1·9	27
QD 3	2nd flow from top near Trinidad, Wash.	8·6	3·4	44
QD 5	1st flow from top near Yakima, Wash.	7·6	4·0	45

Table 11—(*contd.*)

Number	Description	Fe (%)	Mg (%)	Co (p.p.m.)
QD 6	8th flow from top near Yakima, Wash.	10·5	2·7	48
QD 10	Snake R. Canyon, near Lewiston, Idaho	6·8	4·2	41
QD 13	Salmon R., near Cottonwood, Idaho	8·0	2·6	40
QD 16	Grande Ronde Canyon, near Anatone, Wash.	8·8	1·8	29
QD 23	Basal flow in Pine Creek section, NE Oregon	9·4	3·6	52
QD 24	La Fleur, Oregon	9·3	2·4	43
	(ii) Pacific Northwest: Ol. basalts (Pliocene–Recent)			
QD 26	Rimrock flow, W. of Prineville, Oregon	7·7	4·2	47
QD 27	Horse Ridge, SE of Bend, Oregon	7·2	6·2	44
QD 28	Diktitaxitic flow, W of Hood R., Oregon	11·7	2·9	77
QD 29	Simcoe Mt., W of Satus Pass, Wash.	12·2	6·0	72
QD 30	Satus Pass, Wash.	9·6	5·1	58
QD 31	Porpyritic flow, Abert Rim, Ore.	5·4	3·4	30
QD 32	Goldendale, Wash.	9·9	5·0	65
QD 33	Flow interstratified in the Dalles fm., near Mecca Oregon	6·9	3·1	43
QD 34	Recent Ol. basalt, Roberts, Oregon	7·3	9·1	55
QD 35	"The Big Lava Flow", near Willard, Wash.	7·0	4·6	53
	(ii) Other basaltic rocks			
AD 48	Basalt, American Ravine, Silver City, Nev.	7·5	6·6	45
AD 49	Diabase, Humboldt Range, Nev.	9·1	8·5	46
AD 50	Diorite, Mosquito Range, E of Leadville, Colo.	3·9	0·63	19
AD 51	Gabbro, Hermosa Park, Colo.	5·0	2·0	26
AD 52	Dolerite, N. Table Mts., Golden, Color.	7·0		27
AD 53	Gabbro, Spanish Peaks, Colo.	6·6	2·4	28
AD 54	Diorite, dike, W. of Spanish Peaks, Colo.	4·9	2·2	21
AD 55	Ol. gabbro, Cripple Creek, Colo.	13·6		92
AD 56	Quartz gabbro, Iron Hill, Colo.	9·1	3·5	56
AD 57	Basalt, Comstock, Nev.	9·6	6·9	49
AD 58	Diabase, Soap Hill, Nev.	4·3	1·5	19
AD 59	Quartz basalt, Lassen Peak, Calif.	3·6	3·2	33
AD 60	Ol. basalt, Truckee, Calif.	5·5	3·1	32
AD 61	Ol. basalt, Jamestown, Tuolumne Co., Calif.	5·6		26
AD 62	"Anorthite gabbro", near Nevada City, Calif.	3·8	4·5	58
AD 67	Diabase, Squaw Creek, Black Hills, S.D.	8·0	2·5	47
AD 68	Gabbro, Black Hills, S.D.	8·7		73
AD 85	Gabbro, Leesburg, Idaho	11·0	6·9	59

values of from 150 to 220 p.p.m. for oceanites. Faust *et al.* (1956) found that the cobalt content of serpentines derived from ultrabasic rocks ranged from 10 to 70 p.p.m.

The numerous analyses of basaltic rocks by Nockolds and Allen (1953, 1954, 1956), Wager and Mitchell (1943, 1951) and Nockolds and Mitchell (1948) show that most basalts have values for cobalt between 30 and 80 p.p.m. The same authors also show that intermediate rocks, such as andesites, have cobalt contents up to 35 p.p.m., whereas the values for trachytes, phonolites, rhyolites, granodiorites

Table 12. Shales analysed spectrographically

Number	Description	Ca (%)	Fe (%)	Mg (%)	Co (p.p.m.)
	(a) *Cambrian*				
AS 23	Shale W, w. Olenellus, L.E., Weymouth, Mass.	0·10	5·4	1·6	29
AS 24	Upper E., St. John, New Bruns.	0·079	7·8	1·4	31
AS 25	St. Albans shale, Albertan, Georgia Plains, Vt.	0·76	3·75	2·0	4
AS 26	Watauga shale, M.E., Roanoke Co., Va.	0·11	4·6	1·1	18
AS 27	Bonne Terre shale, Elvins, Mo.	16·1	1·6	0·59	8
	(b) *Ordovician*				
AS 1	Martinsburg shale, Chazyan, Westlawn, Pa.	0·17	6·4	2·5	26
AS 2	Athens shale, w. graptolites, Mormanskill, Roanoke, Va.	0·036	6·7	3·8	4
AS 3	Deer R. shale, Trenton-Collingwood or Gloucester, Copenhagen, N.Y.	1·3	5·4	1·5	37
AS 4	Thebes shale, Richmond Cape Girardeau, Mo.	1·1	5·1	0·81	12
AS 6	Utica shale, Utica, N.Y.	5·3	4·6	1·4	22
AS 5	Hudson R. Shale, Kingston, N.Y.	2·8	3·4	1·2	10
AS 7	Hudson R. shale, Lorraine, Martins Creek, Pa.	0·050	4·0	1·4	8
AS 8	Reedsville shale, L. Cincinnatian, Jonesville, Pa.	0·86	4·2	0·64	19
AS 9	Frankfort shale, Chavwick, near Utica, N.Y.	2·1	5·0	2·2	27
AS 10	Orchard Creek shale, Cape Girardeau, Mo.	1·6	0·69	0·52	4
AS 11	Shale w. Triarthrus, Frankfort, Washington Hills, N.Y.	2·4	5·1	1·4	19
AS 12	Maquoteta sh., Cincinnati-Richmond, Graf, Iowa	9·9	1·5	4·6	4
	(c) *Silurian*				
AS 13	Walcott sh., Niagara-Clinton, Rochester, N.Y.	7·5	4·7	1·4	16
AS 14	Sodus sh., Clinton, Rochester, N.Y.	0·41	4·0	1·7	25
AS 15	Williamson sh., U. Clinton, Rochester, N.Y.	6·4	4·7	2·2	15
AS 16	Rochester shale, Middleport, N.Y.	8·5	1·6	3·1	9
AS 17	Shale, phosphatic nodules and iron ore, Bennet Quarry, Clinton, N.Y.	2·1	13·0	1·9	19
AS 18	Waldron sh., Niagaran, Tennel Mill, Vernon, Ind.	13·2	5·4	3·9	17
AS 19	Medina sh., (basal Sil.-U. Ord.) Goes, Greene Co., O.	5·7	4·5	3·4	15
AS 20	Longwood sh. (green facies), Water Gap, Pa.	0·26	3·6	1·5	28
AS 22	Red sh., High Falls, Salinian High Falls, N.Y.	0·79	7·3	1·7	28
AS 21	Black sh., M. Shawangunk, Del. Water Gap, Pa.	0·037	3·5	1·5	10

Table 12—(*contd.*)

Number	Description	Ca (%)	Fe (%)	Mg (%)	Co (p.p.m.)
	(d) *Devonian*				
AS 30	Helderbergian, L. Mempremagog, Quebec	20·4	0·75	0·27	4
AS 31	Heragon sh., near Dougherty, Murray Ca., Okl.	19·6	0·36	0·98	4
AS 32	Frog Mt. sh., Oriskanian, Ragland, Ala.	5·6	2·6	2·1	4
AS 33	Esopus sh., Becraft Mt. N.Y.	0·15	3·9		16
AS 34	Marcellus sh., Catskills, N.Y.	17·2	1·9	0·55	7
AS 35	Marcellus sh., Hamilton Stroudsburg, Pa.	1·9	6·5	1·1	26
AJ 37	Mt. Marion sh., Erian-Hamilton Kingston, N.Y.	9·3	2·8	1·2	14
AS 38	Huron sh., Lewis Center Run, Ohio	2·9	4·9	1·5	40
AS 39	Snider Creek sh., Calloway Co., Mo.	20·0	0·28	1·6	4
AS 40	Genesee sh., Hamilton, 18 miles Creek, N.Y.	10·4	2·3	0·92	14
AS 41	Oneonta sh., U. Dev., Senecan-Portage, Ashokan Dam, N.Y.	3·9	4·8	0·98	17
AS 42	Cashaqua sh., Portage, Cashaqua Creek, Livingston Co., N.Y.	0·75	4·1	1·5	16
AS 43	Marcellus-Genesee sh., Roanoke Co., Va.	16·1	1·5	0·45	8
AS 44	Ohio (Huron) black sh., Portage, Huron Creek, N.Y.	0·51	2·5	1·0	14
AS 45	Conodont sh., uppermost Dev., Cayahoga Co., N.Y.	0·33	4·2	0·89	18
AS 46	Blue sh., Genesee, Mt. Morris, N.Y.	2·5	3·9	1·2	26
AS 47	Catskill shale, Pottsville, Pa.	0·14	2·9	0·80	25
AS 48	Brailler sh., Chautauquan, Roanoke Co., Va.	0·24	4·8	1·0	23
AS 49	Woodford sh., Woodford, Okl.	1·4	3·6	0·73	41
AS 53	Sulfur Springs sh., St. Genevieve, Co., Mo.	9·7	9·2	5·5	115
AS 51	Chattanooga sh., Horse Leg Mtns., Rome Ga.		2·8	1·0	10
AS 50	Chattanooga sh., Sale Creek, Tenn.	0·37	6·3	0·45	88
AS 52	Eureka sh., Chattanooga, Spavinaw, Okl.	0·21	2·6	1·2	32
	(e) *Mississippian*				
AS 55	Bluefield, Stony Ridge Gap, W. Va.	19·6	1·7	0·63	9
AS 56	Warsaw, Keokuk, Iowa	10·4	0·59	0·32	4
AS 57	Cayahoga, Vernon, Ohio	0·39	3·2	0·57	16
AS 58	Orangeville (Sunbury) sh., Cortland, Ohio	0·14	2·0	0·45	8
AS 59	Floyd sh., Meramecan, Bessemer, Ala.	0·11	4·2	1·2	11
AS 60	Gasper sh., Chesterian, Cherokee, Ala.	0·75	3·9	1·2	16
AS 61	Red. sh., Mauch Chunk, Hazelton Quad., Pa.	0·10	5·2	1·1	34
	(f) *Pennsylvanian*				
AS 62	Allegheny, Clearfield, Pa.	0·14	3·7	0·81	18
AS 63	Graphitic sh., Rhode Is. fm., Newport Neck, R.I.	0·11	5·4	1·1	22
AS 64	Red sh., Lower barren coal measure, Carrol Co., Ohio	0·11	2·1	0·38	13

Table 12—(*contd.*)

Number	Description	Ca (%)	Fe (%)	Mg (%)	Co (p.p.m.)
AS 65	Shale w. pelecypods, carbonic	5·0	1·5	0·71	10
AS 66	Warren group, Grand View Pike Spring City, Tenn.	0·08	1·8	0·81	6
AS 67	Varved metashale, Newport Neck, R.I.	0·92	4·4	1·5	25
AS 68	Lower Smithwick sh., Bend, San Saba Co., Tex.	20·4	0·86	0·63	4
	(g) *Triassic*				
AS 69	Newark sh., Granton, N.J.	2·4	6·7	4·3	45
	(h) *Cretaceous*				
AS 28	Mowry sh., Gulfian, Hutton Lake, Wyo.	0·50	1·3	0·31	4
AS 29	Fuson sh., Comanchean, Sheep Mt., Wyo.	13·9	1·9	0·4	5
AS 70	Eagle Ford sh., Austin, Tex.	15·8	1·1	0·32	8

and granites are generally below 15 p.p.m. Patterson and Swaine (1955), and Stonehouse (1954) give figures for basalts similar to those above. Young *et al.* (1954) found that cobalt in kimberlites ranged from 30 to 80 p.p.m.

The cobalt content of granites is commonly such that it is below the sensitivity limit for the emission spectrograph and few analyses are available. Sandell and Goldich (1943) have analysed some granites, mostly from Minnesota, and the

Table 13. Schists analysed spectrographically

Number	Description	Fe (%)	Mg (%)	Co (p.p.m.)
AP 1	Berkshire schist, Mt. Prospect, Salisbury, Conn.	7·6	1·3	32
AP 2	Kyanite mica schist, Hartford, Conn.	3·0	0·95	21
AP 3	Garnetiferous horn. schist, Orange, Conn.	9·5	3·4	56
AP 4	Mica schist, Watertown, Conn.	2·0	0·76	62
AP 5	Schist w. magnetite, Stockbridge, Vt.	8·2	2·4	25
AP 6	Actinolite–talc schist, Stockbridge, Vt.	2·6	19	8
AP 7	Staurolite–biot.–garnet schist, Jordan Falls, Nova Scotia	7·5	1·6	17
AP 8	Biotite schist, New Bedford, Mass.	14·9	7·0	100
AP 9	Phlogopite schist, Montville, N.Y.	6·2	12·6	4
AP 11	Talc schist w. magnetite, Marquette Co., Mich.	10·0	0·49	7
AP 10	Biotite schist, Moose Lake, Minn.	4·6	1·3	21
AP 12	Chlorite schist, Silver City, Nev.	5·8	5·6	16
AP 13	Glaucophane schist, Morgan Hill, Calif.	15·3	2·9	147
AP 14	Mica schist, Cripple Creek, Colo.	7·0	0·63	4
AP 15	Calcitic chlorite schist, Carlon Co., Wyo.	6·0	5·6	29
AP 16	Chlorite schist, Black Hills, S.D.	11·0	11·2	112
AP 19	Green schist, Yöjärvi, Finland	8·2	3·6	27
AP 21	Hornblende schist, New York, N.Y.	11·8	3·5	68
AP 20	Sericite schist, Salair, U.S.S.R.	1·2	0·56	8
AP 24	Garnet hornblende schist, Cap a l'Aigle, Quebec	5·5	0·87	8

Table 14. Silicate minerals analysed spectrographically

Number	Description	Fe (%)	Mg (%)	Co (p.p.m.)
YFM 1	Hornblende, gabbro, pyroxene hornfels facies, Adirondacks, N.Y.	6·9	9·8	72
YFM 2	Garnet coexisting with YFM 1	16	5·0	88
YFM 3	Muscovite, pegmatite, Branchville, Conn.	2·2	0·14	5
YFM 4	Muscovite, pegmatite, Buckfield, Maine	5·0	0·23	4
YFM 5	Biotite, pegmatite, Russel, Lawrence Co., N.Y.	8·0	17	16
YFM 6	Biotite, pegmatite, Holderness, New Hampshire	12	4·7	65
YFM 7	Biotite, 2-mica schist, sill.–ky. subfacies, Deep River, Conn.	13	2·8	65
YFM 8	Garnet, coexisting with YFM 7	19	1·4	23
YFM 9	Biotite, garnet 2-mica schist, sill.–ky. subfacies, Deep River, Conn.	15	3·4	83
YFM 10	Muscovite, coexisting with YFM 9	2·5	0·52	9
YFM 11	Garnet, coexisting with YFM 9	21	1·2	16
YFM 12	Biotite, garnet–biotite–quartz–plagioclase gneiss, Deep River, Conn.	10·7	4·8	45
YFM 13	Biotite, 2-mica schist, Hartland formation, ky.–musc.–quartz subfacies, Naugatuck, Conn.	16	3·9	58
YFM 14	Muscovite, coexisting with YFM 13	2·8	0·49	6
YFM 15	Garnet, coexisting with YFM 13	12	1·7	10
YFM 16	Biotite, 2-mica schist, Hartland formation, Naugatuck, Conn.	13	2·0	32
YFM 17	Muscovite, coexisting with YFM 16	2·8	0·46	4
YFM 18	Hornblende, garnet–hornblende biotite schist, amphibolite facies, Oppdal, Norway	6·6	3·4	33
YFM 19	Biotite, coexisting with YFM 18	9·8	5·6	47
YFM 20	Garnet, garnet–actinolite schist, amphibolite facies, Oppdal, Norway	0·18	1·7	31
YFM 21	Actinolite, coexisting with YFM 20	12	5·6	59
YFM 22	Garnet, garnet–hornblende schist amphibolite facies, Oppdal, Norway	16	1·7	26
YFM 23	Hornblende, coexisting with YFM 22	8·9	4·8	59
YFM 24	Sphene, pegmatite, Renfrew Co., Ontario	1·8	<0·1	<4
YFM 25	Spinel, Camango, Mexico	8·8	11·7	256
YFM 26	Enstatite, coexisting with YFM 25	6·4	29	85
YFM 27	Diopside, coexisting with YFM 25	2·7	10·2	73
YFM 28	Olivine, coexisting with YFM 25	7·8	42	164

values obtained ranged from less than 1 p.p.m. to 4·5 p.p.m. and Smales *et al.* (1957) give a value of 2·2 p.p.m. for the Westerley, R.I., granite.

2. *Sediments and sedimentary rocks*

Data on the cobalt content of sediments is sparse. Stanton (1944) found that the cobalt contents of several New Zealand limestones averaged 4 p.p.m., however if only pure limestones are considered this value is close to 1 p.p.m. Similar values were obtained by Dixon and Kidson (1940). Hirst and Nicholls (1958) separated the acid-soluble and -insoluble portions of some limestones and the soluble fractions

Table 15. Iron and manganese ores analysed spectrographically

Number	Description	Fe (%)	Co (p.p.m.)	Co/Fe ($\times 10^{-4}$)
YGM 1	Manganese ore, Sheorajpur, India	4·5	117	26
YGM 2	Manganese ore, Sheorajpur, India	4·8	130	27
YGM 4	Clay ironstone, Cedar Pt., Md.	35	<4	<0·1
YGM 5	Hematite, Ioditz, Germany	35	<4	<0·1
YGM 6	Magnetite, Sanford ore, Moriah, Essex Co., N.Y.	59	12	0·21
YGM 7	Magnetite, Magnet Cove, Ark.	46	64	1·4
YGM 9	Limonite, Buchersberg, Hartz, Germany	41	<4	<0·1
YGM 10	Magnetite, Furneau, Quebec	41	143	3·5
YGM 11	Magnetite, Lyon Mtn., N.Y.	19	29	1·5
YGM 12	Magnetite, Krageral, Norway	41	7	0·17
YGM 13	Limonite, Salisbury, Conn.	36	68	0·19
YGM 14	Limonite, Wayne Co., Mo.	46	10	0·22
YGM 16	Bog iron ore, Lake Saltonstall, E. Haven, Conn.	29	4	0·12
YGM 17	Hematite, Fayal Mines, Eveleth, Mesabi dist., Minn.	22	42	1·9
YGM 18	Hematite, Marquette, Mich.	37	5	0·14

mostly contained less than 1 p.p.m. cobalt. The cobalt contents of the insoluble fractions, presumably clay, ranged from 28 to 160 p.p.m., averaging 46 p.p.m. Ronov *et al.* (1955) give 11 p.p.m. as the average cobalt content of some clays from the Russian platform and similar values for clay have been found by Ishibashi (1959) and Tatsumoto (1957).

Deep-sea clay sediments from the Pacific have higher concentrations of cobalt than those from the Atlantic. Hutchinson *et al.* (1955) give the mean values for red clay from two Atlantic cores of 25 and 19 p.p.m. and 194 p.p.m. cobalt for a Pacific core. Smales *et al.* (1957) give mean values of 21 p.p.m. for an Atlantic core and 91 p.p.m. for some Pacific clays and similar high values, averaging 160 p.p.m. cobalt, have been noted by Goldberg and Arrhenius (1958) for Pacific clays Smales *et al.* (1957) recorded values ranging from 3 to 122 p.p.m. for the cobalt content of some pelagic carbonate oozes but the carbonate content of these oozes was not recorded. These same authors give a value of 224 p.p.m. cobalt for one "radiolarian ooze". Manganese nodules have cobalt concentrations ranging from 12 to 7100 p.p.m. averaging 2500 p.p.m. (Smales *et al.*, 1957; Goldberg, 1954).

3. *Sulphides*

Many analyses are available on the cobalt content of sulphides and these have recently been summarized by Fleischer (1955). Gavelin and Gabrielson (1947) suggested that the cobalt will enter arsenopyrite, pyrite, pyrrhotite and chalcopyrite with decreasing ease in that order. Bjorlykke (1954), Bjorlykke and Jarp (1950) and Carstens (1943) give values ranging up to 12,500 p.p.m. cobalt for some Norwegian pyrites and postulated that there is a correlation between high cobalt content and high temperature of formation of the pyrite. Carstens (1943) suggested sedimentary pyrites contain less than 100 p.p.m. Hegemann (1943) found that in

Table 16. Pyrites analysed spectrographically

Number	Description	p.p.m. Co
Tintic district, Utah		
YEM 1	Laclede	<4
YEM 2	Laclede	<4
YEM 3	Tesora	<4
YEM 4	Tesora	4
YEM 5	Tesora	<4
YEM 6	Columbus Tunnel	84
YEM 7	Shoebridge Bonanza	60
YEM 8	United Tintic no. 5, main shaft	4
YEM 9	United Tintic no. 5, main shaft	4
YEM 10	Sunbeam no. 1	<4
YEM 11	Sunbeam no. 1	52
YEM 12	Sunbeam no. 2	6
YEM 13	Sunbeam no. 2	9
YEM 14	Sunbeam no. 6	19
YEM 15	Sunbeam no. 10	<4
YEM 16	Sunbeam no. 11	7
YEM 17	Sunbeam no. 13	4
YEM 18	Sunbeam no. 15	4
YEM 19	Sunbeam no. 16	<4
YEM 20	Joe Daly no. 2	4
YEM 21	Joe Daly no. 4, main shaft	<4
YEM 22	Joe Daly no. 4, main shaft	<4
YEM 23	Joe Daly no. 4, main shaft	67
YEM 24	Martha Washington, main shaft	5
YEM 25	Martha Washington, main shaft	<4
YEM 26	Swansea, near hoist	6
YEM 27	Swansea, near hoist	<4
YEM 28	Disseminated in quartzite inclusion in monzonite	6
Bathurst–Newcastle area, New Brunswick		
YDM 2	Caribou deposit	<4
YDM 3	Armstrong Brook	<4
YDM 5	B.M. and S. no. 3	<4
YDM 7	B.M. and S. no. 12	610
YDM 8	Heath Steel	490
YDM 10	Sturgeon River	<4
YDM 11	Keymet Mine	230
Central City mining District, Colo., Pb–Zn–Cu mineralization		
YCM 1	Carroll Mine	78
YCM 2	Carroll Mine	48
YCM 6	Carroll Mine	195
YCM 8	Carroll Mine	64
YCM 9	Carroll Mine	38

Table 16—(*contd.*)

Number	Description		p.p.m. Co
YCM 15	Claire Marie Mine		540
YCM 16	Claire Marie Mine		12
YCM 17	Claire Marie Mine		18
YCM 18	Claire Marie Mine		98
Copper Hill, Tenn.			
YBM 7	In black phyllite		930
YBM 9	In green quartzose phyllite	approaching Ducktown	510
YBM 11	In phyllite	Tenn.	115
YBM 14	In phyllite		1650

metamorphosed sulphide deposits the cobalt content of the sulphides increased with increasing degree of metamorphism.

Gavelin and Gabrielson (1947) noted wide variations in the cobalt content of sulphides from the same mine and suggested that temperature is not an important factor in governing the cobalt content of sulphides. Verne *et al.* (1955) also found wide variations in the cobalt content of pyrrhotites from a single ore shoot but found no systematic change in cobalt content according to the position in the shoot. However, Auger (1941) reported that the cobalt content of chalcopyrite increased with depth at Noranda, and Hawley (1952) found that the cobalt content of pyrites from some Canadian gold mines increased with depth.

Wilson and Anderson (1959) suggested that ratios of trace elements in sulphides may be diagnostic for a specific deposit and may depend on the type of rock from which the ore solutions were derived. They suggest that ores have a higher Ni/Co ratio the more basic the rock with which they are associated.

The occurrence of economic deposits of cobalt in various parts of the world have been summarized by Perrault (1946), Perelman *et al.* (1949) and Young (1948).

4. *Natural waters*

Noddack and Noddack (1940) determined the cobalt content of sea water to be approximately 0·1 μg/l., and values ranging from 0·38 to 0·67 μg/l. were obtained by Ishibashi (1953) some samples from the Sea of Japan.

Malyuga (1946) gave 2·1 μg/l. as the average cobalt content of surface waters, and values ranging from 1 to 6 μg/l. were given by Torii (1955). Benoit (1956) found concentrations of cobalt ranging from 2 to 4 μg/l. in solution in water from Linsley Pond in Connecticut.

5. *Meteorites*

Lovering *et al.* (1957) give figures ranging from 3,800 to 7,400 for the cobalt content of iron meteorites with a mean of 5,100 p.p.m. Goldberg, Uchiyama and Brown (1951) and the Noddacks (1930) also give similar figures. The cobalt was

Table 17. Distribution of cobalt in the Stillwater complex

Station		Orthopyroxene*				Clinopyroxene*				Plagioclase†	Comp.
		Fe (%)	Mg (%)	Co (p.p.m.)	$\left(\frac{Co}{Fe+Mg}\right)$†	Fe (%)	Mg (%)	Co (p.p.m.)	$\left(\frac{Co}{Fe+Mg}\right)$‡	Co (p.p.m.)	%An
Upper gabbro	EB 41	8·8	8·7	77	1·48					2·5	62·9
	EB 135	11·5	15·5	107	1·26						
	EB 134	10·0	10·2	85	1·41	8·8	11·5	88	1·40		
	EB 133	9·0	10·5	72	1·47	7·4	8·7	89	1·80		
	EB 43									2·3	74·4
	EB 68									2·0	75·4
Anorth.	EB 142	13·5	10·0	97	1·47	9·3	8·0	64	1·27		
	EB 72									1·7	79·5
Lower gabbro	EB 171	10·5	12·0	76	1·12	6·1	8·6	47	0·91		
	EB 174	10·2	14·0	77	1·00	6·4	10·5	55	1·01		
	EB 176	9·0	8·4	65	1·08						
	EB 216	8·6	13·0	86	1·23	6·0	7·7	55	1·03		
	EB 213	7·2	10·5	65	1·15						
	EB 211	9·4	12·0	83	1·24						
	EB 210	8·0	7·8	79	1·69	6·4	7·2	45	1·11		
Norite	EB 32a									1·0	79·1
	EB 182	9·7	9·8	70	1·03						
	EB 26	8·0	12·0	77	1·20						

* Spectrographic.
† Neutron activation.
‡ Expressed in atoms.

found by Nichiporuk (1958) to be primarily in the Ni rich taenite phase. Smales, Mapper and Wood (1957) noted values ranging from 4 to 960 p.p.m. cobalt for various types of chondrites and figures up to 1300 have been obtained by Wiik (1956) Brown and Patterson (1947) reported a mean value of 270 p.p.m. for 107 analyses in the literature on the silicate phases of stony meteorites.

Cobalt in Basaltic Rocks

"Basaltic rocks" is used here as a general term under which gabbros, norites andesites and related rock types are classified. An attempt is made to determine the crustal abundance of cobalt in these rocks and to determine the coherence relations between cobalt and iron and magnesium. The distribution of cobalt in differentiated sequences of the Still-water and Skaergaard types is discussed first and then its distribution in a world-wide sample of basaltic rocks. Finally the significance of these distributions with respect to the genesis of basaltic rocks is discussed.

Distribution in differentiated intrusives

Analyses of minerals from various levels in the Still-water complex in Montana are given in Table 17. The samples are those described by Hess (1960). The Still-water complex is a steeply dipping basic intrusive which is thought to have undergone differentiation by crystal settling (Hess, 1938, 1939, 1960; Howland *et al.*, 1936). The intrusive shows alternation of mafic and feldspathic layers and superimposed upon this banding is a cryptic layering involving changes in composition

of the mineral phases present. Changes in cobalt content corresponding to the rhythmic banding are found. The cobalt content of the plagioclase is below the limit of detection of the emission spectrograph, whereas substantial amounts of cobalt are found in the mafic bands. However, changes in cobalt contents corresponding to the cryptic layering of the mafic bands are not found. The variation in the cobalt content of the pyroxenes is almost within experimental error and shows no systematic change corresponding to changes in the Fe/Mg ratios. Also there is no systematic change or large variation in the Co/Fe+Mg atomic ratios and these ratios are approximately the same for clino- and ortho-pyroxenes. Hence it appears that the cobalt content of these minerals is a function of the total number of Fe–Mg sites and is independent of the Fe/Mg ratio.

Although no systematic changes in the cobalt content of the pyroxenes is observed, there is a progressive increase in the cobalt content of the plagioclases toward the top of the intrusive. The cause of this increase is uncertain but probably reflects an increase in the cobalt content of the magma. Prolonged precipitation of primarily plagioclase from the magma would result in an increase in the Fe, Mg and Co content of the magma and it is significant that the highest cobalt concentrations in the plagioclases are found above the plagioclase rich anorthosite zone. This hypothesis presupposes excess precipitation of plagioclase as is observed in the Stillwater complex although the mechanism by which this could occur is unknown.

Wager and Mitchell (1951) have examined the distribution of various trace elements in the Skaergaard intrusion. They found that for most of the sequence there is little variation in the cobalt content of the individual minerals, however toward the top of the sequence, in the ferrohortonolite and fayalite ferrogabbros, there is a significant decrease in the cobalt concentrations. The ratio of (atoms Co/atoms Fe+Mg) also decreases from $1{\cdot}42 \times 10^{-4}$ in the hypersthene olivine gabbros to $0{\cdot}64 \times 10^{-4}$ in the ferro-hortonolite ferrogabbros whereas the ratio in the chilled margin rocks is $2{\cdot}8 \times 10^{-4}$. Hence, although no marked changes in the Co/Fe+Mg ratios were noted in the Stillwater complex, there is a progressive decrease in this ratio toward the top of the Skaergaard intrusion. The significance of this with respect to petrogenesis is discussed below.

Geochemical coherence

Attempts have been made by several workers to determine the degree of coherence of cobalt with iron and magnesium. Sandell and Goldich (1943) found that Co varied linearly with Mg for a series of unrelated rocks including both granites and basalts. They calculated 0·00066 for the average Co/Mg ratio. Nockolds and Mitchell (1948) found that the Co/Mg ratio for some Caledonian basaltic and dioritic rock series was approximately constant. Nockolds and Allen (1953, 1954) showed that both Co/Fe and Co/Mg were approximately constant for some alkali and calcalkali assemblages. Their results suggest, however, that in some cases the Co/Mg ratio decreases as Mg decreases. The work of Wager and Mitchell (1951) indicated that in the Skaergaard intrusion there is little relation between Mg content and Co content, and that Co tends to follow Fe more closely than Mg but still the coherence is poor especially in the late stages.

Although must of the evidence is contradictory it indicates that comparison of cobalt concentrations with iron and magnesium concentrations in some fashion will yield the most useful results. In Figs. 7 and 8 the logarithms of the cobalt concentrations are plotted against the logarithms of the iron concentrations and the logarithm

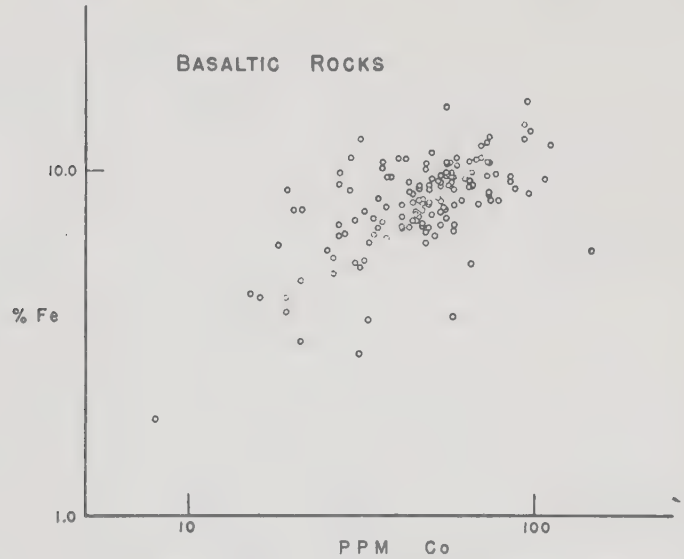

Fig. 7. Plot of Co against Fe for basaltic rocks.

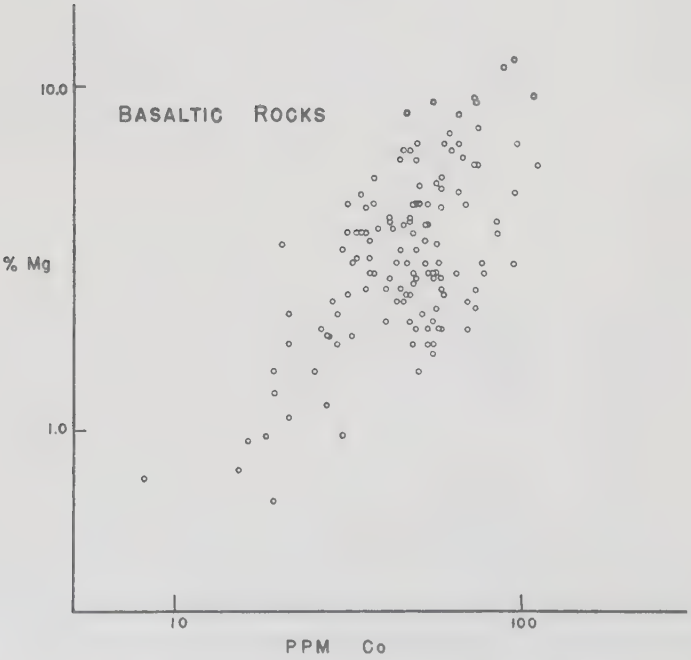

Fig. 8. Plot of Co against Mg for basaltic rocks.

of the magnesium concentrations, respectively, for 135 basaltic rocks. It is evident that neither of the slopes of possible curves drawn through the points is the 45° necessary for a simple proportionality between the variables (the Mg curve being greater as plotted and the Fe curve less).

If, however, the sum of the moles per cent of magnesium and iron is plotted against the cobalt concentrations, a slope close to 45° is obtained, indicating approximate proportionality between the variables (Fig. 9). Visual comparison of this plot

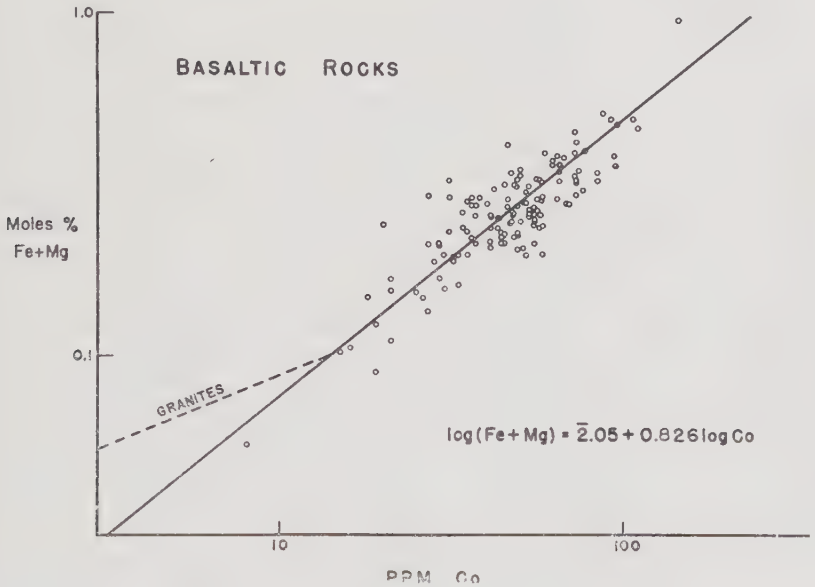

Fig. 9. Plot of Co against (Fe + Mg) for basaltic rocks.

with the plots for iron and magnesium individually indicates better coherence between Co and Fe+Mg than between Co and either Fe or Mg alone. The equation relating Co concentrations with Fe+Mg concentrations was calculated by the reduced major axis method for the 135 samples analysed, and the calculated line has a correlation coefficient of 0·91.

The close approximation of the Co–(Fe + Mg) plot to 45° seems to imply that the cobalt concentrations of basaltic rocks generally are dependent on the number of sites available for cobalt to occupy (represented by the sum of the Fe and Mg molar concentrations). This was also indicated in the Stillwater complex.

The slope of the Co–(Fe+Mg) curve is actually slightly less than 45° and this could result from several causes. Possibly Fe and Mg are preferentially incorporated in the accessory and light minerals with respect to cobalt. The effect of this would only be noticeable at low concentrations and would be such as to reduce the slope. Similarly if the Co/Fe+Mg ratio in the ferromagnesian minerals is slightly higher than that in the magma from which they crystallized then the slope would be slightly less than 45°. Also if cobalt cannot substitute for Fe^{3+} when it is in the Al and Si positions and if a greater proportion of the iron is present in these positions

at low iron concentrations then a slope of less than 45° would result for the Co–(Fe+Mg) plot. With the present data available it is not possible to determine which, if any, of these mechanisms is operative.

General pattern of distribution

A histogram of the logarithm of the concentrations of cobalt in 139 basaltic rocks (Fig. 10) shows the distribution of cobalt to be symmetrical in these rocks.

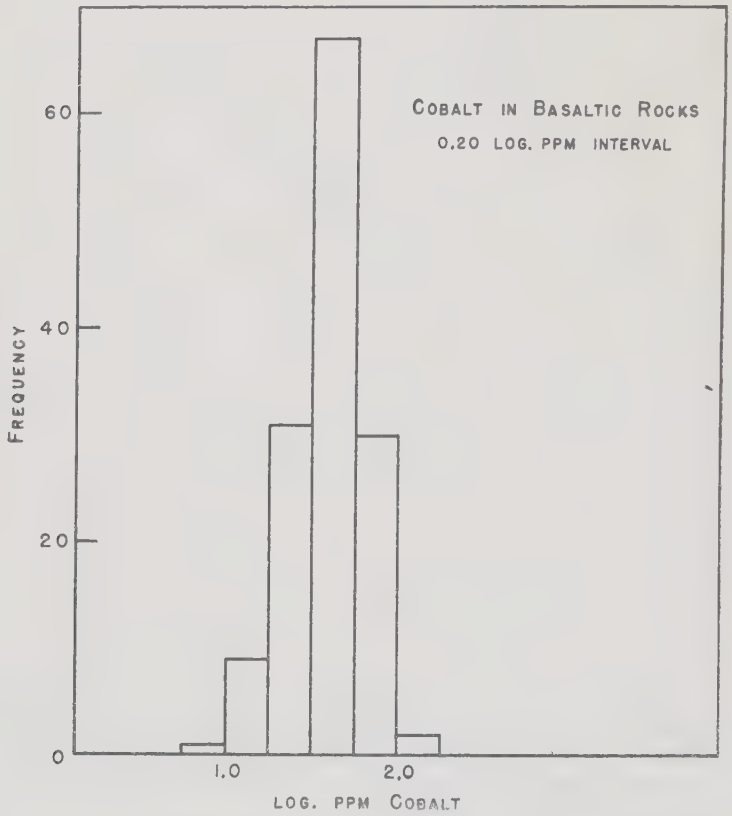

Fig. 10. Histogram of the distribution of cobalt in 139 basaltic rocks.

The slight positive skewness may be due to a preferential sampling bias of rocks low in magnesium and iron. The sample gives an arithmetic mean of 48 p.p.m. and a geometric mean of 46 p.p.m., a reflection of the small dispersion of values. From the previous discussion it is suggested that this is the natural consequence of the narrow spread in the mole per cents of iron plus magnesium in the rocks classified as "basaltic rocks". No significant difference in the cobalt content of basaltic rocks from different regions is apparent though these are the same rock suites for which Turekian and Kulp (1956) found significant regional control of strontium.

Of the twelve samples analysed containing less than 25 p.p.m. cobalt, four are anorthosites, two diorites, two andesites and four basalts. Thus the lowest values

are predominantly intermediate rocks and the light-coloured differentiates of basaltic rocks. Those rocks containing more than 100 p.p.m. are the mafic types. Only two samples analysed here contain more than 100 p.p.m. a dunite and an olivine-rich basalt, but other workers have quoted high figures for picrites and oceanites (Nockolds and Allen, 1953, 1954; Lundegardh, 1956).

Petrogenetic significance

It has been shown above, from a world-wide sampling of basaltic rocks, that the cobalt content of these rocks is approximately proportional to the Fe + Mg content (in moles). The slope of the line in Fig. 9 is, however, a little less than 45° indicating that the Co/Fe + Mg ratio in mafic-rich basaltic rocks is slightly greater than in mafic-poor types. If two basaltic magmas, initially with different Co/Fe + Mg atomic ratios, undergo differentiation such that all the rocks formed from each magma have similar Co/Fe + Mg ratios, as is implied by Fig. 9, then the residual materials must retain the initially different Co/Fe + Mg ratios. Yet, except for rocks from the Skaergaard intrusion, which are discussed below, basaltic rocks with markedly different Co/Fe + Mg ratios have not been found. This implies that basaltic magmas are all formed with similar Co/Fe + Mg ratios and suggests that the process of magma formation does not result in marked differences in this ratio.

Wager and Mitchell (1951) have examined the distribution of various trace elements in the Skaergaard intrusion. Their figures reveal that the Co/Fe + Mg ratio, expressed in atoms, changes from $1{\cdot}42 \times 10^{-4}$ in the lowest rocks exposed to $0{\cdot}64 \times 10^{-4}$ at the top of the intrusion. Hence the constancy of the Co/Fe + Mg ratio found to be characteristic of basaltic rocks in general and the Stillwater complex does not hold for the Skaergaard intrusion. Also for basaltic rocks as a whole the Co/Fe ratio increases with increasing Fe content (Fig. 7) whereas this ratio decreases with increasing Fe content in the Skaergaard intrusion.

This discrepancy could arise from the original Skaergaard magma having a different Co/Fe + Mg ratio from normal basaltic magmas or from the process of differentiation. Analyses of the chilled marginal gabbro of Skaergaard show that the Co/Fe + Mg ratio of the original magma was $2{\cdot}8 \times 10^{-4}$ which is close to the average value of $2{\cdot}9 \times 10^{-4}$ for all basaltic rocks. Thus the cause of the discrepancy must lie in the process of differentiation.

The late differentiates of the Skaergaard intrusion have lower Co/Fe + Mg ratios than the marginal gabbro, so the earlier unexposed differentiates must have proportionately higher ratios. Yet such variations in the Co/Fe + Mg ratios are not found in basaltic rocks in general nor in the Stillwater complex.

Kennedy (1955) and Osborn (1959) have discussed the possible effects of different partial pressures of oxygen on a basaltic magma undergoing differentiation. Fractional crystallization under a moderate partial pressure of oxygen results in the early removal of iron as Fe^{+3} in the form of a spinel, and subsequent differentiation results in the basalt-andesite-dacite series. Under smaller partial pressures of oxygen the iron remains in the divalent state and early spinels are not formed. This leads to the formation of iron rich end products of the Skaergaard type.

Osborn (1959) showed that differentiation along the andesite-dacite line is more common than that of the Skaergaard type. The coherence relations of cobalt

shown by the world wide sample of basaltic rocks (Fig. 9) may reflect the behaviour of cobalt during differentiation along the andesite–dacite line, and we suggest, on the basis of the empirical evidence given above, that this behaviour is different from that during differentiation of the Skaergaard type. Andesite–dacite type differentiation leads to differentiates in which the Co/Fe + Mg ratio remains constant; Skaergaard type differentiation leads to iron-rich, cobalt-poor, end products. This suggestion is based solely on the distribution pattern of cobalt; the cause for the difference in behaviour is not known.

Cobalt in Granitic Rocks

Granites and granodiorites are both discussed here under the general term "granitic rocks". Rhyolites are also included within this group because of their similarity in major element composition to other members of the group.

Geochemical coherence

It was established above that the cobalt content of basaltic rocks approaches a linear relationship to the sum of the molar concentrations of iron and magnesium. However, the deviation from a 45° slope of the regression line for granitic rocks on the Co–(Fe + Mg) plot (Fig. 9) indicates a non-linear relationship for these rocks. For granitic rocks a linear relationship prevails between the cobalt concentrations and the magnesium concentrations as is evidenced by the 45° slope on the logarithmic plot of Co against Mg (Fig. 11). Further, the correlation coefficient for the Co Mg line is 0·91 for the thirty-two samples analysed, compared with 0·57 for the Co–(Fe + Mg) line for the same samples. Thus the coherence relations of cobalt in granitic rocks differ from those in basaltic rocks.

General pattern of distribution

Since neither Mg or Fe is essential for the definition of a granitic rock their concentrations may vary widely in any sampling. Cobalt will then be expected to have a wider dispersion than in the case of basaltic rocks in light of the above discussion. A histogram of the distribution of cobalt values in granitic rocks is given in Fig. 12.

The cobalt content of granitic rocks is dependent on rock type so that any estimate of the abundance of cobalt in granitic rocks must depend on the relative proportions of these various types. The granitic rocks can for convenience be split into two major groups, the high-calcium and the low-calcium types. High-calcium granites are generally higher in Fe and Mg than are low-calcium granites (Daly, 1933; Nockolds, 1954) and so are generally higher in cobalt. The figures for Ca, Fe and Mg in Table 18 for high- and low-calcium granites are taken from a compilation of many analyses of respectively granodiorites and granites by Nockolds (1954). The cobalt values for high- and low-calcium granites obtained using the Co–Mg curve for granites (Fig. 11) and Nockolds Mg values are compared in Table 18 with the mean cobalt concentrations of granites analysed here containing more than, and less than 1 per cent calcium, and the mean values for granitic rocks from western North America and New England.

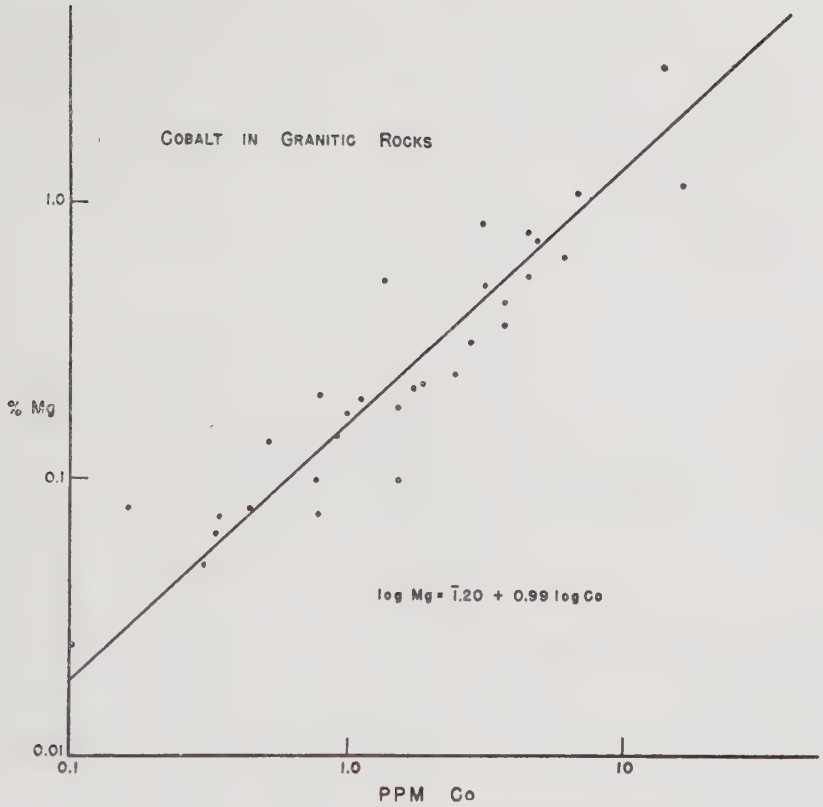

Fig. 11. Plot of Co against Mg for granitic rocks.

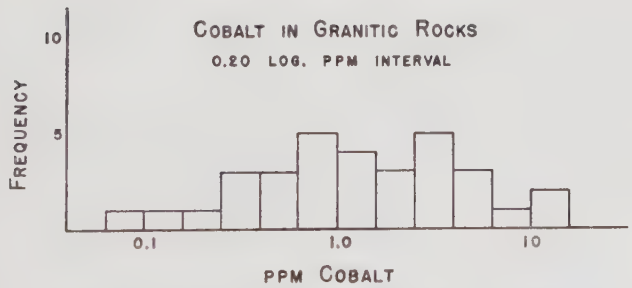

Fig. 12. Histogram of the distribution of Co in granitic rocks.

The cobalt concentrations in high- and low-calcium granites, 6·6 and 0·88 p.p.m., respectively, obtained from the magnesium data of NOCKOLDS (1954) using the Co-Mg regression equation are regarded as the best estimates for the abundance of cobalt in these rocks in view of the large number of analyses involved in NOCKOLDS' compilation and the close coherence between cobalt and magnesium.

Regional differences in the cobalt content of granitic rocks are apparent from the data here presented. However, the difference in cobalt content of granitic rocks from New England and western North America shown in Table 18 is thought to

reflect largely the differences in the type of granitic rocks easily sampled in these two areas, those from western North America being mostly granodioritic and those from New England being mostly granitic. Similarly, unless there is a change in the Mg content of granitic rocks with age, it is considered unlikely that the cobalt content of these rocks is a function of age.

Turekian and Kulp (1956) showed that rhyolites generally have higher Sr/Ca ratios than granites with corresponding calcium contents. No distinction between granites and rhyolites is possible on the basis of their cobalt contents. All the rhyolites analysed fall on the Co–Mg curve for granites.

Distribution of cobalt in the various mineral phases in granitic rocks

The coherence of Co with Mg suggests that most of the cobalt in granitic rocks is in the ferromagnesian minerals. Table 19 gives analyses of quartz, K-feldspar, and biotite from a biotite granite, and an analysis on a Bureau of Standards albite. These figures indicate that a reasonably accurate estimate of the cobalt content of a granite should be possible from the mode of the rock, if a significant amount of ferromagnesian minerals is present, and the concentration of cobalt in them is

Table 18. Cobalt in granitic rocks

Sample	Co (p.p.m.)	Mg (%)	Fe (%)	Ca (%)
Granodiorites*	6·6	0·94	2·96	2·53
Alkali granites*	1·0	0·16	1·42	0·51
Avg. granites > 1% Ca (16)	3·6	0·62	1·97	1·67
Avg. granites < 1% Ca (10)	0·74	0·10	1·25	0·72
Avg. New England granites (11)	1·9	0·24	1·96	1·28
Composite of western North American granites	7·8	0·67	2·79	1·66

* Major elements from Nockolds (1954), Co from Co–Mg curve for granitic rocks (Fig. 11).

Table 19. Minerals from granitic rocks

Mineral	Fe (%)	Mg (%)	Co (p.p.m.)
Biotite*	10·2	4·3	80
Quartz*	0·016	—	0·45
K-feldspar*	0·014	0·011	0·11
Na-feldspar†	0·029	0·097	0·75

* From granodiorite gneiss, Sondrestrom Fjord, Greenland.
† Bureau of Standards, standard albite no. (99).

known. This estimate is liable to be inaccurate, however, at concentrations less than 1 p.p.m. for in this region the contribution of cobalt disseminated through the non-ferromagnesian minerals becomes significant. As two of the granites analysed have less than 0·11 p.p.m. cobalt and several have less than 0·45 p.p.m., the figures given in Table 19 for K-feldspar and quartz, respectively, it is apparent that the

concentration of cobalt in the light minerals is variable. The nature of this variation is not known, except that it is a function of the Mg content, but it is probable that the cobalt content of these minerals is related to the cobalt content of the rock. If the Co, Fe and Mg are low in the material from which the rock crystallized, then it seems likely that the concentrations of these three elements in the light minerals

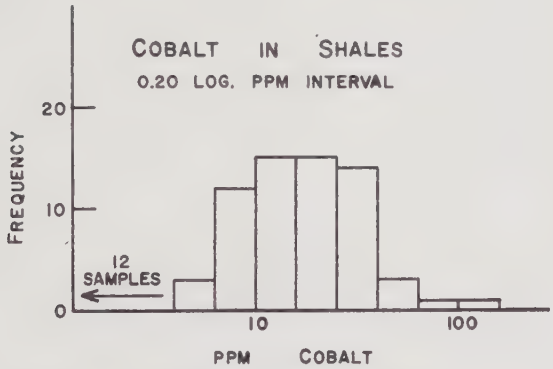

Fig. 13. Histogram of the distribution of Co in shales.

will be less than in those cases where Co, Fe and Mg are more available. Thus the light minerals in a granite containing abundant dark minerals will have more cobalt than those minerals in a granite devoid of dark minerals. This is partially confirmed by a value of 0·055 p.p.m. cobalt obtained from a graphic granite, which has little or no dark minerals. This figure is much less than the values for quartz, K-feldspar, or Na-feldspar given in Table 19.

Cobalt in Sediments

The laws relating the distribution of trace elements to that of major elements in igneous and metamorphic rocks are not operative for sediments. The trace element content of a sediment can be affected by several factors such as the relative proportion of detrital material, variability in the composition of the argillaceous material, and the sulphide, heavy mineral and organic content. The interplay of these factors must result in a complex distribution pattern, hence cobalt in sediments is not expected to show a regularity in behaviour similar to that found in crystalline rocks.

1. *Shales*

General pattern of distribution. Fig. 13 is a histogram of the distribution of Co in shales with the logarithm of the Co content as the variate. The arithmetic mean of this random sample of shales is 19 p.p.m. cobalt, calculated on the basis of a concentration of 2 p.p.m. for those shales containing less than 4 p.p.m. cobalt, the sensitivity limit of the emission spectrographic procedure employed. This mean is larger than that given by some other authors although similar to the average low-grade pelitic rocks analysed by Shaw (1954). Ronov *et al.* (1955) give an average of 11 p.p.m. cobalt for shales of various ages from the Russian platform. Tatsumoto (1957) and Ishibashi (1959) give means of 14 and 9 p.p.m. cobalt, respectively, for Recent

clays from the Sea of Japan and Young (1954) gives 11 p.p.m. as the average of twenty-nine near-shore clays off North America.

Pure limestone and sandstone, though having variable cobalt concentrations, are so low in this element that their effect on sediments composed of mixtures of clay minerals and dark detrital minerals is one of simple dilution.

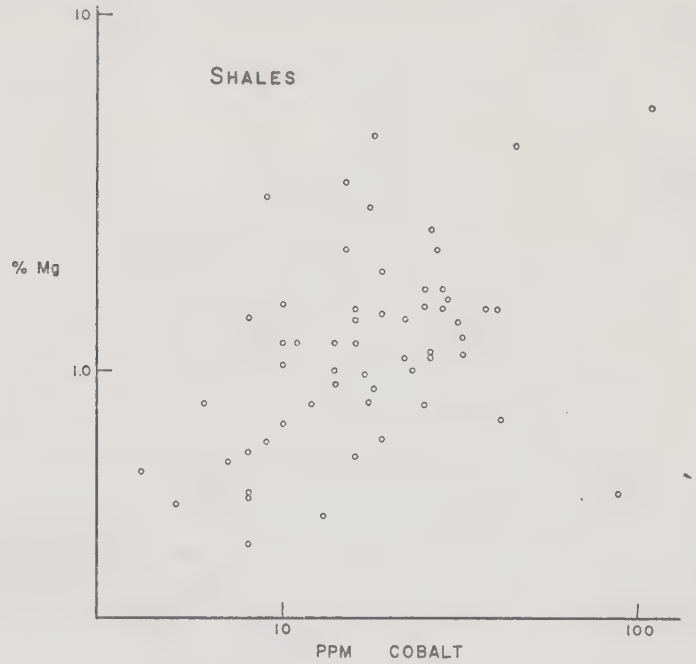

Fig. 14. Plot of Co against Mg for shales.

Geochemical coherence. The coherence relations of cobalt in shales must reflect the behaviour of this element compared to other elements during weathering and its coherence relations in the source materials. Mg tends to be removed in solution preferentially with respect to Fe during weathering (Goldschmidt, 1954; Rankama and Sahama, 1950), whereas it is shown below that Co tends to behave like Fe, except in those cases where separation of Fe and Mn occurs, in which case Co follows Mn. Accordingly, Co shows poor coherence with Mg in shales (Fig. 14) in spite of the coherence of these two elements in crystalline rocks. Better coherence is found between Fe and Co (Fig. 15) but the coherence is much poorer than in basaltic and granitic rocks. This undoubtedly results from differences in the behaviour of Fe and Co during weathering, lack of coherence in the source material, and the effect of the organic component in the shales, since fuels are known to be high in cobalt.

2. *Limestone and sandstone*

Only two carbonate rocks have been analysed here and these analyses give values of 0·61 and 0·36 p.p.m. Co for a limestone and dolomite, respectively. However, several carbonate shells have been analysed (Table 9). These contain up to 0·24 p.p.m. Co but most values are below 0·1 p.p.m. Colorimetric analyses of forty-eight

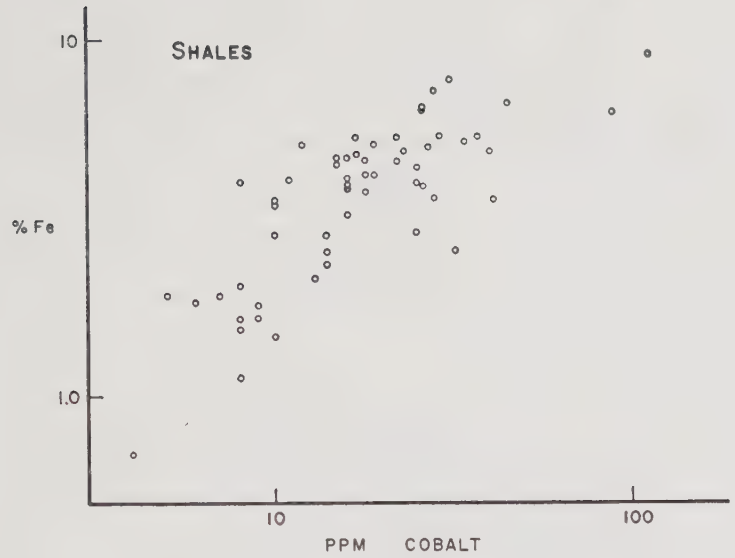

Fig. 15. Plot of Co against Fe for shales.

limestones by Stanton (1944) give an average of 1·6 p.p.m. Co, but if only those limestones are considered which contain greater than 90 per cent calcium carbonate, then an average of 1·2 p.p.m. Co is obtained. Dixon and Kidson (1940) give an average of 4 p.p.m. for thirteen limestones but the calcium carbonate content is not given. Hirst and Nichols (1958) analysed the acetic acid soluble fractions of eight argillaceous limestones and their figures give a mean of 2 p.p.m. for the soluble fraction. However, one of the samples contained 13 p.p.m. in the soluble fraction and if this is excluded from the mean then a value of 0·45 p.p.m. Co is obtained.

The problem of assigning a value for the cobalt content of carbonate material from the limestone data lies in assessing the contribution of non-carbonate material to the total cobalt content of the rock. If the cobalt content of carbonate shells (Table 10) is indicative of the cobalt content of pure carbonate, then minor amounts of argillaceous material in a limestone could substantially affect its cobalt content. Hence the value of 0·09 p.p.m., the average cobalt content of the shells analysed here, is probably the best estimate of the cobalt content of pure carbonate material.

The values of 0·06 and 0·45 p.p.m. Co for quartz and 0·27 p.p.m. Co for a quartzite indicate that if substantial amounts of cobalt are present in a sandstone then the cobalt is mainly in the cement, the heavy minerals, or any argillaceous materials that may be present, and not in the quartz fraction. The figure of 2·7 p.p.m. Co obtained here for a sandstone and the mean value of 4 p.p.m. given by Ishibashi (1959) for ninety-one sandstones are thought indicative of the extent of the contributions of non-quartzose materials in sandstones.

Values of 0·06 p.p.m. and less than 0·02 p.p.m. cobalt for gypsum and anhydrite, respectively, indicate that these sediments contain very little cobalt. The Co/Ca ratio for the two samples is substantially less (by a factor of 70) than that of sea water.

3. *Deep-sea sediments*

A review of previous work on cobalt in deep-sea sediments is given above. We have made a reconnaissance study of the distribution of cobalt in an equatorial mid-Atlantic carbonate-rich core, A 180-74, collected by the Lamont Geological Observatory. This core was selected for study as there is little evidence that it was affected by local turbidity currents, erosion, or solution of carbonate. Also data on

Table 20. Distribution of cobalt in core A 180-74

Depth (cm)	Co (p.p.m.)	Mn (%)	Co/Mn	Co/Fe ($\times 10^4$)	Climate
Top	6				
6	6				Warm
11	5	0·059	0·0085	7·9	
16	8	0·404	0·0020	9·0	
21	4	0·375	0·0011	4·3	
26	5	0·204	0·0024	3·7	Transitional
31	12	0·568	0·0021	7·6	
33	4	0·082	0·0049	2·5	
37	4				
41	7				
46	7				
51	6	0·032	0·019	6·9	
56	6				
61	6				
66	4				
71	5	0·040	0·012	6·8	
76	6				
81	6	0·042	0·014	6·6	
86	8				
91	4				Cold
96	4				
101	6				
106	4				
111	5	0·040	0·010	8·5	
131	<3				
151	4	0·052	0·0077	7·1	
171	5	0·045	0·010	7·8	
191	4				
211	4	0·040	0·010	3·5	
231	6	0·047	0·013	3·6	
251	4	0·043	0·0081	4·5	
271	3				
291	3	0·052	0·0057	4·9	Transitional
311	<3				
351	<3	0·053	<0·0056	6·0	
391	3	0·045	0·0067	4·7	
421	3	0·053	0·0057	4·3	Warm
451	<3	0·052	<0·0057	5·2	
480	4	0·056	0·0071	3·7	

Mn and Fe values from Wangersky (1958).
Climatic data from Erickson and Wollin (1956).

the accumulation rates of the clay and carbonate fractions (Broecker *et al.*, 1958), the distribution of several elements other than cobalt (Wangersky, 1958), and the distribution of temperature-dependent foraminiferal tests (Erickson and Wollin, 1956) are available for this core.

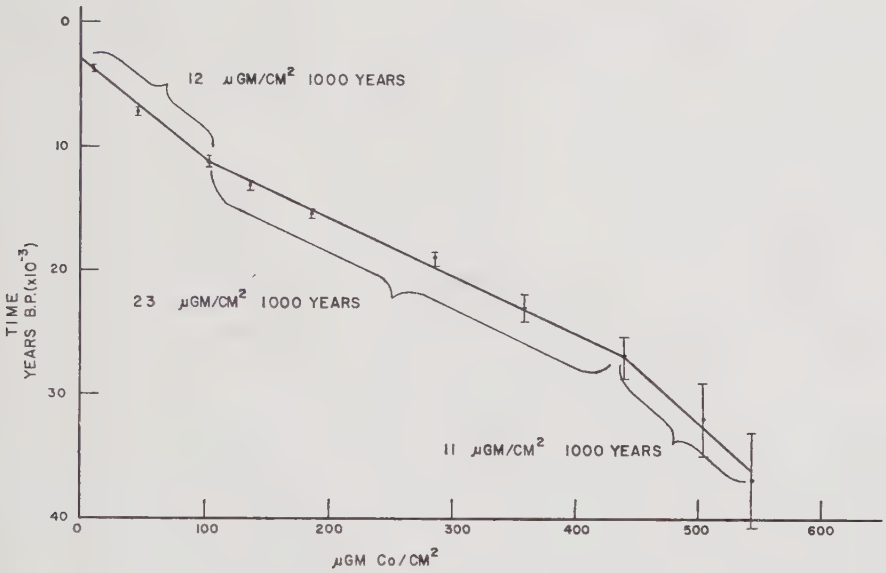

Fig. 16. Rates of accumulation of Co in core A 180-74.

The analytical data on cobalt for core A 180-74 are presented in Table 20 together with the Mn and Fe data from Wangersky (1958) and the climate as inferred by Erickson and Wollin (1956) from the paleontological data.

The rates of accumulation of cobalt in the core were calculated following the method of Broecker *et al.* (1958), and the cumulative curve for cobalt in the core as a function of time is given in Fig. 16 (the data are presented in Table 21). Two marked changes in the rate of accumulation of cobalt are evident at 11,000 years and 26,000 years before present. This has also been observed for both the clay and carbonate fractions (Broecker *et al.*, 1958). However, at the 11,000 year break the accumulation rate of cobalt changes by a factor of 1·9, while that of the clay fraction changes by 3·7 and that of the carbonate fraction by 2·1. At the 26,000 year break, within the errors, the clay and cobalt accumulation rate changes are the same.

The relatively high cobalt/clay ratio found in the Pacific deep-sea sediments and to a lesser degree in the Atlantic (see above) compared to the average concentration of cobalt in shales suggests that the concentration of this element in deep-sea sediments might be the result of several independent effects. Wedepohl (1960) has discussed this question for several elements and concludes that the two components supplying these elements to the deep-sea floor, are detrital clays and volcanic exhalations.

We do not think that volcanic exhalations should be an important contributor of such elements as cobalt, and offer a preliminary calculation to demonstrate that

Table 21. Sedimentation rate data for core A 180-74

Sample depth (m)	Age (years)	Δ Depth (m)	Δ Age (years)	Δ Wt. sed* (g/cm²)	Avg. Co (p.p.m.)	Δ Co (μg)
		2·5	3630 ± 170	1·8	6	11
0–5	3630 ± 170					
		8·0	3470 ± 300	5·9	6	35
9–12	7100 ± 250					
		9·0	4100 ± 390	6·7	8	57
18–21	11,200 ± 300					
		10·0	1900 ± 460	7·4	4·5	33
28–31	13,100 ± 350					
		10·0	2300 ± 460	7·4	6·7	50
38–41	15,400 ± 300					
		21·0	3500 ± 670	15·5	6·5	100
57–64	18,900 ± 600					
		19·5	4100 ± 1250	14·4	5	72
77–80	23,000 ± 1100					
		20·0	3700 ± 2000	14·8	5·5	81
97–103	26,700 ± 1800					
		19·5	5600 ± 3500	14·4	4·5	65
114–125	32,000 ± 3000					
		21·0	~5000	15·5	(2·5)	39
135–146	37,000 ± 4000					
		41·0		30·3	4·5	138
175–186	~40,000					

* Calculated assuming a density of 0·74 g/cm³ for the core.
Age data from Broecker *et al.* (1958).

the two independent sources for cobalt, and presumably other metals, are detrital clay and dissolved material in streams feeding the oceans.

If we use a cobalt concentration of 2 μg/l. for fresh surface waters draining into the sea (see above); a transfer of fresh water from the continents to the sea at the rate of 37×10^3 km³/yr (Wüst, 1936); and 361×10^6 km² for the total surface area of the oceans, the average removal rate of cobalt per unit area of ocean floor for a steady state is 20·5 μg/cm² per 1000 years which represents only the dissolved load of the fresh-water supply. The exact manner and locus of removal of cobalt from the sea are left determined.

Using the accumulation rates of cobalt and clay for different climatic conditions evidenced in core A 180-74 it is possible to get an estimate of the contribution of each of the sources of cobalt mentioned above at that site by the following calculation.

Consider the relation:

$$xL + y = R$$

where x is the average concentration of cobalt in original detrital clay and is independent of climate;

L is the rate of accumulation of detrital clay at a particular site on the bottom of the ocean and is a function of climate;

y is the rate of removal of dissolved cobalt from the ocean at the same site and is independent of climate;

R is the accumulation rate of cobalt at the same site and is a function of climate.

We can solve for x and y if we have two climatic conditions for which L and R are known. Actually we have three climatic conditions in core A 180-74, for which values of L and R have been obtained (Table 22).

Table 22. Accumulation of clay and cobalt in core A 180-74

Zone	Climatic condition	Time range (years before present)	L (g clay/cm^2 per 1000 years)	R (μg Co/cm^2 per 1000 years)
A	a Post-glacial	0–11,000	0·22	12
B	b Last glacial	11,000–26,000	0·84	23
C	c Last "interstadial"	26,000–?	0·34	11

The two values of x obtained by solving A and B simultaneously and B and C simultaneously are, respectively, 18 p.p.m. Co and 25 p.p.m. Co. The corresponding values of y are 8 μg Co/cm^2 per 1000 years and 3 μg Co/cm^2 per 1000 years.

The range of 18–25 p.p.m. for the cobalt concentration of detrital clays brackets narrowly the average value we have obtained for shales (19 p.p.m. Co) and the range of 3–8 μg Co/cm^2 per 1000 years for the supply of cobalt from the dissolved phase is comfortably smaller than the amount supplied to the sea and available for removal on our simple model. Probably most of the cobalt is removed from the sea at the continental margins.

On the basis of this calculation it is possible to explain the higher cobalt concentrations of Pacific relative to Atlantic deep-sea clays (see above). If the supply rate of detrital material per unit of oceanic area is greater for the Atlantic than for the Pacific basin, as is most certainly the case, and if the residence time of the detrital material in the oceans is short while the residence time of dissolved cobalt in the oceans is very much longer, the detrital clay with its original cobalt concentration will be accumulating at different rates in the two oceans while the removal rate of the dissolved cobalt will be the same for the two oceans. These assumptions are, of course, grossly simplified.

Kuhlenberg (1960) has calculated the "residence time" of detrital clay particles in the ocean as about 100 years, while the "residence time" for cobalt as calculated by Goldberg and Arrhenius (1958) is $1{\cdot}8 \times 10^4$ years. (The two "residence times" are not calculated the same way but we are looking for order of magnitude differences and for this the comparison is valid.)

Though the rate of mixing between ocean basins is not accurately known there is evidence (Broecker *et al.*, 1960) that the residence time of an element of water mass in either of the major ocean basins is of the order of 1000 years. This would result in an isolation by basins of the clay fraction and a degree of mixing of the cobalt in solution.

On this model a crude calculation can be made of the ratio of the rates of detrital

clay accumulation for the Atlantic and Pacific. Using the average of the cobalt data of Hutchinson *et al.* (1955), Smales *et al.* (1957), and Goldberg and Arrhenius (1958) for Atlantic deep-sea clays (22 p.p.m. Co) and Pacific deep-sea clays (148 p.p.m. Co) and our average value for shales (19 p.p.m. Co) we arrive at a ratio of 43 for the detrital clay deposition rates of the Atlantic relative to the Pacific. The average rate of accumulation of clay in core A 180-74 (Atlantic) is about 0·58 g/cm^2 per 1000 years (Broecker *et al.*, 1958) while Arrhenius (1954) calculated a rate of 0·073 g/cm^2 per 1000 years for the Pacific giving a ratio of Atlantic to Pacific of 8. Considering the crudeness of the assumption no better agreement should be expected.

At present we are investigating this problem for several elements on well dated cores from the Atlantic in order to evaluate the processes of metal ion supply and removal from the oceans.

Cobalt in Metamorphic Rocks

1. *Regional metamorphism*

General pattern of distribution. A comparison of the arithmetic means of the cobalt concentrations in schists and shales shows that there is a significant difference between the cobalt contents of these two rock types, the value of 40 p.p.m. for schists being approximately double the value of 19 p.p.m. for shales. There is, however, commensurately more Fe in schists, so that there is little difference in the Co/Fe ratios. The difference in the cobalt content of shales and schists is thought to result from sampling. In any sampling of schists, typical micaceous schists are normally chosen, quartzofeldspathic rocks, calcareous rocks and pegmatites are commonly avoided. Hence the equivalents of calcareous shales, which may form pyroxene-amphibole rocks on being metamorphosed, and the equivalents of Si–Na–K rich shales, which could form quartzofeldspathic metamorphic rocks, are not sampled. Also if metamorphic segregation occurs, such that some of the Si, K and Na is removed from the shale to form pegmatites, then the resulting schist will contain more Co, and also more Fe, than the original shale. All these factors will tend to result in a higher value for the cobalt content of a sampling of schists than one of shales.

Changes in cobalt content with metamorphic grade. Shaw (1954) found no change in the cobalt content of the Littleton formation with changing metamorphic grade. This is a very heterogeneous formation and Shaw was careful to choose only those samples which were definitely pelitic. However, his sampling procedure was based on the assumption that no metamorphic segregation had occurred. The similarity in the Co/Fe ratio found here for schists and shales indicate that if there is a change in the cobalt concentration of a pelitic sediment with metamorphic grade then there must be a similar change in the iron concentration.

Geochemical coherence. From the above implication that the Co/Fe ratio remains approximately constant during metamorphism and because of the partial coherence of Fe and Co in shales, these two elements should be coherent to a limited degree in schist. From the few schists analysed here this appears to be the case. However, the analyses of minerals from metamorphic rocks listed in Table 14 indicate that in

its partition relations between various metamorphic minerals cobalt tends to behave more like magnesium than iron. In all cases except the Adirondack gabbro, the order of increasing cobalt concentration of coexisting minerals is the same as the order of increasing magnesium concentration. Hence the close similarity of the Co/Fe ratios in shales and schists does not necessarily imply that Co behaves like Fe during metamorphism but only that if there is segregation of dark and light fractions then Co is in the dark fraction together with Fe and Mg, or alternatively, no change in the total Fe, Mg and Co content of the rock takes place during metamorphism. Cobalt appears to behave more like Mg than Fe during metamorphism.

Partition of cobalt between coexisting minerals. It was shown above that cobalt preferentially enters the ferromagnesian minerals in granitic and basaltic rocks and the same is true for metamorphic rocks. It will be shown below that the partition of cobalt between these minerals may be a function of metamorphic grade, hence the minerals cannot be arranged in any order indicating their preference for cobalt without reference to the metamorphic grade. However, it is evident from Table 14 that in amphibolite facies rocks, the order of decreasing cobalt content of ferromagnesian minerals is biotite–hornblende–garnet–muscovite.

Table 23 gives the ratio of the Co/Mg ratios and cobalt concentrations between coexisting minerals. From this preliminary study it appears that the partition of cobalt between coexisting metamorphic minerals is a functions of metamorphic grade. The partition ratio changes with grade such that entry into different minerals is more selective at lower temperatures. Hence if sufficient samples were available partition ratios could provide indices of metamorphic grade in those cases where diagnostic minerals were absent.

Although Co and Mg are similar in their partition relations between metamorphic minerals, the data in Table 23 indicate that some differences do occur. The Co/Mg ratio in garnet is consistently higher than that in hornblende, and lower than that in biotite.

Cobalt in Sulphides

Several workers have studied the cobalt contents of sulphide minerals and their work has been summarized in the section on previous work. A reconnaissance study of cobalt in pyrites has been made here and the analyses are listed in Table 16. The cobalt contents of these pyrites are lower than most listed in the literature. Wilson and Anderson (1959) suggested that the trace element content of sulphides is a function of the type of rock from which the ore solutions were derived. The Tintic, New Brunswick and Colorado samples given in Table 16 are all from areas of quartz porphyry intrusions and the low cobalt content of these pyrites may reflect the low cobalt content of quartz porphyries.

However, this cannot be the sole factor in determining the cobalt content, for several samples from the Tintic district show markedly different cobalt contents from others from the same district. No correlation between location or mineral association and the high cobalt pyrites was found. Similar variations in the same ore body have been found by Carstens (1943). Although no index of temperature of formation of these sulphides is available, it is unlikely, in view of the random distribution of the high-cobalt sulphides, that this is important in determining the

Table 23. Partition of cobalt between metamorphic minerals

Sample	Metamorphic facies	$\frac{(Co)x}{(Co)y}$	$\frac{(Co/Mg)x}{(Co/Mg)y}$
Hornblende (x)/biotite (y)			
6–12–110*	Granulite	0·77	0·71
YFM 18, 19	Amphibolite	0·65	1·15
37046*	Amphibolite	0·65	0·80
672–46*	Epidote amphibolite	0·43	0·33
Hornblende (x)/garnet (y)			
YFM 1, 2	Granulite	0·82	1·28
37218*	Granulite	1·50	0·70
YFM 20, 21	Amphibolite	1·9	0·58
YFM 22, 23	Amphibolite	2·3	0·53
37046*	Amphibolite	1·6	0·96
372–18*	Amphibolite	1·5	0·70
6–51–54A*	Epidote amphibolite	3·8	0·43
7–9–110*	Epidote amphibolite	3·0	0·51
Biotite (x)/garnet (y)			
YFM 7, 8	Amphibolite	2·8	1·4
YFM 9, 11	Amphibolite	5·2	1·8
YFM 13, 15	Amphibolite	5·8	2·5
7–9–110*	Epidote amphibolite	3·3	0·61

* Data from De Vore (1955a, b).

cobalt content of these minerals. Adequate evaluation of the factors controlling the distribution of cobalt in sulphides must await further data.

Theoretical Considerations

Since the distribution of trace elements in the geologic realm is controlled by the behaviour of the common elements forming the major framework it is natural to try to generalize the relationship between the two groups on the basis of one or more periodic functions of the elements involved.

1. *Distribution of cobalt during magmatic differentiation*

Goldschmidt's (1954) classic laws are based on ionic radius and charge considerations and have had strong predictive value. In the case of basaltic rocks the distribution of cobalt relative to magnesium and iron appears to follow the size rule as is most clearly demonstrated by Figs. 7 and 8, viz. the Co/Mg ratio increases with decreasing Mg concentration and the Co/Fe ratio decreases with decreasing Fe concentration. The difference between the Goldschmidt radii for Fe^{2+} (0·83 Å) and Co^{2+} (0·82 Å) is small, however, and the rule can hardly be said to be strongly confirmed on the basis of the behaviour of cobalt.

The Stillwater complex is instructive in this regard. Though for cobalt the rules appear to hold, the data for nickel (Turekian and Carr, 1960) indicate that the Ni/Mg ratio decreases drastically with the decrease in magnesium content of the late differentiates while the identical ionic radii for Ni and Mg (0·78 Å) would not predict this. It does not help to use Pauling's ionic radius data since he gives Mg 0·65 Å and Ni 0·69 Å predicting an increase of the Ni/Mg ratio in the later fractions.

In the case of basaltic rocks then Goldschmidt's laws, though apparently useful for cobalt, lack sufficient generalizing power. When granitic rocks are also considered the radius, and charge laws are only useful as a reconnaisance tool.

In view of similar difficulties encountered with other elements, particularly in the case of those elements which easily form covalent and metallic bonds in natural crystals, other factors have also been considered.

Electronegativities, described by Pauling (1940), or the ability of atoms in a molecule to attract electrons to themselves, were empirically and somewhat arbitrarily quantified by him as a measure of the ionic character of a bond. On the assumption that the more ionic the bond, as determined by the electronegativity function, the more stable the bond relative to a competing ion's bond, Ringwood (1955) set up an order of expected substitution of different ions for each other in an available lattice. By this scheme the element with the lower electronegativity will be preferentially incorporated. The electronegativities of Fe, Mg and Co (Table 24) indicate that cobalt would be enriched in the latest stages. This was not observed.

Hori (1954) constructed an "index of diadochy" based on charge, ionic radius, co-ordination number and the "repulsion exponent of the cation". The value of the index for Mg, Fe and Co is 0·14 but obviously the Mg/Fe ratio changes in a crystallizing magma hence ruling out the general usefulness of this suggestion.

Dismayed by equilibrium models Ahrens (1953) and De Vore (1955a) have discussed the trace element incorporation in growing crystals as a problem in the kinetics of crystal growth. Ahrens suggested that when two ions of the same valence and equal or similar radii compete for a given structure site in a growing crystal, the one with the greater electrical intensity (field) should arrive first. A measure of the field is given by the "field function" or F and is defined by $F = I/r$, where I is the ionization potential and r is the radius of the ion. Values of I, r and F for Co, Fe and Mg are given in Table 24. If the ion which arrives first is incorporated into the lattice then according to this theory cobalt should be preferentially enriched with respect to both Fe and Mg in the early differentiates. Fig. 8 shows that Mg is enriched relative to cobalt in the Mg-rich and presumably early differentiates of basaltic rocks, suggesting that some factor other than F controls the distribution of cobalt.

De Vore (1955a) suggested that important amounts of some trace elements, including cobalt, do not occupy regular lattice sites but occur at growth surfaces, imperfections, and various interfaces within the crystals and that the mechanism of absorption is responsible for the fixation of the trace elements during crystallization. However, since the cobalt concentrations of basaltic rocks are a function of the sum of the molar per cents of Mg and Fe and hence apparently the number of Fe–Mg lattice sites, it seems probable that this may have had a control on the incorporation of cobalt.

Table 24. Ionic characteristics of Mg, Fe and Co

Ion	Radii (Å)			I (eV)	F (eV/Å)	E
	G	P	A			
Co^{2+}	0·82	0·72	0·72	17·4	24·2	1·70
Mg^{2+}	0·78	0·65	0·66	15·0	22·8	1·20
Fe^{2+}	0·83	0·75	0·74	16·2	22·0	1·65
Co^{3+}			0·63	33·7	53·5	
Fe^{3+}	0·67		0·64	30·7	48·0	1·8

G = Goldschmidt (1926), P = Pauling (1927), A = Ahrens (1952), I = ionization potential (Herzberg, 1945; Harrison *et al.*, 1948), F = field function (Ahrens, 1953), E = electronegativity (Pauling, 1940; Haissinsky; 1946).

Several of the ideas presented above are based on the concept of a trace element entering a lattice site rather than simply substituting for another element diadochically. Although this may seem hair splitting, the difference, we believe, is significant. The lattice site idea essentially presumes that a certain framework is being constructed into which accomodation must be made.

For a trace element, frameworks occur not only in the crystalline phase but also in the less ordered liquid phase. Thermodynamically the partition of a trace element between liquid sites and crystal sites is determined by the condition of equal partial molal free energies for the trace element component in each phase.

Empirically, then, the partial free energies of cobalt in each phase are identical when the fraction of occupied crystal octahedral sites in which cobalt is found is the same as the fraction of occupied transient liquid "octahedral" sites in which cobalt is found, over the normal range of temperatures encountered in basic and ultrabasic rocks.

Though this view lacks some of the erudition inherent in using periodic properties of elements it does clear the air of preconceptions which might, in the present state of knowledge, be more of a hindrance than a help in predicting the behaviour pattern of trace elements during the crystallization of a magma.

2. *Distribution of cobalt between coexisting metamorphic minerals*

Ramberg (1952) explained the distribution of major elements in coexisting minerals on the basis of their polarizing power. He suggested that highly polarizing cations will prefer bonding with highly polarizable anions. Ionization potentials provide a rough index of the polarizing power of the cations (Table 24). The polarizability of the anions will depend on the nature of the surrounding ions. By considering the effect of the neighbouring Si atoms on the 0 atoms in various lattices, Ramberg deduced that the polarizability of the 0 atoms in silicates decreased stepwise in the order orthosilicates, metasilicates, phyllosilicates, tectosilicates. Complications arise through substitution of Si by Al and the presence of other cations. This hypothesis emplains the distribution of major elements between many metamorphic minerals such as the greater concentration of highly polarizing Fe^{2+} with respect to Mg^{2+} in hornblendes coexisting with biotites. However, De Vore (1955b) showed that although major elements are distributed in coexisting minerals as

anticipated by this hypothesis, many minor elements are distributed in the reverse order. As indicated by the analyses in Table 17, cobalt is one of these. Its distribution follows Mg more closely than Fe^{2+} in spite of its similarity in polarizability to Fe.

De Vore tried to establish degrees of correlation between trace elements and major elements in minerals and gave the order of decreasing correlation of the major elements with cobalt as Mg–K–Na–Ca. No explanation as to the cause of this correlation was given. It is interesting to note that although the total cobalt content of a metamorphic pelitic rock is roughly a function of the Fe content, the partition of cobalt between the various minerals bears little relation to their Fe content.

Crustal Abundance of Cobalt

In all the major rock units a relationship between cobalt concentrations and iron and magnesium concentrations has been demonstrated. For the purpose of assessing abundances this is not critical in the case of basalts, shales and schists as the iron, magnesium and cobalt concentrations show small ranges of values. Thus the mean values for the cobalt concentrations in these rocks can be taken as the true abundances (Table 25). Mean values for limestones and sandstones are not very meaningful in view of the large contribution from non-essential constituents toward the total cobalt content of these rocks. Hence only the figures for pure calcium carbonate, obtained from the values for carbonate shells, and for pure quartz, derived from the data on quartz and quartzite, are listed in Table 25.

Table 25. Abundance of cobalt in various geologic realms

	Co (p.p.m.)	Co/Fe ($\times 10^4$)	Co/Mg ($\times 10^4$)
Crystalline rocks			
Basaltic rocks	48	6·0	12
Granodiorites	7	2·5	7·0
Granites	1	0·6	6·4
Schists	40	5·3	9·3
Near shore sediments			
Shales	19	4·9	14
"Pure" limestone	0·1	—	—
Quartzite	0·3	—	—
Deep sea sediments			
Atlantic clays	21	5·8	12
Pacific clays*	160	25	76
Cosmic†	—	30	48

* From Goldberg and Arrhenius (1958).
† From Suess and Urey (1956).

The wide range of cobalt concentrations in granitic rocks and the dependence of the concentrations on the magnesium content present a problem in estimating the average abundance of cobalt in these rocks. The granitic rocks have been split into

two groups, granodiorites and granites, and the cobalt abundances determined using the average Mg content for these two rock types given by Nockolds (1954) and the Co–Mg curve for granites (Fig. 11).

Estimation of the crustal abundance of cobalt depends on the model used. Wickman (1954), by equating the abundances of various elements in sediments with those in igneous rocks, estimated a granite/basalt ratio of 2:1 for the "average weathered igneous rock". This ratio may, however, be only indicative of those rocks, or perhaps more correctly, the fraction of those rocks which have undergone chemical weathering, viz. near surface continental rocks. The abundance of cobalt in these rocks, calculated using the above ratio is 17 p.p.m. As an estimate of the crustal abundance of cobalt, this figure is biased in favour of granitic rocks as no account is taken of the mainly basaltic sub-oceanic crust. Also, Poldervaart (1955) and Worzel and Shurbet (1955) suggested that the continental crust may be primarily granodioritic. Hence assuming basalt and granodiorite in proportions 1:1 provides a better basis for estimating crustal abundances and on this basis 27 p.p.m. is calculated as the crustal abundance of cobalt. It must be emphasized that any estimate of "crustal abundance" is a function of the assumptions made and if these are revised then the abundance must be recalculated.

The silicate phases of stony meteorites fall on the Co (Fe + Mg) curve for basaltic rocks (Fig. 9) and have a Co/Fe + Mg atomic ratio of $3{\cdot}9 \times 10^{-4}$ (Brown and Patterson, 1947) which is similar to that for basalts ($2{\cdot}8 \times 10^{-4}$). The similarity of these ratios suggests that, if the earth is formed from meteoritic material, then no marked differentiation of Co with respect to Fe + Mg took place in the silicate material during the earth's formation. Hence the silicate mantle should have a Co/Fe + Mg atomic ratio similar to that for basalts and the silicate phases of stony meteorites.

The high Co/Fe + Mg atomic ratio (65×10^{-4}) for the metallic phases of stony meteorites (Goldschmidt, 1954) suggests that the depletion of cobalt in the earth's crust and mantle with respect to "cosmic material" results from concentration of cobalt in the earth's core.

Acknowledgements—We wish to thank Mr. R. Armstrong for his criticism and assistance and Miss Elizabeth Swink for her varied help. This work would not have been possible without the cooperation of geologists in providing samples. Aside from the samples obtained and previously acknowledged in an earlier study (Turekian and Kulp, 1956) significant contributions of material have also been made by the following: Messrs. R. Ames, C. Field, E. Hansen and Dr. J. Salisbury, Yale University; Dr. P. W. Gast, University of Minnesota; Dr. W. B. Hamilton, United States Geological Survey; Prof. H. H. Hess, Princeton University; Dr. L. Lundgren, University of Rochester.

This project was supported to a major degree by a grant from the National Science Foundation.

References

Ahrens L. H. (1952) The use of ionization potentials—I. *Geochim. et Cosmochim. Acta* **2,** 155–169.

Ahrens L. H. (1953) The use of ionization potentials—II. Anion affinity and geochemistry. *Geochim. et Cosmochim. Acta* **3,** 1–29.

Arrhenius G. (1954) Origin and accumulation of alumino-silicates in the ocean. *Tellus* **6,** 215–220.

Auger P. E. (1941) Pyrite of Canadian gold deposits. *Econ. Geol.* **36,** 401–423.

Benoit R. J. (1956) Studies on the biogeochemistry of cobalt and related elements. Unpublished thesis, Yale University.

Bjorlykke H. (1945) Innholdet av kobalt i svavelkis fra norske nikkelmalmer. *Norsk Geol. Tidsskr.* **25,** 11–15.

Bjorlykke H. and Jarp S. (1950) The content of cobalt in some Norwegian sulfide deposits. *Norsk. Geol. Tidsskr.* **28,** 151–156.

Broecker W. S., Turekian K. K. and Heezen B. C. (1958) The relation of deep sea sedimentation rates to variations in climate. *Amer. J. Sci.* **256,** 503–517.

Broecker W. S., Gerard R., Ewing M. and Heezen B. C. (1960) Natural radiocarbon in the Atlantic Ocean. *J. Geophys. Res.* **65,** 2903–2931.

Brown H. and Patterson C. (1947) The composition of meteoritic matter. *J. Geol.* **55,** 405–411, 508–510.

Carstens C. W. (1943) Uber den Co-Ni-gehalt norwegischer Schwegelkies-vorkommen. *Kgl. Norske Videnski Selsk. Forh.* **15,** 165–168.

Clark L. M. (1958) Cobalt determination in soils and rocks with 2-nitroso-1-napthol. *Analyt. Chem.* **30,** 1153–1156.

Daly R. A. (1933) *Igneous Rocks and the Depths of the Earth.* McGraw-Hill, New York.

DeVore G. W. (1955a) The role of absorption in the fractionation and distribution of elements. *J. Geol.* **63,** 159–190.

DeVore G. W. (1955b) Crystal growth and the distribution of elements. *J. Geol.* **63,** 471–494.

Dixon J. K. and Kidson E. B. (1940) The influence of Southland limestones on the cobalt content of pastures and Morton Mains. *N.Z. J. Sci. Technol.* A **22,** 1–6.

DuRietz (1955) The content of chromium and nickel in the Caledonian ultrabasic rocks of Sweden. *Geol. Foren. Stockholm Förh.* **78,** 233–299.

Erickson D. B. and Wollin G. (1956) Correlation of six cores from the Equatorial Atlantic and the Caribbean. *Deep Sea Res.* **3,** 104–125.

Faust G. T., Murata K. J. and Fahey J. J. (1956) Relation of minor element content of serpentines to their geological origin. *Geochim. et Cosmochim. Acta* **10,** 316–320.

Fleischer M. (1955) Minor elements in some sulfide minerals. *Econ. Geol.* 50th Anniversary Volume, 970–1024.

Friedlander G. and Kennedy J. W. (1956) Nuclear and radio-chemistry. John Wiley, New York.

Fryklund V. C. and Harner R. S. (1955) Comments on minor elements in pyrrhotites. *Econ. Geol.* **50,** 339–344.

Gavelin S. and Gabrielson O. (1947) Spectrochemical investigations of sulfide minerals from the ores of the Skellefte district. The significance of minor constituents for certain practical and theoretical problems in economic geology. *Sveriges Geol. Undersökn.* C, No. 491, 1–45.

Goldberg E. D. (1954) Marine geochemistry—I. Chemical scavengers of the sea. *J. Geol.* **62,** 249–265.

Goldberg E. D. and Arrhenius G. O. S. (1958) Chemistry of Pacific pelagic sediments. *Geochim. et Cosmochim. Acta* **13,** 153–212.

Goldschmidt V. M. (1926) Geochemische Verteilungsgesetze der Elemente. *Skr. norske Videnskap Akad. Mat.-naturv. Kl.* No. 2, 1–156.

Goldschmidt V. M. (1954) *Geochemistry.* Oxford University Press, London.

Haissinsky M. (1946) Echelle des electronegativities de Pauling et chaleurs de formation des composes inorganiques. *J. Phys. Radium* **7,** 7–18.

Harrison G. R., Lord R. C. and Loofbourow J. R. (1948) *Practical Spectroscopy.* Prentice Hall, New York.

Hawley J. E. (1952) Spectrographic studies of pyrite in some Canadian gold mines. *Econ. Geol.* **47,** 260–304.

Hegemann F. (1943) Die geochemische Bedeutung von Kobalt und Nickel in Pyrit. *Z. angew. Miner.* **4,** 122–239.

Herzberg G. (1945) *Atomic Spectra and Atomic Structure.* Dover Publications, New York.

Hess H. H. (1938) Primary banding in norite and gabbro. *Trans. Amer. Geophys. Un.* Pt. 2, 264–268.

Hess H. H. (1939) Extreme fractional crystallization of basaltic magma. *Trans. Amer. Geophys. Un.* Pt. 3, 430–437.

Hess H. H. (1960) Stillwater igneous complex. *Geol. Soc. Amer. Mem.* **30,** 230.

Hirst D. M. and Nichols G. D. (1958) Techniques in sedimentary geochemistry—I. Separation of the detrital and non-detrital fractions of limestones. *J. Sed. Petrol.* **28,** 468–481.

Hori F. (1954) On the diadochic substitution in silicates. *Miner. J., Japan* **1,** 109–125.

Howland A. L., Peoples J. W. and Sampson E. (1936) *The Stillwater Igneous Complex.* Montana Bur. Mines and Geol. Misc. Contr. No. 7.

Hutchinson G. E., Benoit R. J., Cotter W. B. and Wangersky P. J. (1955) The nickel, cobalt and copper contents of deep-sea sediments. *Proc. Nat. Acad. Sci., Wash.* **41,** 160–162.

Ishibashi M. (1953) Minute elements in sea water. *Records Oceanogr. Works, Japan* **1,** No. 1, 88–92. *Chem. Abstr.* **48,** 6175 (1954).

Ishibashi M. (1959) Chemical studies on the ocean (lxxx). Cobalt content of shallow water deposits (1). *Kyoto Univ. Inst. Chem. Res. Bull.* **37,** 26–31, 31–38.

Johnson F. R. and Graham E. R. (1952). Trace elements and Missouri soil types—1. Copper and cobalt contents of twenty-six soil types. *Res. Bull. Missouri Agr. Expt. Sta.* No. 517.

Kennedy G. C. (1955) Some aspects of the role of water in rock melts. *Geol. Soc. America Spec. Paper* 62, 489–504.

Kuhlenberg (1960) The residence time of particulate matter in the sea. *Abstracts, Internat. Assoc. Phys. Oceanog. at XII General Assembly I.U.G.G., Helsinki,* pp. 150–151.

Lovering J. F., Nichiporuk W., Chodos A. and Brown H. (1957) The distribution of gallium, germanium cobalt, chromium, and copper in iron and stony-iron meteorites in relation to nickel content and structure. *Geochim. et Cosmochim. Acta* **11,** 263–278.

Lundegardh P. H. (1945) Distribution of vanadium, chromium, cobalt and nickel in eruptive rocks. *Nature, Lond.* **155,** 733.

Lundegardh P. H. (1949) The geochemistry of chromium nickel and zinc. *Sveriges Geol. Undersökn.* C, No. 513, 1–56.

Lundegardh P. H. (1956) Petrology of the Uppsala region, eastern Sweden. *Sveriges Geol. Undersökn.* C, No. 544, 1–74.

Lundegardh P. H. (1957) The titaniferous ore-bearing gabbro of Helsingland, central Sweden. *Sveriges Geol. Undersökn.* C, No. 549, 1–34.

Malyuga D. P. (1946) Geochemistry of disseminated nickel and cobalt in the biosphere. *Trudy Biogeokhim. Lab., Akad. Nauk SSR* **8,** 75–141. *Chem. Abstr.* **47,** 7961 (1953).

Meinke W. W. (1955) Trace element sensitivity: comparison of activation analysis with other methods. *Science* **121,** 177–184.

Mitchell R. L. and Scott R. O. (1947) Concentration methods in spectrochemical analysis—II. Recovery of trace constituents in plant materials and soil extracts by mixed organic reagents. *Trans. J. Soc. Chem. Ind., London* **66,** 330–336.

Myers A. T. and Barnett P. R. (1953) Contamination of rock samples during grinding as determined spectrographically. *Amer. J. Sci.* **251,** 814–830.

Nichiporuk W. (1958) Variations in the content of nickel, gallium, germanium, cobalt, copper and chromium in the kamacite and taenite phases of iron meteorites. *Geochim. et Cosmochim. Acta* **13,** 233–247.

Nockolds S. R. (1954) Average chemical compositions of some igneous rocks. *Bull. Geol. Soc. Amer.* **65,** 1007–1032.

Nockolds S. R. and Allen R. (1953) The geochemistry of some igneous rock series. *Geochim. et Cosmochim. Acta* **4,** 105–142.

Nockolds S. R. and Allen R. (1954) The geochemistry of some igneous rock series—I. *Geochim. et Cosmochim. Acta* **5,** 245–285.

Nockolds S. R. and Allen R. (1956) The geochemistry of some igneous rock series—II. *Geochim. et Cosmochim. Acta* **9,** 34–77.

Nockolds S. R. and Mitchell R. L. (1948) The geochemistry of some Caledonian plutonic rocks: a study in the relationship between the major and trace elements of igneous rocks and their minerals. *Trans. Roy. Soc. Edinb.* **61,** 533–575.

Noddack I. and Noddack W. (1930) The abundances of the chemical elements. *Naturwiss. Rdsch.* **18,** 757–764.

Noddack I. and Noddack W. (1940) Die Haufigkeiten der Schwermetalle in Meerestieren. *Ark. Zool.* A **32,** No. 4, 1–35.

Osborne E. F. (1959) Role of oxygen pressure in the crystallization and differentiation of basaltic magma. *Amer. J. Sci.* **257,** 609–647.

Patterson E. M. and Swaine D. J. (1955) Petrochemical study of tertiary tholeiitic basalts: middle lavas of the Antrim plateau. *Geochim. et Cosmochim. Acta* **8,** 173–181.

Pauling L. (1927) The sizes of ions and the structure of ionic crystals. *J. Amer. Chem. Soc.* **49,** 765–790.

Paulling L. (1940) *Nature of the Chemical Bond.* Cornell University Press, Ithaca, N.Y.

Perelman F. M., Zvorykin A. Y. and Gudima N. V. (1949) *Kobalt.* Akad. Nauk. SSSR, Moscow.

Perrault R. (1946) *Le Cobalt.* Dunod, Paris.

Poldervaart A. (1955) Chemistry of the earths crust. *Geol. Soc. Amer. Spec. Paper* 62, 119–144.

Ramberg H. (1952) Chemical bonds and the distribution of cations in silicates. *J. Geol.* **60,** 331–355.

Rankama K. and Sahama Th.G. (1950) *Geochemistry.* University of Chicago Press, Chicago.

Reed G. W. (1959) Activation analysis applied to geochemical problems. *Researches in Geochemistry* (Edited by Ableson P. H.). John Wiley, New York.

Ringwood A. E. (1955) The principles governing trace element behaviour during magmatic crystallization—I. The influence of electronegativity. *Geochim. et Cosmochim. Acta* **7,** 189–202.

Ronov A. B., Malyuga D. P. and Makarova A. I. (1955) Distribution of small amounts of nickel, cobalt and copper in the clays of the Russian platform. *Dokl. Akad. Nauk SSR* **105,** 129–132.

Sandell E. B. (1947) Contamination of silicate samples crushed in steel mortars. *Analyt. Chem.* **19,** 652–653.

Sandell E. B. and Goldich S. S. (1943) The rarer metallic constituents of some American igneous rocks. *J. Geol.* **51,** 99–115, 167–189.

Sandell E. B. and Perlich R. W. (1939) Determination of nickel and cobalt in silicate rocks. *Industr. Engng. Chem. (Anal.)* No. 11, 309–311.

Scott R. D. and Mitchell R. L. (1943) Concentration methods in spectrographic analysis—I Recovery of cobalt, molybdenum, copper and zinc from plant materials and soil extracts by 8-hydroxyquinoline. *Trans. J. Soc. Chem. Ind., London* **62,** 4–8.

Shaw D. M. (1954) Trace elements in pelitic rocks. *Bull. Geol. Soc. Amer.* **65,** 1151–1182.

Smales A. A., Mapper D. and Wood A. J. (1957) The determination of small quantities of nickel, cobalt and copper in rocks, marine sediments and meteorites. *Analyst* **82,** 75–88.

Smythe L. E. and Gatehouse B. M. (1955) Polarographic determination of traces of Cu, Ni, Co, Zn and Cd in rocks using rubeanic acid and 1-nitroso-2-naphthol. *Analyt. Chem.* **27,** 901–903.

Stanton B. J. (1944) The cobalt content of some South Island (New Zealand) limestones. *N.Z. J. Sci. Technol.* A **25,** No. 5, 221–224.

Stonehouse H. B. (1954) As association of trace elements and mineralization at Sudbury. *Amer. Miner.* **39,** 452–474.

Suess H. E. and Urey H. C. (1956) Abundances of the elements. *Rev. Mod. Phys.* **28,** 53–74.

Tatsumoto M. (1957) Chemical investigations of deep-sea deposits—XXII. Cobalt and nickel in sea deposits. *J. Chem. Soc. Japan, Pure Chem. Sect.* **78,** 38–42; *Chem. Abstr.* **48,** 11,251 (1954).

Torii T. (1955) Occurrences of cobalt in mineral springs of Japan. *J. Chem. Soc. Japan, Pure Chem. Sect.* **76,** 707–710; *Chem. Abstr.* **50,** 11,569 (1956).

Turekian K. K. (1957) Additional trace element analyses of standard granite G1 and standard diabase W1. *Science* **126,** 745–746.

Turekian and Kulp J. L. (1956) The geochemistry of strontium. *Geochim. et Cosmochim. Acta* **10,** 245–296.

Turekian K. K. and Carr M. H. (1960) The geochemistries of cobalt chromium and nickel. *Report XXI Session, Intern. Congr.* Pt. I, pp. 14–26.

Turekian K. K. and Carr M. H. (1961) Chromium, cobalt and strontium in some Bureau of Standards rock reference samples. *Geochim. et Cosmochim. Acta.* In press.

Verne C., Fryklund J. R. and Harner R. S. (1955) Comments on minor elements in pyrrhotite. *Econ. Geol.* **50,** 339–344.

Wager L. R. and Mitchell R. L. (1943) Preliminary observations on trace elements in the rocks of the Skaergaard intrusion, Greenland. *Miner. Mag.* **26,** 283–296.

Wager L. R. and Mitchell R. L. (1945) Distribution of vanadium, chromium, cobalt, and nickel in eruptive rocks. *Nature, Lond.* **156,** 207–208.

Wager L. R. and Mitchell R. L. (1951) The distribution of trace elements during strong fractionation of basic magma—a further study of the Skaergaard intrusion, East Greenland. *Geochim. et Cosmochim. Acta* **1,** 129–208.

Wager L. R. and Mitchell R. L. (1953). Trace elements in a suite of Hawaiian lavas. *Geochim. et Cosmochim. Acta,* **3,** 217–223.

Wangersky P. M. (1958) Mechanisms of marine sedimentation. Unpublished thesis, Yale University.

Warren H. V. and Delavault R. E. (1957). Biogeochemical prospecting for cobalt. *Trans. Roy. Soc. Canad.* **51,** 33–37.

Wedepohl K. H. (1960) Spurenanalytische Untersuchungen on Tiefseetonen aus dem Atlantik. *Geochim. et Cosmochim. Acta* **18,** 200–231.

Wickman F. E. (1954) The "total" amount of sediments and the composition of the "average igneous rock". *Geochim. et Cosmochim. Acta* **5,** 97–110.

Wiik H. B. (1956) The chemical composition of some stony meteorites. *Geochim. et Cosmochim. Acta* **9,** 279–289.

Wilson H. D. B. and Anderson D. T. (1959) The composition of Canadian sulfide ore deposits. *Bull. Canad. Min. Met.* **62,** 326–339.

Worzel J. L. and Shurbet G. L. (1955) Gravity interpretations from standard oceanic and continental crustal sections. *Geol. Soc. Amer. Spec. Paper* 62, 87–100.

Wust G. (1936) Die Gliederung des Weltmeeres. *Hydrog. Rev.* **13,** 46–56.

Young E. J. (1954) Trace elements in recent marine sediments. *Bull. Geol. Soc. Amer.* **65,** 1329.

Young R. S. (1948) *Cobalt.* Reinhold, New York.

Young R. S. (1957) The geochemistry of cobalt. *Geochim. et Cosmochim. Acta* **13,** 28–41.

Young R. S., Benfield D. A. and Strachan K. G. A. (1954) Cobalt in kimberlites. *Amer. Miner.* **39,** 143–144.

Geochimica et Cosmochimica Acta, 1961, Vol. 23, pp. 61 to 77. Pergamon Press Ltd. Printed in Northern Ireland

Activities and structure of some borosilicate melts

W. J. Knapp and H. Flood
Department of Engineering, University of California, Los Angeles, California

(*Received* 14 *August* 1960)

Abstract—The application of structural models to some calcium borosilicate melts was made to develop simple expressions of activities as functions of composition. Their applicability was tested with freezing point depression data from phase diagrams. The activity values obtained were compared with those computed from the calorimetric heat of fusion. Data from published phase diagrams for the systems $Ca_2B_2O_5$–$Ca(BO_2)_2$, $Ca_3(BO_3)_2$–Ca_2SiO_4, $Ca(BO_2)_2$–$CaSiO_3$, and $Ca_2B_2O_5$–$CaSiO_3$ were used. Simple ionic models seemed applicable to melts where isolated ions may be expected; in melts containing mixed ions in chains and rings, the so-called "group" model may be useful.

The authors, are respectively, Professor of Engineering, University of California, Los Angeles, and Professor of Inorganic Chemistry and Director, Institute of Silicate Science, Norwegian Institute of Technology, Trondheim, Norway.

I. Introduction

In recent years, increasing attention has been directed to the determination of the structure of silicate and borate melts by several experimental and analytical methods. For example, the work of Bockris and his associates (Bockris and Lowe, 1954; Bockris *et al.*, 1955, 1956; Bockris and Mellors, 1956) involving measurements of viscosity, electrical conductance, and density, presents a series of structural models for liquid silicates and borates. Förland (1955) has studied the structure of binary silicate melts high in silica, using data on the freezing point depression (cryoscopy), and recently (Förland, 1958) investigated the sulphate side of the system Na_2SO_4–Na_2SiO_3 by similar methods. Knapp and Flood (1957a, b) also have developed some melt models, using freezing point depression data, for a number of borosilicate melts. Bååk and Ölander (1955) considered the structure of melts in the system $CaSiO_3$–CaF_2. McKinnis and Sutton (1959) have suggested structural changes associated with the melting of silicates in glass-making.

This paper is a review of the deduction of melt structures by the calculation of activities from freezing point depression data. The method is presented together with applications to several systems of borosilicates. The data used were taken from liquidus curves of experimentally determined phase diagrams described in the literature, together with calorimetric values for the heat of fusion of components.

II. Models for Melts

The development of simple expressions for activities of components in melts has been presented previously (Knapp and Flood, 1957a,b). For purposes of calculation, three hypothetical types of melts may be considered: (1) melts composed of undissociated (molecular) components, (2) melts of dissociated (simple ionic) components, and (3) melts of dissociated components, where the ions are polymeric (e.g. rings and chains) in nature. A brief review of expressions of activities for each of the foregoing types is given here. Borosilicate melts are of the (2) and (3) types.

1. *Melts of undissociated (molecular) components*

Consider the molecular binary system A–B (Fig. 1), where solid solution formation is negligible. In a melt of composition A_xB_{1-x} at temperature T in equilibrium with solid A, the activity a_A of component A, referred to pure liquid A (at the same temperature) as the standard state, is given by the following:

$$-RT \ln a_A = \Delta H_f\left(1 - \frac{T}{T_0}\right) \tag{1}$$

where ΔH_f = heat (enthalpy) of fusion of pure A at its melting point;
T_0 = melting-point temperature of pure A.

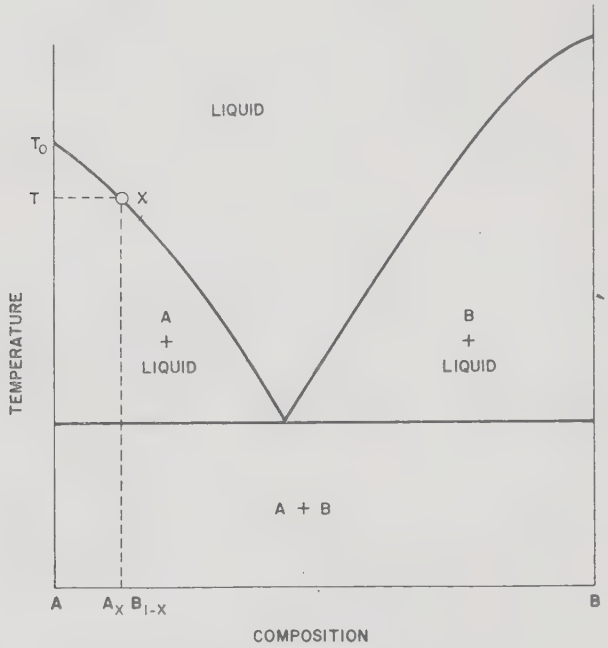

Fig. 1. Phase diagram for the molecular system A—B.

(In using the foregoing relation, the variation of ΔH_f with temperature is neglected). a_A may be further expressed, for a simple mixture of A and B molecules with mole fractions N_A and N_B as

$$a_A = N_A\gamma_A \tag{2}$$

γ_A = activity coefficient of component A.

Equation (1) may now be expressed as

$$\ln N_A + \ln \gamma_A = -\frac{\Delta H_f}{R}\left(\frac{1}{T} - \frac{1}{T_0}\right) \tag{3}$$

When experimental data are available, it is helpful to plot $\ln N_A$ against $1/T$ for several points on the liquidus of the phase diagram; the tangent to the resulting curve at $N_A = 1$ can be used to calculate a heat of fusion (ΔH_f) value. On the

other hand, if ΔH_f is known, the shape of the curve may indicate the extent of deviations from ideality (values of γ_A may be calculated for one composition at each temperature). If the $\ln N_A$ vs. $1/T$ plot is a straight line, whose slope gives a ΔH_f value in good agreement with that determined calorimetrically, the melt may be considered one whose deviations from ideal solution behaviour are small. Large negative deviations from ideality may be interpreted as a complex formation between A and B.

2. *Molten mixtures of simple ions*

Consider the system M_1X_1–M_2X_2, where the components are completely dissociated in melts; therefore, a particular melt in this system is composed of $n_{M_1^+}$ $n_{M_2^+}$ moles of metallic radicals (or cations) and $n_{X_1^-}$, $n_{X_2^-}$ moles of non-metallic radicals (or anions).

Temkin (1945) expresses the activity of component M_1X_1 in an ideal melt of this kind by

$$a_{M_1X_1} = N_{M_1}N_{X_1} \tag{4}$$

where N_{M_1} and N_{X_1} are the cation and anion fractions defined as

$$N_{M_1} = \frac{n_{M_1^+}}{n_{M_1^+} + n_{M_2^+}}, \qquad N_{X_1} = \frac{n_{X_1^-}}{n_{X_1^-} + n_{X_2^-}}$$

The statistical interpretation of the foregoing expressions is that the melt may be considered as two independent mixtures, i.e. the cation mixture and the anion mixture. In ideal and regular ionic mixtures, the cations M_1^+ and M_2^+ are randomly distributed over the cation positions (regardless of the number of the electrical charge), and the same is the case for the anions.

The partial molar entropy of the salt component then is equal to the sum of the partial entropies of the cations and anions, as

$$\bar{S}_{M_1X_1} = \bar{S}_{M_1^+} + \bar{S}_{X_1^-} = -(R \ln N_{M_1^+} + R \ln N_{X_1^-})$$

and therefore in ideal mixtures

$$\bar{S}_{M_1X_1} = -R \ln (N_{M_1^+} N_{X_1^+}) = -R \ln a_{M_1X_1} \tag{5}$$

The ideal Temkin model has proved to be valid for dilute ionic melt mixtures (Kordes *et al.*, 1951). In addition, theoretical expressions have been derived (Flood *et al.*, 1954) for activity coefficients in systems with deviations from ideality, which have proved to be useful for equilibria calculations of iron-slag reactions in basic open-hearth processes.

3. *Melts containing polymeric ions*

In melts containing polymeric ions, such as acid silicate and borate systems, it may be difficult to use the ionic model since neither the degree of polymerization (e. g. groups, rings and chains) nor the acid–base equilibria are known. For such polymeric melts, the possibility has been suggested by Flood *et al.* (1947) that the system could be considered, from a statistical viewpoint, a mixture of randomly

distributed silicate or borate groups (possibly occurring in pairs) of the types shown in Table 1.

Table 1. Group types for borates and silicates

General group family	Group types				
$SiO_n(4-2n)$ $BO_m(3-2m)$	SiO_4^{4-}, BO_3^{3-},	$SiO_{3\cdot5}^{3-}$, $BO_{2\cdot5}^{2-}$,	SiO_3^{2-}, BO_2^{1-},	$SiO_{2\cdot5}^{1-}$, $BO_{1\cdot5}^{0}$,	SiO_2^0

Each of the silicate groups proposed in Table 1 may be considered a silicon tetrahedrally bonded with 4, 3.5, 3, 2.5, or 2 oxygens (counting a bridged oxygen as $\frac{1}{2}$ and an unbridged oxygen as 1) and a borate group as a boron triangularly bonded with 3, 2.5, 2, or 1.5 oxygens. In this model, the degree and nature of polymerization are not determined, but the activities are related to the fractions of groups proposed in Table 1. This is based on the assumption that the differences in bonding energies of these groups are relatively small (and the heat of mixing is therefore negligible), so that the activity is chiefly determined by the entropy of mixing of the groups. This is shown by the following (at temperature T):

$$\bar{G}_1 = RT \ln a_1 = \bar{H}_1 - T\bar{S}_1 \approx -T\bar{S}_1 \tag{6}$$

where $\bar{G}_1$ = partial molar Gibbs free-energy change for a group component on mixing;

a_1 = activity of group component (i.e. $CaSiO_3$, $CaBO_{2.5}$, etc.);

$\bar{H}_1$ = partial molar heat (enthalpy) of mixing ≈ 0 for component 1;

$\bar{S}_1$ = partial molar entropy change.

Then for a random distribution of unpaired groups:

$$\bar{S}_1 = -R \ln N_1 \tag{7}$$

where $N_1 = \dfrac{n_1}{\Sigma n_g}$ (the group fraction);

n_1 = number of groups in question;

Σn_g = total number of all groups.

Hence

$$a_1 \approx N_1 \tag{8}$$

III. Application of Melt Models

Several examples of the application of melt models to some system of borosilicates may now be given. As suggested above, the activities of components may be calculated from different structural models. In general, if ideal behaviour is assumed, the partial molar entropy of a component is given by:

$$\bar{S}_1 = -R \ln a_1 = -R \ln \frac{n_1}{n_1 + n_2 + \ldots + n_m} \tag{9}$$

where $n_1, n_2, \ldots, n_m$ are the different structural equivalent units (ions, groups, etc.) in the molten mixture. The activity then is:

$$a_1 = \frac{n_1}{n_1 + n_2 + \ldots + n_m} \tag{10}$$

If well-determined phase diagrams are available, the activities of components computed with equation (10) may be given for corresponding temperatures along the liquidus curves.

To evaluate a model, activities may also be calculated with equation (1), providing the calorimetric heat of fusion is available, and may be compared with those from the model. In the examples to follow, the phase diagrams have been well studied, and experimentally determined points only of the liquidus curves have been used for computations.

1. $B_2O_5^{4-}$*-rich melts between* $Ca_2B_2O_5$ *and* $Ca(BO_2)_2$

The $CaO–B_2O_3$ phase diagram has been determined by Carlson (1932) (Fig. 2), and the heats of fusion of the calcium borates have been measured by King *et al.* (1948). Since the Ca^{2+} ion is the common cation in these melts, activities may be exprssed in terms of the anion composition.

The metaborate ion is known to exist in the solid state as $(BO_2)_3^{3-}$ rings (in Na and K compounds) and as infinite chains $(BO_2)_n$ (in $Ca(BO_2)_2$) (Wells, 1951). Therefore, it is simplest to visualize melts of this type as consisting of (a) simple ions like $B_2O_5^{4-}$ and $(BO_2)_n^{n-}$. On the other hand, it may also be worth while to consider such a melt as (b) a group mixture of chain molecules of different lengths, symbolized by the formula

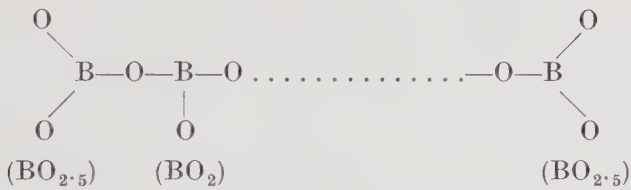

If the model of the ionic type is valid, an activity expression based on the existence of $B_2O_5^{4-}$ and $(BO_2)_3^{3-}$ ions is the most simple alternative. For this model (using equation (10))

$$a_{Ca_2B_2O_5} = N_{B_2O_5} = \frac{n_{B_2O_5}}{n_{B_2O_5} + n_{(BO_2)_3}} \qquad \text{(ionic model)}$$

An example of the actual computation of $a_{Ca_2B_2O_5}$, or $N_{B_2O_5}$, can be given for this ionic model. Let us choose from the results of Carlson (1932) an experimental point on the liquidus curve, whose co-ordinates are about 1280°C and 58·4 per cent CaO by weight (see Fig. 2). If this composition is recalculated in terms of $Ca_2B_2O_5$ and $Ca(BO_2)_2$ as components, it may be expressed at approximately 74·0 moles per cent $Ca_2B_2O_5$ and 26·0 moles per cent $Ca(BO_2)_2$. The activity computation for this composition then is simply:

$$a_{Ca_2B_2O_5} = N_{B_2O_5} = \frac{n_{B_2O_5}}{n_{B_2O_5} + n_{(BO_2)_3}} = \frac{0{\cdot}740}{0{\cdot}740 + 2/3(0{\cdot}260)} = 0{\cdot}81$$

This result, and the results of similar computations for other points on the liquidus curve (for this ionic model), are given in Table 2 and are shown graphically in Fig. 3.

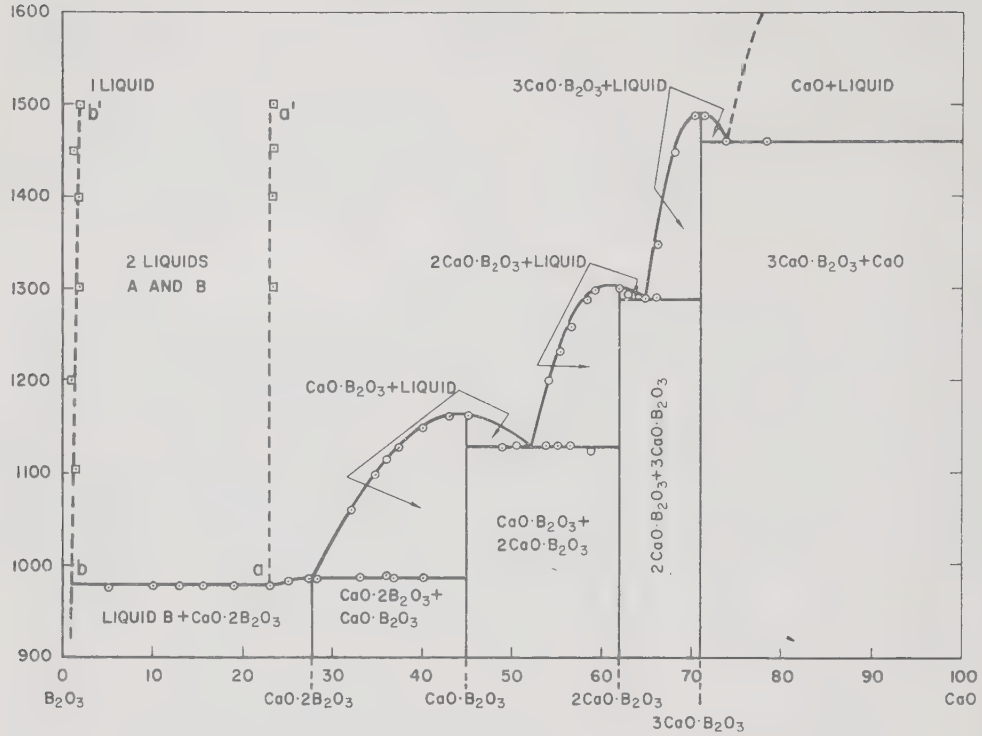

Fig. 2. Phase diagram for the system CaO—B_2O_3, after CARLSON (1932).

Table 2. Data for the diborate-rich side of the system $Ca_2B_2O_5$–$Ca(BO_2)_2$

Liquidus temp. (°C)	$\frac{n_{B_2O_5}}{n_{B_2O_5} + n_{(BO_2)_3}}$	$a_{Ca_2B_2O_5}$*
1280	0·81	0·80
1255	0·73	0·70
1224	0·62	0·59
1183	0·52	0·47

* From ΔH of fusion (KING *et al.*, 1948) $T_f = 1330$°C.

For the group model of polymeric chain molecules, and activity expression such as

$$a_{CaBO_{2\cdot5}} = N_{BO_{2\cdot5}} = \frac{n_{BO_{2\cdot5}}}{n_{BO_{2\cdot5}} + n_{BO_2}} \qquad \text{(group model)}$$

can be tried.

The shape of the liquidus curve indicates that the diborate ion is dissociated to a certain degree in molten $Ca_2B_2O_5$.

The activity vs. $1/T$ plot for a valid model would allow for the estimation of the

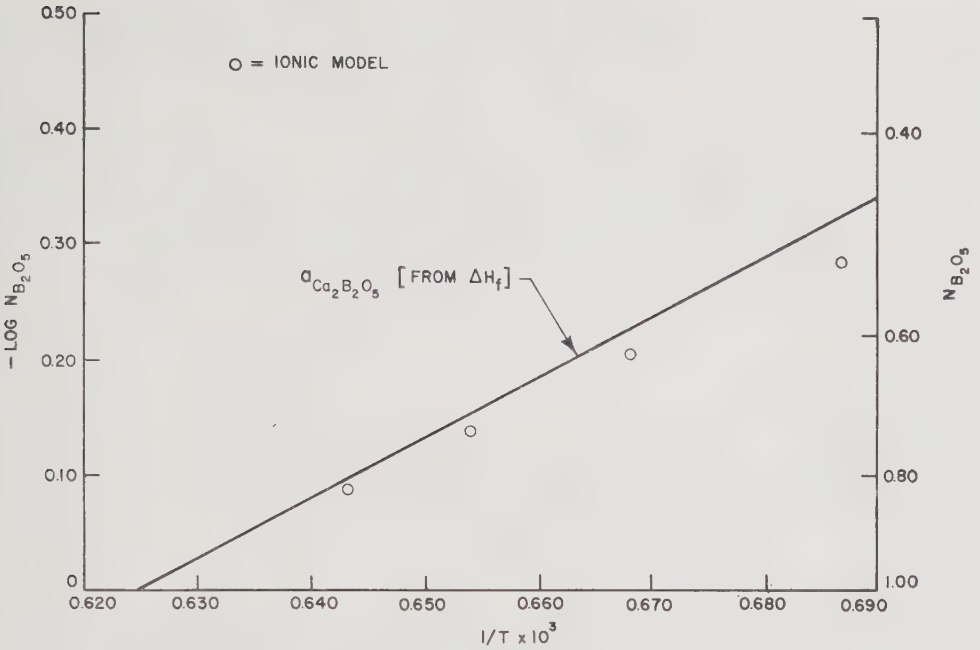

Fig. 3. Activities of melts of example 1 from the diborate side of the system $Ca_2B_2O_5$—$Ca(BO_2)_2$ (ionic model).

theoretical melting-point temperature of undissociated $Ca_2B_2O_5$. This is determined simply be extrapolating the $-\log N$ vs. $1/T$ plot to intersect the $1/T$ axis; the value of $1/T$ intersected gives the desired temperature.

The applicability of the foregoing models is evaluated by plotting $-\log N$ vs. $1/T$, as shown in Fig. 3 and 4. Plots of $-\log a$, calculated from the calorimetric

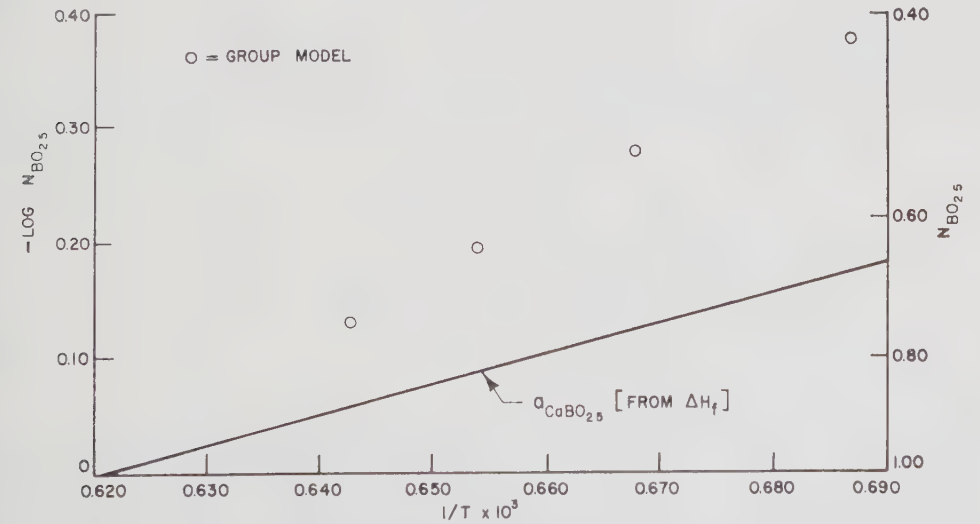

Fig. 4. Activities of melts of example 1 from the diborate side of the system $Ca_2B_2O_5$—$Ca(BO_2)_2$ (group model).

(King *et al.*, 1948) heat of fusion of $Ca_2B_2O_5$, are also shown (Fig. 3 and 4); these activities are plotted so that their intercept on the $1/T$ axis is common with the intercept corresponding to the estimated melting-point temperature mentioned above.

Fig. 3 indicates that the ionic model of $B_2O_5^{4-}$ and $(BO_2)_3^{3}$ ions gives activities in good agreement with values from experimental data. The existence of appreciable amounts of higher $(BO_2)_n^{n-}$-polymers seems to be improbable since this will increase deviations from the calorimetric heat of fusion. The group model does not

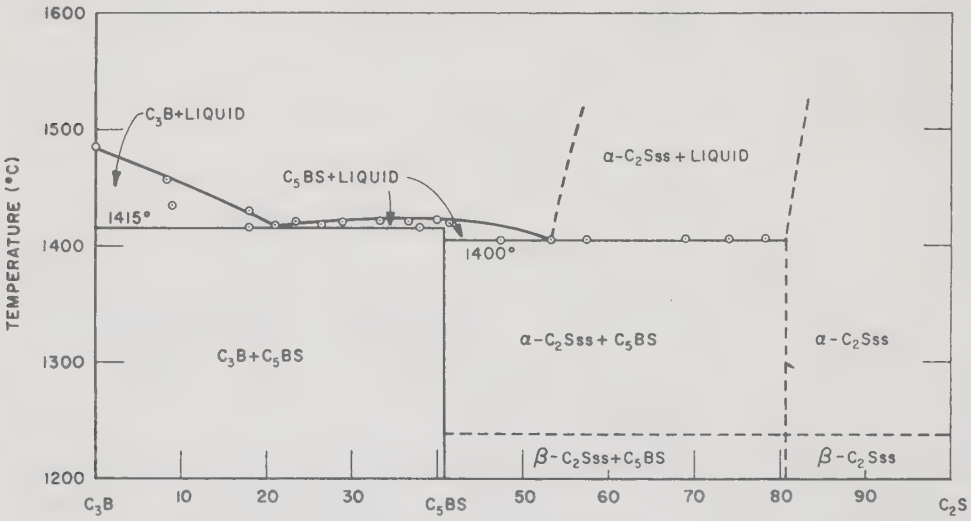

Fig. 5. The system $3CaO{\cdot}B_2O_3$—$2CaO{\cdot}SiO_2$, after Flint and Wells (1936).

seem to be applicable to these melts (Fig. 4). A value for the theoretical melting-point temperature of $Ca_2B_2O_5$ (undissociated), determined from Fig. 3 as indicated in the foregoing, is about 1330°C. (This result probably is somewhat low, since the presence of minor amounts of other types of ions, not foreseen in the present model, will tend to increase the depression of the fusion point.) By using the theoretical melting-point temperature of undissociated $Ca_2B_2O_5$ with equation (3), the dissociation of the $B_2O_5^{4-}$ ion, in liquid $Ca_2B_2O_5$ at its melting point, can also be calculated; the results indicate that at least 0·92 of the $B_2O_5^{4}$ ions are undissociated, whereas the dissociation products should be approximately 0·06 BO_3^{3} and 0·02 $(BO_2)_3^{3-}$, according to a dissociation reaction such as

$$3B_2O_5^{4-} \rightleftharpoons 3BO_3^{3-} + (BO_2)_3^{3-}$$

Pertinent data for these melts are given in Table 2.

2. BO_3^{3-}*-rich melts between* $Ca_3(BO_3)_2$ *and* Ca_2SiO_4

The liquidus curve on the calcium borate side of the diagram of Flint and Wells (1936) (Fig. 5) was used. The Ca^{2-} ion is common to both components, so we shall concern ourselves with the anion content. With a mixture of BO_3^{3-} and SiO_4^{4-} anions, it seems reasonable that a simple ionic model may be used, as no strong

tendency for polymerization or other reaction of anions should be expected. In this case, the activity expression is simply

$$a_{Ca_{1\cdot5}BO_3} = N_{BO_3} = \frac{n_{BO_3}}{n_{BO_3} + n_{SiO_4}} \qquad \text{(ionic model)}$$

where a = activity
N = mole fraction
n = number of moles

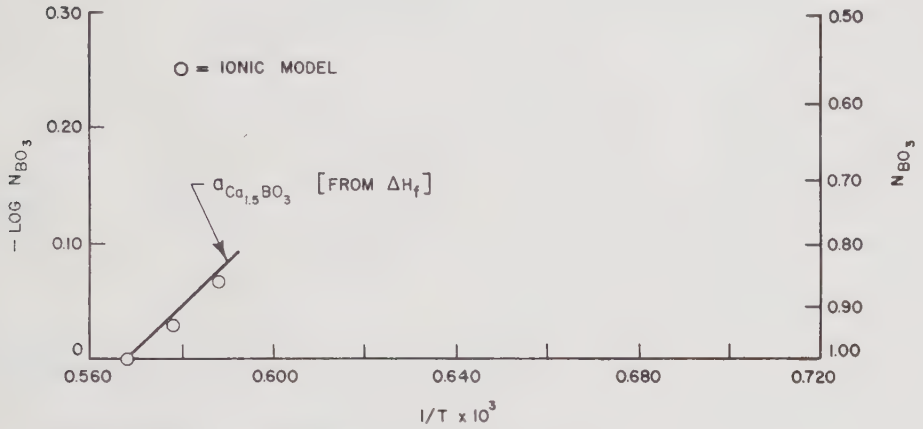

Fig. 6. Activities of melts of example 2 from the borate side of the system $Ca_3(BO_3)_2$—Ca_2SiO_4.

As discussed previously, (Knapp and Flood, 1957a,b) it is helpful to plot $-\log N_{BO_3}$ vs. $1/T$, as shown in Fig. 6. Since only two points were available for testing the model, the result must be considered as a preliminary indication. The activity of $Ca_{1\cdot5}BO_3$ determined from the calorimetric heat of fusion (King *et al.*, 1948) of $Ca_3(BO_3)_2$ is also plotted in Fig. 6. The agreement of calculated N_{BO_3} values with $a_{Ca_{1\cdot5}BO_3}$ values from calorimetric data lends support to the applicability of the simple ionic model, and indicates a high degree of ideality of the mixture (activity coefficients are lower than 1·025). Activity data for the foregoing melts are given in Table 3.

3. *Melts between* $Ca(BO_2)_2$–$CaSiO_3$

The heat of fusion of $CaSiO_3$ can be considered as well established from calculations based on the phase diagrams $CaSiO_3$–$BaSiO_3$ (Eskola, 1932), $CaSiO_3$-K_2-SiO_3 (Morey *et al.*, 1930) $CaSiO_3$–$MgSiO_3$ (Allen *et al.*, 1909) and $CaSiO_3$–CaF_2 (Bäak and Ölander, 1955) giving a value of approximately 13,400 cal/mole.

The phase diagram of Flint and Wells (1936) for this system was used (Fig. 7). The most simple approach is to consider these melts as being simple ionic in nature. The metasilicate ions may be considered as $(SiO_3)_3^{4-}$ rings, for the reasons proposed by Bockris (Bockris and Lowe, 1954; Bockris and Mellors, 1956; Bockris *et al.*, 1955, 1956) and others (Bäak and Ölander, 1955). The metaborate ions may be assumed to be $(BO_2)_3^{3}$ rings, in agreement with the work in

Table 3. Data for borate-rich side of the system $Ca_2(BO_2)_2$–Ca_2SiO_4

Liquidus temp. (°C)	$\frac{n_{BO_3}}{n_{BO_3} + n_{SiO_4}}$	$a_{Ca_{1.5}BO_3}$*
1487	1·00	1·00
1457	0·93	0·92
1428	0·86	0·84

* From ΔH of fusion (King *et al.*, 1948).

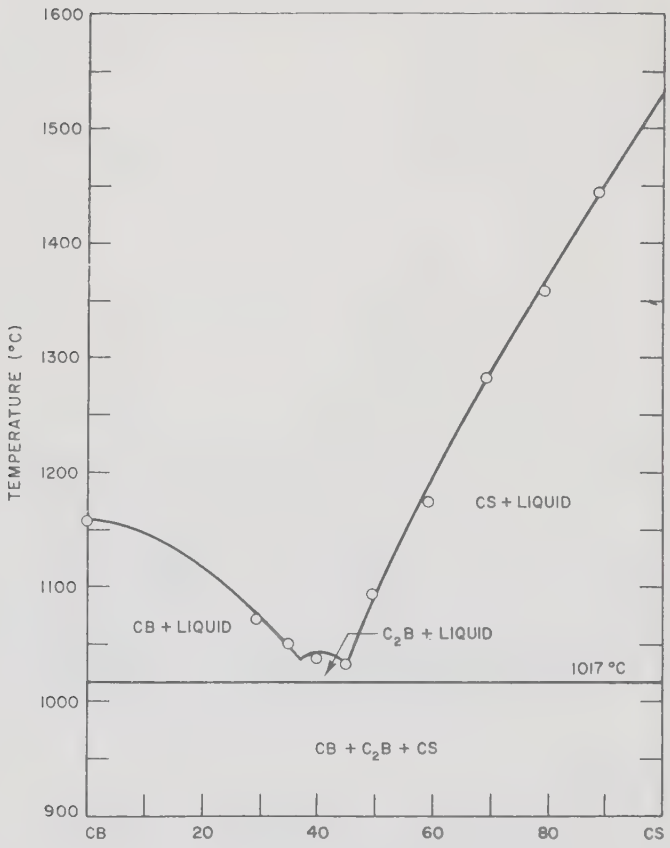

Fig. 7. The join $CaO{\cdot}B_2O_3$—$CaO{\cdot}SiO_2$, after Flint and Wells (1936).

Section (1) and since the structure of solid metaborates is known to be characterized by the presence of rings and chains. Activity expressions, based on the ions proposed in the foregoing and assuming no interaction of anions, are as follows:

Borate-rich side

$$a_{Ca_{1.5}(BO_2)_3} = N_{(BO_2)_3} = \frac{n_{(BO_2)_3}}{n_{(BO_2)_3} + n_{(SiO_3)_3}} \qquad \text{(ionic model)}$$

Silicate-rich side

$$a_{(CaSiO_3)_3} = N_{(SiO_3)_3} = \frac{n_{(SiO_3)_3}}{n_{(SiO_3)_3} + n_{(BO_2)_3}} \qquad \text{(ionic model)}$$

However, it is seen that activity values given by the above expressions are obviously incorrect as compared with values derived from heats of fusion of the components (see Table 4). Therefore, the ionic model proposed above does not seem to be applicable.

Table 4. Data for the system $Ca(BO_2)$–$CaSiO_3$ (ionic model)

Borate-rich side			Borate-rich side		
Liquidus temp. (°C)	$\frac{n_{(BO_2)_3}}{n_{(BO_2)_3} + n_{(SiO_3)_3}}$	$a_{Ca_{1\cdot5}(BO_2)_3}$*	Liquidus temp. (°C)	$\frac{n_{(SiO_3)_3}}{n_{(SiO_3)_3} + n_{(BO_2)_3}}$	$a_{(CaSiO_3)_3}$†
1162	1·00	1·00	1540	1·00	1·00
1070	0·82	0·53	1454	0·83	0·58
1050	0·78	0·36	1363	0·68	0·30
			1285	0·55	0·16
			1177	0·44	0·06
			1095	0·35	0·03

* From ΔH of fusion (King *et al.*, 1948).

† From ΔH of fusion (Bääk and Ölander, 1955).

Another possibility is that the anions combine to form mixed rings (or chains) possessing a completely random distribution, such as

$(SiO_3)_n^{2n-} + (BO_2)_n^{n-} =$

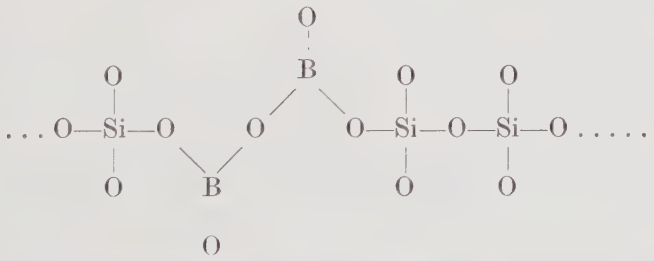

In such melts, it seems reasonable that the group model is appliable. The pertinent activity expressions are as follows:

Borate-rich side

$$a_{Ca_{0\cdot5}BO_2} = N_{BO_2} = \frac{n_{BO_2}}{n_{BO_2} + n_{SiO_3}} \qquad \text{(group model)}$$

Silicate-rich side

$$a_{CaSiO_3} = N_{SiO_3} = \frac{n_{SiO_3}}{n_{SiO_3} + n_{BO_2}} \qquad \text{(group model)}$$

The activities given by these expressions, based on the group model, are in good agreement with activities determined from the calorimetric heats of fusion of $Ca(BO_2)_2$ (King *et al.*, 1948), and $CaSiO_3$, as shown in Fig. 8 and 9 as well as in

Table 5. It therefore seems to be quite evident that mixed Si—O—B— ring ions or chains are formed.

Table 5. Data for the system $Ca(BO_2)_2$–$CaSiO_3$ (group model)

Borate-rich side			Silicate-rich side		
Liquidus temp. (°C)	$\frac{n_{BO_2}}{n_{BO_2}+n_{SiO_3}}$	$a_{Ca_{0.5}BO_2}$*	Liquidus temp. (°C)	$\frac{n_{SiO_3}}{n_{SiO_3}+n_{BO_2}}$	a_{CaSiO_3}†
1162	1·00	1·00	1540	1·00	1·00
1070	0·82	0·80	1454	0·83	0·83
1050	0·78	0·77	1363	0·68	0·68
			1258	0·55	0·55
			1177	0·44	0·40
			1095	0·35	0·28

* From ΔH of fusion (KING *et al.*, 1948).

† From ΔH of fusion (BÅÅK and ÖLANDER, 1955).

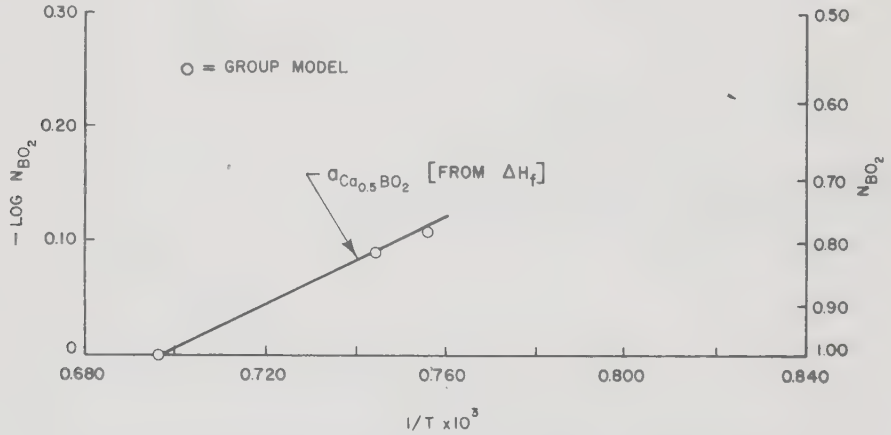

Fig. 8. Activities of melts of example 3 from the boater side of the system $Ca(BO_2)_2$—$CaSiO_3$ (group model).

4. *Melts between* $Ca_2B_2O_5$–$CaSiO_3$

Data from the phase diagram of FLINT and WELLS (1936) Fig. 10 were used. As the metaborate ion is considered to be a stronger acid than the metasilicate ion, and the disilicate ion to be a stronger base than the diborate ion, a considerable acid–base reaction (oxygen–ion transfer) between the diborate and metasilicate should not occur. The most simple ionic model for these melts is to assume the existence of $(SiO_3)_3^{6-}$ ions and $B_2O_5^{4-}$ ions (for reasons discussed in previous examples). The pertinent activity expressions are as follows:

$$a_{Ca_2B_2O_5} = N_{B_2O_5} = \frac{n_{B_2O_5}}{n_{B_2O_5} + n_{(SiO_3)_3}} \qquad \text{(ionic model)}$$

$$a_{(CaSiO_3)_3} = N_{(SiO_3)_3} = \frac{n_{(SiO_3)_3}}{n_{(SiO_3)_3} + n_{B_2O_5}} \qquad \text{(ionic model)}$$

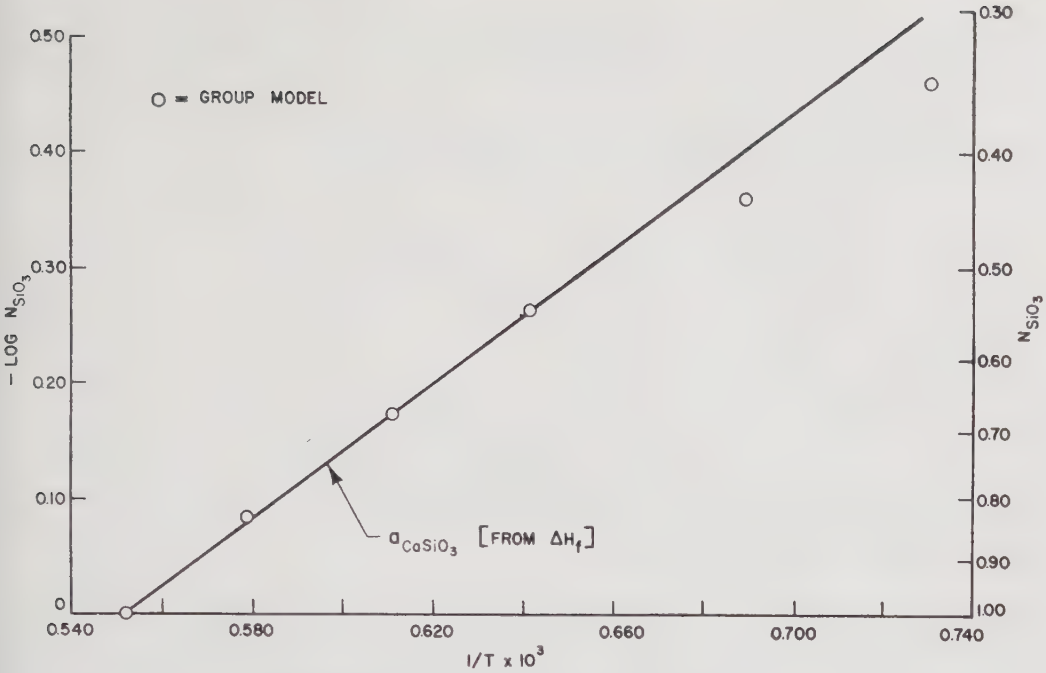

Fig. 9. Activities of melts of example 3 from the silicate side of the system $Ca(BO_2)_2$—$CaSiO_3$ (group model).

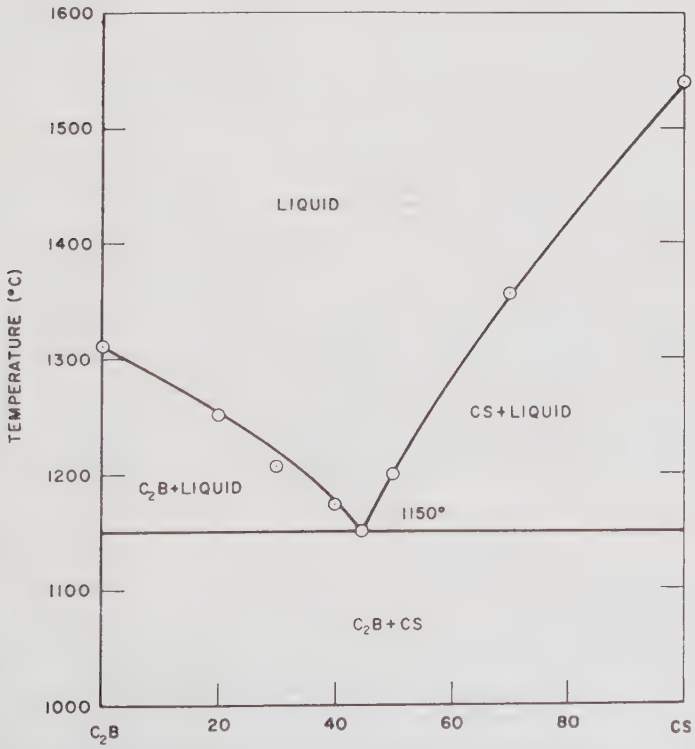

Fig. 10. The system 2 $CaO{\cdot}B_2O_3$—$CaO{\cdot}SiO_2$, after Flint and Wells (1936).

for borate-rich and silicate-rich melts, respectively. However, it is seen in Table 6 that these expressions do not fit the experimental data and that the foregoing ionic models are not applicable.

Another ionic model may be considered for borate-rich melts of this system. Assume that mixed ions of the following type are formed:

$$B_2O_5^{4-} + 1/3(SiO_3)_3^{6-} = \begin{matrix} O & & O & & O \\ \diagdown & & | & & \diagup \\ B & - & O & - & Si \\ \diagup & & | & & \diagdown \\ O & & O & & O \end{matrix} \begin{matrix} & & & & \\ - & O & - & B & \\ & & & & \end{matrix} \begin{matrix} O \\ \diagup \\ \\ \diagdown \\ O \end{matrix}$$

The appropriate activity expression is

$$a_{CaB_2O_5} = N_{B_2O_5} = \frac{n_{B_2O_5} - 3n_{(SiO_3)_3}}{n_{B_2O_5}} = \frac{n_{B_2O_5} - n_{SiO_3}}{n_{B_2O_5}} \quad \text{(ionic model)}$$

However, again this expression gives activity values not in agreement with those from heat of fusion data (see Table 6).

Table 6. Data for the system $Ca_2B_2O_5$–$CaSiO_3$ (ionic model)

Borate-rich side				Silicate-rich side		
Liquidus temp. (°C)	$\frac{n_{B_2O_5}}{n_{B_2O_5} + n_{(SiO_3)_3}}$	$\frac{n_{B_2O_5} - 3n_{(SiO_3)_3}}{n_{B_2O_5}}$	$a_{Ca_2B_2O_5}$*	Liquidus temp. (°C)	$\frac{n_{(SiO_3)_3}}{n_{(SiO_3)_3} + n_{B_2O_5}}$	$a_{(CaSiO_3)_3}$†
1312	1·00	1·00	1·00	1540	1·00	1·00
1245	0·89	0·64	0·71	1350	0·55	0·27
1205	0·82	0·33	0·58	1195	0·34	0·07
1170	0·75	0·00	0·47			

* From ΔH of fusion (King *et al.*, 1948).

† From ΔH of fusion (Bååk and Ölander, 1955).

Since none of the ionic models proposed above for these melts seems to be valid, it may be that a simple ionic model must include a number of mixed-ion types to describe the melt structure completely. In view of this possibility, as well as because of the polymeric nature of the metasilicate ion, it seems promising to try the model of mixed groups to give the following activity expressions:

Borate-rich melts

$$a_{CaBO_{2.5}} = N_{BO_{2.5}} = \frac{n_{BO_{2.5}}}{n_{BO_{2.5}} + n_{SiO_3}} \quad \text{(group model)}$$

Silicate-rich melts

$$a_{CaSiO_3} = N_{SiO_3} = \frac{n_{SiO_3}}{n_{SiO_3} + n_{BO_{2.5}}} \quad \text{(group model)}$$

The above expressions based on the group model, give activity values in satisfactory agreement with values from heat of fusion data (see Fig. 11 and 12 and

Table 7). It appears that the group model is useful in these melts (as in example 3) because of the polymerized condition of the anions.

Table 7. Data for the system $Ca_2B_2O_5$–$CaSiO_3$ (group model)

Borate-rich side			Silicate-rich side		
Liquidus temp. (°C)	$\frac{n_{BO_{2.5}}}{n_{BO_{2.5}} + n_{SiO_3}}$	$a_{CaBO_{2.5}}$*	Liquidus temp. (°C)	$\frac{n_{SiO_3}}{n_{SiO_3} + n_{BO_{2.5}}}$	a_{CaSiO_3}†
1312	1·00	1·00	1540	1·00	1·00
1245	0·85	0·85	1350	0·65	0·64
1205	0·75	0·75	1195	0·43	0·42
1170	0·67	0·69			

* From ΔH of fusion (King *et al.*, 1948).

† From ΔH of fusion (Bååk and Ölander, 1955).

A simplified picture of the structural characteristics of silicate-rich melts may be the following:

When a $B_2O_5^{4-}$ is added, it splits and causes the breaking of an $(SiO_3)_n^{2n}$ ring (or chain). The groups resulting from the split $B_2O_5^{4-}$ attach themselves to the broken ends of the $(SiO_3)_n^{2n-}$ ring (chain), forming $BO_{2.5}$ end groups without changing the number of SiO_3 groups, as follows:

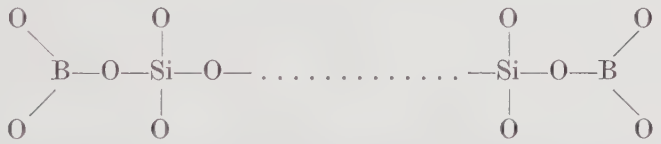

In the case of borate-rich melts in this system, additions of $(SiO_3)_n^{2n-}$ to the pure borate may cause splitting of $B_2O_5^{4}$ ions to form mixed ions containing several $(SiO_3)^{2-}$ groups, for instance:

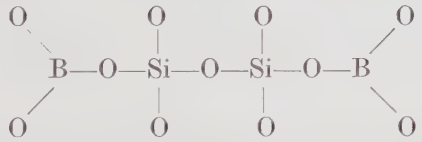

Such melts may be most simply considered in terms of their content of $BO_{2.5}$ and SiO_3 groups, from a statistical viewpoint.

IV. Conclusions

Simple structural models may be developed for the borosilicate melts studied and are useful in expressing activities as functions of composition. Such models also may allow for the deduction of melt structures. It should be emphasized that the successful use of a structural model is not necessarily an assurance of the uniqueness of the model. All possible models should be evaluated and, if possible, confirmed by data from independent experiments.

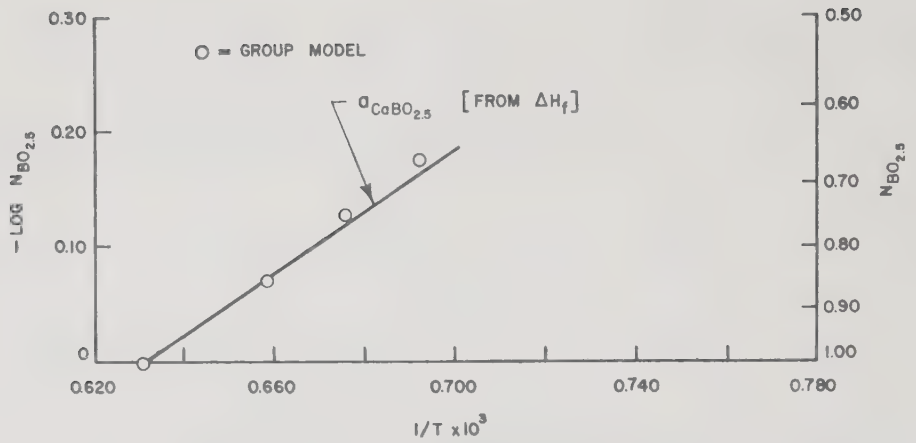

Fig. 11. Activities of melts of example 4 from the borate side of the system $Ca_2B_2O_5$—$CaSiO_3$ (group model).

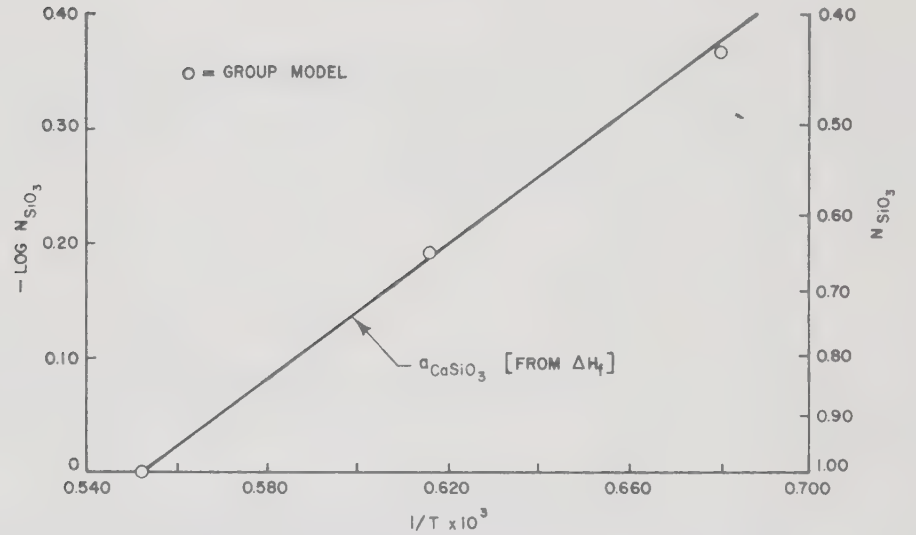

Fig. 12. Activities of melts of example 4 from the silicate side of the system $Ca_2B_2O_3$—$CaSiO_3$ (group model).

Simple ionic models seemed to be applicable to borosilicate melts where isolated ions may be expected; the so-called "group" model may be useful for melts with mixed ions existing as rings and chains.

References

Allen E. T., White W. P., Wright F. E., and Larsen E. S. (1909) Diopside and its relations to calcium and magnesium metasilicates. *Amer. J. Sci.* 4th Series, **27**, 1–47.

Bååk T. and Ölander A. (1955) The system $CaSiO_3$–CaF_2. *Acta Chem. Scand.* **9**, No. 8, 1350–1354. (In English).

Bockris J. O'M. and Lowe D. C. (1954) Viscosity and structure of molten silicates. *Proc. Roy. Soc.* A **226**, No. 1167, 423–435.

Bockris J. O'M., Mackensie J. D. and Kitchener J. A. (1955) Viscous flow in silica and binary liquid silicates. *Trans. Faraday Soc.* **51,** 1734–1748.

Bockris J. O'M. and Mellors G. W. (1956) Electric conductance in liquid lead silicates and borates. *J. Phys. Chem.* **60,** 1321–1328.

Bockris J. O'M., Tomlinson J. W. and White J. L. (1956) Structure of the liquid silicates – Partial molar volumes and expansivities. *Trans. Faraday Soc.* **52,** No. 3, 299–310.

Carlson E. T. (1932) The system $CaO–B_2O_3$. *Bur. Stand. J. Res.* **9,** No, 6, 825–832; RP510, p. 830

Eskola P. (1922) Silicates of strontium and barium. *Amer. J. Sci.* 5th Series, **4,** No. 23, 331–375; p. 358.

Flint E. P. and Wells L. S. (1936) System lime-boric oxide-silica. *J. Res. Nat. Bur. Stand.* **17,** No. 5, 727–752; RP 941.

Flood H., Förland T. and Roald B. (1947) Acidic and basic properties of oxides. III –Relative acid base strengths of some polyacids. *Acta Chem. Scand.* **1,** No. 9, 790–798. (In English).

Flood H., Förland T. and Grjotheim K. (1954) Uber den Zusammenhang zwischen Konzentrationen und Aktivitäten in geschmolzenen Salzmischung. (Relation between concentration and activity in molten mixtures of salts). *Z. anorg. Chem.* **276,** No. 5, 289–315.

Flood H., Fykse O. and Urnes S. (1955) Über den Zusammenhang zwischen Konzentrationen und Aktivitäten in geschmolzenen Salzmischungen II. (Relation between concentration and activity in molten mixtures of salts—II). *Z. Elektrochem.* **59,** No. 5, 364–370.

Förland T. (1955) Freezing point depression and its structural interpretation. *Office of Naval Research Tech. Report* No. 63, Contract N6 ONR 269, Task Order 8 NR 032–264, The Pennsylvania State University.

Förland T. (1958) Investigation of silicate groups in fused mixtures by phase diagram measurements. *J. Amer. Ceram. Soc.* **41,** No. 112, 524–527.

King E. G., Torgeson D. R. and Cook O. A. (1948) High temperature heat contents of $3CaO·B_2O_3$, $2CaO·B_2O_3$ and $CaO·2B_2O_3$. *J. Amer. Chem. Soc.* **70,** No. 6, 2160–2163.

Knapp W. J. and Flood H. (1957a) Activities in borosilicate melts. I—Some melts in the system $CaO–B_2O_3$. *J. Amer. Ceram. Soc.* **40,** No. 7, 246–249.

Knapp W. J. and Flood H. (1957b) Avtivities in borosilicate melts. II—Some mixtures of calcium borates—calcium silicates. *J. Amer. Ceram. Soc.* **40,** No, 8, 262–268.

Kordes E., Bergamnn W. and Vogel W. (1951) Freezing-point lowering of molten salts by addition of extraneous salts—I. *Z. Elektrochem.* **55,** No. 7, 600–606.

McKinnis C. L. and Sutton J. W. (1959) The glassmelting process. I—A theory of the nature of silicate melts and of their interaction with silica. *J. Amer. Ceram. Soc.* **42,** No. 4, 194–199.

Morey G. W., Kracek F. C. and Bowen N. L. (1930) The ternary system $K_2O–CaO–SiO_2$. *J. Soc. Glass Technol.* **14,** No. 54, 149–187.

Temkin M. (1945) Mixtures of fused salts as ionic solutions. *Acta Physiochim. U.R.S.S.* **20,** 411–420.

Wells A. F. *Structural Inorganic Chemistry* (2nd Ed.). Oxford University Press, New York.

Geochimica et Cosmochimica Acta, 1961, Vol. 23, pp. 78 to 99. Pergamon Press Ltd. Printed in Northern Ireland

On the evaluation of glauconite and illite for dating sedimentary rocks by the potassium–argon method*

J. F. Evernden, G. H. Curtis, J. Obradovich and R. Kistler

(*Received* 23 *June* 1960)
(*in revised form* 24 *August* 1960)

Abstract—Potassium–argon dates of stratigraphically known biotite-bearing tuffs, lava flows and intrusions when used as controls show that illite and glauconite samples selected carefully with regard to geologic history and prepared properly are suitable for obtaining dates almost as accurate as those from igneous biotite.

A tentative time-scale is constructed for the Tertiary epochs.

Introduction

Data accumulating from various geochronology laboratories appear to indicate that glauconite is of dubious usefulness for the purpose of obtaining accurate dates of sedimentary strata by the potassium–argon method. Recent work on illite seems to show even less promise for that mineral (Hurley *et al.* 1959). After an examination of the factors influencing the reliability of glauconite and illite dates, we compare a stratigraphically well-controlled sequence of such dates with a time-scale controlled by biotite dates. For glauconites that meet the required geologic conditions for argon retention, agreement with the biotite-controlled time-scale is remarkably good above the Cambrian. It appears from the illite ages presented that useful dates can be obtained from this mineral if careful sample preparation and selection procedures are followed. The consistency and large number of age data within the Tertiary are sufficient to permit construction of a tentative time-scale for the epochs of this period.

We are greatly indebted to numerous organizations and individuals whose assistance in the sample collecting was unstinted. We acknowledge the assistance of all individuals and organizations in the Appendix to this paper.

The pertinent data for all samples are tabulated in the Appendix. The sample localities are given to the accuracy known to us. The age figures are computed on the basis of Wetherill's (1957) estimate of the decay constants ($\lambda_\varepsilon = 0{\cdot}584 \times 10^{-10}$ year^{-1}, $\lambda_\beta = 4{\cdot}72 \times 10^{-10}$ year^{-1}).

Factors Detrimental to the Accuracy of Potassium–Argon Dates

The factors detrimental to the accuracy of potassium–argon dates of illite and glauconite are both chemical and physical, and fall into the general categories of diagenetic or chemical changes and diffusion losses. Surface weathering effects, though suspected of influencing results obtained on some samples, are too little known to permit discussion at this time.

* This work was supported by the Mary Sprague and Adolph C. Miller Institute for Basic Research in Science, the Atomic Energy Commission, and the National Science Foundation.

To be of value for dating purposes, clay minerals must have crystallized without inheriting radiogenic argon at the approximate time the stratum in which they occur was deposited or, if of detrital origin, have been free or freed of radiogenic argon at that time. If the clays are mixed with detrital potassium-bearing minerals other than clay, they must be mechanically separable from such minerals. The necessary condition in clay minerals of their being free from radiogenic argon at the time of formation of the stratum in which they occur may conceivably be met in several ways: (a) clays derived from ancient clay-bearing sedimentary rocks might be cleansed of their radiogenic argon during the weathering and transportation processes; (b) the clay minerals might have crystallized in the zone of weathering by soil-forming processes and shortly thereafter been washed into the basin of deposition; (c) the clay minerals might have grown authigenically in the stratum at about the time of deposition of accompanying sedimentary minerals; (d) detrital clay might lose whatever radiogenic argon it contains by diagenesis shortly after deposition.

For glauconite, the consensus supports an authigenic origin (alternative (c) above). It may be significant to note that the diameters of glauconite crystals in sandstones are of the order of 1 μ (Grim, 1952). For the clay minerals of claystones and shales, no such origin can be assumed. Weaver (1958), on the basis of X-ray analyses of clay minerals from thousands of samples, contends that the great majority of clay minerals in sedimentary rocks are detrital in origin and that these clays are only slightly modified in their depositional environments. Grim (1958), on the other hand, although agreeing with Weaver as to the origin of most clay minerals, believes that certain environments are conducive to diagenetic changes in some of the clay minerals, these changes usually being only partial. Milne and Earley (1958) appear to hold Grim's view concerning the importance of basin environment. Hurley (1959), in collaboration with others, has shown that detrital illite in modern river and estuarine sediments derived from ancient shale source rocks has retained much if not most of its radiogenic argon. Even illite samples from deep-ocean bottoms appear to be contaminated with detrital illite, presumably carried there by wind or ocean currents. It would appear that the wide-scale application of potassium–argon dating to the ubiquitous shales necessitates that either alternative (d) above operates on an unsuspected scale (at least on small grain sizes in certain environments) or that it is possible to separate authigenic and detrital clay minerals.

A cursory inspection of a tabulation of potassium content of glauconites vs. geologic age of the glauconites suggests an increase of potassium content with increasing age. Hurley (1959) has previously noted this. This is not a uniform increase but an increase indicated by averaging obtained potassium percentages over periods of 50 million years. The data suggest an average value of about 5·0 per cent for zero age, 5·5 per cent for 100-million year, and 6·2 for 500-million year glauconite. Weaver has presented evidence which indicates that clay alteration is simply upgrading of degraded clays by cation adsorption, principally addition of potassium and water, this addition taking place shortly after deposition. If the apparent trend in Hurley's and our data is real, potassium can be added to the clay lattice long after deposition. Whether such an addition will affect the

age of a Cambrian glauconite by as much as 10 per cent is uncertain. Mere addition of potassium in the amounts and according to the time schedule indicated would decrease the apparent age of a Cambrian glauconite by only 4 per cent. A schedule of late potassium addition, however, could be imagined which would decrease the apparent age of a Cambrian glauconite by 10–15 per cent. Such a schedule seems unlikely.

We have shown elsewhere (Evernden *et al.*, 1960), that the rate of argon diffusion in crystal lattices is markedly affected by lattice disturbances of any kind. Argon diffusion in glauconite and phlogopite is greatly increased during the period water is driven from the lattice. If glauconite is held under confining water pressures sufficient to prevent loss of water, argon diffusion is strongly retarded. From this we may surmise that addition of water and potassium to a clay lattice, although not changing the lattice in any major way, accelerates the outward diffusion of argon. Thus, it seems reasonable to presume that addition of potassium has a greater effect on the apparent age of a glauconite than mere addition of potassium would imply. Such an explanation of generally low Cambrian glauconite ages is not completely satisfactory in the light of Hurley's data suggesting moderate concordance of potassium–argon and rubidium–strontium ages in some Paleozoic glauconites, both indicated ages being too low.

Finally, diffusion losses of argon independent of chemical change of the clay mineral can lead to indicated ages which are much too young. In the paper cited (Evernden *et al.*, 1960), we indicated the possibly extreme influence of such diffusion. We present more evidence of such diffusion losses in this paper.

Biotite Control Data

The time-scale control data used are potassium–argon biotite dates obtained by us and others on stratigraphically known material from the Lower Pliocene to the Middle Ordovician. These data are shown on Table 1 and a more complete description of our samples is contained in the Appendix. We have accepted the stratigraphic ages assigned to these samples either in the literature or by personal communications.

Comparison of Glauconite Dates with Control Data

Table 1 is a compilation of all dates presented in this paper. The symbols under the column headed "Quality" are to be interpreted as follows: (***) means that the age indicated is within 5 per cent of the control time-scale, (**) means that the age indicated is within 10 per cent of the control time-scale, and (*) means that the age indicated is within 20 per cent of the control time-scale. (– – –) indicates a difference of more than 20 per cent between the indicated age and the control time-scale.

Limiting attention to the glauconite data for the moment, it can be seen that many of these potassium–argon ages are satisfactory. Several of those that are unsatisfactory can be rationalized on the basis of their known geologic history. Thus, the Kreyenhagen series is a nice example of the effect of burial and associated heating on the diffusion of argon from the micron-size grains of glauconite. KA 170 (Paleocene) is probably too low for the same reason. The quality of the

Table 1

Stratigraphic age	K/A age (years)	Mineral	% K	Run no.	Quality
Upper Pliocene	$5{\cdot}2 \times 10^6$	Glauconite	5·0	KA 192	*
Lower Pliocene	11	Biotite	6·1	KA 132	
Lower Pliocene (Clarendonian)	12	Biotite	6·4	KA 414	
Upper Miocene	10	Glauconite	5·3	KA 322	– – –
Upper Miocene (Barstovian)	15	Biotite	4·2	KA 161	
Upper Miocene (Barstovian)	15	Biotite	4·8	KA 449	
Lower Miocene (Zemorrian)	23	Glauconite	5·1	KA 171	– – –
Lower Miocene (Burdigalian)	25	Glauconite	4·1	KA 445	***
Lower Oligocene	32	Biotite	6·4	KA 175	
Oligocene Eocene boundary	33	Sanidine	4·7	KA 483	
Upper Eocene	31	Glauconite	6·2	KA 324	**
Base of Upper Eocene (Kreyenhagen)	43	Glauconite	5·4	KA 189	*** surface
Base of Upper Eocene (Kreyenhagen)	33	Glauconite	4·6	KA 285	– – – 6311 ft
Base of Upper Eocene (Kreyenhagen)	36	Glauconite	5·0	KA 154	– – – 8012–8063 ft
Base of Upper Eocene (Kreyenhagen)	31	Glauconite	5·4	KA 147	– – – 8230 ft
Base of Upper Eocene (Kreyenhagen)	27	Glauconite	5·2	KA 265	– – – 9220 ft
Base of Upper Eocene (Kreyenhagen)	25	Glauconite	5·4	KA 160	– – – 10,790 ft
Base of Upper Eocene (Kreyenhagen)	18	Glauconite	5·2	KA 267	– – – 12,175 ft
Base of Upper Eocene	39	Glauconite	3·9	KA 166	***
Top of Middle Eocene	42	Glauconite	5·8	KA 153	***
Middle Eocene (Type Lutetian)	47	Glauconite	6·0	KA 163	***
L. Middle Eocene (Claiborne)	39	Glauconite	6·2	KA 165	*
Base of Middle Eocene	42	Glauconite	5·4	KA 173	*
U. Lower Eocene (U. Wilcox)	52	Glauconite	4·5	KA 438	***
Lower Eocene (Alpine)	51	Glauconite	4·7	KA 440	***
L. Eocene or Paleocene	38	Glauconite	4·6	KA 162	– – –
Paleocene (Martinez)	46	Glauconite	4·9	KA 178	– – – 8100 ft
Paleocene (Martinez)	59	Biotite	2·5	KA 176	
Mid-Paleocene ("basal Eocene")	57	Glauconite	5·0	KA 274	***
Paleocene	46	Glauconite	3·7	KA 170	– – – 8155 ft
Paleocene	58	Glauconite	4·0	KA 172	*** 8100 ft
Maestrichtian	70	Glauconite	4·4	KA 152	***
Maestrichtian (2nd concentrate)	70	Glauconite	5·4	KA 439	***
Lower Campanian	81	Glauconite	5·3	KA 315	***
Santonian-Maestrichtian	81	Biotite	7·0	KA 177	
Lower Santonian	83	Glauconite	4·8	KA 323	***
Coniacian (Emscher)	87	Glauconite	3·5	KA 298	***
Middle Turonian	84	Glauconite	6·5	KA 306	***
Lower Turonian	86	Glauconite	6·8	KA 316	***
Cenomanian (Soester Greensand)	79	Glauconite	6·2	KA 309	*
Basal Cenomanian	91	Glauconite	5·0	KA 198	***
Albian/Cenomanian (?)	96	Biotite	6·2	KA 404	
Upper Albian	96	Glauconite	5·0	KA 186	***

Table 1 (Continued).

Stratigraphic age	K/A age (years)	Mineral	% K	Run no.	Quality
Albian	97	Glauconite	5·9	KA 273	***
Base of Middle Albian	94	Glauconite	6·5	KA 282	*
Lower Albian	94	Glauconite	5·9	KA 310	**
Aptian/Albian	102	Glauconite	4·8	KA 279	***
Aptian (Bargate Beds)	110	Glauconite	5·6	KA 446	***
Lower Aptian	115	Glauconite	4·4	KA 442	***
Upper Hauterivian	31	Glauconite	5·4	KA 311	– – –
Pre-Valanginian, post-Oxfordian	128	Biotite	6·3	KA 81	
Upper Portlandian	139	Glauconite	6·4	KA 313	** high
Lower Portlandian	125	Glauconite	6·6	KA 270	***
Post-Oxfordian	136	Biotite	7·0	KA 97	
Oxfordian	136	Glauconite	5·7	KA 312	***
Lower Oxfordian	26	Glauconite	3·3	KA 272	– – –
Callovian	139	Glauconite	6·0	KA 318	***
Callovian	131	Glauconite	6·0	KA 317	**
Top of Lower Jurassic	169	Biotite	3·6	KA 431	
Upper Lias	21	Glauconite	5·4	KA 308	– – –
Permian	254	Biotite	6·5	KA 276	
L. Upper Pennsylvanian	246	Illite	5·1	KA 262	**
Upper Carboniferous	278	Biotite	6·4	KA 461	
Pre-Stephan Zone, post-Kulmgraywacke	327	Biotite	4·9	KA 291	
Westphalian	295	Illite	2·9	KA 337	***
L. Lower Mississippian	305	Illite	2·1	KA 338	**
Upper Devonian	344	Biotite	6·2	KA 332	
Lower Devonian	347	Illite	4·2	KA 340	**
Basal Devonian	362	Illite	5·3	KA 339	**
Mid-Lower Silurian	284	Illite	5·6	KA 341	– – –
Mid-Lower Silurian	267	Illite	5·7	KA 342	– – –
Middle Ordovician	421	Biotite	6·2	KA 462	
Middle Ordovician	297	Bentonite	4·2	KA 289	– – –
Middle Ordovician	485	Illite	2·8	KA 343	** high
Lower Ordovician	406	Glauconite	6·1	KA 296	*
Lower Ordovician	423	Glauconite	7·0	KA 292	**
Lower Ordovician	434	Glauconite	6·5	KA 294	**
Lower Ordovician	420	Glauconite	6·4	KA 290	**
Top of Cambrian	457	Illite	5·8	KA 344	***
Base of Middle Cambrian	645	Illite	6·1	KA 258	– – – Bulk shale
Base of Middle Cambrian	708	Illite	6·2	KA 259	– – – 16–150 μ
Base of Middle Cambrian	646	Illite	6·0	KA 260	– – – 8–16 μ
Base of Middle Cambrian	530	Illite	5·9	KA 261	*** less than 8μ
Base of Middle Cambrian	447	Glauconite	4·8	KA 443	*
Base of Middle Cambrian	399	Glauconite	6·4	KA 293	– – –
Base of Middle Cambrian	406	Glauconite	5·2	KA 191	– – –
Top of Lower Cambrian	413	Glauconite	6·8	KA 299	– – –
Lower Cambrian	457	Glauconite	5·4	KA 444	– – –
Basal Cambrian	436	Glauconite	6·6	KA 271	– – –

Lower Ordovician glauconite dates is high (less than 10 per cent error) whereas the Cambrian dates obtained by us are useless. Cambrian glauconites from boreholes in Sweden and Gotland appear to give ages essentially the same as those given by Lower Ordovician glauconites from boreholes in the same area.

KA 308 is an interesting confirmation of the influence of post-depositional processes on argon retention. This is a sample of Upper Lias (Lower Jurassic) glauconitic sandstone from the Feltrine Alps of northern Italy. This area was deformed during the Alpine orogeny. The indicated potassium–argon age (21 million years) appears to date that orogeny rather than the time of deposition of the glauconite. Many of the unsatisfactory dates, however, are on samples about which we know too little to be able to explain the inaccuracies. We suspect, though we cannot give good supporting evidence, that several of the poor ages obtained are the result of using weathered material.

It appears from these data that it is possible to obtain useful potassium–argon ages from glauconites over a time span of approximately 400 million years if the glauconites used fulfill certain rigid conditions of geologic history (the Swedish glauconites were selected for lower Paleozoic because of their apparently ideal burial history). The use of glauconite in dating programs requires a careful investigation and evaluation of the geologic history of each sample used if significant results are to be obtained. With only one exception, all of our non-concordant glauconite dates are too young, thus seeming to indicate that during the authigenic processes leading to the generation of glauconite, pre-erosion argon is completely eliminated from the reconstituted debris. The sole exception to this rule is an upper Miocene glauconite from New Zealand that yielded an age of 30 million years (Lipson, 1958).

Our data suggest that the burial history of glauconite samples is one of the major items to be evaluated prior to their dating. The heating which occurs concomitant with burial may be sufficient to cause excessive argon loss. We realize that there are examples of deeply buried glauconites (such as our KA 172) which have yielded accurate ages. We can only suggest at this time that such dates are obtained from coarser-grained glauconites. There is a large variation in the sizes of the crystal grains of different glauconite samples.

Comparison of Illite Dates with Control Data

The illitic samples dated are from several different depositional environments. KA 308, 334, 340, 339, 341, 342, 343, 343A and 344 were obtained from shaly members of limestone sequences. All except 343A are determinations on bulk samples of the shale. KA 258, 259, 260 and 261 are clay fractions obtained from the same sample of Gros Ventre shale, a shale in a sequence of marine detrital sediments. The sized fractions were obtained after disaggregation of the sample rather than after crushing. The Fithian illite (KA 262) is a fine-grained underclay of a Pennsylvanian cyclothem. A bulk sample of this illite was used in our run. All of these illite samples were prepared and provided by the laboratory of Pan-American Petroleum Corporation.

The data obtained on these runs are included in Table 1 and it is clearly seen that they are not characterized by excessive age except for the bulk and

coarse-grained Gros Ventre samples. KA 343 yielded an age approximately 10 per cent too old whereas all of the others are within 10 per cent of the control age or are too young. These figures contrast the results of Hurley. The one sample that, in bulk, yielded a greatly excessive age is the Gros Ventre shale, the only normal marine shale in our samples. However, the sized fractions of this shale showed a continuous decrease of indicated age with decreasing grain size, the smallest sizes used (less than 8 μ) yielding an age within 1 per cent of the control age. The older ages obtained for the coarser fractions do show that they are contaminated, but whether the contamination is potassium-bearing minerals other than clay is not known. Microscopic and X-ray examination showed that a part of the material was fine-grained mica, quartz, and possibly potassium feldspar.

The hypothesis that the excellent fit of all illite dates to the biotite control is a fortuitous interplay between loss of radiogenic argon by diffusion and retention of pre-erosion radiogenic argon appears untenable. This idea might be entertained if the samples were taken from one geologic period and one geosynclinal basin, but they were taken from several different basins and they span 300 million years.

Either these samples are composed of uncontaminated authigenic or soil-formed clays (unlikely, in view of Hurley's and Weaver's work) or the contaminating pre-erosion argon has been removed by diagenesis shortly after burial. It may be significant that the clays obtained from limestone sequences, even when used in bulk, yielded satisfactory ages whereas the Gros Ventre does contain appreciable pre-erosion radiogenic argon in coarse grain sizes. Milne and Earley (1958) have pointed out that rapid deposition inhibits clay diagenesis by reducing the time for chemical interaction between sea water and clay. The clay associated with the limestone was in all probability at the water–clay interface of the sea bottom much longer than the Gros Ventre clay material. The Fithian illite, being an underclay of a Pennsylvanian cyclotherm, was also a product of slow deposition and slow subsidence. As noted above, we are not sure that the excess argon is not carried in minerals other than clay.

It thus appears that illite has not been eliminated as a mineral of promise for potassium–argon dating. Its usefulness does seem to depend upon the efficacy of diagenesis in removing radiogenic argon from detrital illite shortly after burial, at least in the finer grain sizes. Diffusion coefficients for illite appear to be similar to those for glauconite (Evernden *et al.*, 1960); therefore, burial and heating will be expected to influence argon retention in illite, the coarser grain sizes of much clay material possibly decreasing the percentage losses under given conditions.

Tertiary Time-scale

A tentative time-scale of the Tertiary can be constructed on the basis of the data presented here. Before so doing, we wish to make it clear that we realize the existence of paleontological disputes regarding the stratigraphic position of such boundaries as Cretaceous–Paleocene, Eocene–Oligocene, and Oligocene–Miocene. In addition, some world-wide correlations are insecure. At this time, we can contribute little to these problems though it is hoped that eventually absolute age-dating will help in their resolution.

Results obtained by using the potassium-argon method can be reproduced to

an accuracy of 1–2 per cent. The best dates obtained from early Paleozoic samples, therefore, have an uncertainty of from 5 to 10 million year, whereas the best dates obtained from Tertiary samples have an uncertainty of less than 1 million year. This raises the critical problem of palaeontologic correlations, for uncertainties of 5–10 million years in radioactive age determinations are sufficiently large to mask the uncertainties inherent in palaeontologic correlations between basins and probably between continents; but radioactive age uncertainties of 1 million year will probably be small enough both to demonstrate and resolve such paleontologic difficulties. Keeping in mind that the so-called boundaries between eras, periods and epochs are based upon the early misconception of periodic world-wide orogeny or catastrophe, and that these boundaries exist only locally at type-localities or in the imaginations of geologists, it is evident that the accuracy with which these boundaries can be established is limited by many factors. Difficulties of technique, of obtaining material precisely at boundaries of type sections, and of interpolating between dated points and boundaries of type sections, lead to results whose accuracy decreases as a function of age. It appears unlikely that we can know the time boundaries of any of the periods before the Mesozoic era more closely than 5–15 million years, and of the periods during and after the Mesozoic, more closely than 2–5 million years. The stages of the Cretaceous and the epochs of the Cenozoic may possibly be established to an accuracy of 1–2 million years, but only after resolution of the present paleontological disputes.

The time-scale presented is based upon the biotites and (***) results in Table 1. Base of Miocene is largely based upon the Burdigalian glauconite (KA 445). The Zemorrian date (KA 171) is suspect as it was obtained on a core from 5700′; therefore, we cannot state an absolute-age correlation between Zemorrian of California and Burdigalian of Europe.

It is to be noted that the Eocene–Paleocene and Paleocene–Cretaceous boundaries are significantly older than the values suggested previously (Evernden, 1959). The change is due to our learning of the influence of heating upon argon retention in glauconites. The previous time-scale was based upon dating results here listed but now thought to be invalid.

The time-scale follows:

	($\times 10^6$ years)
Pliocene–Miocene	12
Miocene–Oligocene	25
Oligocene–Eocene	33
Eocene–Paleocene	55
Paleocene–Cretaceous (Montian–Danian)	62
Paleocene–Cretaceous (Danian–Maestrichtian)	67

References

Curtis G. H., Evernden J. F. and Lipson J. (1958) *Age Determination of Some Granitic Rocks in California by the Potassium-Argon Method.* California Division of Mines, Special Report No. 54.

Evernden J. F. (1959) Dating of Tertiary and Pleistocene rocks by the potassium-argon method *Proc. Geol. Soc. London* No. 1565, 17–19.

Evernden J. F. *et al.* (1960) Argon diffusion in glauconite, microcline, sanidine, leucite and phlogopite. *Amer. J. Sci.* **258,** 583–604

Grim R. E. (1952) *Clay Mineralogy.* McGraw-Hill, New York.

Grim R. E. (1958) Concept of diagenesis in argillaceous sediments. *Bull. Amer. Ass. Pet. Geol.* **42,** 246–253 (1958).

Hurley P. M. *et al.* (1959) Authigenic versus detrital illite in sediments. *Bull. Geol. Soc. Amer.* **70,** No. 12, Pt. 2, 1622.

Lipson J. (1958) Potassium-argon dating of sedimentary rocks. *Bull. Geol. Soc. Amer.* **69,** 137–150.

Milne I. H. and Earley J. W. (1958) Effect of source and environment on clay minerals. *Bull. Amer. Ass. Pet. Geol.* **42,** 328–338.

Weaver C. E. (1958) Geologic interpretation of argillaceous sediments. I—Origin and significance of clay minerals in sedimentary rocks. *Bull. Amer. Ass. Pet. Geol.* **42,** 254–271.

Wetherill G. W. (1957) Radioactivity of potassium and geologic time. *Science* **126,** 545–549.

Appendix I

Biotite Control Dates

KA 81 biotite; K = 6·25 per cent; A/K = $7{\cdot}71 \times 10^{-3}$; A_{40}^{At} = 9 per cent; $t = 128 \times 10^6$ years.
Biotite concentrated from quartz diorite composing the Shasta Bally batholith.
Stratigraphic age: The intrusion is of the same age as intrusions in the foothills of the Sierra Nevada to the southeast which cut sedimentary rocks containing Oxfordian–Kimeridgian fossils. The intrusion is overlapped non-conformably by sedimentary rocks containing a Hauterivian fauna. South-westward a few miles from the intrusion these same beds lie conformably above beds containing Valanginian fossils.
Donor: N. E. A. Hinds, University of California, Berkeley.
Remarks: see Curtis, *et al.* (1958) p. 5, for further description and comments. The date is probably close to the Jurassic–Cretaceous boundary.

KA 97 biotite; K = 7·04 per cent; A/K = $8{\cdot}25 \times 10^{-3}$; A_{40}^{At} = 6 per cent; $t = 136 \times 10^6$ years.
Biotite concentrated from biotite-bearing quartz diorite or gabbro.
Stratigraphic age: The pluton intrudes rocks containing Oxfordian–Kimeridgian fossils.
Location: From a quarry near Horseshoe Bar on the American River 3 miles northeast of Loomis, California ($NE\frac{1}{4}$ sec. 18, T. 11N, R8E., MDB and M).
Remarks: see Curtis *et al.* (1958) p. 6, for discussion of this sample. The intrusion cannot be older than upper Oxfordian.

KA 132 biotite; K = 6·12 per cent; A/K = $6{\cdot}24 \times 10^{-4}$; A_{40}^{At} = 66 per cent; $t = 10{\cdot}7 \times 10^6$ years.
Biotite separated from biotite latite welded tuff.
Stratigraphic age: Lower Pliocene based on flora.
Location: West Walker River Canyon, California, 9·7 miles north of Fales.
Hot Springs, Hwy. 395, on east side of river.
Remarks: Seems satisfactory.

KA 161 biotite; K = 4·20 per cent; A/K = $8{\cdot}94 \times 10^{-4}$; A_{40}^{At} = 91 per cent; $t = 15{\cdot}2 \times 10^6$ years.
Biotite separated from rhyolitic crystal vitric tuff.
Stratigraphic age: Barstovian age (Upper Miocene) based on excellent fauna.
Location: 205 ft below top of Caliente Formation in Dry Canyon near the north-west corner of San Guillermo Quad., California.
Donor: D. E. Savage, University of California, Berkeley.

Remarks: The tuff has excellent faunal control, almost identical with the type Barstovian fauna in the Barstow syncline (see KA 449).

KA 175 biotite; K = 6·38 per cent; A/K = $1{\cdot}88 \times 10^{-3}$; A^{A}_{40j} = 50 per cent; $t = 32 \times 10^6$ years.
Biotite concentrated from biotite rhyolite welded tuff.
Stratigraphic age: Lower(?) Oligocene.
Location: Summit tuff, 375 ft above base of Tertiary volcanic sequence in Sheep Pass, Egan Range, Nevada. This is the lowest welded tuff deposit in the section.
Donor: H. Williams, University of California, Berkeley.
Remarks: The date suggests a lower Oligocene age.

KA 176 biotite; K = 2·53 per cent; A/K = $3{\cdot}52 \times 10^{-3}$; A^{At}_{40} = 53 per cent; $t = 59 \times 10^6$ years.
Biotite separated from biotite-bearing glauconitic sandstone.
Stratigraphic age: Paleocene–Martinez(?).
Location: Core (8092–8102 μ) from Standard Oil Co. well No. 62–13C(13 20S–15E, M.D.B. and M., California).
Donor: Standard Oil Co. of California.
Remarks: The biotite appears to be of volcanic origin and may therefore date closely the period of deposition.

KA 177 biotite; K = 6·96 per cent; A/K = $4{\cdot}86 \times 10^{-3}$; A^{At}_{40} = 11 per cent; $t = 81 \times 10^6$ years.
Biotite separation from granodiorite.
Stratigraphic age: "Upper Colorado (Niobrara)"-Reeside, 1948; "probably post-Montana"-Lyons, 1944. (Santonian-Maestrichtian).
Location: Clancy granodiorite, Kain Quarry on Clancy Creek, 1 mile west of Clancy, Montana
Donor: A. Knopf, Stanford University, Stanford, California.
Remarks: The radioactive age would appear to make this older than Maestrichtian.

KA 276 biotite; K = 6·50 per cent; A/K = $15{\cdot}92 \times 10^{-3}$; A^{At}_{40} = 12 per cent; $t = 254 \times 10^6$ years.
Biotite separated from Dartmoor granite.
Stratigraphic age: Post Lower Westphalian, pre Upper Permian (?).
Location: Haytor Quarry, Haytor.
Donor: J. F. Kirkaldy
Remarks: Age compatible with time-scale suggested by Kulp.

KA 291 biotite; K = 4·94 per cent; A/K = $2{\cdot}09 \times 10^{-2}$; A^{At}_{40} = 8 per cent; $t = 327 \times 10^6$ years.
Biotite separated from Harzburger gabbro.
Stratigraphic age: Post-Kulmgrauwacke, pre-Stephan zone of Upper Carboniferous.
Location: Near Harzburg, Harz.
Donor: Amt für Bodenforschung, Hannover.
Remarks: Appears satisfactory.

KA 332 biotite; K = 6·20 per cent; A/K = $2{\cdot}20 \times 10^{-2}$; A^{At}_{40} = 11 per cent; $t = 344 \times 10^6$ years.
Biotite separated from biotite rhyolite.
Stratigraphic age: Near top of Upper Devonian.
Location: 2 miles east of Rubicon Power Station, Snobs Creek, Warburton, Victoria, Australia.
Donor: E. Irving, National University, Canberra, Australia.
Remarks: Appears to be an excellent date.

KA 404 biotite; K = 6·15 per cent; A/K = $5{\cdot}75 \times 10^{-3}$; A^{At}_{40} = 9 per cent; $t = 96 \times 10^6$ years.
Biotite separated from bentonite.
Stratigraphic age: Upper Cenomanian (?). The bentonite occurs in a thick (5000 ft ±) shale

approximately 500 ft stratigraphically beneath the contact with the Venado formation. Fossils approximately 250 ft stratigraphically above the bentonite have been identified as Cenomanian–Turonian by E. C. Allison, Dept. Paleontology, University of California. Inoceramus cf. I. labiatus in the Venado formation indicates early Turonian age. Fossils several thousand feet lower than the contact with the Venado formation in Putah Creek, 25 miles to the south, have been tentatively indentified as Upper Albian in age.
Location: Cache Creek, California.
Donor: C. M. Gilbert
Remarks: Appears to be an excellent date in the lower part of the Upper Cretaceous.

KA 414 biotite; K = 6·37 per cent; A/K = $7{\cdot}04 \times 10^{-4}$; $A_{40}^{At} = 56$ per cent; $t = 12{\cdot}0 \times 10^6$ years.
Biotite separated from biotite rhyolite tuff.
Stratigraphic age: Lower Clarendonian (Lower Pliocene). Bottom of C_1 zone of Axelrod in the Coal Valley formation.
Location Basal tuff in Coal Valley formation, Coal Valley, Nevada.
Donor: D. E. Savage.
Remarks: The sample has excellent vertebrate faunal control and appears to be close to the boundary between Lower Pliocene and Upper Miocene in this area.

KA 449 biotite; K = 4·83 per cent; A/K = $8{\cdot}90 \times 10^{-4}$; $A_{40}^{At} = 40$ per cent; $t = 15{\cdot}2 \times 10^6$ years.
Biotite separated from biotite dacite tuff.
Stratigraphic age: Barstovian (Upper Miocene) at type locality.
Location: Barstow syncline north of Barstow, California.
Donor: M. McKenna, University of California, Berkeley, California.
Remarks: This date agrees with that of KA 161.

KA 461 biotite; K = 6·60 per cent; A/K = $17{\cdot}5 \times 10^{-3}$; $A_{40}^{At} = 16$ per cent; $t = 278 \times 10^6$ years.
Biotite separated from toscanite.
Stratigraphic age: Upper Carboniferous (Kuttung series).
Location: Lower Hunter Valley, South Wales, Australia.
Donor: E. Irving.
Remarks:

KA 431 biotite; K = 3·63 per cent; A/K = $1{\cdot}04 \times 10^{-2}$; $A_{40}^{At} = 19$ per cent; $t = 169 \times 10^6$ years.
Biotite separated from diorite.
Stratigraphic age: Diorite pluton intrudes marine volcanics (Talkeetna formation) of early Jurassic age. Ammonites of late early Jurassic age occur in the Talkeetna formation about 1 mile from the intrusion. Pliensbachian? Eroded boulders of this pluton occur in the Naknek formation (Oxfordian).
Location: Headwaters of the Oshetna River, Talkeetna Mountains, Alaska.
Donor: A. Grantz, U.S.G.S., Menlo Park, California.
Remarks: The low potassium value is due to the presence of hornblende in the sample, not to chloritized mica.

KA 483 sanidine: K = 4·73 per cent; A/K = $1{\cdot}95 \times 10^{-3}$; $A_{40}^{At} = 21$ per cent; $t = 33{\cdot}1 \times 10^6$ years.
Sanidine separated from rhyolitic tuff.
Stratigraphic age: close to Oligocene–Eocene boundary (Chadronian fauna).
Location: Presidio County, Texas, 4 miles east of Rio Grande river.
Donor: G. H. Curtis.
Remarks: Low potassium value is due to high sodium content of the feldspar. Appears to be an excellent result.

KA 462 biotite; K = 6·23 per cent; A/K = $2·76 \times 10^{-2}$; A^{At} = 23 per cent; $t = 421 \times 10^6$ years.
Biotite separated from tuff.
Stratigraphic age: Mid-Ordovician near top of (Carter's limestone, Stone's River group).
Location: core from Wenonah no. 8, Bessemer, Alabama.
Donor: H. Faul.
Remarks: H. Faul obtained an age of 420×10^6 years on this sample.

Appendix II

Glauconites and Illites

KA 147 glauconite; K = 5·44 per cent; A/K = $1·85 \times 10^{-3}$; A_{40}^{At} = 49 per cent; $t = 31·5 \times 10^6$ years.
Concentrate from glauconitic sandstone.
Stratigraphic age: Upper Eocene (Lower Kreyenhagen, A-2 zone of Laiming).
Location: core from 8230 ft in Bandini no. 64–30B (30–19S–16, M.D.B. and M.) California.
Donor: Standard Oil Company of California.
Remarks: Excessive burial and heating invalidate age determination.

KA 152 glauconite; K = 4·41 per cent; A/K = $4·15 \times 10^{-3}$; A_{40}^{At} = 65 per cent; $t = 70 \times 10^6$ years.
Concentrate from glauconitic sandstone.
Stratigraphic age: Maestrichtian stage of Upper Cretaceous (Ripley Formation).
Location: Gulf Coast, outcrop.
Donor: Shell Oil Company.
Remarks: Appears to be an excellent determination. A second glauconite separation from another portion of the same sample yielded the following: (KA 439) K = 5·54 per cent; A/K = $4·08 \times 10^{-3}$; A_{40}^{At} = 27 per cent; $t = 69 \times 10^6$ years.

KA 153 glauconite; K = 5·82 per cent; A/K = $2·49 \times 10^{-3}$; A_{40}^{At} = 18 per cent; $t = 42 \times 10^6$ years.
Concentrate from glauconitic sandstone.
Stratigraphic age: Very top of Middle Eocene of California (Domengine Fm.).
Location: Core from 4579–99 ft in Magnet Oil Fearron no. 2 (18–20S–15E, M.D.B. and M.) California.
Donor: Standard Oil Company of California.
Remarks: Possibly influenced slightly by burial.

KA 154 glauconite; K = 5·00 per cent; A/K = $2·11 \times 10^{-3}$; A_{40}^{At} = 58 per cent; $t = 36 \times 10^6$ years.
Concentrate from glauconitic sandstone.
Stratigraphic age: Base of Upper Eocene of California (Basal Kreyenhagen).
Location: Core from 8012–8063 ft in General Petroleum Espe Road 75–33 (33–16S–17E, M.D.B. and M.), California.
Donor: Standard Oil Company of California.
Remarks: Excessive burial and heating invalidate age determination.

KA 160 glauconite; K = 5·38 per cent; A/K = $1·46 \times 10^{-3}$; A_{40}^{At} = 52 per cent; $t = 25 \times 10^6$ years.
Concentrate from glauconitic sandstone.
Stratigraphic age: Base of Upper Eocene of California (basal Kreyenhagen).
Location: Core from 10,790 ft in Artnell Honolulu Kreyenhagen no. 81 X (14–21S–14E, M.D.B. and M), California.
Donor: Standard Oil Company of California.
Remarks: Excessive burial and heating invalidate age determination.

KA 162 glauconite; K = 4·63 per cent; A/K = 2·27 × 10^{-3}; A_{40}^{At} = 25 per cent; t = 38 × 10^6 years.
Concentrate from glauconitic sandstone.
Stratigraphic age: Lower Eocene or Paleocene (Mathews' Landing Marl).
Location: Gulf Coast, outcrop?
Donor: Shell Oil Company.
Remarks: Age determination appears poor. Too little known of sample history to permit explanation of poor result.

KA 163 glauconite; K = 6 02 per cent; A/K = 2·78 × 10^{-3}; A_{40}^{At} = 38 per cent; t = 47 × 10^6 years.
Concentrate from glauconitic sandstone.
Stratigraphic age: Lutetian Stage of Middle Eocene (type locality).
Location: Fosse near Survilliers in Paris Basin, outcrop.
Donor: Francois Lampietti.
Remarks: Appears to be an excellent determination.

KA 165 glauconite; K = 6·22 per cent; A/K = 2·30 × 10^{-3}; A_{40}^{At} = 27 per cent; t = 39 × 10^6 years.
Concentrate from glauconitic sandstone.
Stratigraphic age: Lower Mid-Eocene (Winona sand of Lower Claiborne).
Location: Gulf Coast, outcrop?
Donor: Shell Oil Company.
Remarks: Age determination appears poor. History of sample unknown.

KA 166 glauconite; K = 3·85 per cent; A/K = 2·33 × 10^{-3}; A_{40}^{At} = 39 per cent; t = 39 × 10^6 years.
Concentrate from glauconitic sandstone.
Stratigraphic age: Base of Upper Eocene of Gulf Coast (Moody Branch Fm. at base of Jackson).
Location: Gulf Coast, outcrop?
Donor: Shell Oil Company.
Remarks: Age determination appears poor. Burial history of sample unknown.

KA 170 glauconite; K = 3·70 per cent; A/K = 2·73 × 10^{-3}; A_{40}^{At} = 47 per cent; t = 46 × 10^6 years.
Concentrate from glauconitic sandstone.
Stratigraphic age: Paleocene (top of Paleocene at 8028 ft).
Location: Core from 8150–60 ft in Amerada Clover 53–28 (28–16S–17E, M.D.B. and M.).
Donor: Standard Oil Company of California.
Remarks: Excessive burial and heating invalidate the age determination.

KA 171 glauconite; K = 5·09 per cent; A/K = 1·32 × 10^{-3}; A_{40}^{At} = 66 per cent; t = 23 × 10^6 years.
Concentrate from glauconitic sandstone.
Stratigraphic age: Lower Miocene of California (Lower Zemorrian) Base of lower Santos shale-top of Phacoides sand at 5705 ft on cores.
Location: Core from 5688–5716 ft in Hub Petroleum Cymric no. 1 (22–29S–21E, M.D.B. and M.), California.
Donor: Standard Oil Company of California.
Remarks: Appears to be good result. Possibly slight loss due to burial and heating.

KA 172 glauconite; K = 3·95 per cent; A/K = 3·48 × 10^{-3}; A_{40}^{At} = 39 per cent; t = 58 × 10^6 years.
Concentrate from glauconitic sandstone.
Stratigraphic age: Paleocene (top of Paleocene at 8063 ft).
Location: Core from 8092–8102 ft in General Petroleum Espe Road 75–33 (33–16S–17E, M.D.B. and M.), California.

Donor: Standard Oil Company of California.
Remarks: Appears to be an excellent result. Burial has had little effect.

KA 173 glauconite; K = 5·43 per cent; A/K = 2·50 × 10^{-3}; A_{40}^{At} = 23 per cent; t = 42 × 10^6 years.
Concentrate from glauconitic sandstone.
Stratigraphic age: Base of Middle Eocene of Gulf Coast (Stave Creek Fm.).
Location: Gulf Coast, outcrop?
Donor: Shell Oil Company.
Remarks: Appears to be a poor age determination. History of sample unknown.

KA 178 glauconite; K = 4·94 per cent; A/K = 2·73 × 10^{-3}; A_{40}^{At} = 70 per cent; t = 46 × 10^6 years.
Stratigraphic age: Paleocene of California (Martinez).
Location: Core from 8092–8102 ft in Standard Oil Company no. 62–13C (13–20S–15E, M.D.B. and M.), California.
Donor: Standard Oil Company of California.
Remarks: Excessive burial and heating invalidate age determination.

KA 186 glauconite; K = 4 98 per cent; A/K = 5·76 × 10^{-3}; A_{40}^{At} = 22 per cent; t = 96 × 10^6 years.
Concentrate from glauconitic sandstone.
Stratigraphic age: Upper Albian Stage of Lower Cretaceous (Upper Greensand of Dorset Coast).
Location: near Lyme Regis, England, outcrop.
Donor: C. M. Gilbert, University of California, Berkeley, California.
Remarks: Appears to be an excellent age determination.

KA 189 glauconite; K = 5·42 per cent; A/K = 2·55 × 10^{-3}; A_{40}^{At} = 37 per cent; t = 43 × 10^6 years.
Concentrate from glauconitic sandstone.
Stratigraphic age: Base of Upper Eocene of California (basal Kreyenhagen).
Location: Hernandez Valley, California, roadcut.
Donor: R. L Rose, San Jose State College, San Jose, California.
Remarks: Appears to be an excellent age determination.

KA 191 glauconite; K = 5·21 per cent; A/K = 26·4 × 10^{-3}; A_{40}^{At} = 12 per cent; t = 406 × 10^6 years.
Concentrate from glauconitic sandstone.
Stratigraphic age: Base of Middle Cambrian (50 ft above Gros Ventre shale).
Location: Wyoming, outcrop.
Donor: Pan-American Petroleum Corporation, Tulsa, Oklahoma.
Remarks: A poor result. Typical of most Cambrian glauconites.

KA 192 glauconite; K = 5·00 per cent; A/K = 0 3044 × 10^{-3}; A_{40}^{At} = 93 per cent; t = 5·2 × 10^6 years.
Concentrate from glauconitic sandstone.
Stratigraphic age: Upper Pliocene.
Location: Mendocino County, California.
Donor: B. A. Ogle.
Remarks: Appears to be an excellent result.

KA 198 glauconite; K = 4·95 per cent; A/K = 5·41 × 10^{-3}; A_{40}^{At} = 18 per cent; t = 91 × 10^6 years.
Concentrate from glauconitic sandstone.
Stratigraphic age: Basal Cenomanian stage of Upper Cretaceous (Pecten asper zone).
Location: Upper Greensand at top of Telegraph Hill, Haldon Hills, Devonshire, England.
Donor: C. M. Gilbert.
Remarks: Appears to be too young

KA 258 "illite"; K = 6·12 per cent; A/K = 45·0 × 10^{-3}; A_{40}^{At} = 5 per cent; t = 645 × 10^6 years.
Bulk sample of Gros Ventre Shale.
Stratigraphic age: Base of Middle Cambrian.
Location: Wyoming, outcrop.
Donor: Pan-American Petroleum Corporation.
Remarks: Presence of pre-erosion argon invalidates age determination.

KA 259 "illite"; K = 6·23 per cent; A/K = 50·1 × 10^{-3}; A_{40}^{At} = 12 per cent; t = 708 × 10^6 years, 16–150 μ size cut from disaggregated Gros Ventre Shale from same locality as KA 258.
Stratigraphic age: Base of Middle Cambrian.
Location: Wyoming, outcrop.
Donor: Pan-American Petroleum Corporation.
Remarks: Presence of pre-erosion argon invalidates age determination.

KA 260 "illite"; K = 6·01 per cent; A/K = 45·1 × 10^{-3}; A_{40}^{At} = 8 per cent; t = 646 × 10^6 years, 8–16 μ size cut from disaggregated Gros Ventre Shale from same locality as KA 258.
Stratigraphic age: Base of Middle Cambrian.
Location: Wyoming, outcrop.
Donor: Pan-American Petroleum Corporation.
Remarks: Presence of pre-erosion invalidates age determination.

KA 261 "illite"; K = 5·86 per cent; A/K = 35·8 × 10^{-3}; A_{40}^{At} = 8 per cent; t = 530 × 10^6 years, less than 8 μ size cut from disaggregated Gros Ventre Shale from same locality as KA 258.
Stratigraphic age: Base of Middle Cambrian.
Location: Wyoming, outcrop.
Donor: Pan-American Petroleum Corporation.
Remarks: Very nearly the correct age for base of Middle Cambrian. This result may be a fortuitous interplay of detrital argon and argon loss from small grains; however, KA 259, 260 and 261 do illustrate the decreasing influence of pre-erosion argon as the grain size decreases.

KA 262 "illite"; K = 5·07 per cent; A/K = 15·3 × 10^{-3}; A_{40}^{At} = 32 per cent; t = 246 × 10^6 years.
Bulk sample of Fithian illite.
Stratigraphic age: The Fithian illite is the underclay of the Macoupin cyclothem of the McLeansburg Group. Lower Upper Pennsylvanian (Lower Stephanian–Missouri Series).
Location: Type locality of Fithian illite, Fithian, Illinois.
Donor: Pan-American Petroleum Corporation.
Remarks: Appears to be an excellent age determination. Possibly, the absence of pre-erosion argon is due to the fine-grained or authigenic nature of the Fithian illite.

KA 265 glauconite; K = 5·16 per cent; A/K = 1·54 × 10^{-3}; A_{40}^{At} = 33 per cent; t = 27 × years.
Concentrate from glauconitic sandstone.
Stratigraphic age: Base of Upper Eocene of California (basal Kreyenhagen).
Location: Core from 9220 ft in Guijarral Service no. 87X (21–20S–16E, M.D.B. and M.) California.
Donor: Standard Oil Company of California.
Remarks: Excessive burial and temperature invalidate age determination.

KA 267 glauconite; K = 5·23 per cent; A/K = 1·07 × 10^{-3}; A_{40}^{At} = 45 per cent; t = 18 × 10^6 years.
Concentrate from glauconitic sandstone.
Stratigraphic age: Base of Upper Eocene of California (basal Kreyenhagen).
Location: Core from 12,175 ft in Kettleman M.D. Corp. 38–19 (19–23S–19E, M.D.B. and M.), California.
Donor: Standard Oil Company of California.
Remarks: Excessive burial and temperature invalidate age determination.

KA 270 glauconite; K = 6·64 per cent; A/K = 7·53 × 10^{-3}; $A_{40}^{\Delta t}$ = 7 per cent; t = 125 × 10^6 years.
Glauconite pellets from limestone.
Stratigraphic age: Upper Jurassic ("Portland sand").
Location: Okus Quarry, Swindon. Sample from 15 ft below ground level.
Donor: J. F. Kirkaldy, Queen Mary College, University of London.
Remarks: Appears to be too young for stratigraphic age. Burial history unknown to us.

KA 271 glauconite; K = 6·55 per cent; A/K = 2·88 × 10^{-2}; $A_{40}^{\Delta t}$ = 4 per cent; t = 436 × 10^6 years.
Concentrate from glauconitic sandstone.
Stratigraphic age: Basal Cambrian.
Location: Core from 118·6 m in Böda Hamm Borehole, Öland, Sweden.
Donor: J. Ecklund, Geological Survey of Sweden, Stockholm.
Remarks: Too young.

KA 272 glauconite; K = 3·30 per cent; A/K = 1·53 × 10^{-3}; $A_{40}^{\Delta t}$ = 45 per cent; t = 26 × 10^6 years.
Concentrate from glauconitic sandstone.
Stratigraphic age: Lower Oxfordian Stage of Upper Jurassic (Heersumer Schlichten).
Location: Core from 1169 m, north of Braunschweig, Germany.
Donor: Amt für Bodenforschung, Hannover, Germany.
Remarks: Excessive burial and heating invalidate the age determination.

KA 273 glauconite; K = 5·87 per cent; A/K = 5·84 × 10^{-3}; $A_{40}^{\Delta t}$ = 29 per cent; t = 97 × 10^6 years.
Concentrate from glauconitic sandstone.
Stratigraphic age: Albian stage of Lower Cretaceous.
Location: Core from 430 m near Salzgitter.
Donor: Amt für Bodenforschung, Hannover.
Remarks: Appears to be an excellent result.

KA 274 glauconite; K = 5·02 per cent; A/K = 3·41 × 10^{-3}; $A_{40}^{\Delta t}$ = 29 per cent; t = 57 × 10^6 years.
Concentrate from glauconitic sandstone.
Stratigraphic age: "Basal" Eocene (according to J. F. Kirkaldy). Mid-Paleocene (according to R. Brinkmann). Uppermost Thanet sands.
Location: Seacliff at Oldhaven Gap, $\frac{1}{2}$ to $\frac{3}{4}$ miles west of Reculver, Kent.
Donor: J. F. Kirkaldy; D. J. Shearman, Imperial College of Science and Technology, London.
Remarks: Appears to be an excellent result.
Bakeout temperatures are critical when using glauconite. The following data are illustrative of this point:

Run no.	Bakeout temp. (overnight) (°C)	t (× 10^6 years)	$A_{40}^{\Delta t}$ (%)
KA 274B	260	34	29
KA 274 II	190	49	29
KA 274	85	57	29

KA 279 glauconite; K = 4·77 per cent; A/K = 6·14 × 10^{-3}; $A_{40}^{\Delta t}$ = 42 per cent; t = 102 × 10^6 years.
Concentrate from glauconitic sandstone.
Stratigraphic age: Albian–Aptian boundary of Lower Cretaceous.
Location: Core from 613 m near Salzgitter.
Donor: Amt für Bodenforschung, Hannover.
Remarks: Appears to be an excellent result.

KA 282 glauconite; K = 6·52 per cent; A/K = 4·64 × 10^{-3}; A_{40}^{At} = 21 per cent; t = 94 × 10^6 years.
Concentrate from glauconitic clay.
Stratigraphic age: Base of Middle Albian Stage of Lower Cretaceous (base of Galt [glauconitic clays], overlies Folkstone).
Location: Seacliff, ½ mile east of end of promenade at Folkstone.
Donor: J. F. Kirkaldy, D. J. Shearman.
Remarks: Appears to be slightly young.

KA 285 glauconite; K = 4·57 per cent; A/K = 1·94 × 10^{-3}; A_{40}^{At} = 39 per cent; t = 33 × 10^6 years.
Concentrate from glauconitic sandstone.
Stratigraphic age: Base of Upper Eocene of California (basal Kreyenhagen).
Location: Core from 6311 ft in Federal Noble no. 26 (10–15S–17E, M.D.B. and M.), California.
Donor: Standard Oil Company of California.
Remarks: Deep burial invalidates age determination.

KA 289 bentonite; K = 4·22 per cent; A/K = 1·88 × 10^{-2}; A_{40}^{At} = 5 per cent; t = 297 × 10^6 years.
Bentonite bed in Ludibundus Limestone.
Stratigraphic age: Middle Ordovician (Ludibundus limestone).
Location: Core from 89 m in Smedsby gärd, Östergötland, Sweden.
Donor: J. Ecklund.
Remarks: Excessive burial and heating may have invalidated age determination.

KA 290 glauconite; K = 6·43 per cent; A/K = 2·74 × 10^{-2}; A_{40}^{At} = 4 per cent; t = 420 × 10^6 years.
Concentrate from glauconitic sandstone.
Stratigraphic age: Lower Ordovician (On top of Dictyonema shale).
Location: From borehole at Borensberg, Sweden.
Donor: J. Ecklund.
Remarks: Appears to be a good date.

KA 292 glauconite; K = 6·96 per cent; A/K = 2·78 × 10^{-2}; A_{40}^{At} = 19 per cent; t = 423 × 10^6 years.
Concentrate from glauconitic sandstone.
Stratigraphic age: Uppermost Arenig of Lower Ordovician (Expansus limestone).
Location: Core from 31·4 m in Böda Hamm, Öland, Sweden.
Donor: J. Ecklund.
Remarks: Appears to be a good date.

KA 293 glauconite; K = 6·42 per cent; A/K = 2·60 × 10^{-2}; A_{40}^{At} = 10 per cent; t = 399 × 10^6 years.
Concentrate from glauconitic sandstone.
Stratigraphic age: Base of Middle Cambrian (Oelandicus zone).
Location: Core from 34·15 m in Bredsätter Borehole, Närke, Sweden.
Donor: J. Ecklund.
Remarks: Too young.

KA 294 glauconite; K = 6·49 per cent; A/K = 2·85 × 10^{-2}; A_{40}^{At} = 2 per cent; t = 434 × 10^6 years.
Concentrate from glauconitic sandstone.
Stratigraphic age: Basal Arenigian Stage of Lower Ordovician.
Location: Stora brottet, Latorp, Sweden, 15 ft below surface.
Donor: N. Spjeldnaes, Geological Museum, University of Oslo, Norway.
Remarks: Appears to be an excellent age determination.

KA 296 glauconite; K = 6·14 per cent; A/K = 2·65 × 10^{-2}; A_{40}^{At} = 12 per cent; t = 406 × 10^6 years.
Concentrate from glauconitic sandstone.
Stratigraphic age: Middle Tremadocian stage of Lower Ordovician.
Location: Core from 33·1 m in Gammalsby Borehole, Öland, Sweden.
Donor: J. Ecklund.
Remarks: Appears too young.

KA 298 glauconite; K = 3·48 per cent; A/K = 5·18 × 10^{-3}; A_{40}^{At} = 32 per cent; t = 87 × 10^6 years.
Concentrate from glauconitic sandstone.
Stratigraphic age: Coniacian stage of Upper Cretaceous (Emscher).
Location: Core from 711 m, near Hannover.
Donor: Amt für Bodenforschung, Hannover.
Remarks: Appears to be an excellent age determination.

KA 299 glauconite; K = 6·84 per cent; A/K = 2·70 × 10^{-2}; A_{40}^{At} = 8 per cent; t = 413 × 10^6 years.
Concentrate from glauconitic sandstone.
Stratigraphic age: Near top of Lower Cambrian.
Location: Core from 389 m in File Haidar Borehole, Gotland.
Donor: J. Ecklund.
Remarks: Too young. Heating?

KA 306 glauconite; K = 6·54 per cent; A/K = 5·00 × 10^{-3}; A_{40}^{At} = 17 per cent; t = 84 × 10^6 years.
Concentrate from glauconitic sandstone.
Stratigraphic age: Middle Turonian Stage of Upper Cretaceous (Bochumer Greensand).
Location: Near Herne, Germany.
Donor: Amt für Bodenforschung, Hannover.
Remarks: Appears to be an excellent age determination.

KA 308 glauconite; K = 5·41 per cent; A/K = 1·23 × 10^{-3}; A_{40}^{At} = 63 per cent; t = 21 × 10^6 years.
Concentrate from glauconitic sandstone.
Stratigraphic age: Upper Lias Stage of Lower Jurassic (Toarciano).
Location: Alpi Feltrini–Coston Delle Vette, Italy.
Donor: P. Gallitelli, University of Modena, Italy.
Remarks: Excessive burial and heating are the probable causes for the inaccurate age. It is interesting to note that the age obtained for this sample is that of the Alpine Orogeny (Miocene) which affected the Alpi Feltrini.

KA 309 glauconite; K = 6·24 per cent; A/K = 4·71 × 10^{-3}; A_{40}^{At} = 17 per cent; t = 79 × 10^6 years.
Concentrate from glauconitic sandstone.
Stratigraphic age: Cenomanian stage of Upper Cretaceous (Soester greensand).
Location: Core from well near Dortmund, Germany.
Donor: Amt für Bodenforschung, Hannover.
Remarks: Appears to be too young.

KA 310 glauconite; K = 5·88 per cent; A/K = 5·60 × 10^{-3}; A_{40}^{At} = 19 per cent; t = 94 × 10^6 years.
Concentrate from glauconitic sandstone.
Stratigraphic age: Lower Albian stage of Lower Cretaceous.
Location: Core from well near Salzgitter, Germany.
Donor: Amt für Bodenforschung, Hannover.
Remarks: Appears to be too young.

KA 311 glauconite; K = 5·43 per cent; A/K = 1·85 × 10^{-3}; A_{40}^{At} = 77 per cent; t = 31 × 10^6 years.
Concentrate from glauconitic sandstone.
Stratigraphic age: Upper Hauterivian Stage of Lower Cretaceous.
Location: Core from well near Salzgitter.
Donor: Amt für Bodenforschung, Hannover.
Remarks: Indicated age much too young. Burial and heating are probable causes of invalid age.

KA 312 glauconite; K = 5·73 per cent; A/K = 8·21 × 10^{-3}; A_{40}^{At} = 20 per cent; t = 136 × 10^6 years.
Concentrate from glauconitic sandstone.
Stratigraphic age: Oxfordian stage of Upper Jurassic (Plicatilis Schichten).
Location: Core from 29·4 m in Pegnitz 10, Oberpfalz.
Donor: J. H. Ziegler, Bayerisches Geologisches Landesamt. Munich, Germany.
Remarks: Appears to be a quite good age determination. Somewhat young.

KA 313 glauconite; K = 6·38 per cent; A/K = 8·42 × 10^{-3}; A_{40}^{At} = 13 per cent; t = 139 × 10^6 years.
Concentrate from glauconitic sandstone.
Stratigraphic age: Upper Portland Stage of Upper Jurassic (Münder Mergel).
Location: Core from 24 m in well near Hannover.
Donor: Amt für Bodenforschung, Hannover.
Remarks: Appears to be an excellent age determination.

KA 315 glauconite; K = 5·30 per cent; A/K = 4·86 × 10^{-3}; A_{40}^{At} = 30 per cent; t = 81 × 10^6 years.
Concentrate from glauconitic sandstone.
Stratigraphic age: Lower Campanian Stage of Upper Cretaceous.
Location: Core from approx. 500 m depth from well near Hannover.
Donor: Amt für Bodenforschung, Hannover.
Remarks: Appears to be an excellent age determination.

KA 316 glauconite; K = 6·80 per cent; A/K = 5·11 × 10^{-3}; A_{40}^{At} = 38 per cent; t = 86 × 10^6 years.
Stratigraphic age: Lower Turonian Stage of Upper Cretaceous (Essener Greensand).
Location: Core from well near Dortmund.
Donor: Amt für Bodenforschung, Hannover.
Remarks: Appears to be an excellent age determination.

KA 317 glauconite; K = 6·00 per cent; A/K = 7·91 × 10^{-3}; A_{40}^{At} = 11 per cent; t = 131 × 10^6 years.
Concentrate from shale (glauconite pellets in clay matrix).
Stratigraphic age: Callovian stage of Upper Jurassic (Ornatentone).
Location: Core from 35·6 m in Pegnitz 10, Oberpfalz.
Donor: J. H. Ziegler.
Remarks: Too young.

KA 318 glauconite; K = 5·96 per cent; A/K = 8·42 × 10^{-3}; A_{40}^{At} = 11 per cent; t = 139 × 10^6 years.
Concentrate from shale (glauconite pellets in clay matrix).
Stratigraphic age: Callovian Stage of Upper Jurassic (Ornatentone).
Location: Core from 33·0 m in Pegnitz 10, Oberpfalz.
Donor: J. H. Ziegler.
Remarks: Appears to be somewhat young.

KA 322 glauconite; K = 5·28 per cent; A/K = 5·62 × 10^{-4}; A_{40}^{At} = 57 per cent; t = 9·5 × 10^6 years.
Concentrate from glauconitic sandstone.
Stratigraphic age: Upper Miocene.
Location: Core from well near Kadenberge (25 km south-west of Stade).
Donor: Amt für Bodenforschung, Hannover.
Remarks: Too young when compared with dates for western U.S.A.

KA 323 glauconite; K = 4·78 per cent; A/K = 4·94 × 10^{-3}; A_{40}^{At} = 34 per cent; t = 83 × 10^6 years.
Concentrate from glauconitic sandstone.
Stratigraphic age: Lower Santonian of Upper Cretaceous.
Location: Core from well near Salzgitter.
Donor: Amt für Bodenforschung, Hannover.
Remarks: Appears to be an excellent determination.

KA 324 glauconite; K = 6·16 per cent; A/K = 1·85 × 10^{-3}; A_{40}^{At} = 64 per cent; t = 31 × 10^6 years.
Concentrate from glauconitic sandstone.
Stratigraphic age: Upper Eocene.
Location: Core from well near Nevenhaus (few kilometres west of Nordhorn).
Donor: Amt für Bodenforschung, Hannover.
Remarks: Too young if Oligocene of Europe is time equivalent of Oligocene of western U.S.A. However, possibly indicative of lack of such time equivalency.

KA 337 "illite"; K = 2·86 per cent; A/K = 18·7 × 10^{-3}; A_{40}^{At} = 32 per cent; t = 295 × 10^6 years.
Bulk sample of shaly member in limestone.
Stratigraphic age: Westphalian stage of Lower Pennsylvanian (Otterville L/S).
Location: (?).
Donor: Pan-American Petroleum Corporation.
Remarks: Appears to be an excellent determination.

KA 338 "illite"; K = 2·06 per cent; A/K = 19·4 × 10^{-3}; A_{40}^{At} = 34 per cent; t = 305 × 10^6 years.
Bulk sample of shaly member of Sycamore Limestone.
Stratigraphic age: Lower Tournaisian Stage of Lower Mississippian (Sycamore Limestone).
Location: (?).
Donor: Pan-American Petroleum Corporation.
Remarks: Appears to be too young

KA 339 "illite"; K = 5·30 per cent; A/K = 23·4 × 10^{-3}; A_{40}^{At} = 28 per cent; t = 363 × 10^6 years.
Bulk sample of shaly member of Haragan limestone.
Stratigraphic age: Gedinnian Stage of Devonian (Basal Devonian) (Haragan 1/s).
Location:
Donor: Pan-American Petroleum Corporation.
Remarks: Probably young.

KA 340 "illite"; K = 4·19 per cent; A/K = 22·3 × 10^{-3}; A_{40}^{At} = 28 per cent; t = 347 × 10^6 years.
Bulk sample of shaly member of Haragan limestone. Different rock sample from KA 339.
Stratigraphic age: Gedinnian Stage of Lower Devonian.
Location:
Donor: Pan-American Petroleum Corporation.
Remarks: Too young.

KA 341 "illite"; K = 5·64 per cent; A/K = 17·9 × 10^{-3}; A_{40}^{At} = 37 per cent; t = 284 × 10^6 years.
Bulk sample of shaly member of Chimney Hill limestone.
Stratigraphic age: Lower Llandovery Stage of Lower Silurian.
Location:
Donor: Pan-American Petroleum Corporation.
Remarks: Too young.

KA 342 "illite"; K = 5·67 per cent; A/K = 16·7 × 10^{-3}; A_{40}^{At} = 53 per cent; t = 267 × 10^6 years.
Bulk sample of shaly member of Chimney Hill Limestone (Different sample from KA 341).
Stratigraphic age: Lower Llandovery Stage of Lower Silurian.
Location:
Donor: Pan-American Petroleum Corporation.
Remarks: Too young.

KA 343 "illite"; K = 2·79 per cent; A/K = 32·3 × 10^{-3}; A_{40}^{A} = 54 per cent; t = 485 × 10^6 years.
Bulk sample of shaly member of Bromide limestone.
Stratigraphic age: Mid-Champlanian stage of Mid-Ordovician (Bromide limestone).
Location:
Donor: Pan-American Petroleum Corporation.
Remarks: Too old. Pre-erosion argon? See KA 343-A.

KA 343A "illite"; K = 2·82 per cent; A/K = 32·7 × 10^{-3}; A_{40}^{At} = 23 per cent; t = 490 × 10^6 years.
Same rock sample as KA 343 but a sized sample obtained after disaggregation of rock. KA 343A contained all sizes of less than 74 μ diameter.
Stratigraphic age: Mid-Champlanian stage of Mid-Ordovician (Bromide limestone).
Location:
Donor: Pan-American Petroleum Corporation.
Remarks: Too old. Pre-erosion argon? Note that the grain sizes here used contain sizes that showed detrital contamination in the Gros Ventre samples (KA 258–261).

KA 344 "illite"; K = 5·84 per cent; A/K = 30·2 × 10^{-3}; A_{40}^{At} = 13 per cent; t = 457 × 10^6 years.
Bulk sample of shaly member of Butterly dolomite.
Stratigraphic age: Top of Cambrian (Butterly dolomite).
Location:
Donor: Pan-American Petroleum Corporation.
Remarks: Appears to be an excellent age determination.

KA 438 glauconite; K = 4·46 per cent; A/K = 3·10 × 10^{-3}; A_{40}^{At} = 23 per cent; t = 52 × 10^6 years.
Concentrate from glauconitic sandstone.
Stratigraphic age: Upper Lower Eocene–Upper Wilcox (Bashi Formation).
Location: Gulf Coast, outcrop?
Donor: Shell Oil Company.
Remarks: Appears to be an excellent age determination.

KA 440 glauconite; K = 4·72 per cent; A/K = 3·03 × 10^{-3}; A_{40}^{At} = 38 per cent; t = 51 × 10^6 years.
Concentrate from glauconitic sandstone.
Stratigraphic age: Lower Eocene (Alpine).
Location: Core from 196–199 m in Kressenberg 5, near Teisendorf (Obb.).
Donor: J. H. Ziegler.
Remarks: Appears to be an excellent age determination.

KA 442 glauconite; K = 4·35 per cent; A/K = 6·99 × 10^{-3}; A_{40}^{At} = 23 per cent; t = 115 × 10^6 years.
Concentrate from glauconitic sandstone.
Stratigraphic age: Lower Aptian stage of Lower Cretaceous (Lower Green Sand–Hythe Beds).
Location: Brook roadcut, 4 miles NNE of Haslemere. Grid ref: 931–387(169).
Donor: J. F. Kirkaldy.
Remarks: Appears to be an excellent age determination.

KA 443 glauconite; K = 4·83 per cent; A/K = 29·5 × 10^{-3}; A_{40}^{At} = 12 per cent; t = 447 × 10^6 years.
Concentrate from glauconitic sandstone.
Stratigraphic age: Base of Middle Cambrian
Location: Outcrop on Robin's Tump, Shropshire. Grid Ref: 484–954(129).
Donor: J. F. Kirkaldy.
Remarks: Too young, as are all of the Cambrian glauconites that we have tried.

KA 444 glauconite; K = 5·42 per cent; A/K = 30·2 × 10^{-3}; A_{40}^{At} = 11 per cent; t = 457 × 10^6 years.
Concentrate from glauconitic sandstone.
Stratigraphic age: Lower Cambrian- Ab 4 Zone.
Location: Pit. Grid Ref: 487–962(129).
Donor: C. J. Stubblefield, Geological Survey of Great Britain, London.
Remarks: Too young.

KA 445 glauconite; K = 4·14 per cent; A/K = 1·46 × 10^{-3}; A_{40}^{At} = 69 per cent; t = 25 × 10^6 years.
Concentrate from glauconitic sandstone.
Stratigraphic age: Lower Miocene–Burdigalian.
Location: Core from 45·0–47·7 m in F.Z.6, Bad Hall, Austria.
Donor: E. Braumüller, Rohoel-Gewinnungs A. G., Vienna, Austria.
Remarks: Appears to be an excellent age determination.

KA 446 glauconite; K = 5·55 per cent; A/K = 6·58 × 10^{-3}; A_{40}^{At} = 18 per cent; t = 110 × 10^6 years.
Concentrate from glauconitic sandstone.
Stratigraphic age: Aptian stage of Lower Cretaceous (Bargate Beds–Lower Green Sand).
Location: Stock Farm Quarry. Grid Ref: 876–383(169).
Donor: J. F. Kirkaldy.
Remarks: Appears to be an excellent age determination.

Geochimica et Cosmochimica Acta, 1961, Vol. 23, pp. 100 to 115. Pergamon Press Ltd. Printed in Northern Ireland

Some observations on the distribution of thallium, cadmium and bismuth in silicate rocks and the significance of covalency on their degree of association with other elements

R. R. Brooks and L. H. Ahrens
Department of Chemistry, University of Cape Town

(*Received* 12 *October* 1960)

Abstract—Cd, Tl and Bi have been estimated in forty-four rock samples, using the anion exchange–spectrochemical procedure described by Brooks *et al.* (1960). Estimates of the crustal abundances of these elements have been made on the basis of two parts granite (plus compositional equivalent) and one part basalt (plus gabbro and diabase), and are as follows: Cd (0·08 p.p.m.), Tl (0·7 p.p.m.) and Bi (0·17 p.p.m.). The Cd value is lower than previous estimates. The Tl value is also lower than other estimates but as it is based on quite extensive data (recent data of Russian and Japanese workers, plus data from this paper) it is suggested with considerable confidence.

The Rb–Tl association is considered in some detail. The association of these two elements is in certain respects closer than that of the classical pair K–Rb. The presence of a significant degree of covalency in the Tl—O bond may slightly but distinctly influence the Rb–Tl association (see Taylor and Heier, 1960). A high degree of covalency is evidently present in the Cd—O bond and is the probable reason why a Cd–Ca association (radii of Cd^{2+} and Ca^{2+} almost identical) is virtually non-existent. The significance of the presence of a high degree of covalency in the metal-oxygen bonds of certain other elements is also discussed.

Possible high crustal enrichment of Tl and Bi, but not Cd, is noted.

Introduction

Brooks *et al.* (1960) have described an anion exchange–spectrochemical procedure which they used to estimate Zn, Cd, Tl, Bi and Sn in nineteen rocks of various types. For some of these elements, geochemical data are still quite scant; Bi is a notable example. Data on Cd are also comparatively few. There is also a distinct need for more data on Tl in basic rocks. Accordingly, a modification of this anion exchange–spectrochemical procedure was used to estimate Cd, Tl and Bi in a further forty-four rocks. The selection includes a high proportion of basic rocks and five deep-seated rocks (eclogites). The results are given in Table 1(a); description of the rock samples is given in Table 1(b).

Cd, Tl and Bi form bonds with oxygen that have varying degrees of covalent character and it is in part the purpose of the present study to investigate the significance of covalency on the degree of association of pairs of elements whose cations carry the same charge and have similar radii.

Discussion

In the discussions which follow, each element will be considered in turn.

Thallium

(i) *Abundance.* Estimates of the abundance of thallium in the crust and in certain specific rock types are given in Table 2.

The crustal value recommended in the present paper is based on the data of Ishimori and Takashima, those of the large number of determinations recently carried out by Russian workers (see Table 2) and the new data given here (Table 1a). This value (0·7 p.p.m.) is lower than some recent (post—1945) crustal abundance

Table 1(a). The determination of Bi, Cd and Tl in rocks

No.	Type	Concentrations (p.p.m.)								
		Tl			Bi			Cd		
		1	2	Av	1	2	Av	1	2	Av
1	Soevite	—	—	—	0·04	0·03	0·04	0·19	0·11	0·15
2	Syenite	0·08	0·08	0·08	0·02	0·03	0·03	—	—	—
3	Syenite	0·05	0·06	0·06	0·02	0·02	0·02	0·04	0·04	0·04
4	Syenite	0·20	0·23	0·22	0·03	0·03	0·03	—	—	—
5	Foyaite	0·11	0·11	0·11	0·04	0·04	0·04	0·04	0·04	0·04
6	Foyaite	0·06	0·05	0·06	0·03	0·05	0·04	—	—	—
7	Rhyolite	0·05	0·04	0·05	0·03	0·03	0·03	—	—	—
8	Rhyolite	0·34	—	0·34	0·02	—	0·02	0·05	—	0·05
9	Acid dyke	0·12	0·11	0·11	0·04	0·04	0·04	—	—	—
10	Rhyolite	0·98	0·80	0·89	0·20	0·23	0·22	—	—	—
11	Rhyolite	0·20	—	0·20	0·21	—	0·21	0·05	—	0·05
12	Q. Feldspar	0·07	—	0·07	0·04	—	0·04	0·03	—	0·03
13	Dolerite	0·04	—	0·04	0·08	—	0·08	0·12	—	0·12
14	Dolerite	0·08	—	0·08	0·15	—	0·15	0·10	—	0·10
15	Dolerite	0·10	—	0·10	0·80	—	0·80	—	—	—
16	Dolerite	0·06	—	0·06	0·15	—	0·15	0·10	—	0·10
17	Dolerite	0·04	0·02	0·03	—	—	—	0·04	0·04	0·04
18	Dolerite	0·15	0·14	0·15	0·28	0·28	0·28	0·22	0·27	0·25
19	Dolerite	0·04	0·04	0·04	—	—	—	0·04	0·04	0·04
20	Dolerite	0·12	0·08	0·10	0·53	0·42	0·48	0·07	0·07	0·07
21	Dolerite	0·08	0·06	0·07	0·18	0·16	0·17	—	—	—
22	Dolerite	0·03	—	0·03	0·76	—	0·76	0·26	—	0·26
23	Dolerite	—	—	—	0·16	—	0·16	0·01	—	0·01
24	Dolerite	0·02	0·02	0·02	0·01	0·02	0·02	—	—	—
25	Dolerite	0·03	—	0·03	0·13	—	0·13	0·08	—	0·08
26	Dolerite	0·04	0·03	0·04	0·03	0·04	0·04	0·02	—	0·02
27	Dolerite	0·03	0·03	0·03	0·03	0·04	0·04	—	—	—
28	Dolerite	0·03	—	0·03	0·01	—	0·01	—	—	—
29	Dolerite	0·03	0·02	0·03	0·03	0·03	0·03	0·04	0·03	0·03
30	Dolerite	0·40	0·50	0·45	—	—	—	0·02	0·02	0·02
31	Dolerite	0·80	1·40	1·10	0·27	0·19	0·23	0·21	0·27	0·24
32	Eclogite	0·03	0·03	0·03	0·02	0·02	0·02	—	—	—
33	Eclogite	0·54	0·58	0·56	—	—	—	0·02	0·04	0·03
34	Eclogite	0·06	0·06	0·06	0·10	0·10	0·10	0·04	0·04	0·04
35	Eclogite	0·16	0·12	0·14	0·03	0·02	0·03	—	—	—
36	Eclogite	0·07	0·07	0·07	—	—	—	—	—	—
37	Basalt	0·07	—	0·07	0·02	0·02	0·02	0·03	—	0·03
38	Carbonatite	0·24	0·13	0·19	0·08	0·05	0·06	0·17	0·08	0·13
39	Carbonatite	0·03	0·02	0·03	0·08	0·04	0·06	0·46	0·26	0·36
40	Glauconite	0·03	—	0·03	0·13	—	0·13	0·03	—	0·03
41	Crocidolite	0·01	—	0·01	0·01	—	0·01	—	—	—
42	Fe-stone	0·01	—	0·01	—	—	—	—	—	—
43	Biotite	5·11	—	5·11	0·21	—	0·21	—	—	—
44	Shale	0·18	—	0·18	0·10	—	0·10	—	—	—

Duplicates were taken only after the ion-exchange enrichment step and represent one rock sample only. The reproducibility of these duplicates therefore refers to the spectrochemical part of the procedure.

Table 1(b). Description of rocks investigated

No.	Description
1	Soevite
2	Nepheline syenite (coarse)
3	Nepheline syenite (fine)
4	Monomineralic syenite. K.Felspar rock.
	All from Ondurakorume alkali complex. Farm Etaneno. No. 44 Otjiwarongo. S.W.A.
5	Foyaite (fine grain)
6	Foyaite (coarse grain)
	Members of small intrusive complex in NW margin of Paresis* complex.
7	Intrusive plug into riebeckite rhyolite of intermediate Series, NW Paresis* complex.
8	Na-rhyolite, lower member of central extrusive complex. Paresis*.
9	Acid dyke rock, intruding W. margin of intermediate volcanic series. W. part of Paresis*.
10	Riebeckite rhyolite flow. W. Paresis*.
11	Rhyolitic dyke rock, intrusive into Damara basement. E. Paresis*.
12	Quartz felspar. Flow underlying agglomerate. S. Paresis*.
13	240 ft
14	260 ft
15	280 ft
16	300 ft
17	340 ft
18	360 ft
19	380 ft
20	420 ft
21	460 ft
22	480 ft
23	500 ft
24	500 ft
25	520 ft
	All from upper dolerite sill, main shaft, Jagersfontein diamond mine, O.F.S. S. Africa. Total thickness of sill 425 ft. Upper contact 150 ft below surface Base of sill 575 ft below surface.
26	660 ft
27	840 ft
28	860 ft
29	920 ft
30	960 ft
	All from 2nd dolerite sill. Total thickness 390 ft. Upper contact 575 ft, lower contact 970 ft.
31	Chilled upper margin of 1st dolerite sill.
32	Eclogite nodule. Bultfontein mine. Kimberley. S. Africa.
33	Eclogite nodule. Roberts Victor mine. O.F.S. S. Africa.
34	Eclogite nodule. Du Toits Pan mine. Kimberley. S. Africa.
35	Eclogite nodule. No locality.
36	Eclogite nodule. No locality.
37	Amygdaloidal basalt. Intrusive into Damara basement. Paresis*.
38	Micaceous carbonatite.
39	Dolomitic carbonatite.
	Same locality as nos. 1–4.
40	Glauconite. Lower portion of Boornaat. Glen Allen Mine. Prieska.
41	Crocidolite asbestos. Buisvlei. Orangeview, Prieska. S. Africa.
42	Banded ironstone, Tseloan, Hemingvlei, Vryburg. S. Africa.
43	Biotite. Clifton, Cape Town, S. Africa.
44	Shale. Malmesbury shale, Mouille point, Cape Town. S. Africa.

* The Paresis igneous complex lies between Outjo and Otjiwarongo, South West Africa.

Table 2. Estimated thallium concentrations (in p.p.m.) in the crust, chondrites and in certain igneous rocks

	Crust	Granites + related rocks	Basalt diabase or gabbro	Sedimentary rocks	Chondrites	No. of samplex
Clarke and Washington (1924)	0·0009	—	—	—	—	EST
Noddack and Noddack (1934)	0·1	—	—	—	0·15	?
Otteman (1940)	—	1·5	—	—	—	4
Preuss (1941)	2·1*	3·0	0·30	2·0	—	4 COMP
Rankama (1949)	0·6	—	—	—	—	EST
Goldschmidt (1954)	0·3	—	—	—	—	EST
Shaw (1957)	1·3	2·5	0·12	0·72		28
Ahrens (1947)	3·0	—	—	—	—	EST
Ahrens (as above, recalculated)	0·9‡	—	—	—	—	EST
Canney (1952)	—	—	—	0·36	—	323
Ishimori (1955)	0·7*	0·90	0·30	—	—	24
Vinogradov (1956)	1·7	—	—	—	—	—
Diomin and Khitarov (1958)	—	0·50	—	—	—	21
Vosresenskaya (1959)	—	0·80	—	—	—	43
Kogarko (1959)	—	0·50	—	—	—	27
Ehmann and Huizenga (1959)	—	—	—	—	0·004	5
Morris and Killick (1960)	—	1·30†	0·09	—	—	6
This paper	0·7*	0·73	0·11	0·34	—	52

* Estimated on 2:1 acid/basic rock ratio.

† One sample only(G–1).

‡ Based on a Rb crustal abundance of 120 p.p.m. The comparatively high value (3·0 p.p.m.) reported by Ahrens (1947) was based on the assumption that his observations on the constancy of the Rb/Tl ratio, estimated at 90, in 164 specimens of potassium minerals from pegmatites held also for common igneous rocks for which at that time very few Tl but considerably more Rb data were available; assuming a value of 280 p.p.m. for Rb (see references below) in the crust, the Tl abundance (calculated at Rb/Tl = 90) = 3 p.p.m. The crustal abundance for Rb has since been considerably lowered to 120 p.p.m. which if used in place of the earlier crustal value reduces the estimated thallium abundance considerably. As, however, considerable data have become available on the abundance of Tl in igneous rocks, calculations as above serve little purpose now.

estimates and is close to the value recommended by Rankama (1949). Recent work by Morris and Killick (1960) on the determination of Tl in five silicates and in G–1 and W–1 using a neutron activation method show results very similar to those reported by the authors. In particular there is a gratifying agreement between the respective values for the abundances in G–1 and W–1.

This comparison is shown in Table 3 below:

Table 3. The thallium content of G–1 and W–1

	G–1	W–1
Brooks *et al.* (1960)	1·3	0·1
Morris and Killick (1960)	1·3	0·17

In general, the estimated abundances given in this paper for granites are very similar to those of Goldschmidt, Ishimori and of most of the several Russian workers, but somewhat less than those of Preuss and of Shaw.

(ii) *The rubidium–thallium association.* The Rb–Tl coherence and the variation of the Rb/Tl ratio has been discussed by Ahrens (1945, 1948); Goldschmidt (1954); Shaw (1952); Tauson and Stavron (1957); Diomin and Khitarov (1958); Zlobin (1958); Borovik-romanova and Sosedko (1960); Taylor and Heier

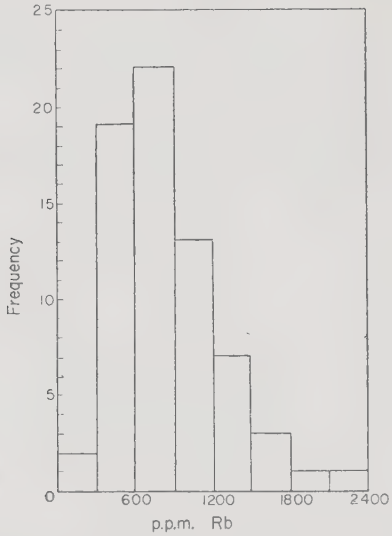

Fig. 1. Frequency distribution diagram for rubidium in 68 biotites from igneous rocks.

(1960), and Zlobin and Lebedev (1960). The principal reasons for this close association are equality of the radii of Rb^+ and Tl^+ and the fact that although the Tl—O bond is evidently more covalent than that of Rb—O both bonds are essentially ionic.

In a discussion of the magnitude of the ratio Rb/Tl in granites, gabbro and basalt and pegmatites, Shaw (1952) concluded that the ratio was at a maximum in granites as indicated in Table 2. Shaw's data were pre-1952. Explanations were offered as to why the Rb/Tl ratio should rise when passing from gabbro and basalt to granite and then fall again in pegmatites. Subsequent data do not support the granite–gabbro + basalt difference.

Table 4 gives some data on Rb, Tl and Rb/Tl ratios in chondrites, granite, gabbro + basalt, alkali rocks, biotite from igneous rocks, pegmatites and lepidolites. Biotites are of interest because though much less abundant than feldspar, they carry the highest Rb and Tl concentrations of igneous rock minerals; maximum concentrations (all silicate minerals including those from pegmatites) for both Rb and Tl are reached in lepidolite and hence this mineral has been included in Table 4.

Some of the data given in Table 4 are shown graphically (Figs. 1 and 2). Fig. 1 is a frequency distribution diagram of Rb in biotites from igneous rocks. The

distribution shows positive skewness with a modal (most frequent) Rb concentration of 650 p.p.m. which may be compared with the average of 900 p.p.m. given in Table 1. Fig. 2 compares the Rb/Tl data of AHRENS (1948), based mainly on 167 minerals from various pegmatites, with those of TAYLOR and HEIER (1960) which refer to alkali feldspars from the Pre-Cambrian basement rocks of southern Norway; the match is quite close.

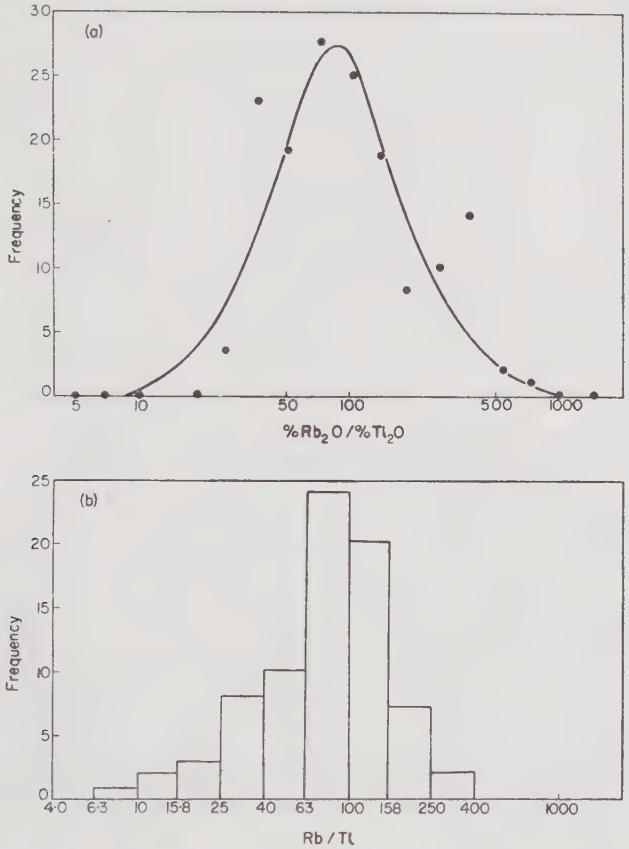

Fig. 2. Frequency distribution diagrams for the rubidium/thallium ratio, (a) in 167 minerals from various pegmatites (AHRENS, 1948). (b) for alkali feldspars from Pre-Cambrian basement rocks of southern Norway (TAYLOR and HEIER, 1960). Correspondence between the two sets of data is quite close.

Lepidolites are often regarded as being formed at a late stage in the sequence of mineralization in a Li-bearing pegmatite and if Rb^+ and Tl^+ enter the structures of these minerals with equal facility— that is to say Rb/Tl (lepidolite) = Rb/Tl (pegmatite emanation or fluid from which lepidolite crystallized) it is of interest to note that the ratio Rb/Tl remains roughly at the same general magnitude (100–300) in the sequence, basalt + gabbro → granite (and also alkali rocks) → pegmatites (as a whole) → pegmatites (very late stage). The available data indicate a slight but distinct fall in the ratio in pegmatites and lepidolites. This could be taken to support TAYLOR and HEIER's (1960) suggestion that the Rb/Tl ratio may fall in a

differentiated sequence due to the fact that the Tl—O bond is weaker than that of Rb—O because of its greater covalency. Their observations were made on some Pre-Cambrian feldspars from Norwegian pegmatites; they report a drop in the Rb/Tl ratio from 100 to 20.

The geochemical coherence of the pairs Rb–Tl and K–Rb make an interesting comparison. In the well known K–Rb pair, K^+ and Rb^+ both form dominantly ionic bonds with O^{2-} and radii differ slightly (K^+ = 1·33 Å and Rb^+ 1·45 Å) whereas in the Rb–Tl pair, radii are identical but the bonds which Tl^+ forms with

Table 4. Rb, Tl and Rb/Tl ratios in certain meteorites, rocks and minerals

	Rb (p.p.m.)	Tl (p.p.m.)	Rb/Tl	
			This paper	Shaw (1952)
Chondrites	4*	0·0004**	10,000	
Basalts + gabbros	30†	0·11††	270	140
Granites	170†	0·75††	200	340
Biotites from granite	900‡	4‡‡	230‡‡	
Alkali rocks	—	—	250§§	
Pegmatites	—	—	115***	90†††
Lepidolites	16,500§	120§	140	

* Based on data of Herzog and Pinson (1955) and K/Rb ratio considerations.

† Based mainly on data of Horstman (1956).

‡ Based mainly on sixty-eight mass spectrometer–isotope dilution estimations of Rb in igneous rock-biotite used for geological age investigations (various workers). See Fig. 1.

§§ From Zlobin and Lebedev (1960).

§ From Ahrens (1948) and Taylor (thirteen unpublished analyses). Only these data have been used because both Rb and Tl have been determined in the same specimen.

** Ehmann and Huizenga (1959) and Reed *et al.* (1960).

†† From this paper, see Table 1(A).

‡‡ Shaw (1952), Diomin and Khitarov (1958), Vosresenskaya (1959), Zlobin (1958), and this paper.

*** This value is based on the average Rb/Tl of Ahrens (1948), one of ninety-two given by Taylor and Heier (1960) and one of 103 given by Borovik-Romanova and Sosedko (1960).

††† This is the modal (most frequent) concentration reported by Ahrens (1948)—see Fig. 2 above. The interval in Fig. 2 is given by a power factor (a log scale has been used) and if a linear scale is used the distribution is strongly positively skewed and of a lognormal type; hence the average (130) is distinctly greater than the modal value (90).

O^{2-} though mainly ionic (depending on the ligand) will probably have some covalency (see above). Covalency arises from the fact that the polarizing power of $Tl^+ > Rb^+$, as indicated by their first ionization potentials 6·1 and 4·2 V, respectively (see Ahrens (1953) in this respect).

Although the Rb–Tl association in igneous rocks may be disturbed by local geological processes (presence of sulphide minerals and halogen transport of Tl, both due to covalency) superimposed on general operative processes (see Editor's Note p. 573 of *Geokhimiya*, No. 5, 1958) and perhaps also by some covalency in the Tl –O bond, the data given in Table 4 indicate that aside from the possible greater dispersion of the Rb/Tl ratio in specific rock types, the Rb–Tl coherence is closer than that of K–Rb in certain respects. Thus, whereas the value of the Rb/Tl ratio has about the same magnitude (100–300) in each of the terrestrial materials including lepidolites referred to in Table 4, K/Rb may drop significantly from its

igneous rock ratio to lower values in some biotites and late phase granites and various small volume residuals reaching a minimum in lepidolite. On the other hand there is the extraordinary drop (x 1/40) between chondrites and the terrestrial Rb/Tl ratio whereas K/Rb in chondrites is apparently the same as in the crust as a whole (AHRENS *et al.*, 1952). The abundances of Tl and of Bi and Hg in common chondrites may in a sense, however, be anomalous (REED *et al.*, 1960); see discussion below.

Although the presence of covalency in the Tl—O bond has not in general strongly disturbed the Rb–Tl association, a high degree of covalency is probably the reason for little or no coherence in other pairs of univalent elements which form cations of about the same size. For example,

Na–Cu
K,Rb–Ag
K,Rb–Au

Whereas the alkali metal–O bonds are essentially ionic, those of Cu, Ag or Au and oxygen are probably essentially covalent. It will be recalled that the order of

Table 5. Estimated Cd concentrations (p.p.m.) in crust and in silicate rocks

	No. rocks analysed	Crustal abundance*	Acid rocks	Basic rocks	Sediments
PREUSS (1941)	—	0·14	0·2	0·02	0·3
SANDELL and GOLDICH (1943)	8	0·14	0·12	0·19	—
VINCENT and BILEFIELD (1960)	15†	0·31	0·36	0·21	—
This paper	35	0·08	0·06	0·11	n.d.

* Estimated on a 2:1 acid/basic rock ratio.
† Skaergaard rocks.

polarizing power of large singly charged cations, as indicated by the first ionization potential is

$$\underset{(5\cdot1)}{\mathrm{Na}} < \underset{(4\cdot12)}{\mathrm{Rb}} < \underset{(4\cdot34)}{\mathrm{K}} \ll \underset{(6\cdot1)}{\mathrm{Tl}} \ll \underset{(7\cdot5)}{\mathrm{Ag}} < \underset{(7\cdot7)}{\mathrm{Cu}} \ll \underset{(9\cdot7)\ \mathrm{V}}{\mathrm{Au}}$$

In this respect, see also the discussion by RINGWOOD (1955) who used electronegativity as a guide to the nature of the bond.

The significance of covalency on the degree of association of certain pairs of divalent elements is discussed below.

Cadmium

(i) *Abundance.* Table 5 shows various abundance data for Cd.

Early (pre-1940) abundance estimates of Cd in rocks are those of CLARKE and WASHINGTON (1924) and GOLDSCHMIDT (1937) who give, respectively, 0·1–1 p.p.m. (magmatic rocks) and 0·5 p.p.m. (upper lithosphere).

PREUSS (1941) reported 0·2 p.p.m in acid rocks and 0·02 p.p.m. in basic rocks.

This large difference ($\times$ 10) between acid and basic rocks was not observed by Sandell and Goldich (1943) who working with a colorimetric procedure reported a fairly uniform Cd concentration in individual basic and acid igneous rocks; average for gabbros, dolerite and greenstone = 0·19 p.p.m. and for granite, 0·12 p.p.m. On the basis of these values the crustal abundance would come out at about 0·14 p.p.m.

The values given by Brooks *et al.* (1960) and in this paper tend to be slightly lower than the above, namely 0·06 p.p.m. for acid rocks and 0·11 p.p.m. for basic rocks, with one sample (Kloof Nek dolerite) containing the maximum of 0·45 p.p.m. (Brooks *et al.*, 1960). On the basis of these figures the crustal abundance would come to about 0·08 p.p.m.

When comparing the sets of data the possibility of analytical error—notably systematic error—should be borne in mind. Thus Vincent and Bilefield (1960) reported 0·33 p.p.m. Cd in standard diabase W–1 whereas the value (0·08 p.p.m.) of Brooks *et al.* (1960) is considerably less. It is unfortunately not possible at present to resolve this problem.

A few Cd data on rocks other than those above are considered in the discussion which follows on aspects of the geochemistry of Cd.

(ii) *Possible association of* Cd *with* Ca. Before examining the geochemistry of Cd (Cd^{2+} radius = 0·97 Å) and its possible association with Ca (Ca^{2+} radius = 1·01 Å), it may be instructive briefly to review the principal features of the geochemistry of Zn and its association with Mg. Neumann (1949) has emphasized many interesting features about the geochemistry of Zn whereas Wedepohl (1953) has reviewed its geochemistry and provided much fresh data. It is quite clear that although Zn is to some extent enriched in certain mafic minerals there is no significant Zn–Mg coherence despite charge equality and a similarity of ionic radii (Zn^{2+} = 0·69 Å; Mg^{2+} = 0.65 Å)· This is probably due to two main facts; first, the Zn—O bond is distinctly more covalent in character than that of Mg—O, and second co-ordination of O about Zn in most silicates (other than some with F^- and water) is usually tetrahedral (non-ionic) and not octahedral which would have accorded with the ionic radius ratio rules (see Neumann, 1949). When bonded (i) to O in compounds or minerals containing radicals (those with CO_3^{2-}, NO_3^-, SO_4^{2-}, PO_4^{3-}, etc.) and (ii) in the presence of F^- (for example, ZnF_2) and water, co-ordination is usually ionic, in which case Zn^{2+}–Mg^{2+} replacement is likely to take place fairly freely; this may account for the enrichment of Zn in biotite and amphibole reported by Wedepohl (1953).

The greater covalency of the Zn—O bond compared with that of Mg—O is evidently due in the first place to poorer screening efficiency of the electronic structure of Zn. As a result the electropositive field, and hence polarizing power, associated with $Zn^{2+} > Mg^{2+}$ as indicated by the second ionization potentials of these elements (Table 6); data on Ca, Cd, Sr and Hg are given for the sake of completion.

As in the Mg–Zn pair, so in the Ca–Cd and Sr–Hg pairs are the ionization potentials of the 18-electron elements distinctly greater than the 8-electron elements. (That of Hg is particularly high and in fact greater than those of Zn and Cd despite the fact that Hg is the heaviest element in the Group Zn–Cd–Hg. This

"anomaly" is evidently associated with the entry of $4f + 5d$ electrons (AHRENS, 1953). The significance of $4f$ and $5d$ entry on the chemistry and geochemistry of elements of the Au, Hg, Tl . . . . . period has been emphasized (AHRENS, 1953). In which case, the bonds between the 18-electron elements (Zn, Cd*, Hg) and oxygen are evidently much more covalent than those between the alkaline earth metals and oxygen. Moreover, the ionization potentials of the Zn–Mg and Cd–Ca

Table 6. Ionic radii, second ionization potentials and ionization potential ratios for Group II elements

	Cation radius (Å)	I_2 (V)	$\frac{I}{\bar{I}}$
8-electron Mg	0·65	15	1·19
18-electron Zn	0·69	17·9	
8-electron Ca	1·01	11·9	1·42
18-electron Cd	0·97	16·9	
8-electron Sr	1·15	11·0	1·71
18-electron Hg	1·12	18·8	

pairs are such that whether considered as simple differences or as ratios, they indicate that the Cd—O, Ca—O bond difference is likely to be greater than that between Zn—O and Mg—O. Electronegativity data support this conclusion; in this respect, see for example, RINGWOOD (1955). Accordingly, one may predict on these grounds that any Cd–Ca association is likely to be less than that between Zn and Mg.

On the other hand, whereas co-ordination of O about Zn tends to be four compared with six about Mg, both Cd and Ca (as one would expect) are octahedrally co-ordinated in their simple oxides each of which has the ionic NaCl structure. This could be taken to indicate that in silicates Cd^{2+} might be accommodated more easily in octahedral structure sites than Zn^{2+} and that a Cd^{2+}–Ca^{2+} substitution is more likely therefore than a Zn^{2+}–Mg^{2+} substitutuon; in which case Ca and Cd would be more closely associated than Zn and Mg. Let us now consider the available data.

SANDELL and GOLDICH (1943) suggested that the higher Cd concentration they found in basalt compared with granite was presumably due to substitution of Cd^{2+} for Ca^{2+}. Similarly GOLDSCHMIDT (1954) has mentioned the detection of Cd in Norwegian bytownite rock and calcic augite from basalt as due to such substitution. On the other hand no sign of a Ca–Cd association was observed by VINCENT and BILEFIELD (1960) in their work on the Cd content of Skaergaard rocks. They found

* Some data other than those of the free atom or ion which indicate that the Cd–ligand bond is likely to be distinctly more covalent than the Ca–ligand bond are:
(i) Refractive indices, for example those of the fluorides (AHRENS, 1958).
(ii) Melting points of CdO and CaO and of their Cd, Ca compounds (m.p. Ca compounds > Cd compounds).
(iii) Lattice energy calculations.
(iv) Colour of certain Ca and Cd compounds; see for example MORRIS and AHRENS (1956).
Moreover, the far greater tendency of Cd to form stable complexes with various ligands indicates that the binding power of Cd > Ca and presumably therefore that the polarizing power of $Cd^{2+} > Ca^{2+}$, which is in support of the ionization potential data.

that the maximum Cd concentration was in fact present in transgressive granophyres, acid rocks of late formation and low in calcium. In this respect it may be noted that Preuss (1941) reported a higher concentration of Cd in acid rocks (0·2 p.p.m.) than in basic rocks (0·02 p.p.m.).

The data given by Brooks *et al.* (1960) and in this paper indicate that the Cd content of basic rocks appears to be a little greater than that of acid rocks. But whether this should be ascribed to substitution of Cd^{2+} for Ca^{2+} is another matter. If anything, the data indicate that such a Ca–Cd association is unlikely for this main reason, i.e. the Cd concentration varies enormously ($\times$ 25) in specific rock types (say, basalt + dolerite) even in a single suite of rocks as at Jagersfontein where no sign of a trend is observable, and such large and seemingly sporadic changes of Cd concentration could hardly be due to its association with Ca, the concentration variation of which is far smaller. Cd is a distinctly chalcophile element and perhaps the presence of sulphides is one cause for some of the large Cd concentration changes: in this respect, it may be noted that there is sometimes a distinct correlation between a high Cd concentration and a high concentration of Bi and Tl, both chalcophile elements, in Jagersfontein dolerites (see Table 1a).

It will be concluded, somewhat tentatively therefore, that a Ca–Cd association in common igneous rocks either does not exist or is very feeble and that in any case such possible coherence is less than in the pair Zn–Mg. If the observations of Vincent and Bilefield (1960) on the Skaergaard rocks hold for other differentiated suites they would support the statement by Rankama and Sahama (1950) that: "Cd together with other elements remains largely in the residual melts and solutions throughout the main stage of crystallization and the pegmatitic stage" and that "owing to its weaker oxyphile nature, cadmium becomes nearly quantitatively enriched in hydrothermal rocks and minerals and its highest concentrations are met in formations belonging to the lowermost temperatures." The observations also provide support to a rule enunciated by Ringwood (1955) on the consequences of covalency in a metal-oxygen bond on the behaviour of a metal during processes of differentiation.

Contrary to the suggestion by Goldschmidt (1954) that apatite is very likely to be a host mineral for Cd in magmatic rocks—a suggestion which on crystallochemical grounds seems very plausible indeed because of the presence of PO_4^{3-} and some F^- (see above)—Vincent and Bilefield (1960) did not find a distinct enrichment of Cd in apatite from ferrogabbro. A value of 0·15 p.p.m. is reported and further determinations by the authors of this paper on three calcium-rich minerals corroborate this finding, and the Cd contents of wollastonite, Damara marble and actinolite were found to be comparatively low (0·05–0·1 p.p.m.). The highest Cd concentrations have been observed in two out of three carbonatites (0·8 p.p.m. Brooks *et al.*, 1960; and 0·36 p.p.m., this paper) analysed and it is presumably in these rocks only that the Cd enrichment is due to substitution of Ca^{2+} by Cd^{2+}.

Bismuth

(i) *Abundance.* Table 7 shows abundance data for Bi.

Very few data are available on the abundance of this element. Noddack and

Noddack (1934) give a value of 0·07 p.p.m. based apparently on the frequency of occurrence of Bi minerals whereas Goldschmidt (1954) gives an estimate of $> 0{\cdot}2$ p.p.m. which is based on the proportions of As, Sb and Bi in ferruginous bauxites and sedimentary iron ores. Preuss (1941) gives a value of 2, nil and 0·6 p.p.m., respectively for acid, basic and sedimentary rocks. Brooks *et al.* (1960) gave an estimate of 0·2 p.p.m. for the crust and this magnitude is supported by the data given in the present paper which together with the previous results indicate a crustal abundance of 0·17 p.p.m. for Bi.

Table 7. Estimated Bi concentrations (p.p.m.) in crust, chondrites and rocks

	No. rocks analysed	Acid rocks	Basic rocks	Sed. rocks	Chond-rites	Crustal abundance
Noddack and Noddack (1934)	—	—	—	—	0·02	0·07
Preuss (1941)	4 comp.	2·0	—	0·6	—	—
Goldschmidt (1954)	Est.	—	—	—	—	0·2
Ehmann and Huizenga (1959)	5	—	—	—	0·0022	—
This paper	50	0·18	0·15	0·11	—	0·17*

* Based on a 2/1 acid–basic rock ratio.

(ii) *Sundry geochemical features.* Several geochemical features, some based on observation and others on crystallochemical speculation have been discussed by Goldschmidt (1954). Reference is made to the possibility of a Bi^{3+}–Ca^{2+} substitution, particularly in early minerals of magnetic rocks. In this respect Goldschmidt (1954) several times mentions (p. 480) a Bi^{3+}–Ca^{2+} substitution in apatite, not only as a suggestion, but seemingly as an observation also; unfortunately neither original data nor original sources are given. Goldschmidt infers from "experience in mineralogy and economic geology" that Bi is concentrated in granitic magmas and in their residual solution and in this latter respect particular mention is made of the concentration of Bi in rare-earth minerals from pegmatites where Bi^{3+} evidently replaces R^{3+} rare earth cations. Several of the above observations will be taken up in the discussion which follows.

If the common igneous rock types are considered, little, if any, Bi–Ca substitution and association are apparent. Thus the Bi content of acid and alkaline rocks (both relatively low in Ca), see also data Brooks *et al.* (1960), is similar in magnitude to the basic rocks (comparatively rich in Ca). Furthermore, no enrichment of Bi was observed in wollastonite, actinolite, apatite or marble. Traces of Bi (0·06, 0·06 and 0·06 p.p.m.) in three specimens of carbonatite (this paper and Brooks *et al.*, 1960) may be due to Bi^{3+}–Ca^{2+} substitution, but the concentration level does not represent an enrichment.

We have not estimated Bi in rare-earth minerals but Bi enrichment in monazite for example is well known and presumably Bi^{3+}–RE^{3+} substitution is the cause.

The spread of Bi concentration in rocks of the same type (for example, Jagersfontein dolerite) is very considerable and ranges from $< 0{\cdot}01$ p.p.m. to 0·80 p.p.m.,

a factor of > 80. This could be due in part at least to the chalcophilic properties of Bi and to a significant degree of covalency in the Bi^{III}—O bond. Brooks *et al.* (1960) have drawn attention to a large difference in Bi content in some granites.

(iii) *Apparent very high degree of enrichment of* Bi *and* Tl *in the earth's crust.* It has been recognized for a considerable time that certain elements (Li, K, Rb and

Table 8. Some selected values of the crustal enrichment index (arranged in order of increasing enrichment)

Element	Abundances in p.p.m. unless indicated as %		Enrichment index
	crust	Earth as a whole	
Ni	35	1·34%	0·0026
Pd	0·004	1·54	0·0028
Au	0·002	0·2	0·01
Co	20	800	0·025
Cr	100	2500	0·04
Ge	1·1	9	0·12
Mg	2·1%	14·4%	0·15
Fe	5·0%	25·1%	0·20
Zn	40	180	0·22
Cd	0·15	0·5	0·30
Cu	55	90	0·61
Si	27·7%	17·8%	1·55
Ca	3·63%	1·39%	2·6
V	120	39	3·0
Sc	20	6	3·3
Na	2·83%	0·67%	4·2
Zr	156	33	5·0
Al	8·13%	1·32%	6·0
Nd + La	42	4·17	10
K	2·59%	0·085%	30
Rb	120	4	30
Sr	450	10	45
Bi	0·2	0·002	100
Ba	1000	6	167
Tl	*1·3	0·004	320
	†0·6	0·004	150

* Shaw's estimate.
† This paper.

C's for example) are apparently strongly enriched in the earth's crust: others (Mg for example) are concentrated in the mantle and others (the siderophile elements Au, Pd and Ni for example) are presumably strongly enriched in the core. If it is assumed that the earth as a whole originated from cosmic substance with a chemical composition equivalent or similar to that of chondrites, it is possible to estimate the degree to which an element may have been enriched in the crust. Given for example that the abundance of potassium in the crust is 2·6 per cent compared with a value

of 0·085 per cent in chondrites, crustal enrichment may be expressed in the form of the ratio,

$$\frac{\text{abundance in crust}}{\text{abundance in earth as a whole}}$$

which for potassium = 30. It is possible to express crustal enrichment in other forms, on a more absolute basis* for example, by taking into account the respective masses of earth ($5{\cdot}976 \times 10^{27}$ g) and of crust ($0{\cdot}024 \times 10^{27}$ g = 0·4 per cent of earth) but for the purpose here the simple ratio above will be used.

Some selected values of the abundance ratios (metals only) are given in Table 8.

It is clear from Table 8 that provided the analytical data are reasonably accurate, Bi and Tl are evidently enriched to a very high degree indeed in the crust. The tendency for Tl^+ to substitute for K^+ in potassium minerals is well established, and hence because of crustal enrichment of potassium, enrichment of Tl (and of Rb) would be expected. An enrichment of Tl which is apparently far greater than Rb is, however, surprising; in fact, the reverse might have been expected because Tl is to some extent chalcophilic and if sulphides are present in the mantle, they could contain Tl but no K + Rb. The crustal enrichment of Bi seems also surprisingly high in this respect. Cd on the other hand is actually depleted in the earth's crust and the index is similar in magnitude to that of Zn (Table 8).

If the index is 250 or greater an element must be concentrated entirely in the crust, as the mass ratio crust/whole earth is 250.

Investigations by Reed *et al.* (1960) (see also Ehmann and Huizenga, 1959) have recently indicated that unlike most elements, the concentrations of the heavy metals Hg, Tl, Pb and Bi are much higher in carbonaceous chondrites than in the common chondrites; for Tl the concentration ratio (carbonaceous chondrite)/(ordinary chondrite) is 200 and for Bi it is 50. If the rare carbonaceous chondrites rather than the common chondrites are more accurately representative of primitive cosmic substance (see Ringwood, 1960, for example) out of which the earth originated, the above comments about high crustal enrichment of Tl and Bi do not apply; this possibility and its implications will, however, not be considered further here.

The possible significance of (i) any high enrichment and (ii) variation of concentration in the principal structural components of the earth will be discussed in detail elsewhere; particular attention will be given to the use of abundance data for setting up limiting compositions*.

Acknowledgements—The authors are indebted to Mr. Key for providing the carbonatites and other specimens, to De Beers Consolidated Mines Ltd. for the eclogites, to Mr. G. Siedner for the specimens from the Paresis complex, to Mr. J. Genis for the Prieska rocks, to Mr. J. F. Truswell for the dolerite suite of rocks and to Dr. S. R. Taylor for his help in collecting the specimens and for helpful comments.

References

Ahrens L. H. (1945) The geochemical relationship between Tl and Rb in minerals of igneous origin. *Trans. Geol. Soc. S. Africa.* **48,** 207.

* *Note added in proof*: A few calculations and discussions of this sort have recently been made by Gast (P. W. Gast (1960) Limitations on the composition of the upper mantle. *J. Geophys. Res.* **65,** 1287–1297).

Ahrens L. H. (1947) The abundance of Tl in the earth's crust. *Science* **106,** 8.
Ahrens L. H. (1948) The unique association of Tl and Rb in minerals. *J. Geol.* **56,** 578.
Ahrens L. H. (1953) The use of ionisation potentials. *Geochimica et Cosmochim. Acta* **3,** 1.
Ahrens L. H. (1958) Variations of refractive index with ionisation potentials in some isostructural crystals. *Miner. Mag.* **31,** 929.
Ahrens L. H., Pinson W. H. and Kearns M. M. (1952) Association of Rb and K and their abundance on common igneous rocks. *Geochim. et Cosmochim. Acta* **2,** 229.
Borovik-Romanova T. F. and Sosedko A. F. (1960) The geochemical ratio between the Tl and Rb content in pegmatites and minerals from the Kola peninsula. *Geokhimiya* **1,** 31.
Brooks R. R., Ahrens L. H. and Taylor S. R. (1960) The determination of trace elements in silicate rocks by a combined spectrochemical-anion exchange technique. *Geochim. et Cosmochim. Acta* **18,** 162.
Canney F. C. (1952) Some aspects of the geochemistry of K, Rb, Cs and Tl in sediments. *Bull. Geol. Soc. Amer.* **63,** 1238.
Clarke F. W. and Washington H. S. (1924) The composition of the earth's crust. *U.S. Geol. Survey* No. 127.
Dromin A. M. and Khitarov D. N. (1958) The geochemistry of K, Rb and Tl applied to problems of petrology. *Geokhimiya* **6,** 570.
Ehmann W. D. and Huizenga J. R. (1959) The determination of Bi, Tl and Cd in stone meteorites by neutron activation analysis. *Geochim. et Cosmochim. Acta* **17,** 1–2.
Goldschmidt V. M. (1937) The geochemical distribution of the elements. *Skr. Norsk. Vidensk. Akad. Mat. Kl.* No. 4.
Goldschmidt V. M. (1954) *Geochemistry.* Oxford University Press.
Herzog L. F. and Pinson W. H. (1955) Sr and Rb content of granite G–1 and diabase W–1. *Geochim. et Cosmochim. Acta* **8,** 295.
Horstmann E. L. (1956) The distribution of Li, Rb and Cs in igneous rocks and sedimentary rocks. *Geochim. et Cosmochim. Acta* **12,** 1.
Ishimori T. and Takashima Y. (1955) *Mem. Fac. Sci. Kyushu* **65,** 74.
Kogarko L. N. (1959) The distribution of alkaline elements and thallium in granitoids of the Turgoyak massif (middle Ural). *Geokhimiya* **5,** 455.
Morris D. F. and Ahrens L. H. (1956) Ionisation potentials and the chemical binding and structures of simple inorganic crystalline compounds—1. *J. Inorg. Nucl. Chem.* **3,** 263.
Morris D. F. and Killick R. A. (1960) The silver and thallium content of rocks. *Geochim. et Cosmochim. Acta* **19,** 139–140.
Neumann A. E. (1949) Notes on the mineralogy and geochemistry of Zn. *Miner. Mag.* **28,** 205.
Noddack I. and Noddack W. (1934) The geochemical distribution coefficients of the elements. *Svensk. Kem. Tid.* **46,** 173.
Otteman J. (1940) Investigations into the distribution of trace elements in Harz minerals. *Z. Angew. Min.* **3,** 142.
Preuss E. (1941) The determination of volatile elements by fractional distillation. *Z. Angew. Min.* **3,** 8.
Rankama K. A. (1949) A note on the geochemistry of Tl. *J. Geol.* **57,** 608.
Rankama K. and Sahama Th. G. (1950) *Geochemistry.* Chicago University Press, Chicago.
Reed G. W., Kigoshi K. and Turkevich A. (1960) Concentrations of some heavy elements in meteorites by activation analysis. *Geochim. et Cosmochim. Acta* **20,** 122–140.
Ringwood A. E. (1955) The principles governing trace element distribution during magmatic crystallisation. *Geochim. et Cosmochim. Acta* **7,** 189.
Ringwood A. E. (1961). In preparation.
Sandell E. B. and Goldich S. S. (1943) The rare metallic constituents of some American igneous rocks. *J. Geol.* **51,** 99.
Shaw D. M. (1952) The geochemistry of Tl. *Geochim. et Cosmochim. Acta* **2,** 118.
Shaw D. M. (1957) The geochemistry of Ga, In and Tl. *Progress in Physics and Chemistry of the Earth.* Vol. 2. Pergamon Press, London.
Tauson L. V. and Stavron O. D. (1957) On the geochemistry of Rb in granitoids. *Geokhimiya* No. 8, 699.

Taylor S. R. and Heier K. S. (1960) The petrological significance of trace element variations in alkali feldspars. *Proceedings of the Twenty-first International Geological Congress, Copenhagen.*

Vincent E. A. and Bilefield L. I. (1960) Cd in rocks and minerals from the Skaergaard intrusion, East Greenland. *Geochim. et Cosmochim. Acta* **19,** 6.

Vinogradov A. P. (1956) The regularity of distribution of the chemical elements in the earth's crust. *Geokhimya* **1,** 6.

Vosresenskaya N. T. (1959) On the geochemistry of thallium and rubidium in igneous rocks. *Geokhimiya* **6,** 495.

Wedepohl K. H. (1953) The geochemistry of zinc. *Geochim. et Cosmochim. Acta* **3,** 93.

Zlobin B. I. (1958) The geochemistry of Tl in alkaline rocks. *Geokhimiya* **5,** — —

Zlobin B. I. and Lebedev V. I. (1960) The geochemical limits of Li, Na, K, Rb and Tl in the alkaline magma and their petrological importance. *Geokhimiya* **2,** 87.

Geochimica et Cosmochimica Acta, 1961, Vol. 23, pp. 116 to 134. Pergamon Press Ltd. Printed in Northern Ireland

Element distribution laws in geochemistry

D. M. Shaw*
McMaster University, Hamilton, Ontario

(*Received* 5 *May* 1960)

Abstract—Recent articles on element distributions have given insufficient attention to geological aspects of the problems, and have neglected to consider the effects of sampling, sample reduction and analysis error on the interpretation of frequency distributions. No single probability function can be expected to suit all elements. These and other considerations lead to the proposal of five rules (given below) concerning trace element distributions which include Ahrens' proposed law (1954a) in a revised form. The first three rules are based on theoretical considerations and require further experimental proof except in the case of certain ore deposits whose lognormal distribution is well established. It is recommended, however, that the lognormal law be used as the basis for discrimination tests in all cases.

(1) The frequency distribution of concentrations of a camouflaged trace element in a homogeneous rock formed by a chemical equilibrium process can be considered as continuous probability functions with limits zero and $+\infty$.

(2) The best probability function to use is the lognormal law, which is justified both by practical utility and theoretical considerations.

(3) The previous rules also apply to those trace and minor elements which are largely concentrated in accessory or ore minerals of simple constitution. Many economic deposits are in this category. The Poisson function may also be convenient in this case, if the discontinuous distribution of mineral grains is considered.

(4) The geochemical variance of a group of data is less than the measured variance, which should be corrected by subtracting manipulation variance (sampling, sample reduction, analysis).

(5) The coefficient of variation c_g (= s.d./mean) of a small body of geochemical data provides a criterion for the choice between a normal and a lognormal law for subsequent statistical tests. When $c_g < 0{\cdot}2$ either law will predict similar probabilities, but when $c_g > 0{\cdot}2$ the lognormal law is more realistic. It is important to correct the observed relative variance c^2 (as in rule 4) to obtain ${c_g}^2$, otherwise the choice will be biassed towards a lognormal law.

Introduction

Numerous articles on the distribution laws of elements in specific geological materials have appeared in recent years. On the one hand there is the series of papers in this journal, initiated by the first paper of Ahrens in which he sought to prove that element distributions are lognormal (this view is qualified in the later papers): Ahrens' several articles (1954a, b, 1957) have been criticized by Chayes (1954), Aubrey (1956), Miller and Goldberg (1955), Durovic (1959), Jizba (1959), and Vistelius (1960).

On the other hand a series of papers in the French mining journals have also been preoccupied with the lognormal distribution, with particular reference to its application for the estimation of ore reserves, but also for scientific problems. Two papers by Matheron (1955, 1956) are of particular interest to geochemists; these and other papers by French authors (Laffitte, 1953; Gy, 1954, Bes de Berc, 1954; Duval, 1955a, b,) also devote considerable attention to the problems of sampling. These authors refer extensively to the works of Krige (1951a, b), Sichel (1949, 1952) and De Wijs (1951, 1953) on lognormal distributions with particular reference to gold values in the mines of South Africa; these original

* On leave of absence 1959–1960 at L'Ecole Nationale Supérieure de Géologie Appliqueé et Prospection Minière, Nancy.

papers were not available to the writer but a summary has been made by DUVAL *et al.* (1955).

The literature review in VISTELIUS' (1960) article indicates that the lognormal distribution has been used by some of the Russian geochemists since 1940 (RASUMOVSKY, KOLMOGOROV, VISTELIUS).

It is unfortunate that the authors of the first sequence referred to did not make use of MATHERON's articles, which include two proposed models to establish the lognormal law, in addition to citing a third by DE WIJS. AHRENS (1954a) had, however, referred to the work of SICHEL and KRIGE in his 1954 papers.

The present article is concerned more with geological aspects of the question than in further elaboration of the mathematical models, since it has recently become evident to the writer that all the authors quoted, with the exception of MILLER and GOLDBERG, have over-simplified the problems and have given insufficient attention to one or other or both of the following points:

(a) a distribution law may be established either empirically, on the basis of a given set of data, or theoretically from a particular model;

(b) geological considerations indicate clearly that the theoretical distribution law will differ according to the situation; i.e. no single law applies to all the situations.

With regard to (a), the procedures of statistical description permit the choice of one or more theoretical distribution laws (probability functions) to describe approximately a given body of data; it is assumed that the proposed geochemical law of AHRENS (1954a, p. 64) falls in this category. The choice of the function used depends on the data and logically precedes any explanation. Alternatively, scientific considerations may lead to the formulation of a statistical probability model appropriate to a given situation before any data have been obtained. The predicted probabilities can then be compared with observed frequencies (e.g. the binomial distribution of point-counting observations, CHAYES and FAIRBAIRN 1951). In practice the two procedures may often be confused and the validity of subsequent criticism becomes uncertain.

With regard to (b) it is only necessary to remark at this point that the distribution models for elements in minerals are not the same as for rocks, and that the model for a major element in either is different from the case of a camouflaged trace element or (usually) from that of an economic metal in a mineral deposit. This matter will be discussed shortly.

A further point is important in the case of the interpretation of the frequency distribution of a group of analyses:

(c) the errors of sampling, preparation and analysis are all reflected in the dispersion of a series of analyses.

Points (a), (b) and (c) will be discussed in reverse order in the following.

A paper by the writer and his colleague J. D. BANKIER (SHAW and BANKIER, 1954) recommended a more extensive use of statistical tests in geochemistry, and appeared almost simultaneously with the first paper of AHRENS quoted above. Normal distributions were assumed throughout that paper and it is now evident that this assumption was unwarranted. The first author accepts all responsibility

for that mistake but the tests described can be modified accordingly. The present article can be regarded as an act of contrition.

Errors of Manipulation

Suppose that a series of analyses for a given element have been made on rocks 1, 2 . . . i . . . n and let the results be x_1, x_2 . . . x_i . . . x_n in wt. per cent. Let us assume that the rocks are similar in such a way that their true contents θ_1, θ_2 . . . θ_i . . . θ_n of the element form a statistical population of mean μ and variance σ^2. Each rock has been collected separately and has undergone three operations to obtain the values x_i:

(a) sampling, or collecting of specimens to represent an exposure in the field;
(b) crushing and quartering, to reduce the size and state of the original sample to a product suitable for the analyst;
(c) analysis.

Each of these operations introduces a source of error, assuming that the rocks are not perfectly homogenous. They will be referred to in general as "manipulation errors".

It will be more convenient in the following discussion to use the *relative standard variation* or *coefficient of variation* c, in place of the standard deviation itself, where

$$c = \text{s.d./mean, and } C = 100\,c$$

The value c^2 will be referred to as *relative variance.*

Whatever the distribution function of the values θ_i, the mean can be estimated by

$$\bar{x} = \frac{1}{n} \sum_{i}^{n} x_i$$

$\bar{x}$ is not always the best estimator of μ for non-symmetrical distributions, but this point will be ignored here (see Matheron, 1955).

The relative standard deviation c of the data is calculated by the expression

$$c^2 = \frac{n^2}{n-1}\left[\sum_{i=1}^{n} x_i^2 - \frac{\left(\sum_{i=1}^{n} x_i\right)^2}{n}\right] \Bigg/ \left(\sum_{i=1}^{n} x_i\right)^2$$

In most geochemical problems c is considered to be a suitable estimator for σ/μ, but this is not necessarily true because of the possibility of the introduction of bias during the three stages of manipulation. Apart from the merits of different sampling and sample reduction schemes a bias can arise simply by the process of hitting a rock with a hammer, whereby brittle minerals may be lost as dust.

If we represent the coefficients of variation introduced by the sampling, crushing and analysis operations by c_s, c_c and c_a, respectively, then

$$c^2 = c_s^2 + c_c^2 + c_a^2 + c_g^2$$

where c_g^2 is the contribution to the total relative variance of the inherent dispersion of the population. In most procedures one sample is taken of each rock, one

crushing and quartering procedure is carried out and p analytical replicates are taken. The above expression becomes

$$c^2 = c_s^2 + c_c^2 + \frac{c_a^2}{p} + c_g^2$$

or

$$c_g^2 = c^2 - \left(c_s^2 + c_c^2 + \frac{c_a^2}{p}\right)$$

Grouping the last expression as c_m^2, the relative variance of manipulation, we have

$$c_g^2 = c^2 - c_m^2 \qquad (1)$$

It is evident that c_g is a better estimator of σ/μ than c. Expressing this relationship as a geochemical rule, we may write: *the geochemical variance of a series of analyses is less than the measured variance, which is therefore biased.*

How can this be used in practice ? Evidently the best thing for a given problem would be to estimate each of the terms c, c_s, c_c and c_a, that is, to collect for each rock numerous samples, crush to numerous fractions, analyse numerous times, then carry out an analysis of variance.* The amount of labour would be prohibitive for small organizations. Most workers content themselves with a measurement of c_a on the basis of a number of replicates, state that it is of the order perhaps of 0·05 (C_a = 5 per cent) and promptly ignore it for the rest of the discussion. It is perhaps tacitly assumed that nothing can be said about c_s and c_c or that they can be disregarded by comparison with c_a. Neither point of view is correct.

In the absence of direct measurements, the likely magnitudes of c_s and c_c can be predicted on the basis of a model proposed by Gy (1954) and adapted to geochemistry by Laffitte (1953, 1957). Details need not be recapitulated here, but the necessary parameters include the mass of the sample (p), the average grain weight π, the average concentration (a_j) of the element in each mineral and in the rock (a) and the modal composition.

From a_j, a and the mode it is possible to calculate the average value for the rock of the expression $(a_j - a)^2$ for each mineral j: representing this mean square by $K^2\,a^2$ the relative standard deviation is c_s ,where $c_s = s/a$ and

$$s^2 = \frac{\pi K^2 a^2}{p}$$

The ratio π/p is the number n of original grains of the rock in the sample and the expression becomes

$$c_s^2 = \frac{K^2}{n}$$

K is a constant which can be roughly evaluated for a given element and rock type. Its value is usually between 0·1 and 10·0; it is least for an element whose concentrations are similar in most of the minerals of a rock (e.g. SiO_2 in an igneous rock) and greatest for an element occurring at a high concentration in one accessory mineral but absent from the others (e.g. P_2O_5 in an igneous rock).

* J. D. Bankier points out (personal communication) that the foregoing arguments involve several theoretical assumptions and demand a more rigorous analysis. As a working method, however, the procedure is empirically justified.

A similar procedure can be applied to the process of sample reduction, the parameters π and p being applied now to the grain size and total mass of the crushed and quartered powder sent to the analyst; c_c can then be calculated.

The principal assumptions of the model concern the grain size of the original rock and of the sample. They are not entirely justified but contribute uncertainties of a lower order of magnitude and can be ignored.

Analysis along the lines indicated by Laffitte indicates a customary range in magnitude of c_s^2 from about 0·0001 to 0·0400 (C_s from 1 to 20 per cent). The upper limit is clearly indeterminate, marking as it does the worst possible sampling imaginable, but the values of c_s^2 for the sampling of coarse-grained porphyroblastic rocks are high unless samples of the order of hundreds of kilograms are taken.

For any sample-reduction operation which is intuitively reasonable the range of c_c^2 is less than c_s^2. This is because the grain size of the final product is critical and can be reduced to a very small magnitude without inordinate labour, especially if mechanical grinders are used. The range of c_c^2 may then be taken as 0·0001 to 0·0010 (C_c from 1 to 3 per cent).

The range in magnitude of c_a^2 depends on the method and the analyst. The original investigation of G–1 and W–1 showed a range from 0·000025 to 0·1600 (C_a from 0·5 to 40 per cent) and it is evident that the precision of gravimetric methods for minor constituents is usually low. The "rapid methods" in use at the Ecole Nationale Supérieure de Géologie Appliquée, Nancy, for major and minor elements in silicate rocks show values usually ranging from 0·0001 to 0·0625 (C_a from 1 to 25 per cent), whereas the quantometric analyses at the same institution show a range (for the same elements) of from 0·0001 to 0·0081 (C_a from 1 to 9 per cent).* For the present we can consider the range of c_a^2 as from 0·0001 to 0·1600 for all methods, acknowledging that good methods show a much smaller range.

We may accordingly express the total manipulation relative variance c_m^2 as follows:

$$c_m^2 \text{ minimum} = 0{\cdot}0001 + 0{\cdot}0001 + 0{\cdot}0001 = 0{\cdot}0003 \ (C = 1{\cdot}7 \text{ per cent})$$

$$c_m^2 \text{ maximum} = 0{\cdot}0400 + 0{\cdot}0010 + 0{\cdot}1600 = 0{\cdot}2010 \ (C = 45 \text{ per cent})$$

The manipulation relative variance in a given experiment may therefore be expected to fall in the range 0·0001–0·2000 (rounding the numbers), assuming that each rock is sampled, reduced and analysed once. It is perhaps fair to say that there are few geochemical organizations where one would expect c_m^2 to reach 0·2000 (i.e. consistently bad techniques), but it is probably equally true to say that there are few where c_m^2 may be held down to 0·0001.

It is difficult to choose a representative figure for c_m^2, but we can first of all admit that c_c^2 may readily be reduced to 0·0001, and many chemical laboratories would consider the value $c_c^2 = 0{\cdot}0025$ ($C = 5$ per cent) for a single analysis to be a reasonable assessment of overall precision for routine analysis of most elements. The magnitude of c_g^2 is less readily controllable, depending as it does on the number of kilograms of rock which the geologist can carry and subsequently crush (except

* These figures are quoted by courtesy of M. Behr, Chief of the Chemical Laboratory, of M. Govindaraju, Chief of the Spectrographic Laboratory and of M. Roubault, Director of the ENSGA.

in the case of mining organizations) and also on the state of combination of the element concerned. However, the value of 0·0075 may represent the sampling relative variance for a coarse-grained rock of which either 500 g or 25 kg have been collected, depending, respectively, on whether one is interested in (a) a major element contained in each principal mineral at a similar concentration, or (b) a minor element strongly concentrated in an accessory mineral. With these restrictions a "representative" value of c_m^2 is 0·0075 + 0·0001 + 0·0025 or about 0·0100, which corresponds to a total coefficient of variation of about 10 per cent. In this case the geochemical relative variance would be

$$c_g^2 = c^2 - 0{\cdot}0100$$

Let us consider now the example of Pb in schists used in our 1954 paper (Shaw and Bankier, 1954). The mean concentration in thirty schists was 27·3 p.p.m. and the sum of the squares of deviations from the mean was 3462·0. The best estimation of the total relative variance (neglecting the rounding in the estimation of the mean) is therefore

$$c^2 = \frac{3462{\cdot}0}{29 \times 27{\cdot}3^2} = 0{\cdot}1602$$

Taking the extreme values of c_m^2 above, the possible values of the geochemical variance are

$$c_g^2 = 0{\cdot}1602 - 0{\cdot}0001 = 0{\cdot}1601$$

and

$$c_g^2 = 0{\cdot}1602 - (0{\cdot}2000) = 0$$

The second case is artificial since c_m^2 cannot exceed c^2. However, it is clear that the dispersion of a series of analyses represents the parent population only to a degree determined by the efficiency of sample manipulation.

To find a distribution law which adequately describes a given population of this kind, it is evident that the manipulation variance must be taken into account, otherwise the bias of the observed variance will influence the law chosen, as shown later.

In the above example, the "representative" value of c_m^2 (0·0100) is applicable (Pb is a trace element, but occurs in garnets, micas and feldspars in the schists). The value of c_g^2 is 0·1602–0·0100 or 0·1502. The correction might or might not change the distribution law chosen, but in any case it certainly would change the prediction of probability in any discrimination tests made on the data.

The Distribution of Manipulation Errors

The discussion in the preceding section is independent of any assumptions regarding the distribution of either the parent population or of the errors. For any body of data one can calculate the mean $\bar{x}$ and the variance s^2 without prejudice to the choice of distribution, but, of course, the two quantities estimate the parameters of a particular normal curve (and only one) which is the best normal curve to describe the observed frequencies. It is always possible, however, that some other curve will describe the data better.

Equation (1) above has been derived to correct the bias of the observed variance

and will carry out that purpose most efficiently if the individual dispersions (e.g. geochemical, analytical, etc.) show a fairly close approximation to normal distributions. If one of them is better represented by some other distribution, then the correction proposed in equation (1) is less efficient than it could be.

We will mainly confine attention in the following to the analytical variance s_a^2; Gy (1954) maintains that sampling errors follow a normal distribution, but this is certainly not always true for analytical errors. Let us consider the distribution of Fe_2O_3 in twenty-eight analyses of G–1 (Fairbairn, 1953). The mean value is 0·93 per cent and s is 0·34, from which we would expect about 99 per cent of the analyses to fall in the range $0{\cdot}93 \pm 3 \times 0{\cdot}34$ or 1·95 to −0·09 per cent. A negative value is impossible, even for the worst analysis; other examples occur in an article by the writer (Shaw, 1954), where, however, their significance was not realized at the time. It is clear that $\bar{x}$ and s in these cases estimate the parameters of normal curves which do not describe the populations at all well.* In other words some other probability function would be more efficient. This point is also discussed by Ahrens (1954b, pp. 121–123), who showed how a logarithmic transform will avoid negative values.

Another point to be borne in mind for later discussion is that numbers whose upper limit is 100 (i.e. concentrations in per cent) cannot conform to a continuous function.

The possibility of predicting negative values clearly depends on the ratio $s/\bar{x}$ or c. If c is greater than 0·33 (it is 0·37 in the example of Fe_2O_3 above) then the range $x \pm 3\,c$ will include negative values, similarly if c is greater than 0·50 there will be negative values in the range $x \pm 2\,c$, etc.

If one wishes to replace a normal distribution in such a way as to prevent the appearance of negative values when $s/\bar{x}$ is large, it is necessary to select a distribution with positive skew (mode less than the mean). Various such distributions are known, e.g. binomial, Poissonian, lognormal, some discontinuous and some continuous. The choice depends on various tests which can be made on the data if it is a large enough sample of the population.

We are concerned here mainly with statistical description but it is worth digressing briefly to consider statistical models. The normal distribution (De Moivre–Laplace–Gauss) became popular largely as a result of Gauss' work on error distributions. If a deviation or an error is the sum of effects which are small, independent, numerous and independent of the magnitude of the quantity measured, then the error distribution obeys the normal law. In fact the distribution is sometimes called "the law of errors". In more recent times, it has become evident that deviations do not always meet these requirements and it is clear from both intuition and mathematical argument that many errors of the type δx_i are a function of the magnitude x_i (see articles by Miller and Goldberg, 1955; Gaddum, 1945; Jizba, 1959). This appears true in many cases in geochemistry and can be used as the base for constructing distribution models. One such model is the lognormal law, but there are others more or less closely related to it (see Jizba, 1959).

* The property of the normal curve to predict negative values was first pointed out in 1879 by Galton (Gaddum, 1945).

It is reasonable as a first approximation to utilize a lognormal distribution in any case where there is a substantial possibility of predicting negative values from a normal distribution (see GADDUM, 1945). The practical consideration of determining what is the limiting value of $s/\bar{x}$ has been discussed by BES DE BERC (1954). Using selected values of $\bar{x}$ and s (e.g. $\bar{x} = 50$, $s = 1$) he calculates the equations of

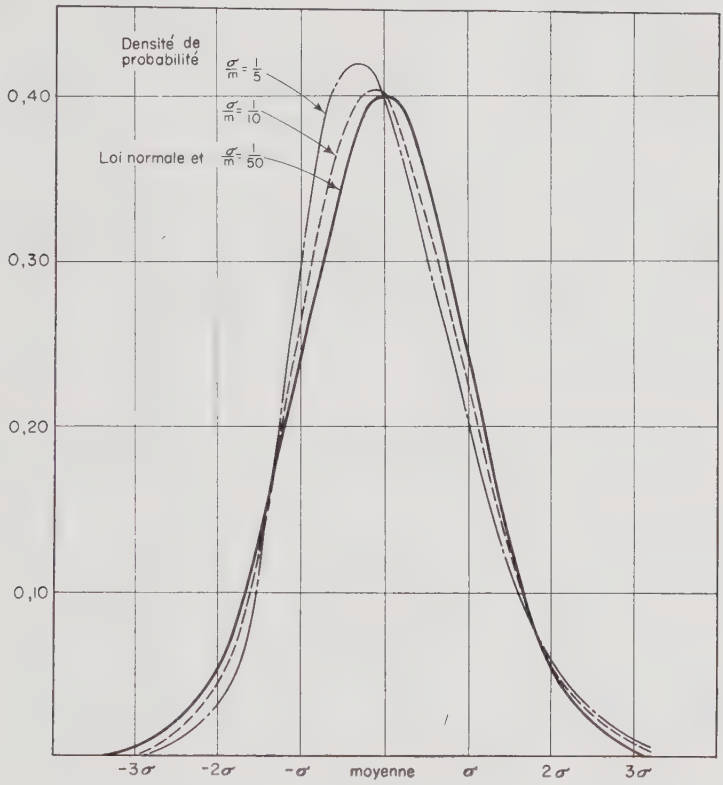

Fig. 1.

the normal curve and the lognormal curve corresponding to these parameters; for the latter he uses the transformations

$$m_{Lx} = \log \frac{\bar{x}^2}{\sqrt{(\bar{x}^2 + s^2)}}$$

and

$$s^2_{Lx} = \log \frac{\bar{x}^2 + s^2}{\bar{x}^2}$$

and then finds the lognormal curve whose parameters are m_{Lx} and s_{Lx}. (This procedure cannot be used for estimations but is suitable in this case.) He then calculates the probabilities for x to fall in the range $\bar{x} \pm s$, $\bar{x} \pm 2s$, $\bar{x} \pm 3s$, etc., and compares with the well known probabilities from the normal curve of 68·3, 95·4, 99·7, etc. These results are also apparent from his diagram (here reproduced as Fig. 1). For the value $s/\bar{x} = 1/50$ the difference in probabilities is negligible and

the two curves are not distinguished on the diagram; for a ratio of 1/10 the differences in probability for the first three ranges are (per cent) +0·6, −0·1, −0·1 and the lognormal curve is slightly displaced; for a ratio of 1/5 the probability differences are +1·9, −0·1, −1·1 and the curves are clearly separated.

Bes de Berc concludes that for values of $s/\bar{x}$ less than 1/5 ($c = 0{\cdot}2$; $C = 20$ per cent) the normal and lognormal curves are virtually indistinguishable for the prediction of probability. We may add that once c becomes much greater than this value, the lognormal curve predicts more reasonable values.

Returning to equation (1), it seems reasonable to use this correction to the observed variance as it stands, provided that none of the individual terms c_s, c_c, c_a exceeds the value of about 0·2. If one or more of them are close to this value it is better to transform the variate from x to log x before using the equation; the resultant variance c_g^2 will then of course be logarithmic and the reasoning of Bes de Berc may be applied in reverse to decide whether the transformation back to x is justified. This procedure is clearly empirical and perhaps needs theoretical justification. In any case the change of variate will not be necessary for any investigation where sampling, sample reduction and analytical errors have been reduced to small terms.

Geological and Mineralogical Aspects of the Choice of Distribution Laws

In the following we shall be concerned entirely with the dispersion of element distributions but must first consider the constitution of rocks in general.

There are two main types of rocks. In the first place there are the crystalline rocks which can be considered as the products of homogenous crystallization or recrystallization, that is their origins are physicochemical. The second type contains in addition the products of mechanical disintegration, of biochemical and of adsorptive origin. The distribution models are not necessarily the same in each case.

Considering the first group, there are two sets of composition properties which can be expected to vary from specimen to specimen of a given rock type. These are the composition of each mineral and the proportion of each mineral in the rock. It follows that the distribution pattern of any element in the rock population depends on both these factors, and is expressed by the sum for all the minerals in the rock of the distributions in the individual minerals. Suppose a particular rock i taken as a sample of the population has the mass G_i g and contains the proportion m_{ij} of mineral j, which in turn contains the proportion a_{ijk} of element k. Then the mass of element k in the mineral is $G_i\, m_{ij}\, a_{ijk}$ g. The variation of a_{ijk} as i takes all possible values gives the distribution of concentrations of k in mineral j. The variation of m_{ij} as i takes all possible values gives the distribution of the proportion of mineral j in the rocks G_i. If the rock contains n minerals the concentration of element k in G_i is

$$x_{ik} = \frac{\sum_{j=1}^{n} G_i m_{ij} a_{ijk}}{G_i} = \sum_{j-1}^{n} m_{ij} a_{ijk}$$

If the whole rock mass (population) is G, so that $G = \sum_{i=1}^{N} G_i$ (N samples), we can express the concentration of element k by X_k where

$$X_k = \sum_{i=1}^{N} \sum_{j=1}^{n} m_{ij} a_{ijk} \tag{2}$$

The distribution of an element in a rock of the first group therefore depends on the product of two variables, each obeying its own distribution law.

The first group contains the igneous and metamorphic rocks, together with the chemical sediments. For the purpose of further argument we will assume that these have formed under conditions of equilibrium crystallization from magmas and solutions of various kinds; a fractional crystallization such as commonly has occurred with magmatic rocks can be considered as a dynamic sequence of stages of related equilibria and we will assume that a given igneous rock represents the product of one of these short periods of equilibrium crystallization.

Since most minerals in a rock contain several elements in common it follows from the Law of Mass Action that (for a system containing definite masses of the reactants) the compositions and relative proportions of these minerals crystallizing in equilibrium are theoretically constant. The law applies only to ideal dilute solutions but an analogous relation will apply: that is, the whole rock mass will contain definite proportions or concentrations M_1, $M_2 \ldots M_j \ldots M_n$ of each mineral, where $M_j = \frac{1}{G} \sum_{i=1}^{N} m_{ij} G_i$, and the following relation will hold

$$M_1^{\alpha_1} \cdot M_2^{\alpha_2} \cdot \ldots \cdot M_j^{\alpha_j} \cdot \ldots \cdot M_n^{\alpha_n} = \text{constant} = c_1 \tag{3}$$

where the values α_j are constants depending on the various reactions involved in the equilibrium.

The total weight of element k in mineral j in the rock mass G is W_{jk} where

$$W_{jk} = A_{jk} M_j G \text{ g}$$

where

$$A_{jk} = \frac{\sum_{i=1}^{N} a_{ijk} m_{ij} G_i}{\sum_{i=1}^{N} m_{ij} G_i}$$

We can therefore modify equation (3) to obtain:

$$A_{2k}^{\beta_1} \cdot A_{2k}^{\beta_2} \cdot \ldots \cdot A_{jk}^{\beta_j} \cdot \ldots \cdot A_{nk}^{\beta_n} = \text{constant} = c_2 \tag{4}$$

since G and the values of W are parameters. This relation can be expressed in words by the following: *the partition of an element between the minerals of a rock mass is a function of the equilibrium conditions and the total composition of the system.* Partition ratios such as

$$P_{2k} = \frac{A_{2k}}{A_{1k}} \qquad P_{jk} = \frac{A_{jk}}{A_{(j-1)k}}$$

can be used where necessary. On the sample level we write

$$p_{ijk} = \frac{a_{ijk}}{a_{i(j-1)k}}, \text{ etc.}$$

The quantities X, M, A and P are parameters of the various populations we are considering: they are estimated by the quantities x_i, m_i, a_i and p_i,. Let us now consider some aspects of the choice of distribution models for these variables, bearing in mind that they are related by virtue of equations (2), (3) and (4).

Choice of Distribution Models or Descriptive Frequency Laws

The first point to be made has already been mentioned. The quantities m_i and a_i are continuous variables but are limited to values between 0 and 1: similarly the upper limit of x_i is the weight G_i. No functions such as the normal or lognormal which are continuous to $+\infty$ can therefore serve as models for the distribution of m_i, a_i or x_i. Whether they are suitable for *approximate description* is an entirely separate question.

If we desire to replace the concentration x_{ik} of an element in a rock by a continuous variable with upper limit of $+\infty$, the simplest is y_{ik} where

$$y_{ik} = \frac{x_{ik}}{1 - x_{ik}}$$

y_{ik} therefore represents the concentration of element k divided by the sum of the concentration of all the other elements in the rock. Where k is a major element the denominator is significantly less than unity and the distribution law is complex (see Jizba, 1957). For a trace element the denominator is close to unity and the distribution of x_{ik} will approximate to that of y_{ik}. We may express this in the following rule: *The distribution law of a camouflaged trace element in a crystalline rock formed in chemical equilibrium will closely approximate a continuous function.* The reason for inserting the qualification "camouflaged" will appear later.

Let us turn now to the minerals of a rock. The elements in a given mineral can be divided into the structure-forming elements and others. Apart from questions of solid solution it is usually considered that minerals have constant composition as far as structure-forming elements are concerned. That is, the values of a_k should be constant (for example a_{si} for quartz in atomic units is taken as 1/3). We do not know whether this is true in general, because analysis errors always interfere: we do know that it is not true for some minerals (S in pyrrhotite). In the majority of minerals where solid solution occurs the equivalent procedure is to consider the sum of the major elements at a particular lattice site (e.g. in olivine the values a_{Mg} and a_{Fe} will vary but $a_{(Mg+Fe)}$ is expected to be 2/7), but vacant sites are well known in minerals such as mica and amphibole.

Genetically we know very little also about the significance of trace elements camouflaged in minerals. It is usually assumed that the entry of Rb into pegmatitic microcline is a function of the supply, of the laws of solution and of the amount of K present, but we do not know where to draw the line between an "essential" and a trace element (e.g. is Al an "essential" element in eclogite pyroxenes?).

From the empirical standpoint we have no data at all. There are plenty of studies of element distributions in mineral series, but these are quite different from the question of mineral composition variation in a single rock type, or in other words in a particular genetic environment. The palaeontologist can do this sort of thing much more readily than the geochemist. We can probably assume that such quantities as the per cent Si in quartz show little variation, but they must show some.

Continuing with the distribution of minerals in a rock, it has been proposed by Allais (unpublished reference in Matheron (1955) that the Law of Mass Action provides a suitable model for establishing a lognormal distribution. Matheron does not clearly distinguish element distributions from mineral distributions so the question must be investigated. Taking the chemical equation

$$A + B = C + D$$

it is readily proved that

$$\frac{dA}{A} + \frac{dB}{B} = \frac{dC}{C} + \frac{dD}{D}$$

Writing $dy = dA/A$ or $y = \log A$ then the effect of small, numerous and independent variations on y will give rise to a normal distribution in $z = \log C$. In other words the effect of a deviation in A is proportional to A. If z obeys a normal law then C is lognormally distributed.

The activities on the left-hand side may be elements and ions forming the minerals C and D, etc., on the right. Mineral distributions should therefore be lognormally distributed.

The argument takes no account of the fact that (a) the mass law applies only to dilute ideal solutions, and (b) if large quantities are involved an unbounded distribution is impossible by reason of the upper limit of unity to values of m (i.e. C, D, etc.).

The model given by the mass action law will, however, be a reasonable approximation in the case of some elements and minerals at low concentrations. The case of trace elements camouflaged in major minerals is different, but lognormal distributions should be shown approximately by accessory minerals in common rocks and by ore minerals in ores which contain a large amount of gangue (the South African gold ores studied by Krige fall in the latter category). The criterion is the ratio $m/(1 - m)$; when m is small then the denominator is close to unity and a distribution close to lognormal can be expected.

Since, however, in these cases the mineral occurs as discrete grains of a certain size the population can be considered alternatively as discontinuous, with a small probability of drawing a sample containing grains of nothing but the accessory or ore mineral. Such a distribution conforms closely to the requirements of a Poisson distribution in which the probability is equal to the overall mean proportion M_j of the mineral j.

Many accessory and ore minerals are of comparatively simple composition, consisting of one major metal united with a non-metal or radical (e.g. Zr in zircon, Pb in galena). In spite of earlier remarks we can take it as likely that the spread of metal values in such minerals will be less than the spread of mineral values in the

samples. When this is true the metal values will conform closely to the mineral distribution law (i.e. the distribution of the x_{ijk} will duplicate that of the m_{ij}) provided that the elements can be disregarded in the other minerals. The latter is seldom the case, since most accessory and ore minerals contain oxygen or sulphur; these occur in other minerals which therefore influence the proportions of the accessory minerals. This, however, is irrevelant to the present question so long as we assume an adequate supply of such elements. The foregoing paragraphs can be summarized in a second rule as follows: *The distribution of the concentration of a minor or trace element in a homogenous crystalline rock will conform closely to a lognormal or a Poisson law, provided that the element is concentrated in an accessory or ore mineral of simple composition.* The qualification of "homogeneous" rock is added to exclude cases of ore deposits in which the primary ore minerals have been subsequently altered or remineralized; an example of this is discussed by Matheron (1956).

In view of the relations expressed in equation (2), the uncertainties regarding the distribution of major minerals in a rock and the magnitude of the denominator in the ratio $x/(1 - x)$, we can at present reach no conclusions regarding the possible distribution laws of major elements in a rock. Jizba's (1959) models are suitable if one can disregard the spread of values in individual minerals.

The position is a little better for trace elements camouflaged in the major minerals. If we assume that the spread of values m_{ij} (mineral proportions) is small (i.e. $m/(1 - m)$ is the same as m) and that the mass action law applies in this case, the distribution of m_{ij} is approximately lognormal. If we then assume that by virtue of their low abundance (probability) the values a_{ijk} (element concentrations in each mineral) follow a Poisson distribution* which approaches a lognormal law, we can reconsider equation (2). This equation shows x_{ik} as a function of the product $m_{ij} \cdot a_{ijk}$. If each of these two variables has a lognormal distribution then so does x_{ijk}. This follows from the fact that we can write log $x_{ijk} = \chi$, log $m_{ij} = \mu$ and log $a_{ijk} = \alpha$, and if α and μ each follow independent normal laws then so does their sum χ. The values x_{ijk} are summed for the n minerals of the rock to obtain x_{ij}, the concentration of element k in the rock. The sum of a group of variables each lognormally distributed is not itself lognormally distributed unless the variables are interrelated in an appropriate way, as is given in this case by equations (3) and (4). The distribution of x_{ij} is therefore approximately lognormal.

Another approach to the problem of the camouflaged trace-element distribution is as follows. A rock is forming from a solution by an equilibrium process. At a given moment t the solution contains u_t moles of a particular trace element, of which a proportion p_t is being incorporated in the rock minerals. During time dt the amount transferred from solution to rock is $p_t u_t dt$, which is equal to the amount lost by the solution $-du$.

$$-du = p_t u_t dt$$

$$d \log u = -p_t dt$$

* The necessary condition of discrete values applies on an atomistic level, i.e., we consider the probability of drawing atoms for a particular site.

If the solution contained u_0 moles at the beginning and the rock contains x_t moles at times t then

$$x_t = u_0 - u_t \quad \text{and} \quad -dx = du$$

We therefore have the relation

$$-d \log u = p_t \, dt = d \log x$$

If a large number of small independent consecutive impulses affect the magnitude of u, each will produce an effect proportional to its duration dt. We may therefore consider these instants dt to have a normal distribution, which is consequently also the case for log u and log x. Consequently, u and x are lognormally distributed.

We are here concerned only with trace elements, and an unbounded distribution is therefore admissable. The conclusions can be summarized in another statement, which is a revision of AHRENS' law (1954, p. 64): *The concentration of a camouflaged trace element in a crystalline rock formed in chemical equilibrium will show a distribution which conforms closely to a lognormal law.*

It should be noted here that AUBREY (1956) discusses in some detail the possibility that the distribution of a trace element will resemble that of the major element which it follows. This is probably the case, allowing the qualification that the relative dispersion for a major element would be expected to be smaller on account of stoichiometric requirements. Unfortunately much of AUBREY's argument is inconclusive because AHRENS' data was not corrected for analytical variance and we have no way of knowing to what degree the dispersions measured represent the real geochemical variance.

Finally, it should be noted that DE WIJS and MATHERON have both attempted to establish the universality of the lognormal law (MATHERON, 1955) for element distributions. It is not clear however whether this universality is to apply only to ore metals in deposits, or to major elements as well; in any case the distinction is not made (the writer has, however, only seen DE WIJS' proof as given by MATHERON). Otherwise the arguments appear quite valid.

Mixed Rocks

The preceding discussion has been restricted to homogeneous crystalline rocks formed under conditions close to chemical equilibrium, previously distinguished as the first group. The second group includes all altered rocks, but among the most important are the majority of sedimentary rocks, in which chemical sediments are mixed with clastic fractions. These merit separate treatment and will not be considered further here, beyond pointing out that since two or more processes may have operated to form a given rock it is to be expected that element distributions will be complex. Mixed distributions, formed by superposition of two populations obeying different laws, will be found.

Use of the Lognormal Law

In the last sections an analysis of the nature of various geochemical populations indicated certain conditions necessary for element distributions to approximate to the lognormal law. These conditions do not apply to major elements, for which

there are no laws to provide simple transformations to be used in day to day geochemical tests.

Faced with the practical necessity to compare geochemical results for any element it is recommended that the lognormal law be used. This is clearly the best model to use for trace elements, and it is better than the normal law for major elements. We have already seen from Bes de Berc's calculations that for small values of $s/\bar{x}$ it is irrelevant which law is used, while for large values of the ratio the lognormal law is better: this applies of course just as much to geochemical dispersions as to analytical ones.

Wherever an adequate number of data has been obtained, the distribution law may be chosen less arbitrarily. It should be noted, however, that "adequate" must be taken to mean an order of magnitude of hundreds or preferably thousands to establish a law with some confidence. (Krige (1951a, b) presents a histogram of 28,334 assays from one gold mine which shows a perfect visual correspondence with a lognormal curve.)

Where the choice between lognormal and normal laws is to be made on the basis of the ratio of $s/\bar{x}$ for a small sample (less than 100), it is important to correct the observed variance c^2 for manipulation error, and base the choice of law on the ratio c_g (see first section). Since $c_g < c$, it is evident that the uncorrected ratio c may indicate a lognormal law in cases where c_g can be used equally well for a normal law. The use of c, in other words, biases the choice towards a lognormal law, and this can be expressed as follows:

The coefficient of variation c_g (= s.d./mean) of a small body of geochemical data provides a criterion for the choice between a normal and a lognormal law for subsequent statistical tests. When $c_g < 0{\cdot}2$ either law will predict similar probabilities, but when $c_g > 0{\cdot}2$ the lognormal law is more realistic. It is important to correct the observed relative variance c^2 (as in rule 4) to obtain ${c_g}^2$, otherwise the choice will be biased towards a lognormal law.

Where this approach is necessary, it is of course useless to make any interpretations from a histogram or other frequency diagram which uses individual values, since these can not be corrected for the manipulation errors.

Comments on the Hypothesis of Lognormal Element Distributions

Several papers by Ahrens already cited maintain the hypothesis that element distributions are approximately lognormal. The law proposed in his first article is as follows: "the concentration of an element is lognormally distributed in a specific igneous rock" (Ahrens 1954a, p. 64). But in the second and third papers this statement has been qualified and modified. Considerable criticism of the original law has been published by the authors cited in the introduction. The criticism can be divided into the following categories:

(a) Insufficient data were presented to establish any distribution law.

(b) Statistical tests such as Pearson's χ^2 test were not used to establish the degree of correspondence between the law proposed and individual frequency distributions (the article by Vistelius demonstrates a better approach).

(c) AHRENS' histograms were constructed without regard to the best class interval to illustrate the observed frequencies.
(d) It was not clear whether AHRENS' law was supposed to be descriptive or to to imply a causal relationship from some unexplained model.
(e) Positive bias in a frequency distribution (the principal evidence used by AHRENS) is a characteristic of numerous probability curves, of which the lognormal is only one example.
(f) No natural frequency distribution will accord with a simple theoretical law.
(g) The existence of positive bias in the distribution curves of one or more elements will necessitate negative bias for others, since the sum of concentrations will always be 100 per cent.

Most of these criticisms have been discussed, either explicitly or implicitly, except the last. This point is clearly true for a substance consisting of two elements only, but where a number of elements are present the situation is far more complex. It is, however, clear that the distribution of a constituent which makes up nearly the whole of a rock (e.g. SiO_2 in glass sand) will have a negative bias. It is also possible, although not essential, that a trace element which has close geochemical coherence with such a major element would itself show a distribution with negative bias.

The controversy has shown (as usual) that there is truth on both sides, although AHRENS' law as originally proposed was expressed in terms too general to be valid. English-speaking geochemists, however, are in debt to AHRENS for having provoked the discussion and for making them rather more aware of the unsuitability of the normal law in most cases; in short, for the point of view expressed by GADDUM (1945, p. 466):

"If it were the normal custom, when scientific observations show uncontrolled variations large compared with the observations themselves, to convert them to logarithms before estimating their mean or variance, the usual result would be an increase in the accuracy and scope of the conclusions drawn from them.

CONCLUSIONS

The present paper has been written in an attempt to reconcile some of the different points of view in a difficult field, and to show that most authors have been guilty of over-simplification and over-generalization.

Most of the points of criticism against the lognormal law of AHRENS (see preceding section) indicate the problems encountered in selecting *any* law. This article has been mainly concerned with two additional points of criticism which are also quite generally applicable:

(h) Observed distributions should not be used to interpret goechemical populations without taking into account the manipulation errors.
(i) It is essential to understand clearly the nature and limits of a given population, in geochemical terms, before trying to find a model to explain it.

The last point is the most important and has been discussed so far in mineralogical terms. From the statistical viewpoint we can summarize the views as follows.

Any collection of numbers or properties can, from the statistical point of view, be treated as a population. From the observed frequencies it is theoretically possible to find a distribution law, i.e. a probability function which describes the population, more or less. It is not, however, of any value whatsoever to try and

find the *reason* why the probability function describes the population, unless it is known that *the population is homogeneous.*

It is very difficult to define the word "homogeneous" in a satisfactory geochemical sense (the writer confesses to a remote suspicion that the "homogeneous geochemical population" is an illusion), but it is often clear that a given population is heterogeneous.

For example an element distribution in a greywacke is heterogeneous, since a greywacke is a mixed rock in the sense of an earlier section. It might be possible to deduce this from frequency diagrams (analogous examples in terms of metal mineralization are given by Tennant and White (1959)), but this will depend on a number of factors. Specifically, one might expect different element distribution models for the various clastic fractions, for the clay mineral fraction and for any diagenetic process such as cementation. In a given greywacke these distributions are superimposed.

It has been shown earlier that a crystalline rock has more claims to be considered as a valid population in the case where it formed at a single chemical equilibrium. This criterion is of course very hard to apply. Can one consider the word "basalt" to imply the concept of a homogeneous population? Not in any strict sense, because: (a) the limits of rock-classification are arbitrary; (b) the limits of an actual rock composition are gradual; (c) there are at least three widespread types of basalt. Obviously one should first restrict the population in time and space: the "diabase dikes and sills of Nipissing age in the Sudbury district" constitute a population which is more likely to be homogeneous, but can still be criticised.

Obviously the question is of less importance when the statistical treatment is being used as a means to a geochemical end. When it is a matter of defining a general law, however, a rigid analysis of the assumptions is necessary.

The rules proposed in the present paper are summarized below. They must be regarded as hypotheses and obviously need to be tested experimentally. Rule 3 is largely a restatement of the findings of Krige, Allais and Matheron and Rule 5 is based in part on the views of Bes de Berc and Ahrens:

(1) The frequency distribution of concentrations of a camouflaged trace element in a homogeneous rock formed by a chemical equilibrium process can be considered as a continuous probability function with limits zero and $+\infty$.

(2) The best probability function to use is the lognormal law, which is justified both by practical utility and theoretical considerations.

(3) The previous rules also apply to those trace and minor elements which are largely concentrated in accessory or ore minerals of simple constitution. Many economic deposits are in this category. The Poisson function may also be convenient in this case, if the discontinuous distribution of mineral grains is considered.

(4) The geochemical variance of a group of data is less than the measured variance, which should be corrected by subtracting manipulation variance (sampling, sample reduction, analysis).

(5) The coefficient of variation c_g (= s. d./mean) of a small body of geochemical data provides a criterion for the choice between a normal and a lognormal law for

subsequent statistical tests. When $c_g < 0{\cdot}2$ either law will predict similar probabilities, but when $c_g > 0{\cdot}2$ the lognormal law is more realistic. It is important to correct the observed relative variance c^2 (as in rule 4) to obtain $c_g{}^2$, otherwise the choice will be biased towards a lognormal law.

Acknowledgements—The writer is grateful to M. le Professeur M. Roubault, Directeur de l'ENSGA, whose many courtesies allowed this paper to be written while in Nancy. Numerous discussions with colleagues, especially A. Bernard and K. Govindaraju at Nancy, and J. D. Bankier at McMaster helped clarify the writer's views. L. H. Ahrens and G. V. Middleton kindly read the manuscript and several points were elaborated in the light of their suggestions. Only the writer however, is responsible for the opinions expressed.

References

Ahrens L. H. (1954a) The lognormal distribution of the elements. *Geochim. et Cosmochim. Acta* **5,** 49–73.

Ahrens L. H. (1954b) The lognormal distribution of the elements (2). *Geochim. et Cosmochim. Acta* **6,** 121–131.

Ahrens L. H. (1957) Lognormal-type distributions—III. *Geochim. et Cosmochim. Acta* **11,** 205–212.

Aitchison J. and Brown J. A. C. (1957) *The Lognormal Distribution.* Cambridge University Press.

Aubrey K. V. (1956) Frequency distributions of elements in igneous rocks. *Geochim. et Cosmochim. Acta* **8,** 83–89.

Bes de Berc O. (1954) Influence sur la précision des calculs du rendement poids et du rendement métal, des erreurs commises sur les teneurs. *Rev. Ind. Minérale* Sect. A, **35,** 366–383.

Chayes F. (1954) The lognormal distribution of the elements : a discussion. *Geochim. et Cosmochim. Acta* **6,** 119–120.

Chayes F. and Fairbairn H. W. (1951) A test of the precision of thin-section analysis by point counter. *Amer. Mineral.* **36,** 704–712.

De Wijs (1951) Statistics of ore distribution—I. *Geol. en Mijnbouw* November.

De Wijs (1953) Statistics of ore distribution—II. *Geol. en Mijnbouw* January.

Durovic S. (1959) Contribution to the lognormal distribution of the elements. *Geochim. et Cosmochim. Acta* **15,** 330–336.

Duval R. (1955a) Contribution à l'étude de l'échantillonage des gisements. *Ann. des Mines* No. 1, 3–27.

Duval R. (1955b) Contribution à l'étude de l'échantillonage des gisements. *Ann. des Mines* No. XII, 76–79.

Duval R., Levy R. et Matheron G. (1955) Travaux de M. D. G. Krige sur l'évaluation des gisements dans les mines d'or sud-africaines. *Ann. des Mines* No. XII, 3–49.

Fairbairn H. W. (1953) Precision and accuracy of chemical analysis of silicate rocks. *Geochim. et Cosmochim. Acta* **4,** 143–156.

Gaddum J. H. (1945) Lognormal distributions. *Nature, Lond.* **156,** 463–466.

Gy P. (1954) L'échantillonage des minerais. Erreur commise dans le prélèvement d'un échantillon sur un lot de minerai. *Rev. Ind. Minerals* Sect. A, **35,** 311–345.

Jizba J. V. (1959) Frequency distribution of elements in rocks. *Geochim. et Cosmochim. Acta* **16,** 79–82.

Krige D. G. (1951a) A statistical approach to some basic mine valuation problems on the Witwatersrand. *J. Chem. Met. Min. Soc. of South Africa.*

Krige D. G. (1951b) A statistical approach to some mine valuation and allied problems on the Witwatersrand. M.Sc. Thesis, University of the Witwatersrand.

Laffitte P. (1953) Etude de la précision des analyses des roches. *Bull. Geol. Soc. Fr.* 6, **3,** 723–745.

Laffitte P. (1957) *Introduction a l'Étude des Roches Métamorphiques et de Gites Métallifères.* Masson, Paris.

Matheron G. (1955) Application des méthodes statistiques à l'évaluation des gisements. *Ann. des Mines* No. XII, 50–75.

Matheron G. (1956) Utilité des méthodes statistiques dans la recherche minière *Rev. Ind. Minerale* January 1956, Special number 1–R. 457–472.

Miller R. L. et Goldberg E. D. (1955) The normal distribution in geochemistry. *Geochim. et Cosmochim. Acta* **8,** 53–62.

Shaw D. M. (1954) Trace elements in pelitic rocks. I—Variation during metamorphism. II—Geochemical relations. *Bull. Geol. Soc. Amer.* **65,** 1151–1182.

Shaw D. M. and Bankier J. D. (1954) Statistical methods applied to geochemistry. *Geochim. et Cosmochim. Acta* **5,** 111–123.

Sichel H. S. (1949) Mine valuation and maximum likelihood. M.Sc. Thesis, University of the Witwatersrand.

Sichel H. S. (1952) New methods in the statistical evaluation of mine sampling data. *Trans. Inst. Min. Met.* March.

Tennant C. B. and White M. L. (1959) Study of the distribution of some geochemical data. *Econ. Geol.* **54,** 1281–1290.

Vistelius A. B. (1960) The skew frequency distributions and the fundamental law of the geochemical processes. *J. Geol.* **68,** 1–22.

Geochimica et Cosmochimica Acta, 1961, Vol. 23, pp. 135 to 144. Pergamon Press Ltd. Printed in Northern Ireland

The relation of discordant Rb–Sr mineral and whole rock ages in an igneous rock to its time of crystallization and to the time of subsequent Sr^{87}/Sr^{86} metamorphism*

H. W. Fairbairn, P. M. Hurley and W. H. Pinson
Department of Geology and Geophysics, Massachusetts Institute of Technology, Cambridge, Mass.

(*Received* 30 *June*, 1960)

Abstract—Interpretation of discordant Rb–Sr ages of coexisting biotite and K-feldspar in igneous rocks, mostly from Sudbury, Ontario, has been attempted using supplementary whole-rock ages. Following a model proposed by Compston and Jeffery, it is postulated that, if the igneous body is a closed system, and a post-crystallization thermal event interrupts the accumulation of Sr^{87} in biotite and K-feldspar, the whole-rock analysis will give the true age and, owing to diffusion of radiogenic Sr out of biotite and K-feldspar, the apparent ages of these two minerals would be less than the whole-rock age. The common intersection of the three radiogenic growth lines (Sr^{87}/Sr^{86} plotted against age) gives the time of metamorphism. For the majority of the twelve examples the model offers an apparently valid explanation of the discrepant ages in terms of known field relations and two orogenic events at 1·2 billion years and 1·6 billion years.

Introduction

Of the various problems which beset isotopic age investigations none is more challenging than the discordant ages shown by coexisting minerals in certain igneous and metamorphic rocks. The disagreement is usually far in excess of possible analytical error and may be caused by redistribution of radiogenic isotopes as a result of reheating of the rock during a metamorphic episode. The particular aspect of this problem under consideration here is the disagreement between Rb–Sr ages of coexisting minerals in rocks of the deformed Pre-Cambrian belt in Ontario just north of Lake Huron. Comparison is also made with K–Ar ages on four of the samples.

The first clue to the riddle of discordant ages was disclosed by Carnegie Institution investigators (Tilton *et al.*, 1959b) in their recent study of biotite, muscovite, K-feldspar, and zircon in gneisses and pegmatites from the Maryland piedmont. They conclude that the gneissic rocks of the region originated at least as long ago as 1100 million years; in the Paleozoic, pegmatites (and probably granites) were intruded 450 million years ago, followed by a metamorphism at 300 million years shown by biotite.

A subsequent clue, marking a distinct advance, has been presented by Compston and Jeffery (1959), who demonstrated that the Rb–Sr age of a *whole-rock* sample of granite in Western Australia was greatly in excess of the Rb Sr ages of the component biotite and K-feldspar. In explanation, they postulated that, if the granite were a closed system, and a post-crystallization thermal event interrupted the accumulation of radiogenic Sr^{87} in biotite and K-feldspar, the whole-rock analysis would give the true age and, owing to diffusion of Sr out of biotite and K-feldspar, the apparent ages of these two minerals would be less than the whole-rock age. In more detail the concept is as follows.

* MIT age studies No. 21.

The Model

Fig. 1 shows the increase* of Sr^{87}/Sr^{86} with time for a hypothetical whole-rock sample of granite and for its component biotite and K-feldspar. It is assumed that, at t_0 when crystallization was complete and the decay of Rb^{87} to Sr^{87} commenced, the initial value of Sr^{87}/Sr^{86} was 0·712. Gast (1960) has assembled abundant evidence in support of this value. As biotite normally has more Rb than K-feldspar and each has more than the whole rock, the accumulation of radiogenic Sr^{87} with time follows the same order. The corresponding radiogenic growth lines have highest slopes for biotite, and lowest for the whole rock. If the radioactive decay

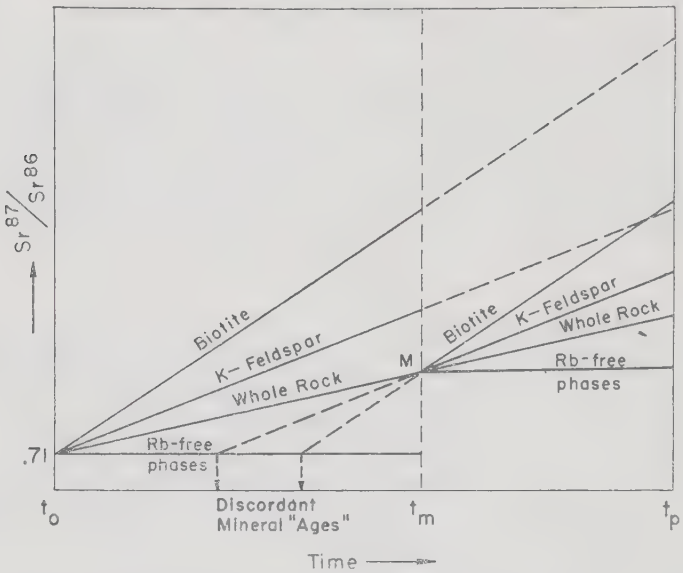

Fig. 1. Schematic diagram of radiogenic Sr growth lines for biotite, K-feldspar, and whole-rock fractions of a granitic rock, showing effect of a thermal episode at time t_m.

proceeded without any interruption to the present (t_p), the growth lines would project straight across the diagram from t_0 to t_p and, since they intersect at t_0 where the initial $Sr^{87}/Sr^{86} = 0{\cdot}712$, we would have three concordant ages and no further problems to solve. This is essentially what Schreiner (1958) demonstrated for granite of the Bushveld complex in the first published investigation of whole-rock age. If, however, at time t_m in Fig. 1 a thermal disturbance intervenes at sufficiently high temperature, it may bring about a redistribution of radiogenic Sr^{87} amongst certain Rb-poor minerals without net loss or gain of Sr in the rock as a whole. Assuming a normal partition redistribution of this radiogenic Sr^{87} between the minerals, and no loss of Sr from the granite upon completion of this thermal episode, the build-up of radiogenic Sr^{87} will begin anew but with a higher initial value of Sr^{87}/Sr^{86} than the original 0·712 (M in the diagram). If Sr^{87}/Sr^{86} at t_p is measured for biotite, and the slope of the radiogenic growth line is computed, the apparent

* For readers unfamiliar with details of the Rb–Sr age method, Rb^{87} decays to Sr^{87}, and Sr^{86}/Sr^{88} is constant for a given mineral. Thus the ratio Sr^{87}/Sr^{86} increases with time for any mineral containing Rb.

age, based on an initial Sr^{87}/Sr^{86} of 0·712, would be at the intersection of the broken-line extension of the biotite growth line with the 0·712 line. Similarly for K-feldspar another "age" may be read from the diagram, somewhat larger than that for biotite. In contrast, the whole-rock age will be considerably larger, as its radiogenic growth line is flatter than the others and was assumed unchanged by the metamorphism at t_m.

Additional evidence of this metamorphic interruption in the post-crystallization history of the granite would be found in all minerals normally low in Rb or lacking it. These now would be expected to have values of Sr^{87}/Sr^{86} greater than the normal 0·712 (see M in the diagram). Their radiogenic growth lines have essentially zero slopes both before and after metamorphism but have different Sr^{87}/Sr^{86} values before and after the event.

In summary the diagram outlines an ideal case in which, assuming no gain or loss of Sr from the rock system, the whole-rock age is the true age and the trisection of the three radiogenic growth lines at M gives co-ordinates for the time of metamorphism t_m and the initial higher value of Sr^{87}/Sr^{86} in the post-metamorphic environment.

The validity of this model was successfully tested by Compston and Jeffery (1959) with a granite from Western Australia. An excellent trisection of radiogenic growth lines for biotite, K-feldspar and the whole rock indicated a metamorphic event at 520 million years and the age of the granite to be 2430 million years. Biotite and K-feldspar "ages" were 650 and 1290 million years, respectively.

The present writers have confirmed the above hypothesis in a number of examples from and near Sudbury, Ontario, now to be presented. Before this Australian work came to our attention interpretation of mineral ages in this region was unsatisfactory (Fairbairn *et al.*, 1960; Tilton *et al.*, 1959a; Wetherill *et al.*, 1960), as no true age "signals" could be heard above the all-pervasive orogenic "noise". We therefore regard the whole-rock approach as a milestone in interpretation of discordant Rb–Sr data.

Scope and Methods of Investigation

Although our investigations were not originally designed for the work which eventually was found necessary, a considerable body of evidence is at hand which we believe confirms the model illustrated by Fig. 1. The diagrams we have constructed give independent evidence of two orogenic periods already suspected along the north shore of Lake Huron and elsewhere and at the same time indicate approximately the true ages of the rocks. Although the precision of whole-rock age determinations will in general be inferior to biotite and K-feldspar (smaller Rb/Sr and consequently flatter slopes in the diagrams), there is no gainsaying the geological importance of the age so determined. If desired, the error may be reduced by replicate analysis. In the diagrams to be presented the limits of error are usually shown for the whole rock only; errors for the component minerals are smaller and have not in all cases been computed.

The data have been obtained by isotope dilution procedures to determine Rb and Sr. The ratio of Sr^{87} to Sr^{86} was obtained either by direct measurement or by computation from an isotope dilution analysis. The growth lines are located by

Table 1. Rb–Sr analytical data

Sample number	Rb (p.p.m. by wt.)	Common Sr (p.p.m. by wt.)	Radiogenic Sr^{87} (p.p.m. by wt.)	Rb^{87}/Sr^{87} (in sample)	Sr^{87}/Sr^{86} (in sample)	Age (million years) for $Sr^{87}/Sr^{86} = 0.712$
B 3086	1926	3·5	9·66	48·2	25·7 (C)	1190 ± 35
F 3086	553	17·0	3·20	36·0	2·63 (C)	1365 ± 40
R 3086	263	43·6	2·29	14·0	1·25 (M)	2065 ± 70
B 3087	2297	4·6	11·54	58·5	24·6 (C)	1195 ± 35
F 3087	630	17·8	4·57	30·8	3·32 (C)	1720 ± 55
B 3094	938	40·7	5·17	33·1	2·01 (C)	1310 ± 40
F 3094	260	55·0	2·18	12·3	1·11 (M)	1985 ± 60
R 3094	234	44·6	2·20	12·5	1·21 (M)	2215 ± 80
B 3200	474	18·2	2·39	25·8	2·93 (C)	1205 ± 40
R 3200	98·7	311	0·78	1·25	0·737 (M)	1870 ± 170
F 3418	186	99·6	1·45	6·25	0·863 (M)	1840 ± 90
R 3418	112	149	0·735	2·84	0·767 (M)	1685 ± 75
F 3424	326	119	2·02	9·55	0·883 (M)	1465 ± 70
R 3424	135	157	0·72	3·27	0·755 (M)	1270 ± 120
B 3479	976	45·8	5·31	32·5	1·90 (C)	1275 ± 40
F 3479	217	43·8	1·37	14·0	1·03 (M)	1490 ± 50
R 3479	193	92·9	1·68	6·71	0·897 (M)	2055 ± 110
F 3767	193	67·8	1·41	8·90	0·926 (M)	1700 ± 85
R 3767	189	161	1·69	4·17	0·815 (M)	2020 ± 120
F 3768	339	87·2	2·10	11·8	0·958 (M)	1470 ± 60
R 3768	160	119	1·27	4·56	0·821 (M)	1880 ± 85
B 3769	382	57·1	2·79	16·0	1·21 (C)	1730 ± 85
R 3769	94·1	369	0·715	1·01	0·732 (M)	1800 ± 225
F 3771	285	122	1·29	8·25	0·820 (M)	1065 ± 75
R 3771	104	295	0·732	1·38	0·737 (M)	1675 ± 185
F 3774	257	43·7	1·80	15·0	1·13 (M)	1655 ± 65
R 3774	172	136	1·56	4·41	0·829 (M)	2140 ± 95

Decay constant used $\lambda_{Rb} = 1{\cdot}47 \times 10^{-11}$ year^{-1} (Flynn and Glendenin, 1959).

To compute Sr^{87}/Sr^{86} for any time t, given Sr^{87}/Sr^{86} and Rb^{87}/Sr^{87} for present time p, and where the fraction of initial Rb^{87} remaining at present time p is $Rb_p{}^{87}/Rb_t{}^{87}$

$$\left(\frac{Sr^{87}}{Sr^{86}}\right)_t = \left(\frac{Sr^{87}}{Sr^{86}}\right)_p \left[1 - \frac{(Rb^{87}/Sr^{87})_p}{(Rb^{87})_p/(Rb^{87})_t}\left(1 - \frac{Rb_p{}^{87}}{Rb_t{}^{87}}\right)\right]$$

$\frac{Rb_p{}^{87}}{Rb_t{}^{87}} = e^{-0.693t/T}$ for any time t and a half-life T of 47 billion years corresponding to the above decay constant.

(M)—Measured directly on unspiked sample.
(C)—Computed from isotope dilution analysis.

computing Sr^{87}/Sr^{86} for specific times for a given value of Rb^{87}/Sr^{87}. The error limits of the lines (standard deviation of arithmetic means) are based on $\pm 0{\cdot}3$ per cent error in measured Sr^{87}/Sr^{86}, $\pm 0{\cdot}5$ per cent in computed Sr^{87}/Sr^{86} and about ± 3 per cent error in the ratio Rb^{87}/Sr^{87}. The age error is then read directly from each diagram, and varies with the slope of the individual lines.

Discussion of Examples

Figs. 2 and 3 show diagrams for two localities in the Creighton granite. Although Fig. 3 is incomplete (no whole rock analysis is available) the biotite and K-feldspar lines intersect at approximately the same time point as in Fig. 2. Following the interpretation given for the model (Fig. 1), the Creighton granite underwent a metamorphic episode approximately 1·2 billion years ago. The unusually large Sr^{87}/Sr^{86} for sample 3087 at the time of metamorphism (Fig. 3) reflects an unusual Rb content (0·2 per cent for biotite). Although comparison of whole-rock ages is not possible for the two localities it is notable that the two K-feldspar "ages" are discordant beyond possible analytical error. The two biotite "ages" show this less conspicuously, but each is clearly discordant with its coexisting K-feldspar. In the absence of metamorphism since crystallization of the granite it would be reasonable to expect concordant K-feldspar, biotite, and whole-rock ages for both samples.

Fig. 4 of the Murray granite shows a reasonably good trisection centering between 1·2 and 1·3 billion years and, because of high Rb/Sr, unusually high precision of the whole-rock age. From the standpoint of field interpretation it is significant that this granite and the Creighton granite have identical whole-rock ages (cf. Fig. 2). In contrast, their biotite and K-feldspar "ages" show confusing differences.

Fig. 5 for the Cutler granite, about 100 miles west of Sudbury, is thought to be another example of metamorphism at about 1·2 billion years. No K-feldspar data are at hand, but the sharply contrasting slopes of the biotite and whole-rock lines make for high precision of the intersection and the postulated time of metamorphism. Although the error in the whole-rock age is large, its geological significance far outweighs its deficiency as a physical quantity.

Fig. 6 lacks a biotite line and the intersection of the K-feldspar and whole-rock lines has an error parallelogram extending from 1·1 to 1·35 billion years. It seems reasonable to assume that this granite, as with the preceding examples, has been involved in the same metamorphism, at about 1·2 billion years.

The Copper Cliff rhyolite was sampled at two localities, with results as shown in Figs. 7 and 8. The single area of agreement is the whole-rock age (2165 and 2215 million years). The K-feldspar whole-rock intersection in Fig. 8 at 1·52 billion years may be evidence of an orogeny around 1·6 billion years ago (Fairbairn *et al.*, 1960), as the error parallelogram extends just beyond this age. No biotite is available from this sample.

The K-feldspar line in Fig. 7 presents an unexplained anomaly, as there is no obvious reason for its slope and Sr^{87}/Sr^{86} ratio to be lower than that of the whole-rock line. Clearly it cannot be explained on the basis of the model of Fig. 1. As there is abundant quartz in the rock (presumably very low in Rb), redistribution of

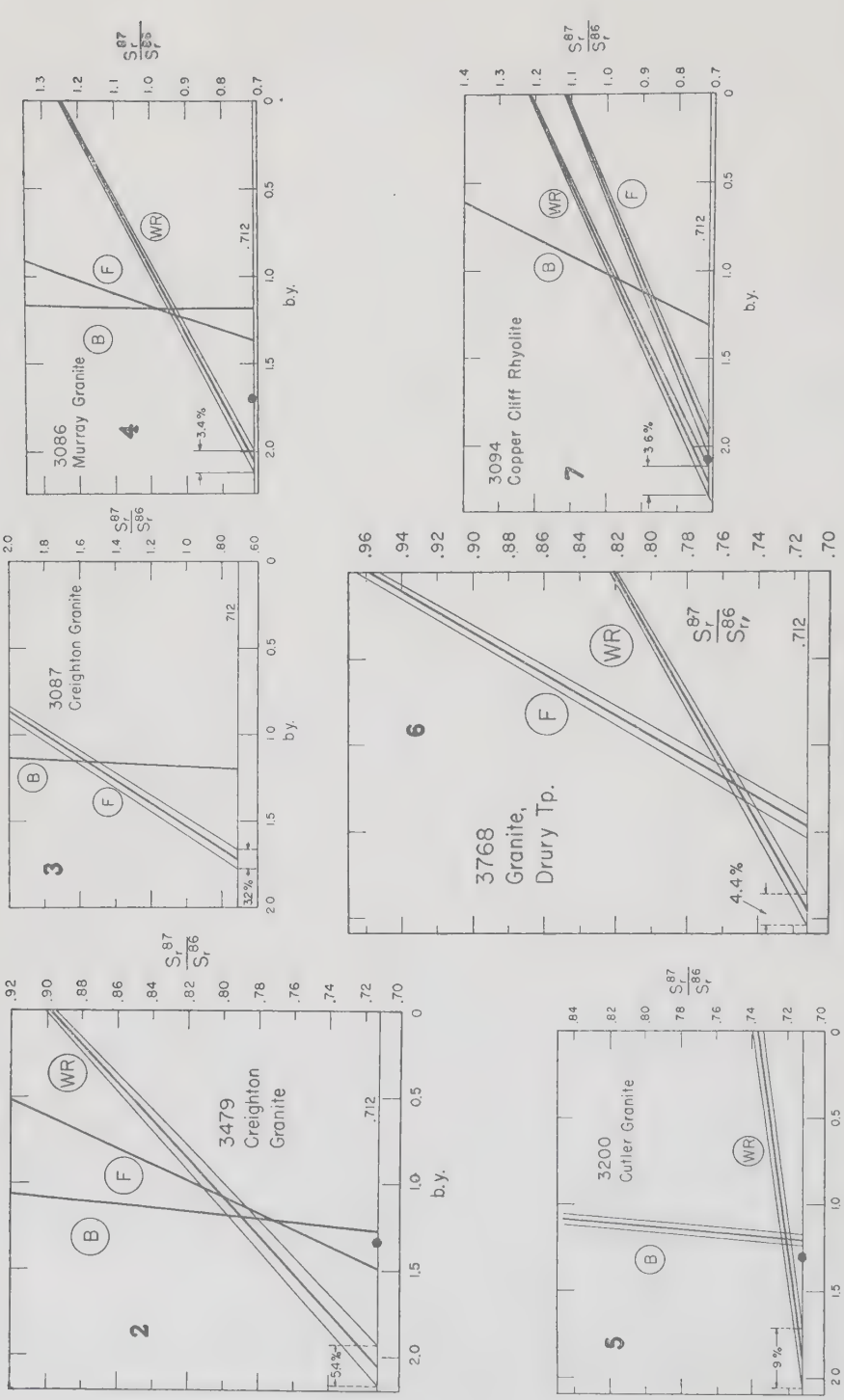

Fig. 2–7. Sr^{87}/Sr^{86} diagrams. See text for description.

Sr during metamorphism should show the normal relation of lowest slope and Sr^{87}/Sr^{86} for the whole-rock line.

The whole-rock age (1665 ± 185 million years) for the rhyolite in Fig. 9 is questionable as a true age according to the model, as it coincides with the 1·6–1·7 billion year orogeny everywhere evident in the region (Fairbairn *et al.*, 1960). There are also field reasons for supposing the rhyolite to be older than this. Absence of biotite in the rock unfortunately leaves the diagram incomplete.

Breccia in the Creighton granite gives the two intersecting lines of Fig. 10. The error parallelogram of the intersection is larger than might be desired but it seems reasonable to interpret it as evidence of the 1·6 billion year orogeny. As the whole-breccia age agrees with that of the unbrecciated Creighton granite the brecciation itself must be younger and for reasons given elsewhere (Fairbairn *et al.*, 1960) is believed to have developed 1·6–1·7 billion years ago.

Concordant biotite and whole-rock ages are shown in Fig. 11, with an intersection of the two lines almost exactly at the normal Sr^{87}/Sr^{86} value of 0·712. The contrast in precision of the two ages is clearly demonstrated. At this locality biotite apparently escaped the recrystallization so prevalent in the region.

Finally in Figs. 12 and 13 we have two examples of whole-rock and K-feldspar intersections at Sr^{87}/Sr^{86} values less than 0·712. In each case the "ages" calculated using 0·712 for the normal Sr correction are discordant. It may be significant that, although the data are derived from different rocks, the intersection is at approximately 0·70 for both, with the micropegmatite substantially older than the rhyolite. Unexplained, however, are the relative age relations indicated by these two diagrams compared with the field relations (Fairbairn *et al.*, 1960). The micropegmatite intrudes the Onaping volcanic formation of which the rhyolite (Fig. 12) is a part, thus disagreeing with the suggested laboratory conclusion.

The preceding example raises the question of the magnitude of departure from the normal value of Sr^{87}/Sr^{86} (=0·712) which can be ascribed to experimental error. It is implicit in this approach to dating of metamorphism that $Sr^{87}/Sr^{86} > 0{\cdot}712$ upon termination of any intermediate thermal episode. In most of the examples presented here Sr^{87}/Sr^{86} at the critical metamorphic intersections is unquestionably larger than 0·712 with respect to any reasonable analytical error. Excluding Fig. 11, which shows no evidence of metamorphism, Fig. 5 is the only diagram with an intersection close to 0·712. It differs from 0·712 by about the same amount as the low intersection (0·70) shown by Figs. 12 and 13. Its error parallelogram, however, is well above the 0·712 level and suggests that the deviation from 0·712 is real. The parallelogram, moreover, is much smaller in terms of Sr^{87}/Sr^{86} error than are those of Figs. 12 and 13, which have upper limits in each case of approximately 0·712. This, together with the unlikelihood of an initial $Sr^{87}/Sr^{86} < 0{\cdot}712$ suggests a non-metamorphic history for the two rocks, comparable with Fig. 11, and analytical error as the source of the anomalous intersections.

Correlation with K–Ar Biotite Ages

Four K–Ar biotite ages have been determined for comparison with the preceding Rb–Sr data. These are indicated at the appropriate point on the age scale in each

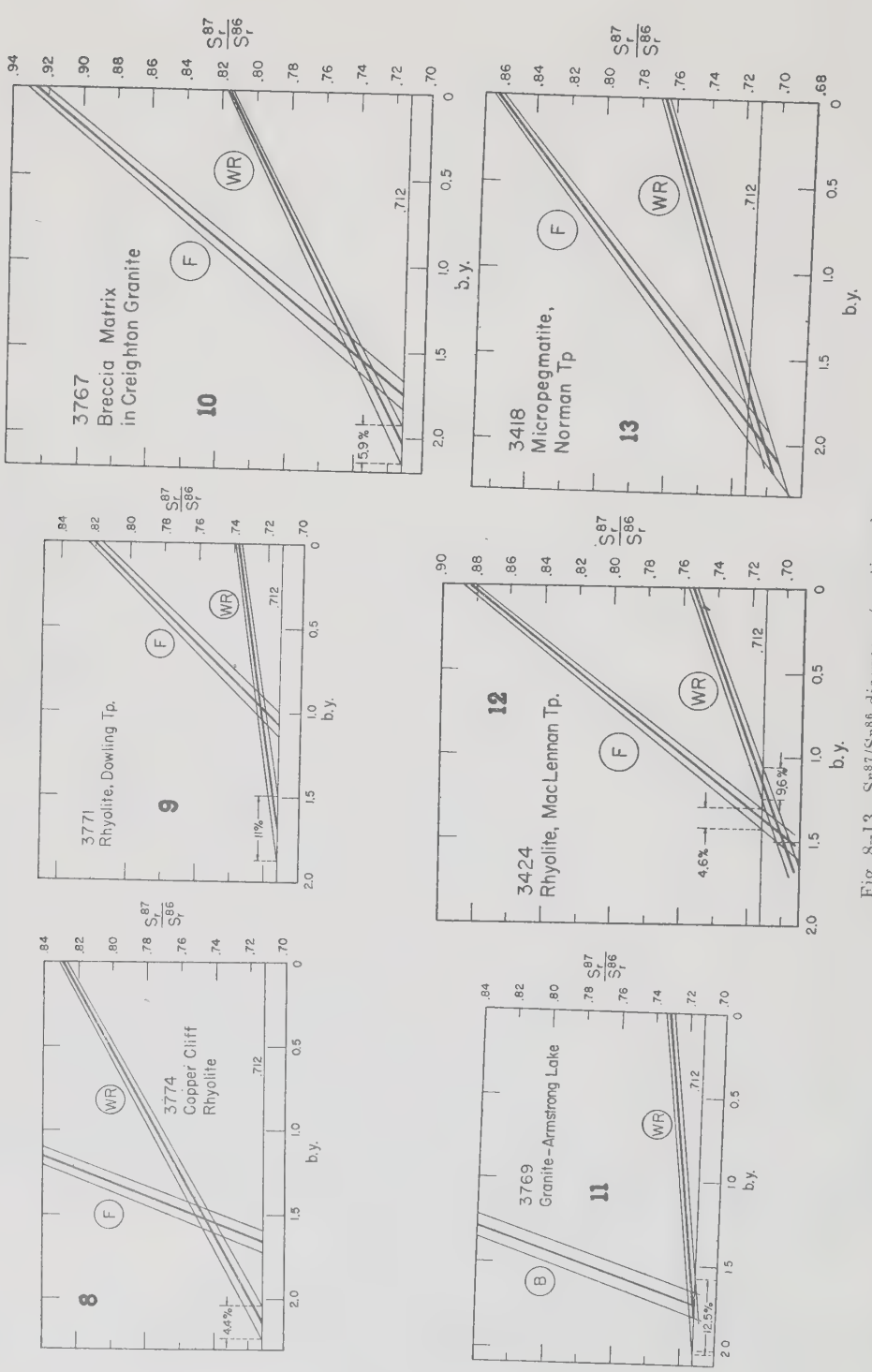

Fig. 8–13. Sr^{87}/Sr^{86} diagrams (continued).

figure by solid circles. The value in Fig. 2 for the Creighton granite at 1·33 billion years is close to the 1·2 billion-year orogeny under discussion. Biotite in the Murray granite (Fig. 4) on the other hand discloses evidence of both the 1·2 (Rb–Sr) and 1·6 billion years (K–Ar) orogenies. That is, the later orogeny had no apparent effect on Ar, in contrast with the Sr, which in this example is an ideal illustration of the model represented in Fig. 1.

Biotite in the Cutler granite (Fig. 5), with a K–Ar age of 1·28 billion years, compares favorably with the intersection at 1·2 billion years. On the other hand, the K–Ar age (2·07 billion years) of biotite in the Copper Cliff rhyolite (Fig. 7) closely approaches the Rb–Sr whole-rock age, indicating that Ar in this sample was not affected by later orogenic events. This is an unexplained feature of much interest for, although the Cutler and Copper Cliff localities are 100 miles apart, they are part of the same deformed belt which parallels the north shore of Lake Huron.

In summary these four K–Ar biotite ages show no consistent pattern with respect to the assumed times of orogeny and Rb–Sr whole-rock ages. The values obtained are obviously comparable with individual Rb–Sr ages but are unpredictable.

Conclusions

The radiogenic Sr model suggested by Compston and Jeffery stands up remarkably well as an explanation of most of the discordant mineral ages at Sudbury. Existing isotopic age evidence of two orogenies (at 1·2 and 1·6 billion years) is confirmed by the radiogenic growth line intersections of most of the examples discussed. Additional studies should of course be made, including isotopic lead ages on zircon. The present data are preliminary and should be amplified by selection of samples which permit successful age analysis by all three current methods, and should include determination of Sr^{87}/Sr^{86} for Rb-poor minerals.

Acknowledgements—The U.S. Atomic Energy Commission, Division of Research, through annual grants to P. M. Hurley as supervisor, subsidized the investigation throughout. We are greatly indebted to J. E. Thomson and the Ontario Department of Mines for generous assistance in collecting material. Two critical samples were provided by the geological staff, International Nickel Company of Canada, through the courtesy of F. Zurbrigg. The co-operation of the Dept. of Mineralogy, Harvard University, and especially of Judith Frondel, made possible a rapid X-ray spectrographic survey of many samples. During the early stages of the work the experience of L. F. Herzog was invaluable for the mass spectrometric measurements. To all these individuals and organizations, as well as to numerous and unnamed students and technical assistants, we extend our thanks.

References

Compston W. and Jeffery P. M. (1959) Anomalous common strontium in granite. *Nature, Lond.* **184,** 1792.

Fairbairn H. W., Hurley P. M. and Pinson W. H. (1960) Mineral and rock ages at Sudbury-Blind River, Ontario. *Proc. Geol. Assoc. Canad.* In press.

Flynn K. F. and Glendenin L. E. (1959) Half-Life and beta spectrum of Rb^{87}. *Phys. Rev.* **116,** 744.

Gast P. W. (1960) Limitations on the composition of the upper mantle. *J. Geophys. Res.* **65,** 1287.

Schreiner G. D. L. (1958) Comparison of the $^{87}Rb \rightarrow {}^{87}Sr$ ages of the red granite of the Bushveld complex from measurements on the total rock and separated mineral fractions. *Proc. Roy. Soc.* A **245,** 112.

Tilton G. R., Davis G. L., Wetherill G. W., Aldrich L. T. and Jäger E. (1959a) The ages of rocks and minerals. *Carn. Inst. Wash. Year Book* **58,** 171–178.

Tilton G. R., Davis G. L., Wetherill G. W., Aldrich L. T. and Jäger E. (1959b) Mineral ages in the Maryland piedmont. *Carn. Inst. Wash. Year Book* **58,** 171.

Wetherill G. W., Davis G. L. and Tilton G. R. (1960) Age measurements on minerals from the Cutler Batholith, Cutler, Ontario. *J. Geophys. Res.* **65,** 2461–66.

Geochimica et Cosmochimica Acta, 1961, Vol. 23, pp. 145 to 150. Pergamon Press Ltd. Printed in Northern Ireland

GEOCHEMICAL NOTES

The determination of indium and thallium in G–1, W–1 and other silicate rocks by a new technique

Following earlier work involving the use of ion exchange spectrochemical techniques (Edge *et al.*, 1959; Brooks *et al.*, 1960; Brooks and Ahrens, 1960a,b; Ahrens *et al.*, 1960 and 1961; Edge and Ahrens, 1961), a new procedure has been developed for the determination of In and Tl in silicates. This method is based on the extraction of the iodo-complexes of these elements into ethylether (Irving and Rossotti, 1952) followed, as in ion exchange enrichment techniques, by a quantitative spectrochemical analysis. Simplicity and high sensitivity are advantages of the procedure full details of which will be published elsewhere.

In and Tl have in the first place been estimated in G–1 and W–1 not only because these rocks may serve as checks but since fresh data on them are desirable. Six other specimens of common rock types were included in the work and the results are given in Table 1.

Table 1. Estimated Tl and In abundances in G–1, W–1 and other silicate rocks

No.	Description	Locality	Tl (p.p.m.)				In (p.p.m.)	
			A	B	C	D	A	E
1	G–1 granite	Westerley R.I. U.S.A.	1·27	1·30	1·30	1·27	0·042	0·026
2	W–1 diabase	Centerville Va. U.S.A.	0·21	0·17	0·10	0·11	0·094	0·064
3	Cape granite	Cape Peninsular, S. Africa	1·30	—	1·40	—	0·070	
4	Quartz feldspar	Paresis igneous complex S.W.A.	0·71	—	—	—	0·070	
5	Nepheline synite		0·59	—	—	—	0·266	
6	Gabbro		0·18	—	—	—	0·120	
7	Hortonolite dunite	Lydenburg Tvl. S.A.	—	—	—	—	0·336	—
8	Malmesbury shale	Mouille Pt., Cape Town	0·12	—	0·18	—	0·027	—

A, This paper. B, Morris and Killick (1960). C, Brooks *et al.* (1960). D, Adams and Vincent (1960). E, Smales *et al.* (1957).

Agreement on G–1 and W–1 is generally good. No information on Tl was available when Ahrens and Fleischer (1960) recently reviewed the trace element data on these two standard rocks but four sets of data are now available (Table 1) and because agreement on G–1 is strikingly close, the average of 1·29 p.p.m. Tl may be recommended with considerable confidence. Agreement on W–1 is not so close but nevertheless quite good and the average of 0·15 p.p.m. should not be far from the true concentration.

The In values given here are about 50 per cent higher than those obtained by neutron activation (Smales *et al.*, 1957) but as two totally different procedures have been used and the concentrations are very low (<0·1 p.p.m.), the results are fairly satisfactory.

Shaw (1957) has reviewed the geochemistry of In and gives several abundance data. The values for the few common rocks given in the present paper are in general agreement with the abundance magnitudes given by Shaw. In an earlier paper, Shaw (1952) points out that there is no apparent regularity in the distribution of In in silicate rocks apart from a tendency to be associated with Sn. This possibility has also been noted by Rankama and Sahama (1950) and by Goldschmidt (1954) who have in addition suggested the possibility of an association with Mn because of a close similarity in ionic radii (Mn^{2+} = 0·81 Å, In^{3+} = 0·80 Å). Wager *et al.* (1958) have observed a sympathetic Mn–In relationship in rock from

Table 2. The Mn and In contents of six silicate rocks

No.	Mn conc. (p.p.m.)	In conc. (p.p.m.)
1	210	0·042
4	600	0·070
2	1300	0·094
6	1300	0·120
5	1530	0·266
7	5500	0·336

the Skaergaard intrusion. Mn determinations are available for six of the rocks discussed here (Taylor, 1960) and in these a relationship between Mn and In is apparent as indicated in Table 2 where Mn and In concentrations are compared. It is obvious that firm conclusions cannot be drawn from the comparatively small number of data available but they indicate that a study of a possible In–Mn association may turn out to be fruitful.

R. R. Brooks
L. H. Ahrens

Department of Chemistry
University of Cape Town

References

Adams D. B. and Vincent E. A. (1960). Unpublished work.

Ahrens L. H., Edge R. A. and Taylor S. R. (1960) The uniformity of concentration of lithophile elements in chondrites. *Geochim. et Cosmochim. Acta.* **20,** 260–272.

Ahrens L. H., Edge R. A. and Brooks R. R. (1961) The combination of ion exchange and spectrographic techniques for the estimation of trace elements in geological materials. *S. Afr. Indust. Chem.* In press.

Ahrens L. H. and Fleischer M. (1960) Second report on a co-operative investigation into the composition of two silicate rocks. *U.S. Geol. Survey Bull.* No. 1113.

Brooks R. R. and Ahrens L. H. (1960a) The application of anion exchange techniques to the spectrochemical detection of the noble metals in silicate rocks. *Spectrochim. Acta* **16,** 783.

Brooks R. R. and Ahrens L. H. (1960b) Some observations on the distribution of Tl, Cd and Bi in silicate rocks and the influence of covalency on their degree of association with other elements. *Geochim. et Cosmochim. Acta.* **23,** 100–115.

Brooks R. R., Ahrens L. H. and Taylor S. R. (1960) The determination of trace elements in silicate rocks by a combined spectrochemical-anion exchange technique. *Geochim. et Cosmochim. Acta* **18,** 162–175.

Edge R. A. and Ahrens L. H. (1961) The Sc, Y, La, Nd, Ce, Sn, Mo and Ga content and K/Rb and K/Cs ratio of some South African granites and related rocks. In preparation.

Edge R. A., Brooks R. R., Ahrens L. H. and Amdurer S. (1959) Some reconnaissance observations on the combined use of ion exchange enrichment and spectrochemical analysis for the determination of trace constituencies in silicate rocks. *Geochim. et Cosmochim. Acta* **15,** 337–341.

Goldschmidt V. M. (1954) *Geochemistry*. Oxford University Press.

Irving H. M. and Rossotti F. J. C. (1952) Solvent extraction in Gp III metal halides. *Analyst* **77,** 801.

Morris D. F. and Killick R. A. (1960) The silver and thallium content of rocks. *Geochim. et Cosmochim. Acta* **19,** 139–140.

Rankama K. and Sahama T. G. (1950) *Geochemistry*. Chicago University Press.

Shaw D. M. (1952) The geochemistry of Tl. *Geochim. et Cosmochim. Acta* **2,** 118.

Shaw D. M. (1951) The geochemistry of Ga, In and Tl. *Progress in Physics and Chemistry of the Earth*. (Vol. 2). Pergamon Press, London.

Smales A. A., Smit J. van R. and Irving H. M. (1957) The determination of In in rocks and minerals by radioactivation. *Analyst* **82,** 539–540.

Taylor S. R. (1960). Unpublished work.

Wager L. R. Smit J. van R. and Irving H. M. (1958) Indium content of rocks and minerals from the Skaergaard intrusion, East Greenland. *Geochim. et Cosmochim. Acta* **13,** 81–86.

Absolute ratio of B^{11}/B^{10} in Searles Lake borax*

C. C. McMullen, C. B. Cragg and H. G. Thode
McMaster University, Hamilton, Ontario, Canada

In 1946, Inghram reported the results of a careful study of the isotopic composition of boron. Two years later, Thode *et al.* (1948) reported variations in the abundance of the isotopes of boron in boric acid prepared from boron minerals obtained from natural sources throughout the world. Since that time there has been considerable controversy in the open literature concerning on the one hand, the absolute ratio of boron isotopes found in nature (Lehman and Shapiro, 1959) and, on the other, whether the isotopic abundances do indeed vary depending on the source of the native boron containing minerals (Parwel *et al.*, 1956; Shiuttse, 1956). Because of this disagreement and the increasing role of boron in reactor design, a further study of the boron isotopes seemed essential.

Two boron standards were carefully prepared from two boric acid samples, highly enriched in B^{10} and B^{11}, respectively. These were obtained from the stable isotope division of Oak Ridge National Laboratories.

The preparation of the standards was as follows: the starting material (H_3BO_3) was converted to methyl borate by heating with synthetic methanol. The methyl borate–methanol distillate (or azeotrope) was then mixed with a stoichiometric amount of 1 M NaOH and seeded with a small borax crystal. The solution was then evaporated to dryness at room temperature and the borax which remained purified by two recrystallizations from distilled water. Washing with ethanol and ether followed, after which the crystals were stored in a desiccator over a saturated aqueous solution of sucrose and sodium chloride. A small portion of each sample was removed at this stage for mass-spectrometric analysis.

Test runs of the distillate in the first step were titrated with standard sodium hydroxide solution and indicated a yield of greater than 95 per cent. The final borax was checked for

* The research for this paper was supported (in part) by the Defence Research Board of Canada, under Grant number 1680-33 Project D 89-16-80-33.

phase impurities by X-ray diffractometer techniques. Comparison of the X-ray spectra of the standards with doubly recrystallized analytic grade borax indicated a high purity standard sample. The two synthetic standards were then prepared by mixing weighed amounts of B^{10}-enriched borax and B^{11}-enriched borax. These were dissolved in a minimum of hot water, held in solution and stirred for about 30 min. Subsequent chilling and evaporation to dryness at room temperature was the final step.

Table 1. Boron isotope ratios for enriched isotope samples

Sample	B^{10} (%)	B^{11} (%)
ORNL	96·6	3·4
A-10	96·6	3·4
B-10	96·5	3·5
ORNL	1·5	98·5
A-11	1·0	99·0
B-11	1·0	99·0

Table 2. Mass spectrometric analyses of boron standards

Sample	B^{11}/B^{10} calculated	B^{11}/B^{10} measured	Discrimination correction factor
Boron-A	4·270	4·249	0·0049
Boron-B	3·956	3·936	0·0051

Table 3. Mass spectrometric analyses of Searles Lake borax

Sample	Observed B^{11}/B^{10}	Absolute B^{11}/B^{10}
Borax (lower deposit brine)	4·020 ± 0·008	4·040 ± 0·008
Borax (upper deposit brine)	4·020 ± 0·008	4·040 ± 0·016
Tincal (115 ft)	4·048 ± 0·012	4·068 ± 0·012
Tincal (30 ft)	4·052 ± 0·012	4·072 ± 0·012

Mass spectrometric analyses of the original enriched borax and the synthetic standards were carried out in a multiple-filament high-sensitivity mass spectrometer employing an electron multiplier detector followed by an electrometer current integrating circuit. The ratios of B^{11}/B^{10} thus obtained permitted an evaluation of the mass discrimination of the instrument at the masses 88 and 89 which were the major ion currents observed ($Na_2BO_2^+$).

Table 1 gives the B^{11}/B^{10} ratios obtained for the components of the standard samples along with the ORNL analysis.

Table 2 records the calculated values of the B^{11}/B^{10} ratio, the results of the mass spectrometric analyses of the standard samples, and the discrimination correction factor.

Four samples of borax obtained from the deposits of Searles Lake California were then analysed to determine the B^{11}/B^{10} ratio. The results of these analyses are presented in Table 3.

These abundance ratios corrected for instrumental mass discrimination (0·5 per cent per mass unit) yield absolute B^{11}/B^{10} ratios from 4·040 to 4·072 for Searles Lake borax. These values are in excellent agreement with those which have been obtained recently in another laboratory (Collins, 1960) from boron minerals found in various locations in the Searles Lake deposit. Consideration of factors which can introduce errors in the results of the investigation reported here indicate that the absolute ratios should be accurate to 0·5 per cent.

It is clear from the present work that previous values given for the absolute value of the B^{11}/B^{10} ratio for natural samples were too high (Inghram, 1946, $B^{11}/B^{10} = 4{\cdot}31$; Thode *et al.*, 1948, $B^{11}/B^{10} = 4{\cdot}35$ average; Macnamara, 1949, $B^{11}/B^{10} = 4{\cdot}18$ Searles Lake). Although these workers attempted to determine the absolute ratio by taking into account non-linear factors inherent in the measurements, mass discrimination effects were apparently particularly large when BF_3 gas samples were involved. Since no attempt was made to

Table 4. Comparison of boron isotope abundances for Searles Lake borax

Sample	B^{11}/B^{10} ratio relative to Tincal (30 ft)	
	Macnamara (1949)	This work
Borax (lower deposit brine)	0·995	0·992
Borax (upper deposit brine)	0·994	0·992
Tincal (115 ft)	0·998	0·999
Tincal (30 ft)	1·000	1·000

calibrate the instruments with standard samples these mass discrimination effects could have led to the large errors. It should be pointed out, however, that where two samples are compared in the measurement of variations in isotope ratio, these mass discrimination effects largely cancel out.

Macnamara (1949) reported the results of the analysis of the same samples shown in Table 3. He analysed BF_3 in a 180° mass spectrometer using magnetic scanning. Table 4 shows a comparison of his results with those of this work.

Although there appears to be approximately the same variations in both of these independent investigations, the errors which are associated with the absolute values indicate that any variations in the B^{11}/B^{10} ratio for Searles Lake borax must be less than 1 per cent.

In addition, the suite of samples obtained from natural sources for which B^{11}/B^{10} isotopic variations had been reported earlier by Thode *et al.* (1948) were reanalysed using the KBF_4 from which the original BF_3 samples were prepared. In this instance, the ion currents represented the isotopic species of $K_2BO_2^+$ ions appearing at masses 120 to 126. The variations in the B^{11}/B^{10} ratios reported earlier for these samples were confirmed, although the absolute ratios were different. A new suite of samples recently obtained from various geological settings have been analysed in the solid source mass spectrometer using portions of the native minerals. The results of this study which again confirm variations in the abundance of the boron isotopes will be reported in a paper to be submitted later.

References

Collins T. L. (1960) Knolls Atomic Power Laboratory. Private communication.

Inghram M. G. (1946) The isotopic constitution of tungsten, silicon and boron. *Phys. Rev.* **70,** 653–660.

Lehmann W. J. and Shapiro I. (1959) Isotopic composition of boron and its atomic weight. *Nature, Lond.* **183,** 1324.

Macnamara J. (1949) *The Natural Variations in the Isotopic Content of Boron.* M.Sc. Thesis, McMaster University.

Parwel A., von Ubisch H. and Wickman F. E. (1956) On the variations in the relative abundance of boron isotopes in nature. *Geochim. et Cosmochim. Acta* **10,** 185–190.

Shiuttse V. (1956) An investigation of the isotopic constitution of boron. *Soviet Physics J.E.T.P.* **2,** 402–405.

Thode H. G., Macnamara J., Lossing F. P. and Collins C. B. (1948) Natural variations in the isotopic content of boron and its chemical atomic weight. *J. Amer. Chem. Soc.* **70,** 3008–3011.

Geochimica et Cosmochimica Acta, 1961, Vol. 23, p. 151. Pergamon Press Ltd. Printed in Northern Ireland

LETTER TO THE EDITORS

In my paper on "Partial molar volumes of some salts in aqueous solutions" (*Geochim. et Cosmochim. Acta* **12**, 103–122, 1957), equation (13) was improperly derived. Inasmuch as this equation is basic to all the calculations in that paper, I should like to re-derive it, this time correctly and using no approximate method.

Starting with

$$V = n_1 v_1^0 + n_2 \phi_2$$

and

$$\overline{V}_2 = (\partial V / \partial n_2)_{T,P,n_1}$$

(symbols defined in the original paper), we have

$$\overline{V}_2 = \phi_2 + n_2 \left(\frac{\partial \phi}{\partial n_2} \right)_{T,P,n_1} = \phi_2 + n_2 \left(\frac{\partial \phi}{\partial N_2} \right) \left(\frac{\partial N_2}{\partial n_2} \right)_{T,P,n_1}$$

But

$$(\partial N_2 / \partial n_2)_{n_1} = N_1 / (n_1 + n_2)$$

Hence

$$\overline{V}_2 = \phi_2 + \frac{N_1 N_2^{1/2}}{2} \left(\frac{\partial \phi_2}{\partial N_2^{1/2}} \right)_{T,P,n_1}$$

Using my equation (12):

$$\phi_2 = \phi_2(\mathrm{O}) + N_2^{1/2} \left(\frac{\partial \phi_2}{\partial N_2^{1/2}} \right)_{T,P,n_1}$$

we get again equation (13):

$$\overline{V}_2 = \phi_2(\mathrm{O}) + \frac{1}{2} N_2^{1/2} (3 - N_2) \left(\frac{\partial \phi}{\partial N_2^{1/2}} \right)_{T,P,n_1}$$

The above steps should substitute equations (7) through (13) in the original paper.

Equation (15) of the original paper also is wrong. In the range of dilute solutions where approximately

$$\overline{V}_2 = \overline{V}_2(\mathrm{O}) + \left(\frac{\partial \overline{V}_2}{\partial N_2} \right)_{T,P} N_2$$

we have, by comparison with equation (13) and because $\overline{V}_2(\mathrm{O}) = \phi_2(\mathrm{O})$, the following relation:

$$\left(\frac{\partial \overline{V}_2}{\partial N_2} \right)_{T,P} = (3 - N_2) \left(\frac{\partial \phi_2}{\partial N_2} \right)_{T,P}$$

At the limit of infinite dilution, we get

$$\left(\frac{\partial \overline{V}_2}{\partial N_2} \right)_{T,P,N_2=0} = 3 \left(\frac{\partial \phi_2}{\partial N_2} \right)_{T,P,N_2=0}$$

Inasmuch as my original equation (13) is valid, the computations based on it remain good.

Branch of Theoretical Geophysics
U.S. Geological Survey
Washington 25, D.C.

E-AN ZEN

Geochimica et Cosmochimica Acta, 1961, Vol. 23, pp. 152 to 153. Pergamon Press Ltd. Printed in Northern Ireland

Academy of Sciences of the U.S.S.R.

Abstracts from Proceedings of the Institute for the Geology of Ore Deposits, Petrography, Mineralogy and Geochemistry

A. I. Perelman. **Some problems of the geochemistry of catagenesis in sedimentary deposits of the type of "cupriferous sandstones".**

"Catagenesis" is a new term applied to the geochemical activity of ground waters. The author discusses catagenesis in red deposits of desert formation and especially the geochemical activity of soda lake waters. Migration and deposition of copper and other metals is discussed.

K. M. Feodotiev. **Outlines of the geochemistry of salts. Geochemical diagrams of salt deposits.**

This work is based on data relating to the crystallization of salts in saline lakes and seas, as well as on the records of salt deposits. The order of crystallization of various minerals in different types of occurrences is illustrated by means of geochemical paragenetic diagrams. Special attention is paid to the elucidation of the prevailing climatic and geological conditions during the process of deposition of salts.

I. G. Chentzov. **Problems of mineralogy and geochemistry of certain sedimentary uranium-ore occurrences.**

This is a detailed study of uranium-vanadium enriched bituminous material as it occurrs in bituminous limestones of Mesozoic-Kainozoic age. First the primary concentration of U, V, Mo, Ni, Co and other metals in the asphaltenes and other bitumens found in limestones is studied with a special study of the distribution of organic matter in various textural types of limestones. Then the concentration of these metals during the diagenetic and subsequent stages is traced to various agencies such as the migration of petroleum, gas and oil-water. A record of 69 minerals found in these deposits provides material for a geochemical paragenetic table-diagram and a double triangular diagram $CaO—UO_3—V_2O_5—nH_2O—SiO_2$ which helps to explain the various orders of deposition of various uranium and vanadium minerals. The localization of uranium-vanadium deposits is also traced to lithological and tectonic factors.

I. G. Chentzov. **Selenium in Palaeogene deposits of Central Asia.**

The content of selenium in certain bituminous limestones in Fergana reaches 0·01%, and in their insoluble residues up to 0·05%. The mean part of selenium is found in the finely dispersed bituminous material and sulphides in the limestones. Ferroselite from these limestones is described. The X-ray data provide the following parameters for the mineral (a) 4·791, (b) 5·715, (c) 3·575 A. Claustolite, native selemium, chalkomenite and cobaltomenite are also described.

A. S. Dudykina. **Paragenetic association of trace elements in garnets of various genesis.**

This is a statistical work on a large number of garnets from various kinds of igneous and metamorphic rocks. It is found that certain trace elements are associated with garnets belonging to a certain group of garnet-bearing rocks.

A. S. Di'dykina. **Paragenetic associations of trace elements of cassiterites of various genetic types of tin deposits.**

The study of trace elements of 271 cassiterites of different genesis has shown that every genetic type is accompanied by a deposit assemblage of trace elements. The cassiterites of sulphide-cassiterites formation, for example, are accompanied by W, Pb, Sb, Ag, In, As and Ga. Cassiterites from pegmatites are accompanied by Zr, Nb and Ta.

K. I. Narbutt, I. P. Laputina, I. D. Shuba, K. A. Kardakov and G. P. Samoilov. **The isotopic composition of ore lead and the age of minerals containing U, Th, and Pb, according to mass-spectrometric and X-ray spectroscopic data.**

The age of a large number of minerals from localities in the Soviet Union has been determined as, for example, lead from galena (19 cases) lead from uranium minerals (8) by isotope method. Then by means of X-ray spectroscopy the age of a large number of minerals ranging from 2390 to 140 m.y. has been determined.

E. I. Semenov and I. D. Shuba. **On the geological age of Lovozero and other alkaline massifs of the Kola peninsula.**

The age of thorite, thorium-apatite, irinite and auerolite and zirconolite from Lovozero, Khibina and Keiva and Africanda was determined by the X-ray spectroscopic method on the basis of Pb/Th ratio. The range of variation is from 400 to 312 m.y. with a mean of 350 m.y., namely Silurian in age.

I. G. Chentzov. **On the presence of uranium in certain rock forming minerals.**

The analyses of minerals fractions of granite has shown that the uranium content of minerals varies from 2·1 to 1860 $\times$ 10%. Over one third of the total uranium is found in the accessory minerals, up to one third in ferric minerals and under one third in feldspars and quartz. The determination of leaching percentages of uranium for various minerals has shown that considerable amounts can be removed from minerals without affecting the intactness of their framework.

S. G. Zeitlin. **The application of ethylenediamintetra-acetate of sodium (trilone B.) in the radiochemical analysis.**

Translations into English of any article mentioned above are available at the price of £3. 10s. or $10. Orders should be sent to: The Secretary, the Pergamon Institute, Headington Hill Hall, Oxford.

Geochimica et Cosmochimica Acta, 1961, Vol. 23, p. 154. Pergamon Press Ltd. Printed in Northern Ireland

ERRATA

A. E. RINGWOOD: Some aspects of the thermal evolution of the earth
Vol. 20, pp. 241–259.

pp. 244 and 248: Transpose Figs. 1 and 2; the captions remain as printed.

G. G. GOLES, R. A. FISH and E. ANDERS: The record in the meteorites—1.
Vol. 19, pp. 177–195.

p. 177. Vol. 18 should read Vol. 19.

p. 177. Delete second footnote.

p. 180. Equation (8): The term $(1/\varepsilon, A)$ should read $(1/\varepsilon)A$.

p. 182. Last line of first paragraph: 5×10^{-29} sec^{-1} should read 5×10^{-20} sec^{-1}.

p. 188. Equation (14): The term A^*/ε should read A/ε.

pp. 191–192. Second line from bottom of p. 191: Delete text beginning "In these cases only minute amounts of xenon . . ." and ending "at which diffusion losses are negligible" on p. 192, fourth line. Delete footnote on p. 192. No paragraph is intended at the fifth line on p. 192.

INFORMATION FOR CONTRIBUTORS

I. GENERAL

1. Papers on *geochemistry* should be submitted to the appropriate Executive Editor—Prof. L. R. WAGER for papers from the United Kingdom and British Commonwealth and for papers in English from Europe; PROF. C. W. CORRENS for papers in German or French; Prof. E. INGERSON for papers from the American continents. Papers submitted for publication will naturally be judged from the standpoint of scientific originality and novelty. Technical details of apparatus used in scientific investigation can, however, be presented in brief notes. Critical comments or preliminary results requiring early publication should be submitted as letters to the editors. Where possible, letters should be confined to 500 words. The preparation of progress reports and review articles will be invited by the editors from time to time. The journal appears as independent and complete numbers, which are combined into volumes of about 300 pages.

2. Only papers which have not been previously published can be accepted. Authors must agree not to publish elsewhere a paper submitted to and accepted by *Geochimica et Cosmochimica Acta*.

3. Fifty reprints of each paper are provided free. Additional copies can be purchased if ordered at the time the first proofs are returned. A reprint order form will accompany first proofs.

II. SCRIPT REQUIREMENTS

1. Scripts must be written in one of the three official languages—English, French or German.

2. The script should be typed (not a carbon copy). The text must be ready for printing and should be carefully checked for errors. Authors will receive proofs for correction. The original script plus two copies will assist in expediting publication.

3. Illustrations should accompany the script mounted on separate sheets. Line diagrams that require to be redrawn should include all relevant details. Half-tone illustrations should be restricted to the minimum necessary. Photographs should be enlarged sufficiently to permit their clear reproduction and if words or numbers appear on them, two copies should be sent, one clearly printed and the other without inscription. All illustrations should be provided with descriptive legends, which should be given on a separate sheet. Any lettering on diagrams—other than Greek letters, symbols, etc.—should be stencilled and should be sufficiently large and bold to permit reproduction when the diagram has been reduced to a size suitable for inclusion in the journal.

4. References in the text should be given by quoting the authors name and year of publication, i.e. AHRENS (1952). *Full references should be listed at the end of each paper, in alphabetical order, in the following manner*

AHRENS, L. H. (1952). The use of ionization potentials—I. Ionic radii of the elements. *Geochim. et Cosmochim. Acta* **2**, 155–169.

and should include the full title of the article, standard abbreviated title of the journal, year, volume number and inclusive page numbers.

5. The text of articles submitted should be concise and in a readily understandable style. The technical description of the methods used should only be given in detail when such methods are new. The essential contents of each paper should be briefly recapitulated in an abstract in English. Such an abstract, may however, be submitted by the author in the language of the original typescript for translation into English by the editorial staff.

6. To conserve space, authors are requested to mark less important portions of the paper (such as description of methods, record of experimental results, etc.) for printing in smaller type.

7. Indices of refraction should be denoted by the symbols α, β, γ, ω, ε, n, and vibration directions by X, Y, Z, O and E.

Pergamon Press are also publishers of the following Journals.

JOURNAL OF NUCLEAR ENERGY (*including* THE SOVIET JOURNAL OF ATOMIC ENERGY*). PART A: REACTOR SCIENCE; PART B: REACTOR TECHNOLOGY; PART C: PLASMA PHYSICS — ACCELERATORS — THERMONUCLEAR REACTORS
HEALTH PHYSICS (*The Official Journal of the Health Physics Society*)
JOURNAL OF INORGANIC AND NUCLEAR CHEMISTRY
TETRAHEDRON (*The International Journal of Organic Chemistry*)
TALANTA (*An International Journal of Analytical Chemistry*)
INTERNATIONAL JOURNAL OF APPLIED RADIATION AND ISOTOPES
BIOCHEMICAL PHARMACOLOGY
ARCHIVES OF ORAL BIOLOGY
* BIOPHYSICS
* JOURNAL OF MICROBIOLOGY, EPIDEMIOLOGY AND IMMUNO-BIOLOGY.
* PROBLEMS OF HEMATOLOGY AND BLOOD TRANSFUSION
* PROBLEMS OF VIROLOGY
* PROBLEMS OF ONCOLOGY
* SECHENOV PHYSIOLOGICAL JOURNAL OF THE U.S.S.R.
* PAVLOV JOURNAL OF HIGHER NERVOUS ACTIVITY
* ELECTRIC TECHNOLOGY, U.S.S.R.
* RADIO ENGINEERING
* RADIO ENGINEERING AND ELECTRONICS
* TELECOMMUNICATIONS
* PHYSICS OF METALS AND METALLOGRAPHY
* THE ABSTRACTS JOURNAL OF METALLURGY
* APPLIED MATHEMATICS AND MECHANICS
CHEMICAL ENGINEERING SCIENCE
JOURNAL OF ATMOSPHERIC AND TERRESTRIAL PHYSICS
PLANETARY AND SPACE SCIENCE
ANNALS OF THE INTERNATIONAL GEOPHYSICAL YEAR
SPECTROCHIMICA ACTA
JOURNAL OF THE MECHANICS AND PHYSICS OF SOLIDS
ACTA METALLURGICA (*for the Board of Governors of Acta Metallurgica*)
INTERNATIONAL JOURNAL OF THE PHYSICS AND CHEMISTRY OF SOLIDS
DEEP-SEA RESEARCH
JOURNAL OF NEUROCHEMISTRY
JOURNAL OF PSYCHOSOMATIC RESEARCH
JOURNAL OF INSECT PHYSIOLOGY
INTERNATIONAL JOURNAL OF AIR POLLUTION
INTERNATIONAL ABSTRACTS OF BIOLOGICAL SCIENCES (*for Biological and Medical Abstracts Ltd.*)
RHEOLOGY ABSTRACTS
VACUUM
OPERATIONAL RESEARCH QUARTERLY
ANNALS OF OCCUPATIONAL HYGIENE
ELECTROCHIMICA ACTA
JOURNAL OF CHILD PSYCHOLOGY AND PSYCHIATRY
JOURNAL OF SMALL ANIMAL PRACTICE
SOLID-STATE ELECTRONICS
INTERNATIONAL JOURNAL OF MECHANICAL SCIENCES

* *Translations of Russian journals published on behalf of the Pergamon Institute, a division of Pergamon International Corporation*

Leaflets giving further details and subscription rates of each of these journals are available on request

FILED IN STACKS 3 Jul'61R
1 Dec'62F
16 Jan63F
22May64F
29Jun64F

THE GEOCHEMICAL SOCIETY

OFFICERS

Tom F. W. Barth, President
Harold C. Urey, Vice-President
Konrad B. Krauskopf, Secretary
George T. Faust, Treasurer

COUNCILLORS

E. F. Osborn, 1958–1960
H. G. Thode, 1958–1960
Albert E. J. Engel, 1959–1961
Friedrich G. Houtermans, 1959–1961
Ralph Cannon, 1960–1962
Th. G. Sahama, 1960–1962

REGIONAL VICE-PRESIDENTS

Louis H. Ahrens
Rui Ribeiro Franco
Ing. Georges Ordoñez
C. W. Correns
J. F. Lovering
Ken Sugawara

COMMITTEES

Auditing Committee:
Joseph J. Tregoning, Chairman
William L. Hill
C. R. Nasser

Constitution and By-Laws Committee:
Michael Fleischer, Chairman
Julian R. Goldsmith
Denis M. Shaw

Education Committee:
H. D. Holland, Chairman
J. A. S. Adams
D. M. Henderson
Kurt E. Lowe
G. D. Nicholls
Hans P. Eugster

Membership Committee:
R. M. Garrels, Chairman
Harvey C. Diehl
Chester B. Slawson
James E. Slosson
Irving Breger

Nominating Committee:
Wm. Pecora, Chariman
Th. G. Sahama
C. E. Tilley
G. Tunell

Programme Committee:
H. T. Evans, Chairman
Gordon J. F. MacDonald
H. E. Lowenstam

Publications Committee:
E. W. Heinrich, Chairman
Julian R. Goldsmith
John C. Maxwell
N. W. Rakestraw
S. C. Robinson
L. R. Wager
Earl Ingerson

Research Committee:
C. G. Dodd, Chairman
W. F. Bradley
R. A. Rowland
T. G. Thompson

Russian Translations Committee:
Earl Ingerson

Standards Committee:
Alvin Van Valkenverg, Chairman
Michael Fleischer
Loren Stieff
George Switzer
George Tilton

Tellers Committee:
Charles Meyer, Chairman
Henry R. Cornwall
Colin O. Hutton